

Taula d'evidències Curs 2020-21

Assignatura ADVANCED AEROELASTICITY
Codi 220351

Activitat avaluable	% Nota final	Alumne/grup	Nota	Pàgina
Entregable Examen Parcial	40	Enunciat	-	2
		Rúbrica correcció	-	4
		CA	6,5	5
		CN	6,5	14
		JO	7	21
		IB	8	29
		EE	10	38
		AI	10	51
Informe Projecte	45	Enunciat	-	59
		Rúbrica correcció	-	69
		CA + CN	6,67	70
		DM + RG	6,67	78
		IB + PS	8,67	99
		AM + AS	8,67	142
		AI	10	171

ADVANCED AEROELASTICITY
 Mid-term Exam – Assignment

- 10/11/2020 -

Control surface reversal condition for a wing

Consider a flat plate on a wind tunnel clamped on one side and free on the other, simulating a wing during flight conditions. The plate has a rigidly attached control surface, the position and size of which are determined by the parameters η and β , as depicted in Figure 1. This control surface can be deflected an angle δ ($\delta > 0$ downwards) in order to increase the total lift on the plate. The plate has an aspect ratio $AR = 6$ and the chord size is $c = 400$ mm. From a structural test, it has been determined that the plate's effective stiffness to a torsional load is $\overline{GJ} = 38$ kN m² and its elastic axis is located at $0.35c$ from the leading edge.

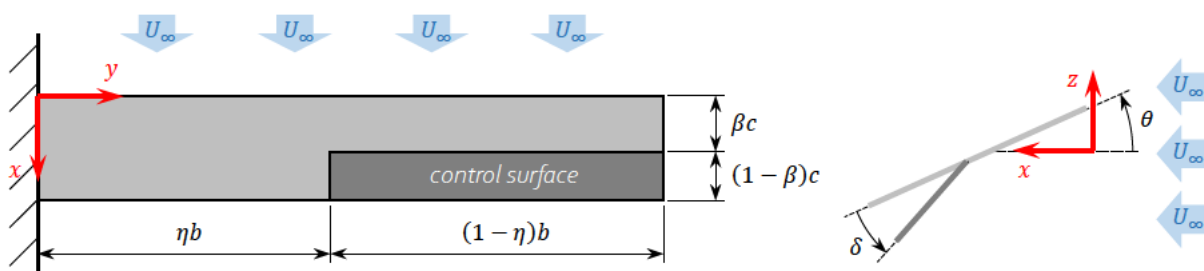


Figure 1.

In this context, we want to determine a position and size for the control surface and, to do so, we require information regarding the control surface reversal condition for different combinations of β and η .

To this end, a report with the following information is requested:

- (a) The divergence speed U_D of the plate.
- (b) A plot with the first 5 modes of the elastic twist associated to their corresponding divergence speeds.
- (c) A plot of U_R/U_D vs. η for $\beta = \{0.5, 0.6, 0.7, 0.8, 0.9\}$ (U_R is the speed at control surface reversal conditions).
- (d) A discussion on the possible sets of values of β and η for which:
 - (d.1) Surface control reversal conditions can be avoided.
 - (d.2) $U_R/U_D > 0.5$.

Note: The use of plots to support the discussion is highly advised.

The report in PDF alongside the code files used to solve the problem must be submitted to Atenea **before 17/11/2020 23:59** in a single compressed ZIP file.

Notes:

- Use lumped panel elements to discretize the plate.
- It can be assumed that all the angles are small and that the panel's section satisfies the requirements for thin airfoil theory to be applied.
- Make sure your code files are well commented (i.e. insert comments to make clear what you are trying to do).
- Make sure all the requested results can be clearly identified in your report.
- Add a detailed and comprehensive description of how you have proceeded to solve the problem. Do not repeat procedures already done in the lectures. However, if you use some of these procedures to obtain some result, you should indicate so and refer to the section from where they come from (e.g. "The procedure ... from page(s) ... in the lecture notes ... has been used to obtain ..." or "Result ... from problem ... is used here to ..."). Also, the report should never contain descriptions of the code (these should be either included as comments in the code itself or, if required, as an appendix to the report). Any additional development or deviation must be explained.
- Private e-mails regarding the assignment will not be answered. If you have any questions you must post them publicly in the course's forum in Atenea. In any case, I will not answer questions regarding theory or methodology to solve the problem.
- (Optional) You can add a section at the end of the report giving your personal thoughts on the first part of the subject. You can answer questions like:
 - How do you feel about the workload that this subject has required from you with respect to the other subjects?
 - Do you think the balance between theory and problems is OK?
 - What are your thoughts regarding the scope of the theory? Should it be extended to explore more topics in detail? Is it too condensed? Have you found it too easy/basic?
 - ...

Rúbrica Mid-term Exam Assignment

Item	Pes	Multiplicadors					Nota (pes x multiplicador)
		1	0.75	0.5	0.25	0	
1) L'estudiant ha obtingut la velocitat de divergència que es demanava a l'apartat (a).	2	Plantejament i resultat correctes	/	Plantejament correcte sense resultat o amb resultat incorrecte	/	Sense plantejament o plantejament i resultat incorrectes	A
2) L'estudiant mostra un gràfic amb els 5 primers modes associats a condicions de divergència demanats a l'apartat (b).	3	Implementació i resultat correctes	/	Intent d'implementació amb resultat incorrecte	/	No aporta resultats ni intents d'implementació	B
3) L'estudiant ha desenvolupat i descrit el model per a obtenir la condició d'inversió de controls requerida per a l'apartat (c).	2	Plantejament teòric correcte	Plantejament teòric gairebé correcte amb errors menors	Part del plantejament teòric correcte amb algun error	Plantejament teòric parcialment correcte amb errors significatius	No s'ha fet cap plantejament o aquest és totalment erroni	C
4) L'estudiant ha realitzat una correcta implementació del model i ha obtingut els resultats demanats a l'apartat (c).	2	Implementació i resultat correctes	/	Intent d'implementació amb resultat incorrecte	/	No aporta resultats ni intents d'implementació	D
5) L'estudiant ha aportat una discussió sobre les situacions plantejades a l'apartat (d).	1	Conclusions correctament justificades	/	Conclusions parcialment justificades	/	No aporta cap discussió sobre les qüestions	E
Bonus. Aspectes favorables més enllà dels demanats.	0-1 (*)	Extra en la nota final al complir-se un (x 0.5), o dos o més (x 1) dels següents criteris: (a) rigor en la presentació de resultats a l'informe, (b) codi ben comentat/documentat, (c) precisió i capacitat de síntesi en el llenguatge, (d) discussions/resultats addicionals respecte els que es demanen.					F
(*) El pes del bonus s'ajusta (fins a un màxim de 10%) per tal que la nota final no superi el 10						Nota final (0-10)	A + B + D + E + F



UNIVERSITAT POLITÈCNICA
DE
CATALUNYA

Control Surface Reversal Condition for a wing

Course 2020-21 QP

Màster universitari en Enginyeria Aeronàutica

Profesor: David Roca Cazorla

Author: C [REDACTED] A [REDACTED]



Contents

1	Problem specification	2
2	Divergence speed of the plate	2
3	Modes of the elastic twist	4
4	Control surface reversal conditions	5
5	Discussion	6
6	Personal thoughts	6

1 Problem specification

The goal of this assignment is to discuss the reversal conditions and divergence of the wing shown in Figure 2. It can be considered as a flat plate on a wind tunnel clamped on one side and free on the other at flight conditions. The plate has a rigidly attached control surface, the position and size of which are determined by the parameters ν and b . For calculus purposes the flight the density chosen for a typical flight level is $\rho = 0.345331\text{kg}/\text{m}^3$.

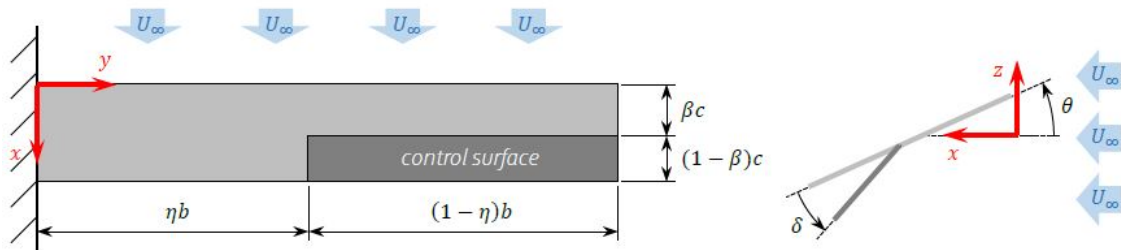


Figure 1: Wing

The wing has the following dimensions:

- $AR = 6$.
- $c = 400\text{mm}$.
- $GJ = 38\text{KNm}^2$
- the elastic axis is located at $0.35c$.

From these values and knowing that $AR = b^2/(c \cdot b)$ it is obtained that the total span $b = 2400\text{mm}$.

2 Divergence speed of the plate

From the structural point of view, our goal is to find the elastic twist angle, θ . When the elastic twist tends to infinite the divergence condition will be found, to do so, the lumped panel elements method has been used. The first step is to discretize the wing, the discretization is the same as it has been done in Problem 3.

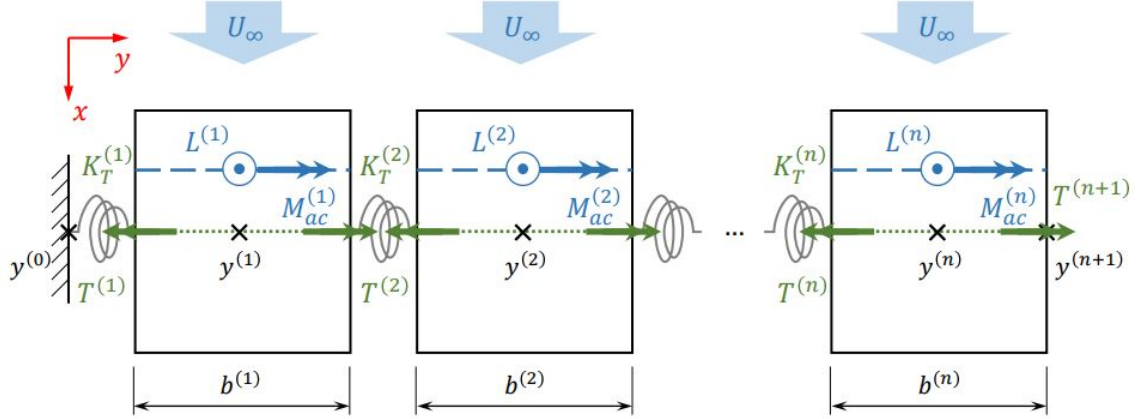


Figure 2: Wing discretization

Doing equilibrium of moments and using the procedure from pages 3 to 4 from problem 4 the next expressions can be found. It is important to notice that the lift is not constant and therefore we have two expressions of lift that can be expressed in the same line.

$$L(i) = q_\infty \cdot \frac{cb}{n} \cdot (C_{L\alpha}(\alpha_0 + \theta(i)) + C_{L\delta} \cdot \delta \cdot \phi(i)) \quad (1)$$

Where,

$$\phi(i) = \begin{cases} 1 & \text{if } 0 \leq i \leq \eta N \\ 0 & \text{if } \eta N \leq i \leq N \end{cases} \quad (2)$$

Introducing this into the equilibrium expression we can obtain the same expression as in Problem 3 page 5. As the term that depends on the deflection angle doesn't multiply the twist angle or structural stiffness the Q term becomes:

$$Q = q_\infty \frac{cbe}{n} \alpha_0 C_{L\alpha} + q_\infty \frac{cbe}{n} C_{L\delta} \delta + q_\infty \frac{c^2 b}{n} C_{mac\delta} \delta \quad (3)$$

And the general equation can be written as:

$$([K_s] - \hat{q}[K_a])\{\theta\} = \{Q\} \quad (4)$$

As the divergence condition $\det(K(\hat{q})) = 0$ doesn't depend on the Q matrix the divergence condition is the same as for a wing with no control surface.

$$q_D = \frac{\pi^2}{4b^2} \frac{GJ}{ceC_{l,\alpha}} = \frac{1}{2} \rho V_D^2 \quad (5)$$

Where V_D is the divergence speed of the plate. Isolating we can get:

$$V_D = \sqrt{\frac{2}{\rho} q_D} = 551.4 \text{ m/s} \quad (6)$$

3 Modes of the elastic twist

Finding the eigenvalues of equation 4 by doing the same procedure as in Problem 3 we can plot the results. Figure 3 shows the modes of the elastic twist, the X-axis shows the dimensionalized y position corresponding to the collocation points, the Y-axis represents the eigenvectors stored in the matrix. The Matlab code used is the same as the one used in class. As was expected, the results have a sinus and cosine behavior according to the analytical solution.

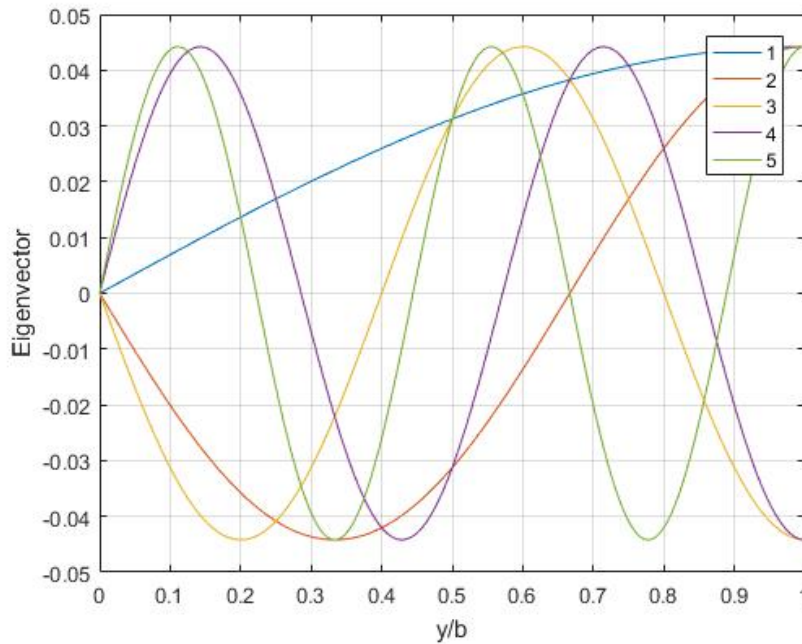


Figure 3: Wing discretisation

Each Eigenvector has an associated divergence speed.

- Mode 1: this is the lowest positive eigenvalue which is equal to 1, the associated divergence speed is the one obtained in the previous section which is 551.4 m/s.
- Mode 2: Eigenvalue = 9, $q_D = 9 \cdot \hat{q} \rightarrow V_D = 1.55e3$
- Mode 3: Eigenvalue = 25, $q_D = 25 \cdot \hat{q} \rightarrow V_D = 2.56e3$

- Mode 4: Eigenvalue = 49, $q_D = 49 \cdot \hat{q} \rightarrow V_D = 3.61e3$
- Mode 5: Eigenvalue = 84, $q_D = 84 \cdot \hat{q} \rightarrow V_D = 4.63e3$

4 Control surface reversal conditions

The control reversal gives the name to a situation in which an increase in the control surface's deflection angle δ causes the lift to decrease. Mathematically can be formulated as:

$$\frac{\partial L}{\partial \delta} = 0 \quad (7)$$

Reminding the obtained equation of the lift (equation 1) the partial derivative can be done:

$$\frac{\partial L}{\partial \delta} = 0 = q_\infty \cdot \frac{cb}{n} \cdot \left(C_{L\alpha} \frac{\partial}{\partial \delta} \{\theta\} + C_{L\delta} \cdot \phi(i) \right) \quad (8)$$

Here we have all the values except the elastic twist matrix which has to be derivated. The elastic, twist similarly as the previous section, can be obtained isolating it from the equation of equilibrium (equation 4).

$$\{\theta\} = \{Q\}([K_s] - q[K_a])^{-1} \quad (9)$$

Then,

$$\frac{\partial}{\partial \delta} \{\theta\} = \frac{\partial}{\partial \delta} \{Q\}([K_s] - q[K_a])^{-1} \quad (10)$$

Where,

$$\frac{\partial}{\partial \delta} \{Q\} = q_\infty \frac{cbe}{n} C_{L\delta} + q_\infty \frac{c^2b}{n} C_{mac\delta} = q_\infty \frac{cb}{n} (C_{L\delta}e + C_{mac\delta}c) \quad (11)$$

Introducing equation 11 into equation 10 and introducing it into equation 8 we can obtain the following expression:

$$\frac{\partial L}{\partial \delta} = q_\infty \cdot \frac{cb}{n} \left(C_{L\alpha} q_\infty \frac{cb}{n} (C_{L\delta}e + C_{mac\delta}c) \cdot ([K_s] - q[K_a])^{-1} + C_{L\delta} \cdot \phi(i) \right) = 0 \quad (12)$$

This equation is the beginning of a Matlab problem which I tried to solve but I couldn't do it. Form that equation and isolating q_R/q_D the control reversal function can be obtained, therefore, the velocities as a function of η .

5 Discussion

Control reversal can be avoided with high values of η , that'd mean reducing the control reversal surface. The same happens with the β values, closer to 1 the chances of having control reversal would be minimum. As a result, the negative pitching moment produced by the control surface would be reduced.

Finally comment that when we have $U_R/U_D < 0.5$ the deflection of the control surface will result in a decrease of the lift, which is the opposite of what we expect.

6 Personal thoughts

From my point of view, I think that all the workload, theory classes, and problems are well balanced. The best of having meet lessons is the support of the whiteboard, I think it's very useful to solve the problems and helps a lot. Theory classes are maybe too dense and the 3 hours are maybe too long and since there are so many equations in the slides you can be easily get lost. Regarding the problems solved in the class were very useful in order to understand the theory despite they can be very long or mathematically complicated. Regarding this assignment I personally regret choosing the assignment instead of the exam, it has happened the same as in all the subjects, the demanded level when we do exams online or project increases a lot. This assignment required mathematical skills with Matlab that I don't have and, with no chance of asking to you how to solve an equation, I couldn't finish it. Also, I found the mathematical development difficult as, in class, we didn't see how to get the reversal conditions of a wing. Doing a presencial exam I think I could have gotten a better result explaining the theory and solving a similar problem.

```

clear
close all

m = 0:1:10;

% Initialize variables

n = zeros(1,length(m)); %Number of elements/PANELS
e = zeros(1,length(m)); %Error

for i = 1:length(m)

    %number of panels
    n(i) = 2^m(i);

    %Initialize matrices
    Ks = zeros(n(i),n(i));
    Ka = eye(n(i),n(i)); %identity matrix
    k = (4*n(i)^2)/(pi^2); %constante

    %Stifness matrix coefficients
    for j=1:n(i) %loop for each pannel

        if (j==1)

            Ks(j,j) = k*3; %diagonal
            if(i>1)
                Ks(j,j+1) = -k*1;
            end

        elseif j==n(i)

            Ks(j,j) = k;
            Ks(j,j-1) = -k;

        else

            Ks(j,j) = 2*k;
            Ks(j,j-1) = -k;
            Ks(j,j+1) = -k;

        end

    end

    %Eigenvalues and eigenvalues
    [V,L] = eig(Ka\Ks);
    L = diag(L);
    L = L(L>0); %obtain the indices which value is positive, i
discard the negative
    qD = min(L); %this is non dimensionalized!!!

    %Error definition
    e(i) = abs(1-qD);

```

```

end

figure
loglog(n,e);
grid on
grid minor
box on
xlabel('Number of panels')
ylabel('Relative error')

%Defining collocation points to plot eigenvectors
y = [0, ((1:n(end))-1/2)/n(end),1]; %it is non diemsionalized; if we want
to give it a value
figure %we jut have to multiply by span,b
hold on
for i=1:5
    plot(y,[0;V(:,i);V(end,i)]); %Adding the boundary conditions
    %first row twist angle = 0 bcz wing root, at the end
    % V(end,i) bcz last co
end

box on
grid on
xlabel('y/b')
ylabel('Eigenvector')
legend('1','2','3','4','5');

%%

rho = 0.348331;
CLa= 2*pi;
GJ = 38000;
c = 400*10^-3;
AR = 6;
b = c*AR;
e = 0.35*c;
qD = (pi*pi*GJ)/(4*b*b*c*e*CLa);

for (i=1:5)

    qDdim = L(i)*qD;
    vel(i) = sqrt(2*qDdim/rho);

end

```



UNIVERSITAT POLITÈCNICA
DE CATALUNYA
BARCELONATECH

Msc. in Aeronautical Engineering

ADVANCES AEROELASTICITY

-Midterm Exam Assignment-

QT 2020-2021

ESEIAAT

17th of November 2020

Professor David Roca Cazorla

Author: C [REDACTED] N [REDACTED]

CONTROL SURFACE REVERSAL CONDITION FOR A WING

For the resolution of this assignment it was considered a flat plate on a wind tunnel clamped on one side and free on the other side, simulating a wing during flight condition. Bearing in mind these annotations it has been considered that it has an altitude of **10.000 m** which gives a density of **0.4127 kg/m³**. The problem refers to a plate rigidly attached to a control surface, its position and size are determined by the parameters η and β [see Fig. 1]. This term **rigid** is a relevant data which means conditions that relies on elastic properties can not be considered (i.e. in [lecture 2 slide 26] there is a specific expression determined for rigid bodies). This control surface can be deflected at an angle δ ($\delta > 0$ downwards) in order to increase the total lift on the plate. The aspect ratio of the plate is **AR = 6** and the chord size **c = 0.4 m**. The plate's effective stiffness to a torsional load is also given, $\overline{GJ} = 38.000 \text{ N}\cdot\text{m}^2$ (according to the theory from [lecture 3] G and J are recognized as Shear modulus of material and Geometrical parameter respectively) and its **elastic axis** is located at **0.35c** from the leading edge, **e = 0.14 m**.

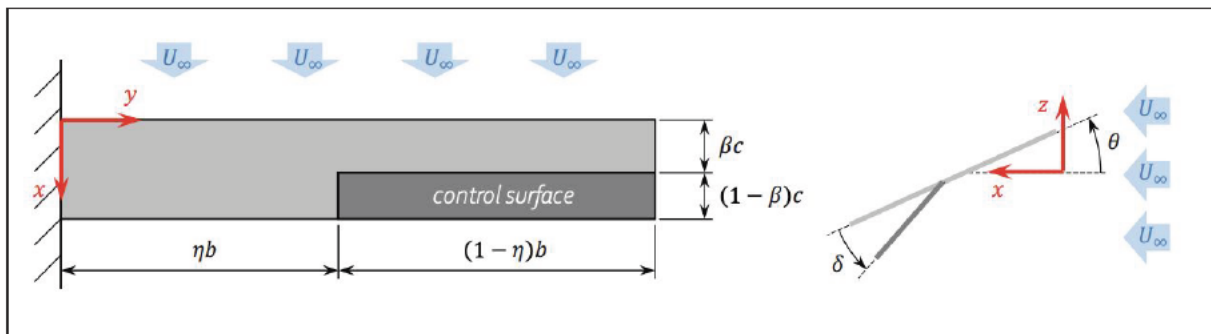


Figure 1

This problem is solved using lumped panel elements which means discretization of the plate/wing in terms of constant panels. A panel can be understood as an airfoil interconnected to each other through torsional spring [lecture 3]. The aim is to determine the position and size for the control surface and to do so, the information regarding the control surface reversal condition for different combinations of η and β is required.

a. *The Divergence speed U_D of the plate*

This part is solved following the procedure carried out in the problem 3 and as a first approximation the following equation has been developed, which means that the torsional spring between two panel is the difference between the elastic twist of two panels divided by the distance:

$$\frac{\theta^{(i)} - \theta^{(i-1)}}{y^{(i)} - y^{(i-1)}} = \frac{T^{(i)}}{GJ}$$

where:

$$T^{(i)} = K_T^{(i)} (\theta^{(i)} - \theta^{(i-1)}) = ct$$

Therefore:

$$K_T^{(i)} = \frac{GJ}{y^{(i)} - y^{(i-1)}} = ct$$

In this equation, T is identified as internal torque by the relative torsion between two panels and theory suggests to keep G and J constant values. From the previous expression, the torsional stiffness of spring is also obtained which is $K_T^{(i)}$. It is important to highlight that $K_T^{(1)}$ is not constant because the distance is not same as $K_T^{(2:N)}$, this condition is applied only at the root. Regarding the control points, it is required to add two extra nodes at root and tip (at the point internal torsional reaction is null).

Continuously the equilibrium over the elastic axis in each panel $i = \{1...n\}$ is applied [lecture 3]:

$$M_{ac}^{(i)} + L^{(i)}e^{(i)} - K_T^{(i)} (\theta^{(i)} - \theta^{(i-1)}) - K_T^{(i+1)} (\theta^{(i)} - \theta^{(i+1)}) = 0$$

according to the theory at $i=1$, $\theta^{(0)} = 0$ (fixed root):

$$M_{ac}^{(1)} + L^{(1)}e^{(1)} - K_T^{(1)}\theta^{(1)} - K_T^{(2)} (\theta^{(1)} - \theta^{(2)}) = 0$$

and for $i=n$ (point at which there is no torsional reaction), $T^{(n+1)} = 0$, $\theta^{(n+1)} = \theta^{(n)}$ (free tip):

$$M_{ac}^{(n)} + L^{(n)}e^{(n)} - K_T^{(n)} (\theta^{(n)} - \theta^{(n-1)}) = 0$$

Due to the presence of a control surface, the properties do not remain constant along the wing (from root to ηb the properties are constant and from this point to tip they differ, $1 - \eta b$) which leads to two slightly different lift expressions are obtained:

for constant properties $M_{ac}^{(i)} = 0$ ($C_{mac} = 0$):

$$L^{(i)} = q_\infty \frac{cb}{n} C_{L,d} (\alpha_0 + \theta^{(i)})$$

for non-constant properties, there is no sum up of θ with δ because of a rigid structure, not elastic:

$$L^{(i)} = q_\infty \frac{cb}{n} [C_{L,\alpha}(\alpha_0 + \theta^{(i)}) + C_{L,\delta}\delta]$$

$$C_{L,\alpha} = 2\pi$$

$$C_{L,\delta} = 6\pi \frac{1+\beta-2\beta^2}{3+4\beta(1-\beta)}$$

Recalling the general equation of moment:

for constant properties $M_{ac}^{(i)} = 0$:

$$-K_T^{(i)}\theta^{(i-1)} + (K_T^{(i)} + K_T^{(i+1)}) - q_\infty \frac{cb}{n} C_{L,\alpha} e^{(i)} \theta^{(i)} - K_T^{(i+1)}\theta^{(i+1)} = q_\infty \frac{cb}{n} C_{L,\alpha} \alpha_0$$

for non-constant properties:

$$M_{ac}^{(i)} + q_\infty \frac{cb}{n} C_{L,\alpha} e^{(i)} + q_\infty \frac{cb}{n} C_{L,\delta} e^{(i)} \delta = [-q_\infty \frac{cb}{n} C_{L,\alpha} e^{(i)} + K_T^{(i)} + K_T^{(i+1)}] \theta^{(i)} - K_T^{(i)} \theta^{(i+1)} - K_T^{(i+1)} \theta^{(i+1)}$$

following the procedure of problem 3 [lecture 3], it is proved that:

$$q_D = \frac{\pi^2}{4b^2} \frac{GJ}{ceC_{L,\alpha}} = \frac{\pi^2}{4(c*AR)^2} \frac{GJ}{ce2\pi}$$

$$U_D = \sqrt{\frac{2q_D}{\rho}} = 473.5 \text{ m/s}$$

- b. It is asked to plot the first five modes of the elastic twist associated to their corresponding divergence speeds:

In order to obtain the plot of figure 2 the boundary conditions explained previously have been set to "V" which stores eigenvectors. In the first row the twist angle is zero because it corresponds to the root and at the end an additional row is set because of a null torsional reaction which belongs to the wing tip.

The divergence speed is obtained computing q_D for the first five cases and they are: [473.49; 1420.5; 2367.5; 3314.4; 4261.4].

Observing the vector, the divergence speed calculated in the previous section can be located at the first position.

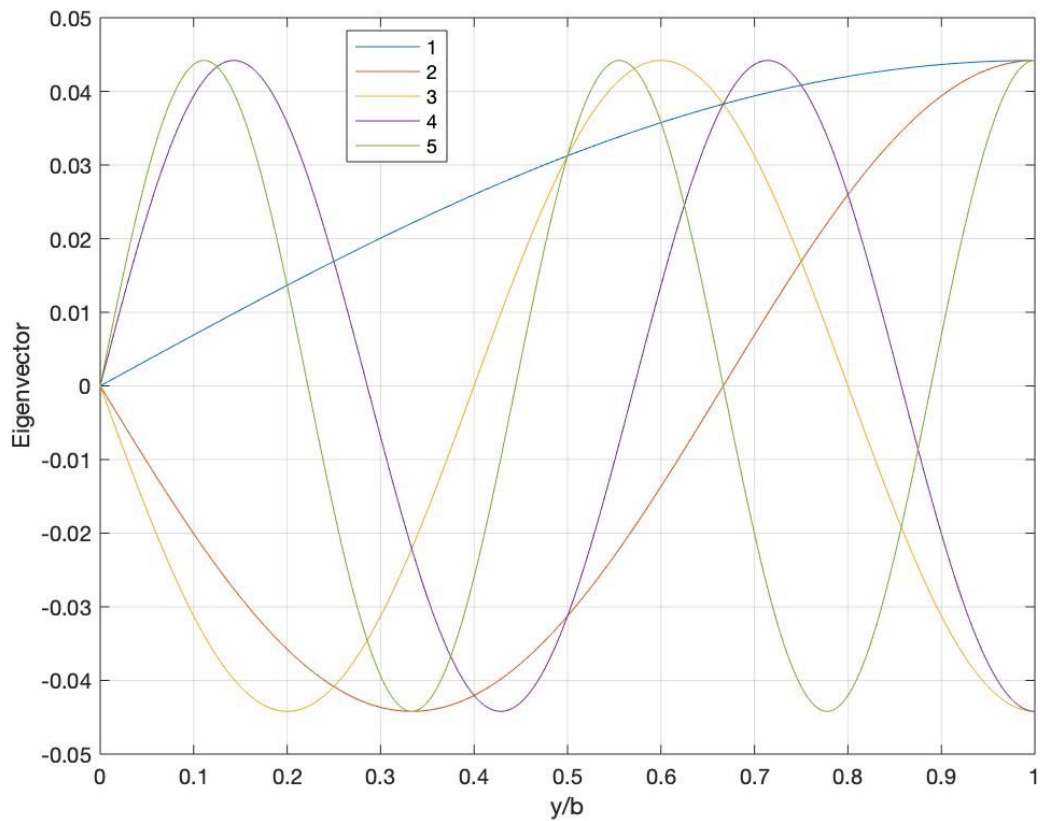


Figure 2: Eigenvector of first 5 modes of the elastic twist

Observing the figure 2 it can be seen that all of them have the same amplitude because of the matlab function “eig” that normalizes the values. Their shape resembles sinus or cosine and this is expected.

$$\theta_i = c1 \sin \left((2i-1) \frac{\pi}{2} \frac{y}{b} \right)$$

where “i” goes from 1 to 5 in this case and the term in blue marks the periodicity.

c. U_R/U_D vs η is requested in this section for $\beta = \{0.5, 0.6, 0.7, 0.8, 0.9\}$

The control surface reversal condition is as follows:

$$\frac{dl}{d\delta} = 0$$

$$L^{(i)} = q_\infty \frac{cb}{n} [C_{L,\alpha}(\alpha_0 + \theta^{(i)}) + C_{L,\delta}\delta\Phi]$$

$$\text{if } i \geq 0 \ \&\& \ i \leq \eta N$$

$$\Phi = 1$$

if $\eta < i \leq N$

$$\Phi = 0$$

deriving the expression of lift:

$$\frac{\partial L}{\partial \delta} = q_\infty \frac{cb}{n} [C_{L,\alpha} \frac{\partial \theta(i)}{\partial \delta} + C_{L,\delta} \Phi] = 0$$

Applying the equilibrium equation:

$$([K_s] - \hat{q} [K_a])\{Q\} = \{Q\}$$

$$\{Q\} = \{Q\}([K_s] - \hat{q} [K_a])^{-1}$$

$$\frac{\partial \theta(i)}{\partial \delta} = \frac{\partial Q}{\partial \delta} ([K_s] - \hat{q} [K_a])^{-1}$$

where force is:

$$Q = q_\infty \frac{cbe}{n} C_{L,\alpha} \alpha_0 + q_\infty \frac{cb}{n} C_{L,\delta} \Phi + q_\infty \frac{cbe}{n} C_{mac,\delta} \delta$$

$$\frac{\partial \{Q\}}{\partial \delta} = q_\infty \frac{cb}{n} (C_{L,\delta} e + c C_{mac,\delta} \delta)$$

$$\frac{\partial L}{\partial \delta} = q_\infty \frac{cb}{n} (C_{L,\alpha} q_\infty \frac{cbe}{n} (C_{L,\delta} e + c C_{mac,\delta} \delta) ([K_s] - \hat{q} [K_a])^{-1} + C_{L,\delta} \Phi) = 0$$

q_∞ has to be computed in matlab in order to obtain q_R so that U_R/U_D can be computed.

d. Discussion on the possible sets of values of β and η :

Surface control reversal conditions can be avoided when η is high or β is closer to 1, as a result the control reversal surface reduces. According to the theory [lecture 2] Control reversal gives name to a situation in which an increase on the control surface's deflection angle, δ , causes the lift to decrease therefore for the opposite case, control reversal would decrease.

Personal Opinion

Personally I find this subject really interesting which can be justified by my decision to select this speciality at first but I did not expect that the level that has been presented and required would be doubled by the professors. When you explain the concepts in class I more or less try to follow them and get to understand them at that moment but due to my insufficient level of background on this subject, things get really difficult for me to understand when solving problems on my own. My coding background is not that good either but I am able to compute, more or less, something that I understand well. I am not sure if the exam would have had the same level as this assignment or easier but sincerely, after studying the problems solved in the class I would be able to solve just the problems that are very similar to the ones solved in class because of my insufficient knowledge in this topic. In this assignment I have done my best, tried to understand some concepts relating one to another but I am not pretty satisfied with what I am presenting. I could do better if I had better knowledge. Regardless of having five or six more assignments for this week, I dedicated a lot of time giving my best to solve this assignment. I also realized that the colleagues who graduated from ESEIAAT, were able to solve the problem probably they had done similar assignments back then. The fact that they have more knowledge about aeroelasticity thanks to the subjects taught in graduation made me feel bad because I could not. The planning of this master's course says everybody is welcome to join this course but once I was in, many professors said this master course is designed for ESEIAAT students. I feel like they are not considering students from other universities. Everyone is here because they are interested in learning more but it will never happen without a little support from part of the professors.

ADVANCED AEROLASTICITY

Control surface reversal condition for a wing

Name: J [redacted] O [redacted]
Assignment: (Mid-term Exam)

Due Date: November 17, 2020

Problem

As a first approach to solve the problem, I have decided to model the wing by two elastically connected surfaces (lumped panels), as shown in the following figure;

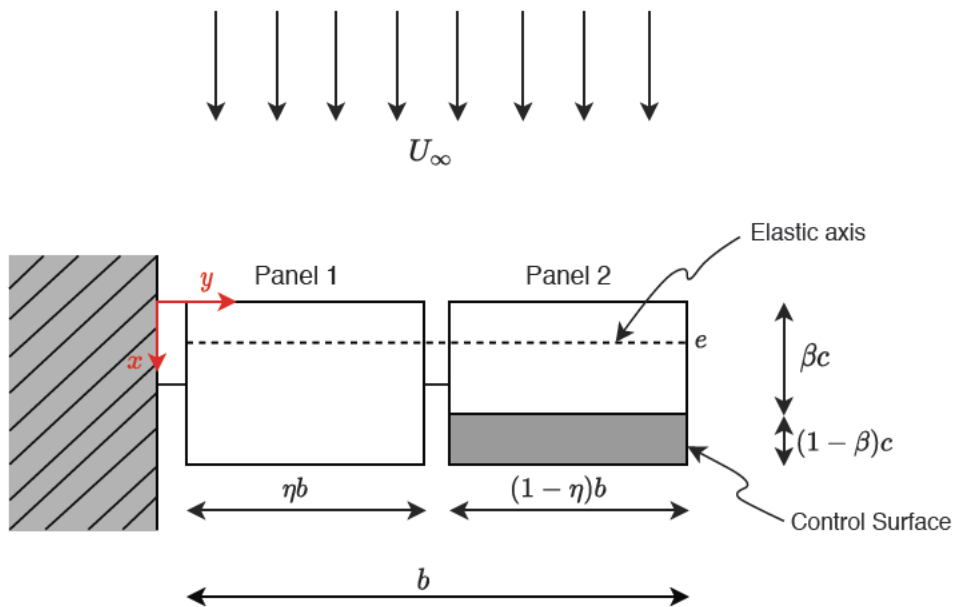


Figure 1: Wing with aileron panel discretization

Note that the surface of each panel is different as they are dependent of η . The gaps between panels are negligible and the torsional spring constants are equal to K_T (for this simplified example). Also, as we are solving a flat plate we assume thin airfoil theory and incompressible flow.

The free body diagram of our idealized wing is the following:

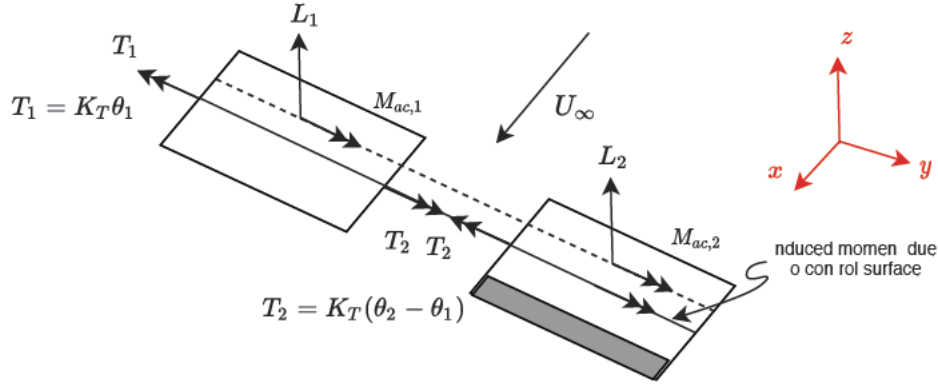


Figure 2: Wing free body diagram

Where the aerodynamic forces acting on each panel are:

$$L_1 = q_\infty S C l_\alpha (\alpha_o + \theta_1) \quad (1)$$

$$L_2 = q_\infty S C l_\alpha (\alpha_o + \theta_2) + q_\infty S C l_\delta (\delta_o) \quad (2)$$

Focusing on the panel with a control surface, it is important to take into account the value of β as it has a dependence on the value of $C_{l,\delta}$ and $C_{m,\delta}$.

This problem has been already solved in class and the results obtained are the following:

$$C_{l,\alpha} = 2\pi \quad (3)$$

$$C_{l,\delta} = 2\pi \frac{\beta-1}{2\beta+1} \quad (4)$$

$$C_{m,\delta} = 3\pi\beta \frac{\beta-1}{4\beta+2} \quad (5)$$

$$(6)$$

Now we can sum moments about the elastic axis for each panel

$$\sum M_1 = 0 = L_1 e + K_T(\theta_2 - \theta_1) - K_T \theta_1 \quad (7)$$

$$\sum M_2 = 0 = L_2 e + K_T(\theta_2 - \theta_1) + q_\infty S c C_{M,\delta} \delta_o \quad (8)$$

substituting equations (1) and (2) into (3) and (4) respectively:

$$5K_T \theta_1 - 2K_T \theta_2 = q_\infty S C l_\alpha (\alpha_o + \theta_1) \quad (9)$$

$$-2K_T \theta_1 + 2K_T \theta_2 = q_\infty S C l_\alpha (\alpha_o + \theta_2) + q_\infty S C l_\delta (\delta_o) \quad (10)$$

This set of equations written in matrix form is:

$$K_T \begin{bmatrix} 5 & -2 \\ -2 & 2 \end{bmatrix} \begin{bmatrix} \theta_1 \\ \theta_2 \end{bmatrix} - \gamma \begin{bmatrix} 1 & 0 \\ 0 & 1 \end{bmatrix} \begin{bmatrix} \theta_1 \\ \theta_2 \end{bmatrix} = \gamma \begin{bmatrix} 1 \\ 1 \end{bmatrix} \alpha_o + \gamma \left(\frac{C_{l,\delta}}{C_{l,\alpha}} + \frac{c}{e} \frac{C_{m,\delta}}{C_{l,\alpha}} \right) \begin{bmatrix} 0 \\ 1 \end{bmatrix} \delta_o \quad (11)$$

where $\gamma = q_{\text{inf}} S e C_{l,\alpha}$.

Dividing both sides of the equation by K_T and defining an arbitrary non dimensional parameter \bar{q} as

$$\bar{q} = \frac{\gamma}{K_T} = \frac{q_{\text{inf}} S e C_{l,\alpha}}{K_T} \quad (12)$$

the system becomes:

$$\begin{bmatrix} 5 & -2 \\ -2 & 2 \end{bmatrix} \begin{bmatrix} \theta_1 \\ \theta_2 \end{bmatrix} - \bar{q} \begin{bmatrix} 1 & 0 \\ 0 & 1 \end{bmatrix} \begin{bmatrix} \theta_1 \\ \theta_2 \end{bmatrix} = \bar{q} \begin{bmatrix} 1 \\ 1 \end{bmatrix} \alpha_o + \bar{q} \left(\frac{C_{l,\delta}}{C_{l,\alpha}} + \frac{c}{e} \frac{C_{m,\delta}}{C_{l,\alpha}} \right) \begin{bmatrix} 0 \\ 1 \end{bmatrix} \delta_o \quad (13)$$

We note that all the values of the problem are constant, α_o and δ_o are inputs, independent of θ_1 and θ_2 .

Lets consider the following notation for the previous equation:

$$[[K_S] - \bar{q}[K_A]] \begin{bmatrix} \theta_1 \\ \theta_2 \end{bmatrix} = \begin{bmatrix} Q_1 \\ Q_2 \end{bmatrix} \quad (14)$$

where $[Q_i]$ are input loads and $[\theta_i]$ the wing deformed system equilibrium state vector. If we also add the following assumption

$$\begin{bmatrix} \theta_1 \\ \theta_2 \end{bmatrix} = \begin{bmatrix} \theta_1^S \\ \theta_2^S \end{bmatrix} + \begin{bmatrix} \delta\theta_1 \\ \delta\theta_2 \end{bmatrix} \quad (15)$$

where $[\delta\theta_i]$ is the vector of perturbation twist angles, the equation in (13) can be rewritten as follows for the existence of the perturbed equilibrium state

$$[K_{ij}^-] \{\delta\theta_i\} = Q_j - [K_{ij}^-] \{\theta_j^S\} = \{0\} \quad (16)$$

To satisfy the previous requirement, we need that the determinant of the stiffness matrix become equal to zero. Regarding our simplification of the problem, the determinant of the stiffness matrix is

$$\nabla ([K_S] - \bar{q}[K_A]) = \bar{q}^2 - 3\bar{q} + 1 \quad (17)$$

The divergence condition then is obtained when computing the roots of this characteristic equation. In this case: $\bar{q}_D = 0.382$ and $\bar{q}_D = 2.618$.

Here we interpret this roots as the eigenvalues of the problem and the smaller one is the nondimensional divergence dynamic pressure.

1 Problem discretization

Now lets consider that instead of having two panels we have a succession of n panels to idealize the wing.

$$V_d = \sqrt{\frac{2q_D}{\rho}} \quad (21)$$

For our case, considering that $\rho = 1.255 \text{ kg/m}^3$, the divergence velocity obtained for in-compressible flow is:

$$V_D = 357.6 \text{ m/s}$$

3 Twist angle configurations

Once we have obtained the \bar{q} values, a plot of the twist angle distribution along the entire wing can be computed for the divergence dynamic pressures. I have considered here that the outer half part of the wing has control surfaces and the other one does not. Also, we suppose that the aileron is the 30% of the total chord in order to compute the different coefficients (then $\eta = 0.5$, $\beta = 0.7$ and 100 panels). The results obtained are the following:

The solution for the system eigen-vectors is:

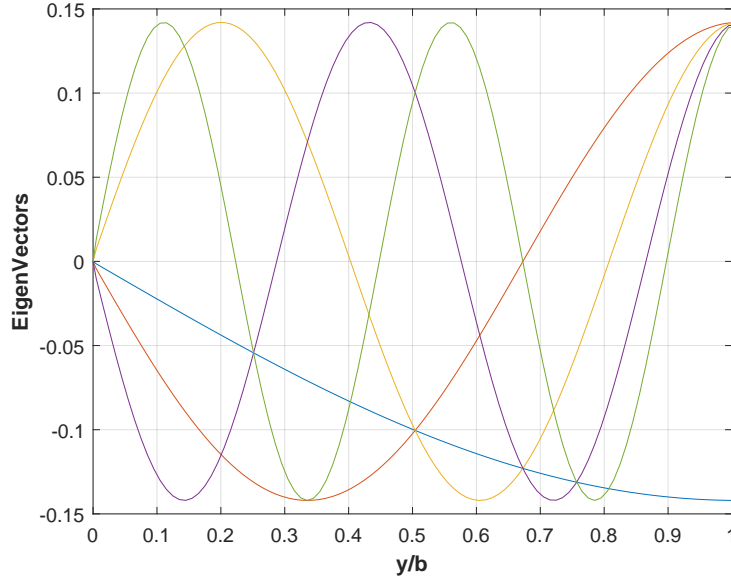


Figure 4: First 5 modes of the elastic twist associated

And the twist distribution along the wing (solving system in Eq. 13 for the divergence) is for the first 5 conditions of divergence:

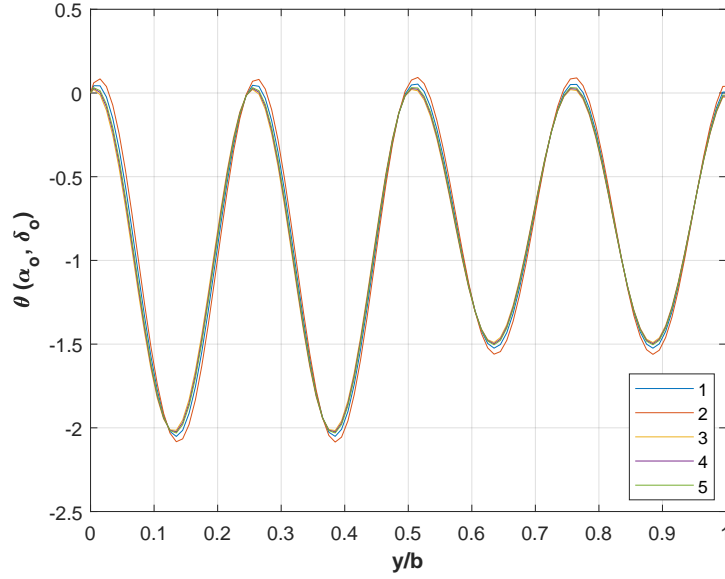


Figure 5: Twist distribution along the wing

We can see that as we do not have a wing with constant properties, the twist angle has greater oscillations in the control surface part of the wing.

At this point it is important to mention that the accuracy of the results is directly influenced by the number of panels selected. The velocity obtained is considering 100 panels. Considering less, the error on the divergence dynamic pressure will be higher and then the velocity will not be accurate.

4 Reversal velocity

The total lift generated by the wing is

$$L_{flex} = \sum L_i = f(\theta_i, \alpha_o \delta_o) \quad (22)$$

As the purpose of the aileron is to generate lift, the reversal condition then will happen when this L_{flex} becomes zero.

$$L_{flex} = L_1 + L_2 = qSC_{L_\alpha} (\theta_1 + \theta_2) + qSC_{L_\delta} \delta_o \quad (23)$$

where the twist angle is a function of \bar{q} .

Then, computing the values of θ_i as a function of \bar{q} we can find a new polynomial with the same order as panels and we will just repeat the procedure done for the divergence dynamic pressure. Which means, finding the non-dimensional dynamic pressure that makes the total lift be equal to zero and compute the corresponding reversal speed using equation (20). For the simple example of two surfaces:

Until now, I will consider only 10 panels in order to make the calculation process of the total lift. This is due to the use of symbolic variables inside matrices, and the manipulations of them is so slow.

5 Reversal vs Divergence velocity

Following the previous procedure to compute the control reversal condition for the aileron, the following results have been obtained for different configurations of η and β :

We can note that for a given value of β , as we increase the area of the wing without control surface, the reversal speed becomes greater and those the U_R/U_D factor. This is normal because we are reducing the aileron area and then its influence over the wing reversal condition.

Also we see that as we increase of β , the U_R/U_D factor value becomes smaller. this is due to the same reason as before, the aileron is smaller.

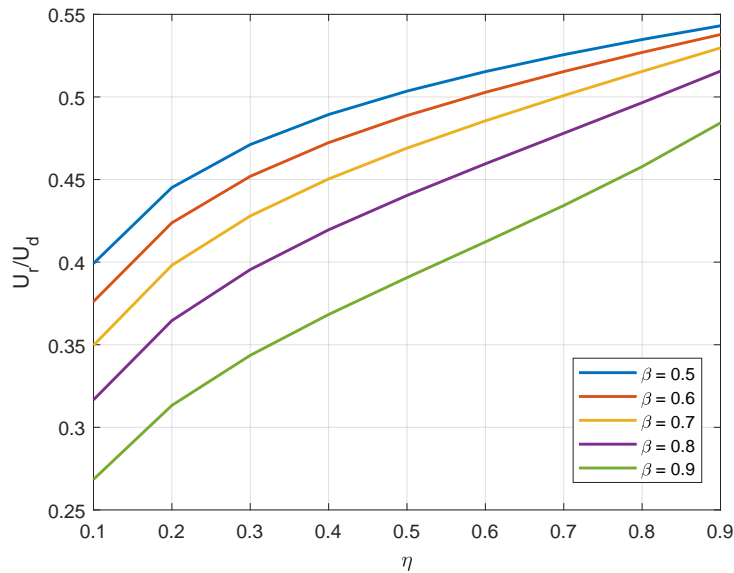


Figure 6: Twist distribution along the wing

6 Discussion

6.1 Avoid reversal

Between the low speed range where the aileron works as intended and the high speed range there is one speed point where the rolling moments of the aileron and the wing twist cancel each other out. There is where reversal occurs. To avoid this we can set the speed at which full aileron deflection produces only a quarter of the rolling moment coefficient as we will never exceed speed. In terms of η and β , a trivial solution is to consider that we do not have a control surface, which means $\eta = 1$ and $\beta = 1$.

6.2 $U_R/U_D > 0.5$

From the plot in figure 7, this condition is achieved for:

- values of β bigger than 0.5 but minor than 0.9.
- values of η bigger than 0.5 (aprox) and minor than 0.85

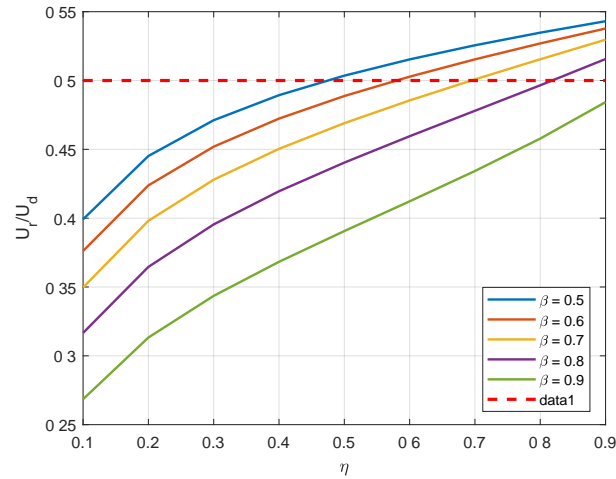


Figure 7: Twist distribution along the wing

7 Feedback

In general I consider that this exercise has been very complete and much of what was learned in class has been addressed. Also, I think that the Master is to enjoy it, we are tired of exams. I am very satisfied with the result and although I know that I am using a bad method to calculate the reversal speed, I hope we correct the exercise in class.

Regarding the content of the subject, I think it is very balanced and what is expected is obtained from it.



UNIVERSITAT POLITÈCNICA DE CATALUNYA
BARCELONATECH

Escola Superior d'Enginyeries Industrial,
Aeroespacial i Audiovisual de Terrassa

Control surface reversal condition for a wing

MUEA

Advanced Aeroelasticity

B [REDACTED], I [REDACTED]

UPC ESEIAAT

17th November of 2020

Contents

1	Introduction	2
2	Divergence speed U_D of the plate	3
3	First 5 modes of the elastic twist and their divergence speeds	4
4	Plot of U_R/U_D for different values of η and β	5
5	Discussion of the sets of values of β and η	8

1 Introduction

A flat plate on a wind tunnel clamped on one side and free on the other will be considered, simulating a wing during flight conditions. The plate has a rigidly attached control surface, the position and size of which are determined by the parameters η and β , as depicted in Figure 1. This control surface can be deflected an angle δ ($\delta > 0$ downwards) in order to increase the total lift on the plate. The plate has an aspect ratio $AR = 6$ and the chord size is $c = 400mm$. From a structural test, it has been determined that the plate's effective stiffness to a torsional load is $\overline{GJ} = 38kNm^2$ and its elastic axis is located at $0.35c$ from the leading edge.

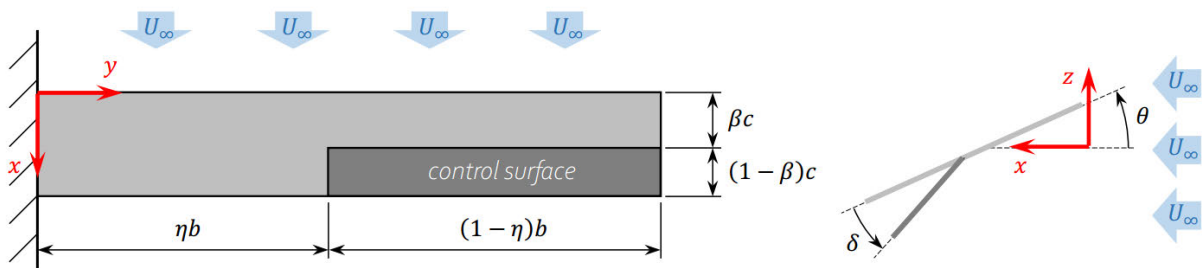


Figure 1: Description of the problem.

The objective is to determine a position and size for the control surface and, to do so, we require information regarding the control surface reversal condition for different combinations of β and η . For this study, lumped panel elements will be used to discretize the plate, assuming their section satisfies the requirements for thin airfoil theory. All angles will be assumed small.

It is understood that this report complements the lectures. This means that the report will contain the explanation of why procedures already done in the lectures are being used but they will not be explained. Some definitions used in the report are referenced to the page of the lecture where they belong but will not be explicitly defined.

2 Divergence speed U_D of the plate

The plate will be discretized in N equal sized panels as described in *Session 3* (slides from 3 to 7) and *Problem 3*, see Figure 2. As for constant properties each panel will have equal effective stiffness and geometry, $c = 0.4m$ width = b/Nm . The non constant property will be that those panels in a position where $y > \eta b$ will be considered as an airfoil with a control surface deflected in an angle δ . $\alpha_0 = 0$ will be considered for the whole problem.

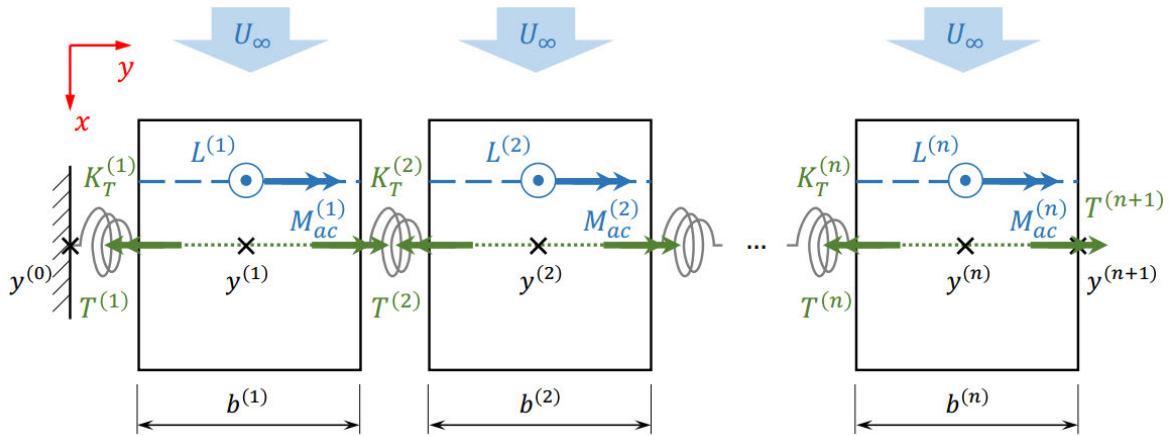


Figure 2: Discretization model.

The divergence speed can be obtained from the homogeneous form of the equilibrium of moments equation for each panel of the wing as seen in *Problem 3*. The divergence speed will be the one corresponding to the dynamic pressure of the first eigenvalue. The equilibrium of moments equation is solved as a system with the structural stiffness term (K_s) and the aerodynamic stiffness term (K_a) multiplying the matrix of θ and the input aerodynamic load (Q) as RHS. The existence of a control surface in some of the panels affects only the RHS because the lift and momentum generated by its deflection do not depend on θ . For this reason the procedure to find the eigenvalues will be the one described in *Problem 3*.

As the first eigenvalue is the non-dimensional form of the divergence dynamic pressure (\hat{q}_D) it is necessary to multiply it by q_{Da} , the analytical solution for the divergence condition mentioned in slide 1 of *Problem 3*, to obtain q_D because it is the one used to nondimensionalize. It is assumed that $\rho = 1.225kg/m^3$. $C_{l,\alpha} = 2\pi$, as seen in *Problem 1*.

$$u_D = \sqrt{\frac{2 \cdot \hat{q}_D \cdot q_{Da}}{\rho}} = 514.159m/s \quad (1)$$

3 First 5 modes of the elastic twist and their divergence speeds

In Section 2 we have calculated the smallest divergence speed choosing the first eigenvalue. The next 4 eigenvalues have already been calculated in the process, with their corresponding eigenvectors. The process to calculate the divergence speed of these modes is the same (Equation 1).

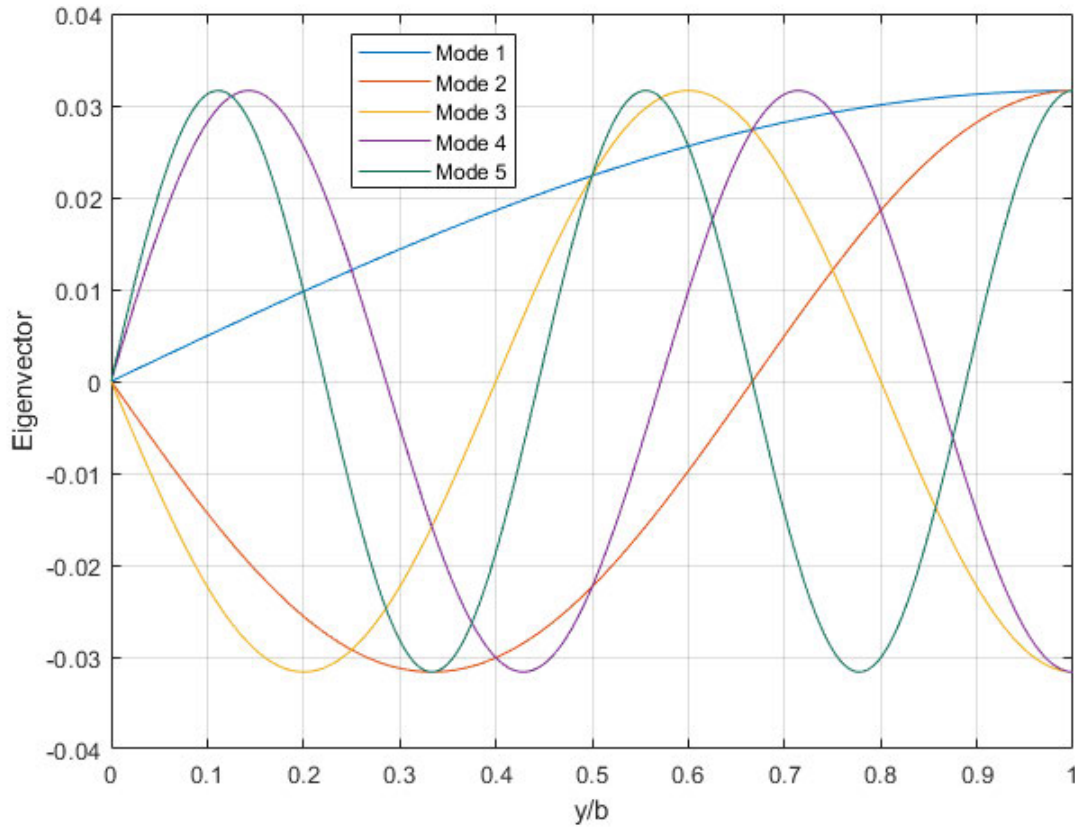


Figure 3: First 5 modes of the elastic twist.

The divergence speeds for these modes are in Table 1.

Mode	Mode 1	Mode 2	Mode 3	Mode 4	Mode 5
Divergence speed [m/s]	514.16	1542.47	2570.79	3599.11	4627.43

Table 1: Divergence speeds.

4 Plot of U_R/U_D for different values of η and β

In order to find the speed for control reversal conditions it is necessary to solve the system imposing control reversal condition. This means that the q_∞ of the equation will be q_R and one of the unknowns of the problem. Having N θ s as unknowns of the problem and N equations we need to add another equation to the system. According to the slides of *Session 2* (pages 4-7), control reversal condition for an airfoil can be written in the following way.

$$\frac{dl}{d\delta} = 0 \quad (2)$$

If we imagine that the plate presented in the problem represents an airplane wing with an aileron, and imagining there would be an equal plate on the other side with an aileron working in the opposite direction, control reversal condition for the airplane would occur when the total lift of the plate becomes smaller with a positive deflection of δ . For this reason, it is logical to think that the control reversal condition asked for the whole plate is the one that occurs when the derivative of the total lift of the plate with respect to δ meets the same condition as the control reversal condition for an airfoil.

$$\frac{dL}{d\delta} = 0 \quad (3)$$

Adding this condition, the number of unknowns equals the number of equations. The total lift of the plate can be calculated as the sum of the lift generated by every panel, and, as the derivative of the sum of two functions is equal to the sum of their derivatives, Equation 3 can be written as follows.

$$\frac{d \sum_{n=1}^{n=N} l^{(n)}}{d\delta} = \sum_{n=1}^{n=N} \frac{dl^{(n)}}{d\delta} = 0 \quad (4)$$

To calculate the aerodynamic coefficients of every panel the results of *Problem 1* will be used. The following equations represent the contribution to the lift of a panel without aileron (Equation 5) and a panel with aileron (Equation 6).

$$l_{flat}^{(n)} = q_R \frac{cb}{N} C_{l,\alpha} \theta^{(n)} \quad (5)$$

$$l_{aileron}^{(n)} = q_R \frac{cb}{N} C_{l,\alpha} \theta^{(n)} + C_{l,\delta} \quad (6)$$

The derivatives of these equations need to be used for Equation 4.

$$\frac{dl_{flat}^{(n)}}{d\delta} = q_R \frac{cb}{N} C_{l,\alpha} \frac{d\theta^{(n)}}{d\delta} \quad (7)$$

$$\frac{dl_{aileron}^{(n)}}{d\delta} = q_R \frac{cb}{N} C_{l,\alpha} \frac{d\theta^{(n)}}{d\delta} + C_{l,\delta} \delta \quad (8)$$

$$\underbrace{\left(K_T \begin{bmatrix} \beta^{(1)} + \beta^{(2)} & -\beta^{(2)} \\ -\beta^{(2)} & \beta^{(2)} \end{bmatrix} \right)}_{\mathbf{K}_s \text{ Structural stiffness}} - \underbrace{q_\infty S e C_{L,\alpha} \begin{bmatrix} 1 & 0 \\ 0 & 1 \end{bmatrix}}_{\mathbf{K}_a \text{ Aerodynamic stiffness}} \underbrace{\begin{Bmatrix} \theta^{(1)} \\ \theta^{(2)} \end{Bmatrix}}_{\mathbf{f}_a \text{ Input aerodynamic load}} = q_\infty S e C_{L,\alpha} \alpha_0 \begin{Bmatrix} 1 \\ 1 \end{Bmatrix}$$

Figure 4: Simplified system of equations for a lumped panel elements problem (constant properties), useful to visualize the problem.

To solve the problem it is necessary to obtain the derivative of θ with respect to δ from the system of equations. With this objective the system of the equilibrium of moments mentioned in Section 2 is derived with respect to δ . The structural stiffness term (K_s) and the aerodynamic stiffness term (K_a) do not depend on δ , so they stay equal. The matrix of θ will turn into a matrix of θ derived with respect to δ and the input aerodynamic load (Q) will remain as follows.

$$RHS_{flat} = 0 \quad (9)$$

$$RHS_{aileron} = M_{ac,\delta} + L(\delta)e_\delta \quad (10)$$

Equation 9 refers to the RHS of the equations of the system corresponding to panels without aileron, while Equation 10 is the RHS of the equations for the panels with aileron. If the RHS is 0 for the panels without aileron, $d\theta/d\delta = 0$. So panels without aileron will not contribute to Equation 3.

$$\frac{dl_{flat}^{(n)}}{d\delta} = 0 \quad (11)$$

In Equation 10, $L(\delta)$ is the contribution to the lift that is multiplied by delta and e_δ is the distance between the aerodynamic center of the aileron and the shear center of the plate. Substituting the values and nondimensionalizing, the RHS of the momentum equation would be the following.

$$R\hat{H}S = \frac{\hat{q}_R e_{\delta}}{C_{l,\alpha} e} C_{l,\delta} \delta + \frac{\hat{q}_R c}{C_{l,\alpha} e} C_{mac,\delta} \delta \quad (12)$$

Where \hat{q}_R is q_R/q_D . And deriving with respect to delta we obtain the following.

$$\frac{d\hat{Q}}{d\delta} = \frac{\hat{q}_R e_{\delta}}{C_{l,\alpha} e} C_{l,\delta} + \frac{\hat{q}_R c}{C_{l,\alpha} e} C_{mac,\delta} \quad (13)$$

The procedure to find the u_R now is to isolate the variable matrix of $d\theta^{(n)}/d\delta$ of the system and introduce it into Equation 4 to iterate around different values of q_R until control reversal condition is met. This process is repeated for a series of β and η to obtain the following graph.

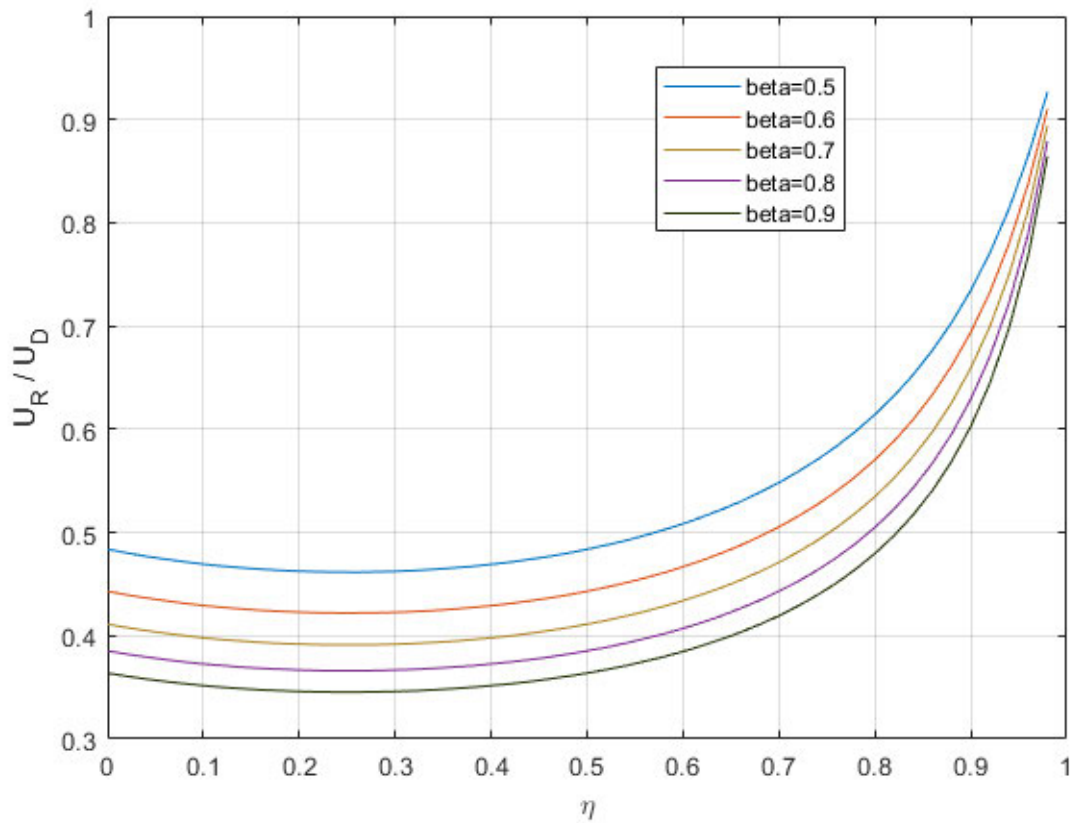


Figure 5: U_R/U_D vs. η for $\beta = \{0.5, 0.6, 0.7, 0.8, 0.9\}$

5 Discussion of the sets of values of β and η

As it can be seen in Figure 5 the shape of an aileron can significantly affect the point where control reversal starts to happen. The plot can be read choosing a β curve and, if the U/U_D is situated under the curve, control reversal is not happening. If the speed is higher, the lift decreases when deflecting the aileron and control is reverted.

It can be seen that the higher the β , the smaller the U_R needed for control reversal to happen. A high β means a thin aileron and a bigger distance between the application point of $L(\delta)$ and the shear center line. So, according to Figure 5, thin ailerons reach control reversal earlier.

As for the dependence on η , the bigger it is the smaller is the aileron. If an aileron is very small the U_R goes to infinite. The bigger the aileron is, the bigger its lift, and the momentum decreasing the aerodynamic moment of the wing, making control reversal happen earlier (U_R decreases). When the aileron is so big that gets very close to the embedding, the stiffness of the wing does not allow the area near it to bend so much, so the aileron starts contributing to the lift with less reduction of θ .

In order to avoid control reversal conditions, the best option would be having no aileron or a very small one. In this case U_R could even be over U_D , making control reversal not possible. Of course, it would make no sense because the objective of having an aileron is to have control over the lift generated. The most feasible options would be when the control reversal speed is the highest but with a reasonable size for the aileron. According to Figure 5, the most suitable values of β would be between 0.5 and 0.8, and of η between 0.6 and 0.85.

Another solution that can be considered to avoid control reversal conditions in flying conditions where the speed is near U_R is to avoid the use of control surfaces near the edge of the wing and use other control surfaces located near the embedding, so the stiffness of the wing prevents the decrease of θ . Increasing the stiffness of the wing can help avoid control reversal too.

U_R/U_D is greater than 0.5 for all the β represented when $\eta > 0.85$. It can be seen in Figure 5 where the curves from the different β cross $U_R/U_D > 0.5$.

ESEIAAT



UNIVERSITAT POLITÈCNICA DE CATALUNYA
BARCELONATECH

Escola Superior d'Enginyeries Industrial,
Aeroespacial i Audiovisual de Terrassa

Partial Exam Advanced Aeroelasticity

Report

Degree: Aerospace Engineering MSc (MUEA)

Subject: 220351-Advanced Aeroelasticity

Delivery date: 17/11/2020

Student: E ■ E ■■■■■■

Professor: David Roca Cazorla

1 Problem definition

Consider a flat plate on a wind tunnel clamped on one side and free on the other, simulating a wing during flight conditions. The plate has a rigidly attached control surface, the position and size of which are determined by the parameters η and β , as depicted in Fig. 2. This control surface can be deflected an angle δ (being $\delta > 0$ downwards) in order to increase the total lift on the plate. The plate has an aspect ratio $AR = 6$, and the chord size is $c = 400\text{mm}$. From a structural test, it has been determined that the plate's effective stiffness to a torsional load is $\bar{G}J = 38\text{ kN} \cdot \text{m}^2$ and its elastic axis is located at $0.35c$ from the leading edge.

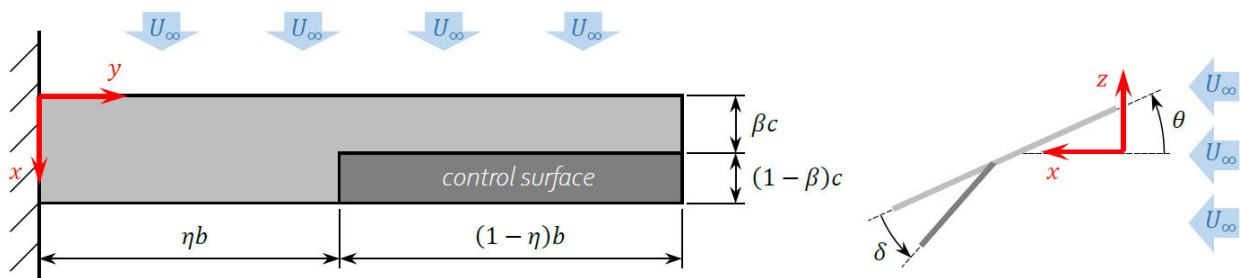


Figure 1: Problem definition. Source: [3]

1.1 Hypotheses

Before writing the equations and drawings applicable to this problem, it is necessary to define the hypotheses that will be assumed during the resolution of this exercise:

Geometrical

- Flat plates
- Small angles $\alpha \ll 1$
- No geometrical torsion by design ($\alpha_{0=0}$)
- $\alpha = \theta + \alpha_0 \rightarrow 0$
- $\delta = ct.$ across all control surface span

Aerodynamic

- Potential incompressible flow (no viscous effects)
- TAT (Thin Airfoil Theory) applicable
- Lift at each section $L(i)$ independent of surrounding panels
- Discretization of wing into N lumped elements

Structural

- Control surface rigidly attached to the wing
- Torsional stiffness $\bar{G}J$ and elastic axis position e are constant across all span

2 Analytical development

2.1 Aerodynamic Coefficients

Before solving the divergence or control reversal problem, it is necessary to define the aerodynamic modellization of the wing. Because we've assumed that lift at each section is completely independent of surrounding areas (which is not true for Prandtl's lifting line theory!), we can compute aerodynamic coefficients for a generic section with control surface:

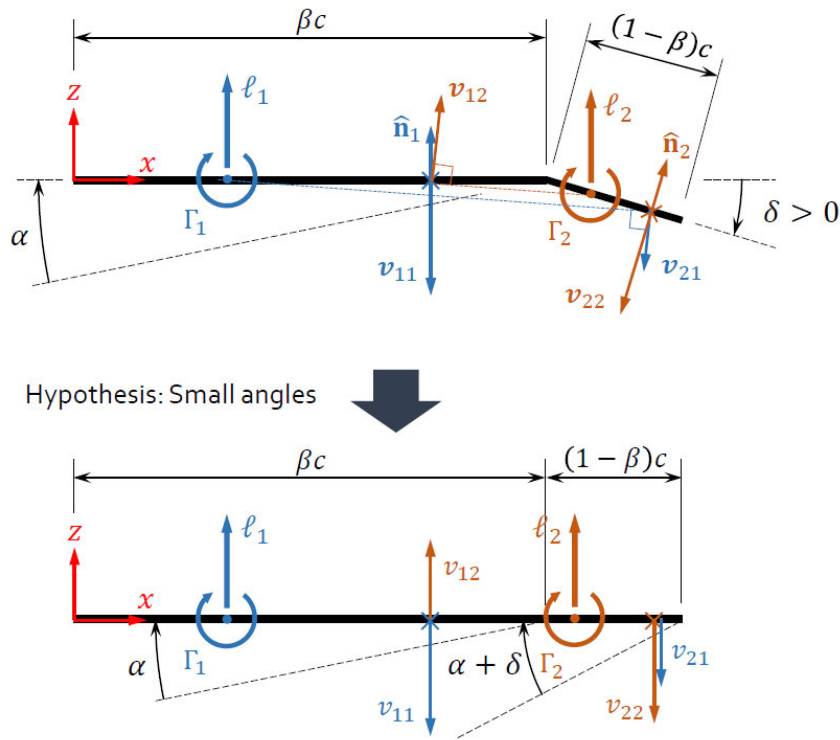


Figure 2: Aerodynamic forces in an generic airfoil with control surface. Source: [1]

The procedure presented in Problem 1-Divergence of an airfoil [1] is here used to retrieve the aerodynamic coefficients of an airfoil with control surface:

$$l = \frac{1}{2} \rho_{\infty} u_{\infty}^2 c \cdot (C_{l, \alpha} \cdot \theta + C_{l, \delta} \cdot \delta) \quad (2.1)$$

$$C_{l, \alpha} = 2\pi \quad (2.2)$$

$$C_{l, \delta} = 2\pi \cdot \frac{3(2\beta + 1) \cdot (1 - \beta)}{3 + 4\beta \cdot (1 - \beta)} \quad (2.3)$$

The aerodynamic center is located at:

$$x_{AC} = \frac{c}{4} \quad (2.4)$$

And the moment about the aerodynamic center only depends on δ , due to the fact airfoil is a simple flat plate with control surface:

$$C_{mac, \delta} = \frac{-3\pi}{2} \cdot \beta \cdot \frac{1 + \beta - 2\beta^2}{3 + 4\beta \cdot (1 - \beta)} \quad (2.5)$$

2.2 Lumped Elements Discretization

The presented wing in Fig. 2 is divided into a total of N lumped panels. Because of the presence of control surface, which can start at an arbitrary span on the wing, panels have been discretized into 2 zones, each of them with uniform spacing. First zone with N_1 panels is the one without control surface; while the second zone with control surface is divided into N_2 panels.

In case a uniform spacing was used for all wing span, panels might not fit with the edges of control surface; so it has been decided to split discretization into 2 zones. In any case, total number of panels N is preserved:

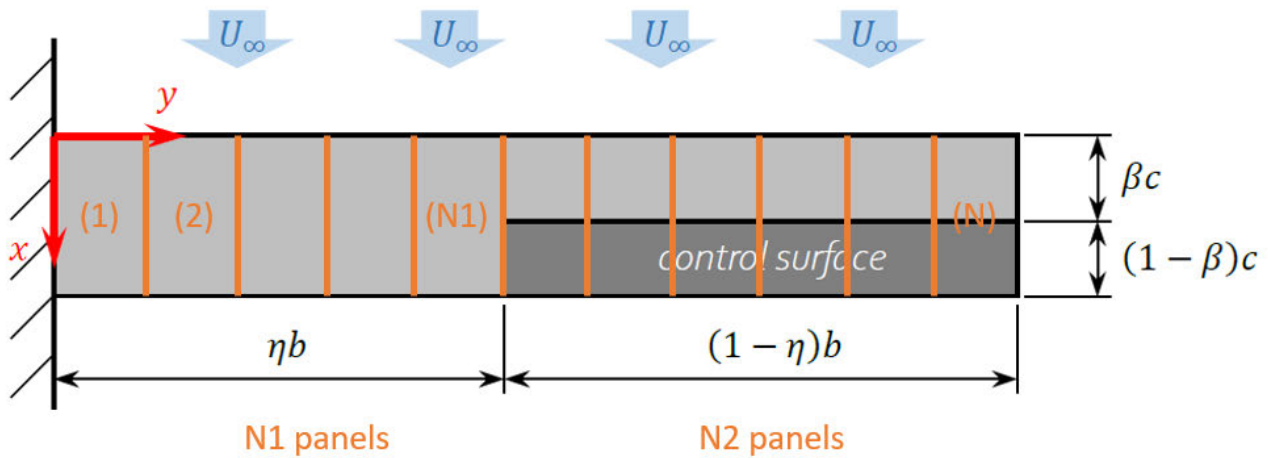


Figure 3: Wing panels discretization

The discretization of wing's semispan into these lumped panels leads to a numerical approximation to the physical problem, in which external forces such as lift are applied each of the finite N panels, while consecutive panels are joint with an equivalent stiffness torsional spring.

Mind that because we're only interested in divergence and control reversal phenomena, studied stiffness is only torsional, so no bending/plunging movement will be studied.

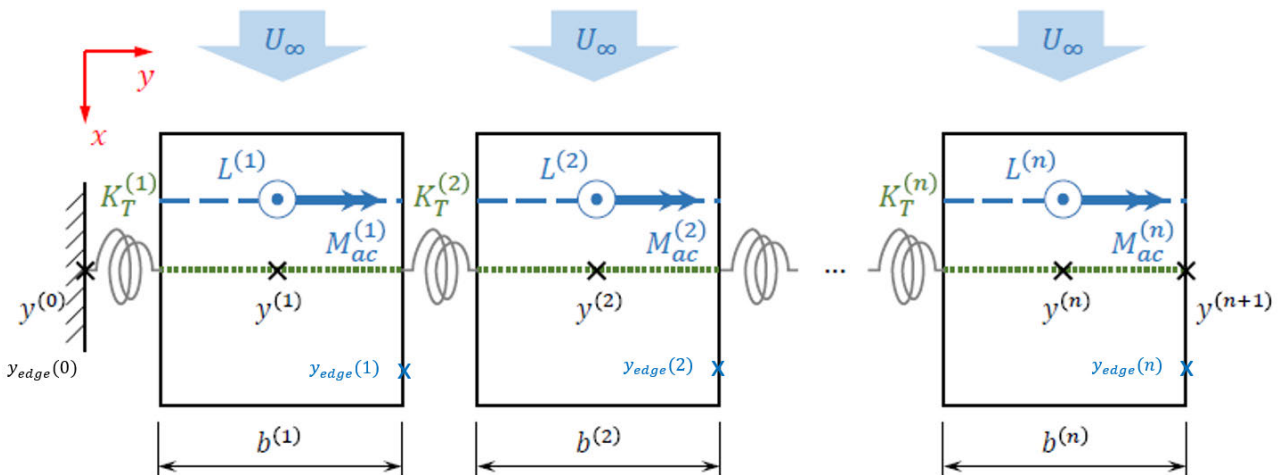


Figure 4: Forces and geometry of lumped panels

For discretization, first are created the positions y_{edge} that delimit each panel. Span of each panel can be computed with the difference of y_{edge} :

$$b^{(i)} = y_{edge}^{(i)} - y_{edge}^{(i-1)} \quad (2.6)$$

Then, y positions are computed at the center of each panel, and also root and wingtip positions are added.

$$y^{(i)} = \frac{y_{edge}^{(i)} + y_{edge}^{(i-1)}}{2} \quad (2.7)$$

Because each panel is assumed as a rigid body connected with torsional springs, number of DOFs is equal to the number of panels N:

$$\{\theta\} = \begin{bmatrix} \theta_1 \\ \theta_2 \\ \dots \\ \theta_i \\ \dots \\ \theta_n \end{bmatrix} \quad (2.8)$$

2.3 Static problem definition

Having defined the discretization to be used in this numerical problem, we can start writing their applicable equations. We know that torsion along a beam is governed by the following relation:

$$\frac{T}{GJ} = \frac{d\theta}{dy} \quad (2.9)$$

Because domain has been discretized into N lumped panels, we can use a 1st order approximation of the derivate:

$$T^{(i)} = \frac{\bar{G}J^{(i)}}{y^{(i)} - y^{(i-1)}} \cdot (\theta^{(i)} - \theta^{(i-1)}) \quad (2.10)$$

From the previous eq. 2.10, torsional stiffness at each panel $k_t^{(i)}$ can be computed as the following:

$$T^{(i)} = k_t^{(i)} \cdot (\theta^{(i)} - \theta^{(i-1)}) \quad (2.11)$$

Being the torsional stiffness $k_t^{(i)}$:

$$k_t^{(i)} = \frac{\bar{G}J^{(i)}}{y^{(i)} - y^{(i-1)}} \quad (2.12)$$

Both divergence and control reversal phenomena are obtained under the hypothesis of **static equilibrium** about the elastic axis:

$$\sum M^{(i)} = I^{(i)} \cdot \frac{d\theta^{(i)}}{dt^2} \quad (2.13)$$

$$M_{ac}^{(i)} + L^{(i)} \cdot e^{(i)} - k_t^{(i)} \cdot (\theta^{(i)} - \theta^{(i-1)}) - k_t^{(i+1)} \cdot (\theta^{(i)} - \theta^{(i+1)}) = 0 \quad (2.14)$$

Being:

$$M_{ac}^{(i)} = q_\infty \cdot (c^{(i)})^2 \cdot b^{(i)} \cdot C_{mac, \delta}^{(i)} \cdot \delta^{(i)} \quad (2.15)$$

$$L^{(i)} = q_\infty \cdot c^{(i)} \cdot b^{(i)} \cdot [C_{l, \alpha} \cdot \theta + C_{l, \delta} \cdot \delta] \quad (2.16)$$

Now, it is time to define and apply the corresponding BCs:

- At $i=1$ the root is clamped: $\theta^{(0)} = 0$

$$M_{ac}^{(1)} + L^{(1)} \cdot e^{(1)} - k_t^{(1)} \cdot \theta^{(1)} - k_t^{(2)} \cdot (\theta^{(1)} - \theta^{(2)}) \quad (2.17)$$

- At $i=N$ the wingtip is free, no torsion is applied: $\theta^{(n+1)} = \theta^{(n)}$

$$M_{ac}^{(n)} + L^{(n)} \cdot e^{(n)} - k_t^{(n)} \cdot (\theta^{(n)} - \theta^{(n-1)}) \quad (2.18)$$

By substituting expressions of moment 2.15 and lift 2.16 into static equilibrium equation 2.14, the following expression is obtained:

$$q_\infty \cdot (c^{(i)})^2 \cdot b^{(i)} \cdot C_{mac, \delta}^{(i)} \cdot \delta^{(i)} + e^{(i)} \cdot q_\infty \cdot c^{(i)} \cdot b^{(i)} \cdot [C_{l, \alpha}^{(i)} \cdot \theta^{(i)} + C_{l, \delta}^{(i)} \cdot \delta^{(i)}] - k_t^{(i)} \cdot (\theta^{(i)} - \theta^{(i-1)}) - k_t^{(i+1)} \cdot (\theta^{(i)} - \theta^{(i+1)}) = 0 \quad (2.19)$$

If we order by terms:

$$-k_t^{(i)} \cdot \theta^{(i-1)} + (k_t^{(i)} + k_t^{(i+1)} - e^{(i)} \cdot q_\infty \cdot c^{(i)} \cdot b^{(i)} \cdot C_{l, \alpha}^{(i)}) \cdot \theta^{(i)} - k_t^{(i+1)} \cdot \theta^{(i+1)} = [q_\infty \cdot (c^{(i)})^2 \cdot b^{(i)} \cdot C_{mac, \delta}^{(i)} + e^{(i)} \cdot q_\infty \cdot c^{(i)} \cdot b^{(i)} \cdot C_{l, \delta}^{(i)}] \cdot \delta^{(i)} \quad (2.20)$$

In matrix form, we can arrange the following system of equations:

$$([K_s] - q_\infty \cdot [K_a]) \{\theta\} = \{Q\} \quad (2.21)$$

The stiffness matrix K_s :

$$[K_s] = \begin{bmatrix} k_t^{(1)} + k_t^{(2)} & -k_t^{(2)} & 0 & \dots & 0 \\ -k_t^{(1)} & k_t^{(1)} + k_t^{(2)} & -k_t^{(2)} & \dots & 0 \\ \dots & \dots & \dots & \dots & \dots \\ 0 & \dots & -k_t^{(n-1)} & k_t^{(n-1)} + k_t^{(n)} & -k_t^{(n)} \\ 0 & \dots & 0 & -k_t^{(n)} & k_t^{(n)} \end{bmatrix} \quad (2.22)$$

While the matrix K_a , containing aerodynamic coefficients affected by θ :

$$[K_a] = \begin{bmatrix} e^{(1)} \cdot c^{(1)} \cdot b^{(1)} \cdot C_{l, \alpha}^{(1)} & 0 & \dots & \dots & 0 \\ 0 & e^{(2)} \cdot c^{(2)} \cdot b^{(2)} \cdot C_{l, \alpha}^{(2)} & 0 & \dots & 0 \\ \dots & \dots & \dots & \dots & \dots \\ 0 & \dots & \dots & e^{(n-1)} \cdot c^{(n-1)} \cdot b^{(n-1)} \cdot C_{l, \alpha}^{(n-1)} & 0 \\ 0 & \dots & \dots & \dots & e^{(n)} \cdot c^{(n)} \cdot b^{(n)} \cdot C_{l, \alpha}^{(n)} \end{bmatrix} \quad (2.23)$$

And the vector of external torque, which contains parameters that do not depend on variable θ , but on enforced δ :

$$\{Q\} = q_\infty \cdot \begin{bmatrix} ((c^{(1)})^2 \cdot b^{(1)} \cdot C_{mac, \delta}^{(1)} + e^{(1)} \cdot c^{(1)} \cdot b^{(1)} \cdot C_{l, \delta}^{(1)}) \cdot \delta^{(1)} \\ \dots \\ ((c^{(i)})^2 \cdot b^{(i)} \cdot C_{mac, \delta}^{(i)} + e^{(i)} \cdot c^{(i)} \cdot b^{(i)} \cdot C_{l, \delta}^{(i)}) \cdot \delta^{(i)} \\ \dots \\ ((c^{(n-1)})^2 \cdot b^{(n-1)} \cdot C_{mac, \delta}^{(n-1)} + e^{(n-1)} \cdot c^{(n-1)} \cdot b^{(n-1)} \cdot C_{l, \delta}^{(n-1)}) \cdot \delta^{(n-1)} \\ ((c^{(n)})^2 \cdot b^{(n)} \cdot C_{mac, \delta}^{(n)} + e^{(n)} \cdot c^{(n)} \cdot b^{(n)} \cdot C_{l, \delta}^{(n)}) \cdot \delta^{(n)} \end{bmatrix} = q_\infty \cdot \{Q_{coeffs}\} \cdot \{\delta\} \quad (2.24)$$

2.4 Divergence speed U_D of the plate

In the previous Section it was obtained the system of equations for static equilibrium 2.41. Thus, it can be used both for divergence u_D and control reversal u_R :

$$([K_s] - q_\infty \cdot [K_a])\{\theta\} = \{Q\} \quad (2.25)$$

Divergence condition q_D occurs when aerodynamic forces are such that θ can not find a finite equilibrium value. In mathematical form:

$$\theta \rightarrow \infty \quad (2.26)$$

For a general N DOFs case, this situation occurs when the previous system of eqs. 2.25 can not be solved, because determinant is zero:

$$\det([K_s - q_D[K_a]]) = 0 \quad (2.27)$$

By applying algebraic manipulation to eqs. 2.25:

$$([K_a]^{-1}[K_s] - q_D[1])\{\theta\} = [K_a]^{-1}\{Q\} \quad (2.28)$$

We can obtain q_D as an eigenvalue problem of the homogeneous system. In this new expression, divergence occurs for those eigenvalues $\lambda_i = 0$. Mind that external torque $\{Q\}$ is not used for divergence computation q_D :

$$([K_a]^{-1}[K_s] - q_D[1] - \lambda_i[1])\{\theta\} = \{0\} \quad (2.29)$$

In the previous expression 2.29, the solution to be found q_D is an unknown, together with eigenvalues λ_i . In order to reduce the number of unknowns of the system so it can be solved, a new variable λ'_i is defined:

$$\lambda'_i = (q_D + \lambda_i) \quad (2.30)$$

And the system to be solved is:

$$\det([K_a]^{-1}[K_s] - \lambda'_i[1]) = \{0\} \quad (2.31)$$

Because divergence occurs at $\lambda_i = 0$, q_D is the minimum positive eigenvalue λ'_i :

$$\lambda'_i = (q_D + \lambda_i); q_D = \min(\lambda'_i > 0) \quad (2.32)$$

From dynamic pressure q_D , divergence velocity u_D is directly calculated:

$$u_D = \sqrt{\frac{2 \cdot q_D}{\rho_0}} \quad (2.33)$$

being $\rho_0 = 1.225[kg/m^3]$ air density at sea level.

Of course, because the system has N DOFs, a total of N values of u_D can be obtained, even they lack physical meaning because the 1st mode is already a catastrophic failure. In any case, higher modes are also computed and saved for later comparison.

In addition, q_D for the case of rectangular wing with constant properties across the span has **analytical solution**, that can be found in [2] pag.6:

$$q_D|_{\text{analytical}} = \frac{\pi^2}{4b^2} \frac{GJ}{ceC_{l,\alpha}} \quad (2.34)$$

2.4.1 Grid Convergence Analysis

In order to assess the effect of mesh size, which is the number of panels for wing discretization, u_D is computed for different N panels. Afterwards, error is assessed as the difference between u_D obtained numerically, and the reference analytical solution for a rectangular wing with constant properties:

$$\varepsilon = \frac{u_D - u_D|_{\text{analytical}}}{u_D|_{\text{analytical}}} \quad (2.35)$$

The obtained results are plotted in a loglog scale:

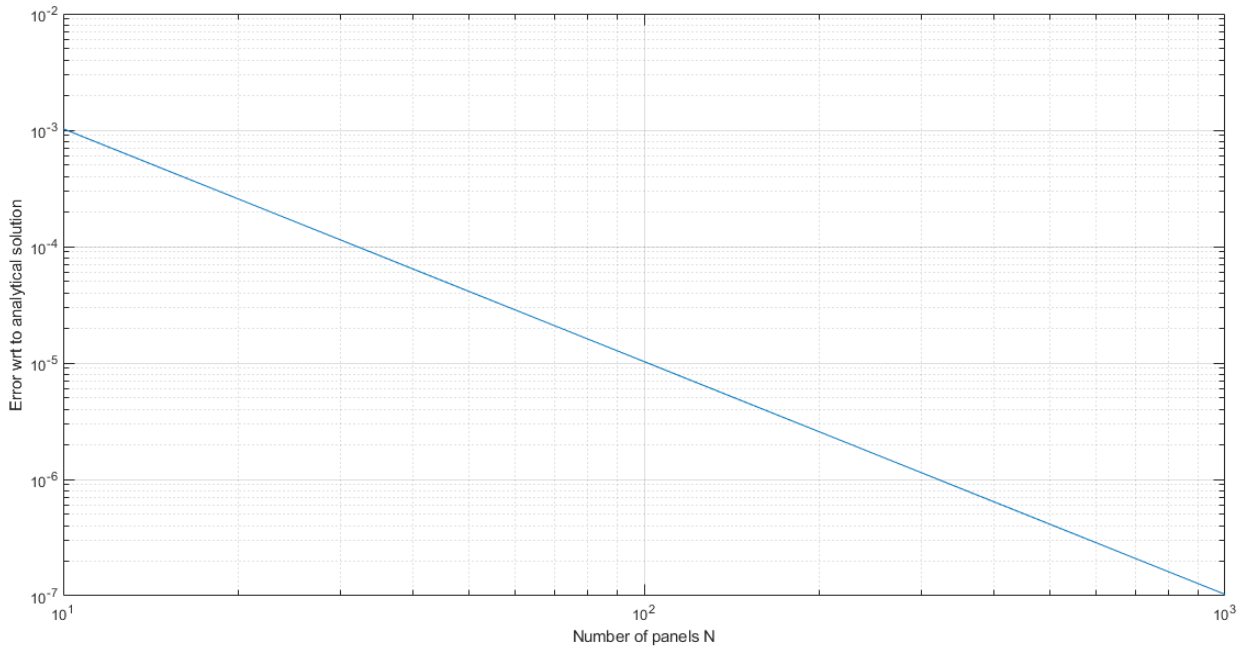


Figure 5: Grid Convergence Analysis for u_D

Due to the reduced computational cost of this problem, it has been decided to use N=1000 panels both for computation of divergence velocity u_D and control reversal u_R , with an estimated error $\varepsilon \approx 1e-7$.

2.4.2 Divergence results

In the following Table 1 are presented the obtained divergence velocities u_D for the first 5 modes:

Divergence Mode	u_D [m/s]
#1	514.2
#2	1542.5
#3	2570.8
#4	3599.1
#5	4627.4

Table 1: Divergence velocities u_D of the wing

At first glance, it can be seen that the obtained divergence velocities u_D are in the supersonic regime $Ma > 1$; so hypothesis of potential incompressible flow is not valid. In order to obtain accurate results, aerodynamic modellization for matrix $[K_a]$ should be revised in case of supersonic compressible flow.

After applying the previous mathematical procedure in Matlab, the obtained divergence value for the 1st mode is:

$$u_D = 514.2 \text{ [m/s]} \quad (2.36)$$

It is worth noting that the obtained divergence velocity u_D does not depend on the position of control surface. This has been checked with Matlab as a code verification. Also, when comparing with analytical solution, obtained numerical results with $N=1000$ are equal:

$$u_D|_{\text{analytical}} = \sqrt{\frac{2 \cdot q_D|_{\text{analytical}}}{\rho_0}} = 514.2 \text{ [m/s]} \quad (2.37)$$

2.5 Plot 5 first modes of elastic twist, associated to corresponding U_D

After obtaining divergence speeds u_D for each mode, also a plot of their eigenvectors is here displayed:

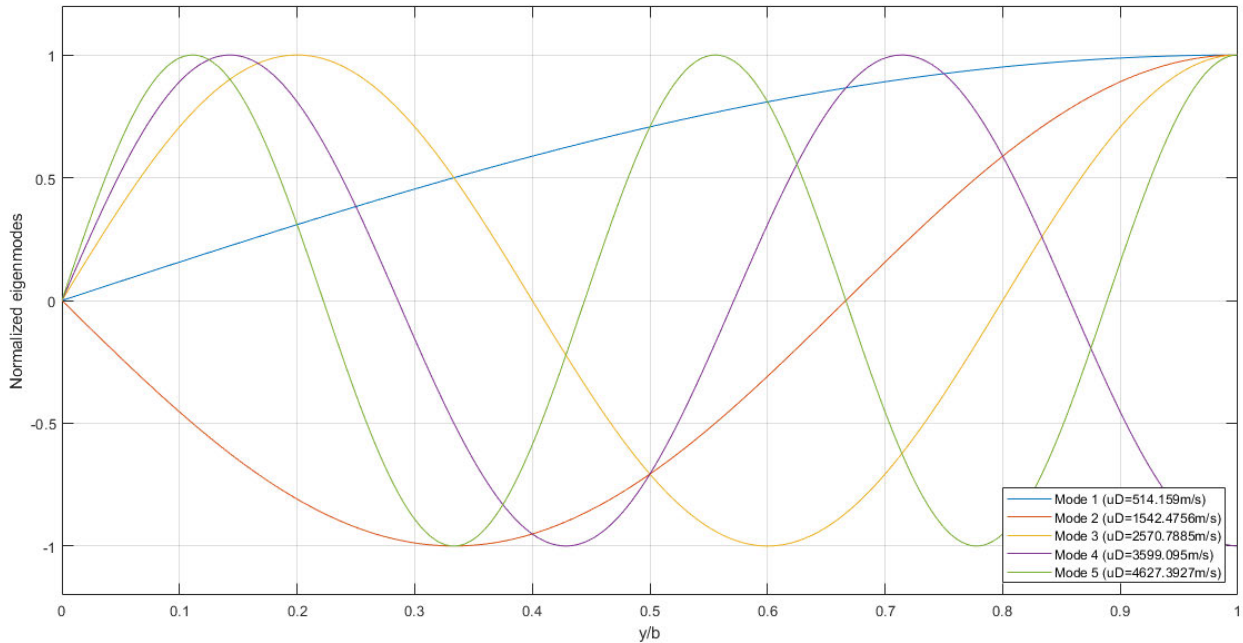


Figure 6: Normalized modes for the first 5 divergence velocities u_D

The modes presented in the previous Fig. 6 are normalized with their maximum value, so their bounds are between $[-1, 1]$. It is clearly seen that 1st mode corresponds to the simplest one, with $\theta = 0$ at wing root and tending to $\theta \rightarrow \infty$ at wingtip.

Higher modes have the same number of inflection points as the N^0 mode. For example, mode #2 tends to divergence at $y/b = 0.32$ and wingtip. However, as commented previously, higher modes are not physically feasible, because 1st mode will occur at a lower velocity u_D and it produces a catastrophic failure.

2.6 Plot U_R/U_D vs. η for $\beta = \{0.5, 0.6, 0.7, 0.8, 0.9\}$ (U_R is the speed at control surface conditions)

Control reversal condition is a static aeroelasticity phenomena that occurs when a deflection of control surface δ does not produce a change in total lift of the wing. In these conditions, it is said that control surface has lost its effectiveness, because it is not useful for controlling the aircraft.

The schematic of how control reversal occurs is here presented Fig. 7:



Figure 7: Control Reversal phenomena schematic

In mathematical form, for an airfoil section, control reversal occurs when:

$$\frac{\partial \{l^{(i)}\}}{\partial \delta} = 0 \quad (2.38)$$

However, because now we're treating with a complete wing, we shall evaluate total lift of the wing, which is the sum of each panel:

$$\frac{\partial \sum_{i=1}^N \{l^{(i)}\}}{\partial \delta} = \sum_{i=1}^N \frac{\partial \{l^{(i)}\}}{\partial \delta} \quad (2.39)$$

We know that general expression of lift at each panel in vector form is the following. For better readiness, the upper indices "i" are omitted, even these are quantities per each panel:

$$\{l\} = q_\infty \cdot \{c\} \cdot \{b\} \cdot \left[\{C_{l, \alpha}\} \cdot \{\theta\} + \{C_{l, \delta}\} \cdot \{\delta\} \right] \quad (2.40)$$

In the previous eq. 2.40, lift at each panel $\{l\}$ depends both on current torsion $\{\theta\}$ and also control surface deflection $\{\delta\}$.

Coming back to the general system of equations for the static problem:

$$\left([K_s] - q_\infty \cdot [K_a] \right) \{\theta\} = \{Q\} \quad (2.41)$$

We isolate deflection at each panel θ :

$$\{\theta\} = \left([K_s] - q_\infty \cdot [K_a] \right)^{-1} * \left(q_\infty \cdot \{Q_{coeffs}\} \cdot \{\delta\} \right) = \left([K_s] - q_\infty \cdot [K_a] \right) \backslash \left(q_\infty \cdot \{Q_{coeffs}\} \cdot \{\delta\} \right) \quad (2.42)$$

Where backslash operator "\" is as useful tool in Matlab to avoid computing the inverse when solving a linear system of equations:

$$A * x = b; \quad x = A \backslash b \quad (2.43)$$

Substituting $\{\theta\}$ in lift eq. 2.40:

$$\{l\} = q_\infty \cdot \{c\} \cdot \{b\} \cdot \left[\{C_{l, \alpha}\} \cdot \left([K_s] - q_\infty \cdot [K_a] \right) \backslash \left(q_\infty \cdot \{Q_{coeffs}\} \cdot \{\delta\} \right) + \{C_{l, \delta}\} \cdot \{\delta\} \right] \quad (2.44)$$

Now we have written the system of equations dependant only on deflection δ ; so control reversal condition as expressed in eq. 2.39 is applied:

$$F = \sum_{i=1}^N \left(\frac{\partial \{l\}}{\partial \delta} \right) = 0 = \sum_{i=1}^N q_R \cdot \{c\} \cdot \{b\} \cdot \left[\{C_{l, \alpha}\} \cdot ([K_s] - q_R \cdot [K_a]) \setminus (q_R \cdot \{Q_{coeffs}\} \cdot \{CS\}) + \{C_{l, \delta}\} \cdot \{CS\} \right] \quad (2.45)$$

Where variable CS is defined as:

$$CS = \frac{\partial \{\delta\}}{\partial \delta} = \begin{cases} 0 & \text{for panels without control surface} \\ 1 & \text{for panels with control surface} \end{cases} \quad (2.46)$$

In order to avoid the trivial solution $q = 0$, we omit the common terms $q_\infty \cdot \{c\} \cdot \{b\}$ from the control reversal function, and preserve the equation inside brackets:

$$F = \sum_{i=1}^N \left(\frac{\partial \{l\}}{\partial \delta} \right) = 0 = \sum_{i=1}^N \left[\{C_{l, \alpha}\} \cdot ([K_s] - q_R \cdot [K_a]) \setminus (q_R \cdot \{Q_{coeffs}\} \cdot \{CS\}) + \{C_{l, \delta}\} \cdot \{CS\} \right] \quad (2.47)$$

This highly nonlinear eq. 2.47 is the function that has to be solved, so the scalar control reversal q_R is found. To do it, function *fsolve* has been used in Matlab, recovering q_R for different configurations of β and η . The obtained results are the following Fig. 8:

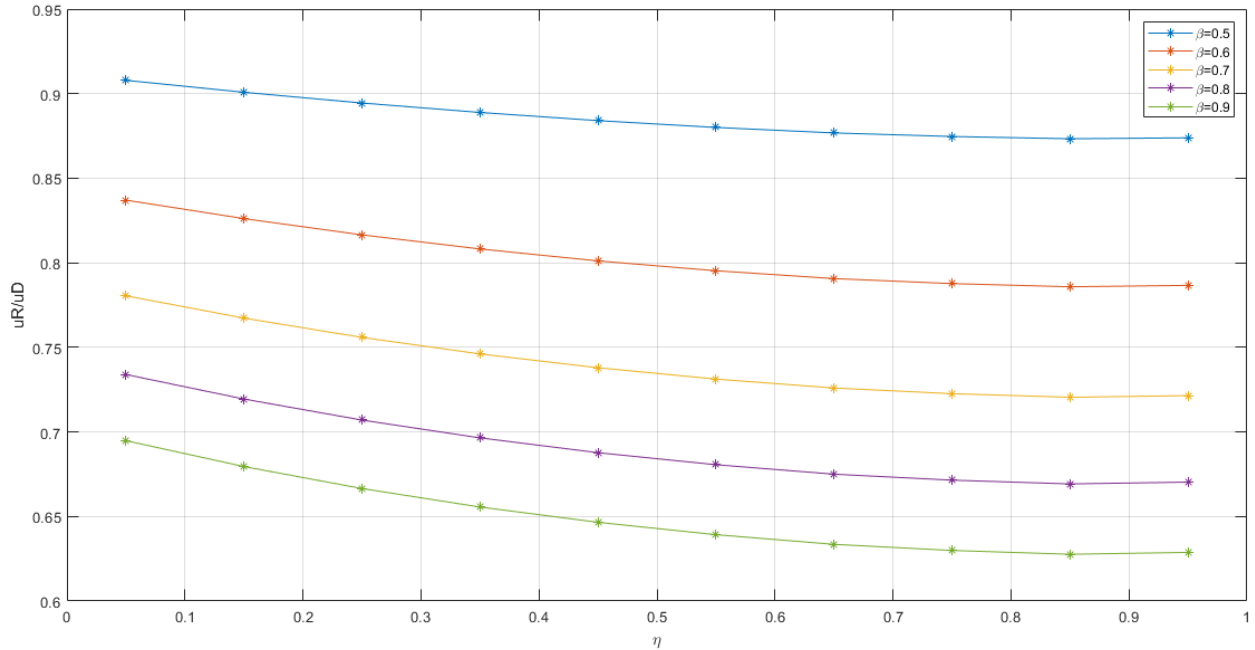


Figure 8: Control Reversal velocity ratio u_R/u_D results

When observing ratio u_R/u_D for different positions β and η of the control surface, the following trend-line is deduced: **for smaller size of control surface** (which is associated to small chord of control surface $\beta \uparrow$ or small span of control surface $\eta \uparrow$), **then control reversal velocity u_R is lower**.

So, the smaller the control surface is, it is more prone to experience control reversal at lower velocities. In any case, it is important to notice that obtained velocities here are in compressible range, so potential incompressible flow hypotheses are no longer valid: analysis should be refined with more accurate aerodynamic modellization in the transonic/supersonic regime.

2.7 A discussion on the possible sets of values of β and η for which:

2.7.1 Surface control reversal can be avoided

For control reversal to be avoided, there are 2 possibilities:

- $u_R/u_D \geq 1$. If control reversal velocity is higher than divergence, then u_D would occur before, and it will be the most limiting factor. Remember u_D results into catastrophic failure, while control reversal u_R is usually a loss of maneuverability, but does not generally end up into a structural failure.
- $u_R < 0$. If no positive control reversal velocity is found from eq. 2.47, then this phenomena would not occur.

For all the range analyzed in Fig. 8, control reversal occurs at lower velocities than divergence, so u_R would be the limiting factor for high speeds.

In order to check a wider design envelope, it was decided to compute u_R for more β positions of control surface:

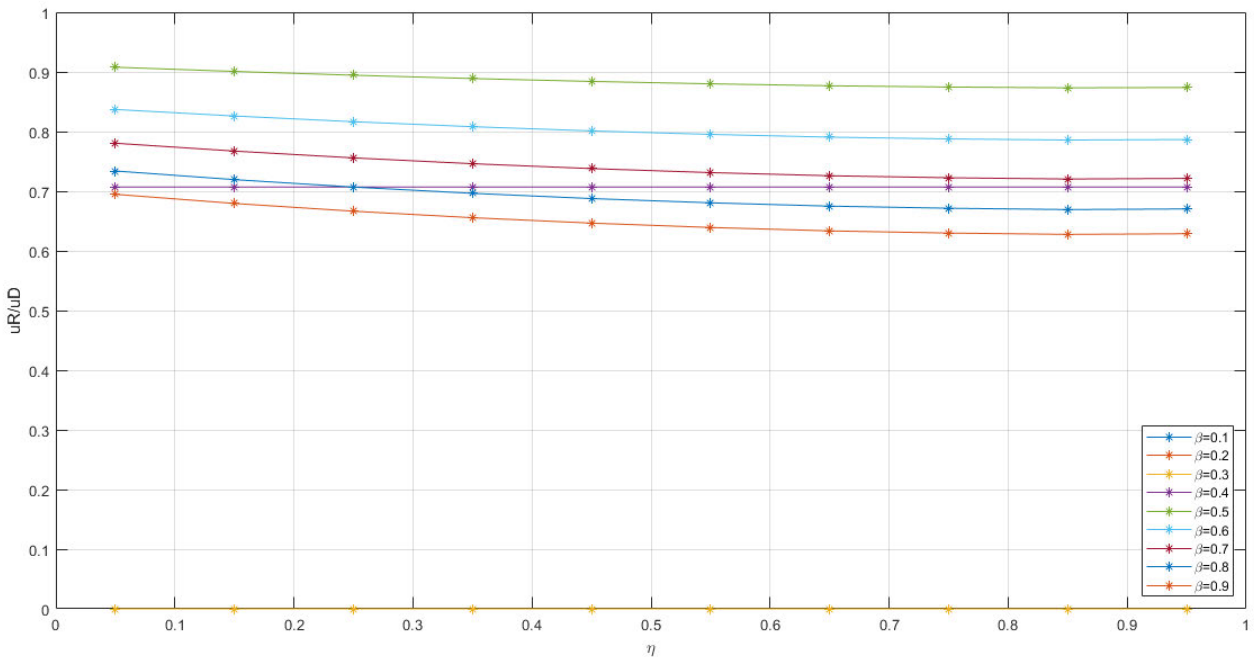


Figure 9: Control Reversal velocity ratio u_R/u_D results. Extended analysis

In this case, it was observed that for $\beta < 0.4$, u_R had no real part, but it was an imaginary number. So, for $\beta < 0.4$, control reversal would not occur.

2.7.2 $U_R/U_D > 0.5$

According to Fig. 8, for all the range $\beta \in \{0.5; 0.9\}$ and $\eta \in \{0.05; 0.95\}$, the relation $u_R/u_D > 0.5$ is true. Thus, this statement is fulfilled for all the analyzed control surface positions in 8.



References

- [1] D. Roca. Problem 1-Divergence of an airfoil (Advanced Aeroelasticity Course). Technical report, Terrassa, 2020.
- [2] D. Roca. Problem 3-Divergence of a wing (Advanced Aeroelasticity Course). Technical report, Terrassa, 2020.
- [3] D. Roca. Mid-term Exam Assignment (Advanced Aeroelasticity Course). Technical report, Terrassa, 2020.

Control surface reversal condition for a wing

Consider a flat plate on a wind tunnel clamped on one side and free on the other, simulating a wing during flight conditions. The plate has a rigidly attached control surface, the position and size of which are determined by the parameters η and β , as depicted in Figure 1.

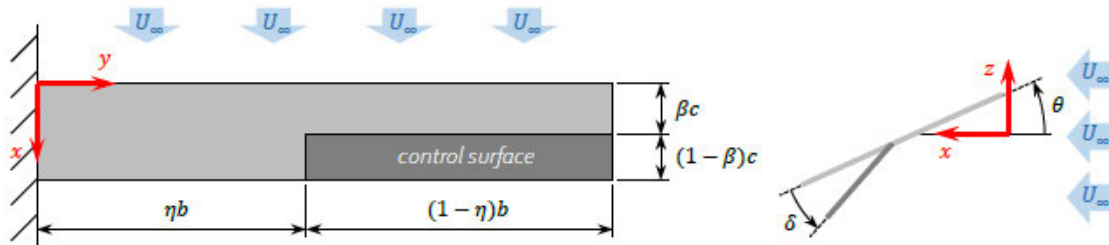


Figure 1: Problem description. Geometry and parameters identification.

This control surface can be deflected an angle δ ($\delta > 0$ downwards) in order to increase the total lift on the plate. The plate has an aspect ratio $AR=6$ and the chord size is $c = 400$ mm. From a structural test, it has been determined that the plate's effective stiffness to a torsional load is $GJ = 38$ kN m² and its elastic axis is located at $0.35c$ from the leading edge.

a) Divergence speed

Continuous beam and uncoupled aerodynamics analytical solution (extracted from page 41 of the lecture 3) which is valid even for deflections of the control surface as it does not affect the static stability of the system:

$$q_D = \frac{\pi^2 G \cdot J}{4b^2 \cdot c \cdot e \cdot cl_\alpha} = 161920 \text{ Pa} \quad (1)$$

Which at sea level will correspond to ($\rho = 1.225$ kg/m³) a flight velocity of:

$$U_D = 514.16 \text{ m/s}$$

Discretised Systems of equation

$$\sum_{SC} M = (K_s - qK_{m,\alpha})\theta + qK_{m,\delta}\delta + C_{m,ac} = 0 \quad (2)$$

$$\vec{l} = q(K_{l,\alpha}(\alpha - \alpha_0) + K_{l,\alpha}\theta + K_{l,\delta}\delta) \quad (3)$$

The divergence condition is when there is not a solution on the moment's equation. This is achieved by solving the following eigen-values problem (equation extracted form lecture 3 page 34):

$$(K_s - qK_{m,\alpha})\theta = 0 \quad (4)$$

Which can be transformed to (equation extracted form lecture 3 page 34):

$$(K_{m,\alpha}^{-1} K_s - qI)\theta = 0 \quad (5)$$



Concretely, the lowest positive eigenvalue is the divergence condition ($q_D = \min(q > 0)$), obtaining the following convergence plot for the lumped system:

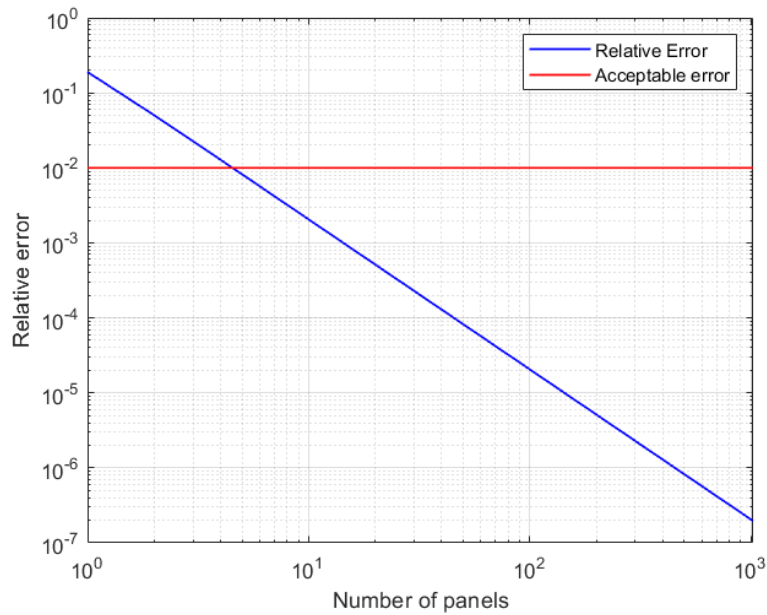


Figure 2: Convergence plot. Lumped panel method.

From this plot it is possible to extract that for more than 8 panels the solution has a relative error to the analytical solution (eq. 1), of less than 1%. However, 100 panel will be used in order to precisely allocate the wing distribution of the control surface η .

b) First 5 eigen-modes of divergence

From the previous development (the eigen-values problem) it is possible to obtain the 5 first eigenmodes of the system:

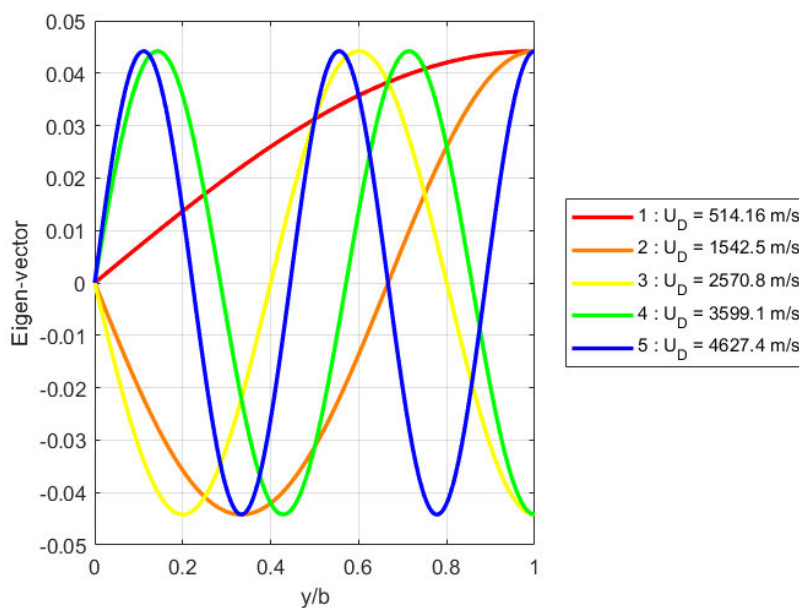


Figure 3: Five first eigen-modes. Lumped panel method.

c) Control surface reversal condition

The control surface reversal condition occurs when a deflection of a determined control surface do not perform the desired control action, instead, it performs the opposite one. At the limit, this condition can be determined when the sensitivity of a magnitude to a deflection of a control surface is null. From this problem two different desired control actions may be studied, on one hand, the sensitivity of the total wing lift vs a deflection of the control surface ($\frac{\partial L}{\partial \delta} = 0$). On the other hand, the sensitivity of the roll moment generation by the control surface ($\frac{\partial M_x}{\partial \delta} = 0$).

To solve this equation, the lift distribution (eq. 3) must be solved as a function of the control surface deflection (δ) and the dynamic velocity (q):

$$\vec{l} = q(K_{l,\alpha}(\alpha - \alpha_0) + K_{l,\alpha}\theta(\delta, q) + K_{l,\delta}\delta) \tag{6}$$

Concretely:

$$\theta = - (K_s - qK_{m,\alpha})^{-1} (qK_{m,\delta}\delta + C_{m,ac}) \tag{7}$$

Where $C_{m,ac} = 0$ and $\alpha_0 = 0$ because it is a symmetric airfoil:

$$\vec{l} = q \left[K_{l,\alpha}\alpha + \left(K_{l,\delta} - K_{l,\alpha} (K_s - qK_{m,\alpha})^{-1} (qK_{m,\delta}) \right) \delta \right] \tag{8}$$

Then, if both conditions are applied what is obtained is:

Total lift condition:

$$\frac{\partial L}{\partial \delta} = q \sum \left(K_{l,\delta} - K_{l,\alpha} (K_s - q_R K_{m,\alpha})^{-1} (q_R K_{m,\delta}) \right)_i = 0 \tag{9}$$

And the rolling moment condition:

$$\frac{\partial M_x}{\partial \delta} = q \sum y_i \left(K_{l,\delta} - K_{l,\alpha} (K_s - q_R K_{m,\alpha})^{-1} (q_R K_{m,\delta}) \right)_i = 0 \tag{10}$$

These equations might be solve using numerical schemes, concretely a simple Bolzano method will be used, using as intervals limits $q_R \in [0, q_D)$. If there is a change of sign between this interval, there exist a solution with cross the x axis:

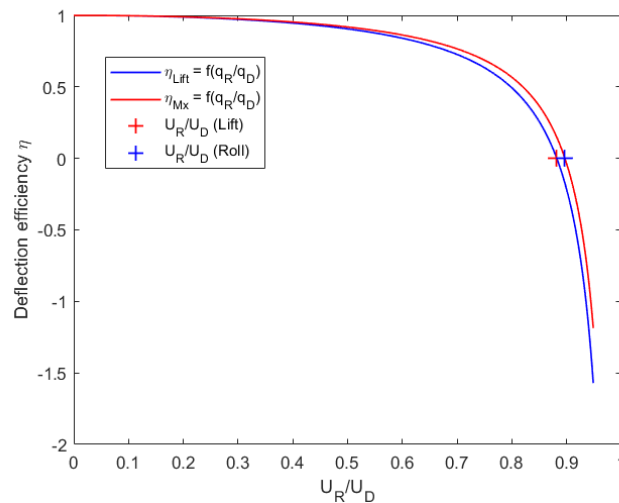


Figure 4: Bolzano solution verification. Lumped panel method.

Finally, the solution for different wingspan and chord span position of the control surface can be plotted:

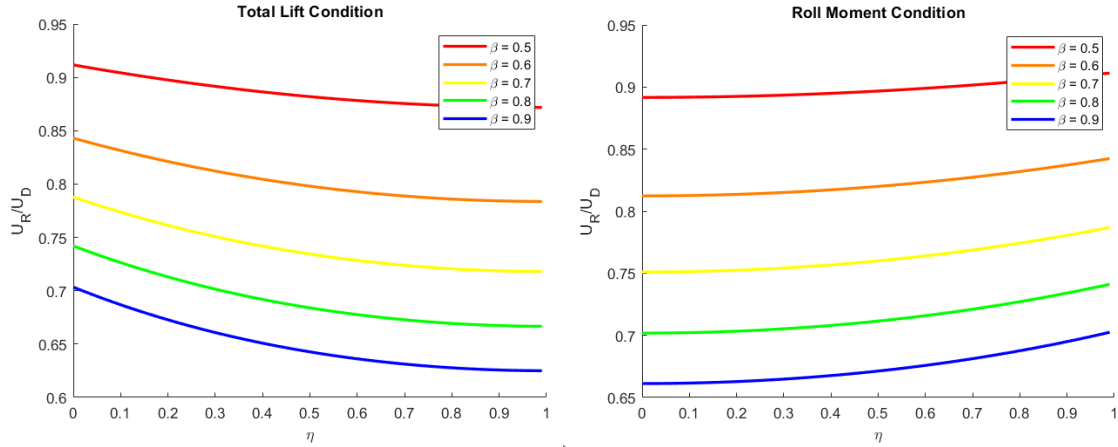


Figure 5: Control reversal condition. Lumped Panel method.

d) Results discussion

d.1 Surface control reversal conditions can be avoided.

Chord proportion of the control surface β :

From the theory lecture 2, page 25 the following expression of flexible airfoil can be extracted:

$$\frac{\partial l}{\partial \delta} = q_{\infty} c C_{l,\delta} \left(\frac{1 + \frac{q_{\infty} (C_{m_{ac},\delta}) (\frac{c}{e})}{q_D}}{1 - \frac{q_{\infty}}{q_D}} \right) = 0 \rightarrow \frac{q_R}{q_D} = -\frac{e}{c} \frac{C_{l,\delta}}{C_{m_{ac},\delta}} \quad (11)$$

Where, from problem 1 page 4:

$$C_{l,\delta} = 6\pi \frac{1 + \beta - 2\beta^2}{3 + 4\beta(1 - \beta)}; \quad C_{m_{ac},\delta} = -\frac{\beta}{4} C_{l,\delta} \rightarrow \frac{q_R}{q_D} = \frac{e}{c} \frac{4}{\beta} \quad (12)$$

To obtain feasible solutions the following conditions must be satisfied:

$$0 < \frac{q_R}{q_D} < 1 \quad (13)$$

From here it is possible to obtain two inequations:

$$\frac{q_R}{q_D} < 1 \rightarrow \frac{e}{c} \frac{4}{\beta} < 1 \rightarrow \beta > \frac{4e}{c} \quad (14)$$

For $\hat{e}=0.1$ (as in this problem):

$$\beta_1(\hat{e} = 0.1) > 0.4 \quad (15)$$

From this equation it can be seen that for β lower than 0.4 it will not exist a control reversal condition within the range of divergence conditions.



The second condition is:

$$\frac{q_R}{q_D} > 0 \rightarrow \frac{e^4}{c\beta} > 0 \tag{16}$$

From the previous results, it is possible to obtain that does not exist a feasible solution that avoids the divergence of the 1D problem. Then, it would occur for the range of β :

$$0.4 < \beta < 1 \tag{13}$$

In addition, control reversal condition can be improved by increasing the chord proportion of the control surface increasing the efficiency of the control surface respect the torsional moment generated.

This effect can be clearly seen at figure 5 obtaining in both cases better control reversal speeds when increasing the control surface chord. Concretely, if $\beta < 0.5$ the following results are obtained:

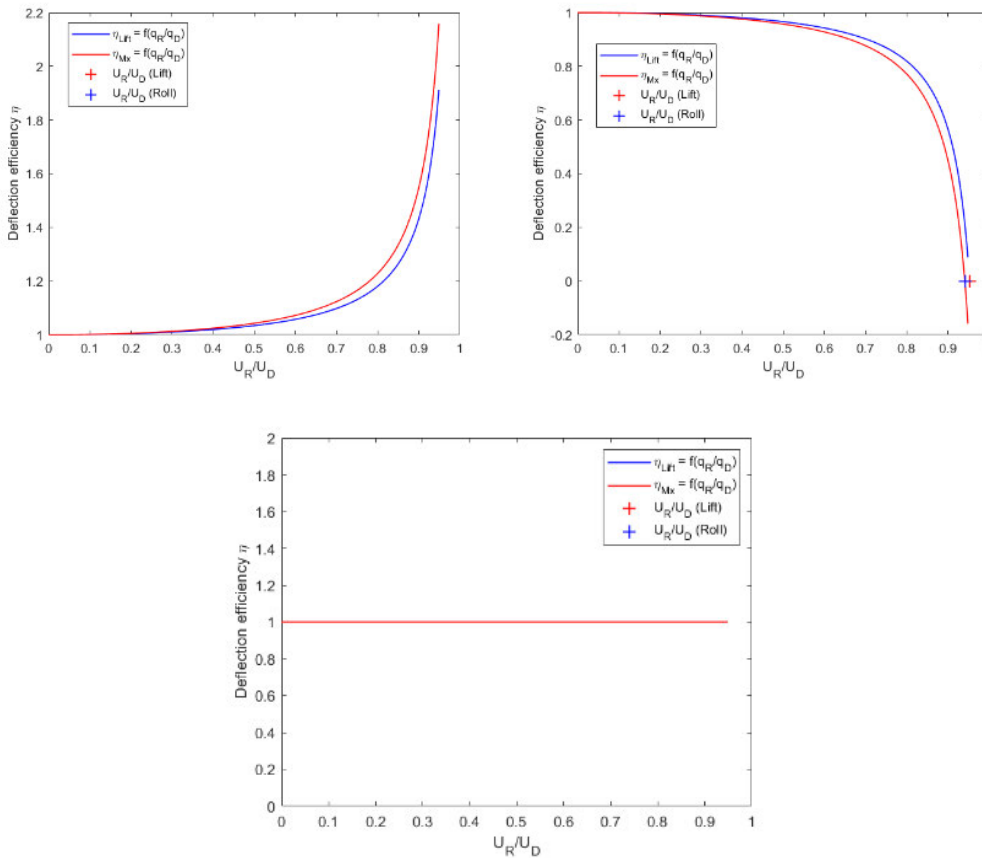


Figure 6: Control reversal condition ($\eta = 0$): a) $\beta = 0.35$. b) $\beta = 0.45$. c) $\beta = 0.4$.

The results for the 2D wing problem are consistent with the flexible 1d airfoil. It can be seen that for $\beta < 0.4$ the control reversal condition will not occur. This effect is maintained, independently of whether the whole wing is considered control surface or just a part of it, and for both control reversal conditions.



Wingspan proportion of the control surface η :

The control force generated by the control surface is a linear function η , whereas the generated torsion of the wing by a deflection is parabolic function:

Torsion moment:

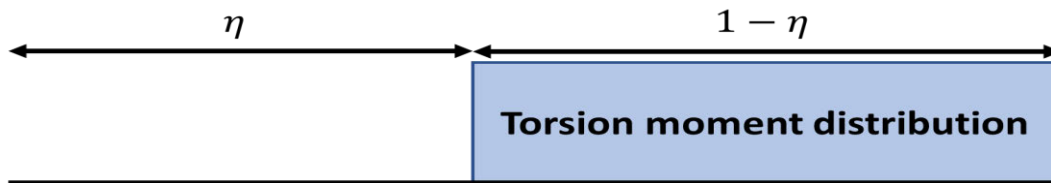


Figure 7: Torsion moment effect by control surface deflection.

And the deflection is:

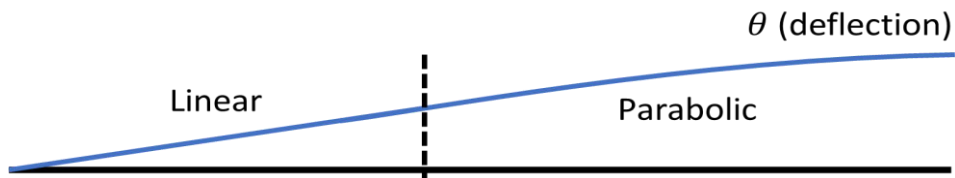


Figure 8: Torsional deflection by control surface deflection.

Then the obtained sensitivity distribution along the wingspan are:

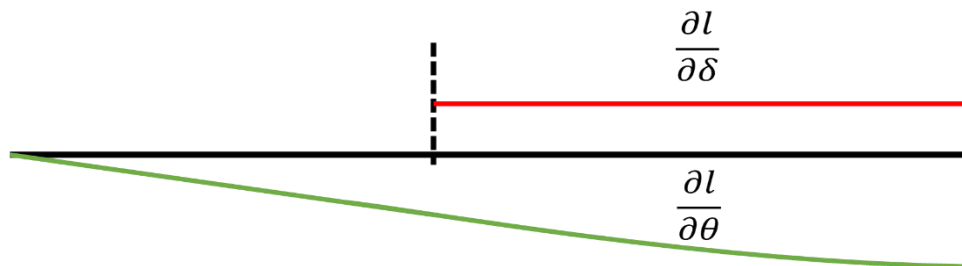


Figure 9: Total lift distribution comparison.

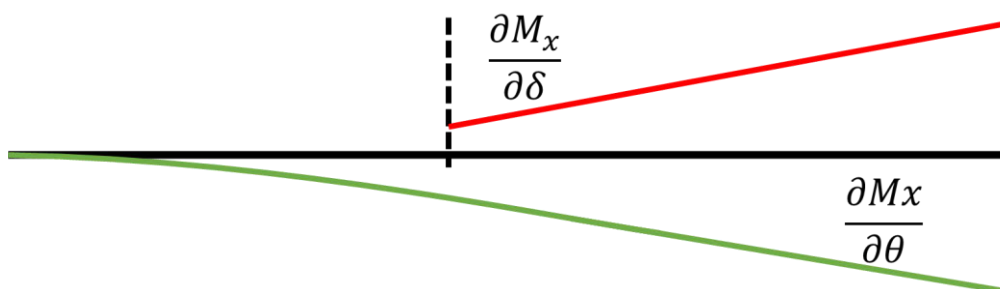


Figure 10: Total Roll Moment distribution comparison.

As it can be seen the balance between the torsion effect due to the control surface deflection and the extra lift generated by the control surface deflection is the main cause of the sensitivity of the η parameter. Because of this effect, the linear part, where no control action is applied generates parasite reduction of the lift that is optimized when increasing the wing part that is used as a control surface. Whereas, the roll moment is optimized by positioning the control surface near the wing tip, as the distance effect is more important than the total lift generation.

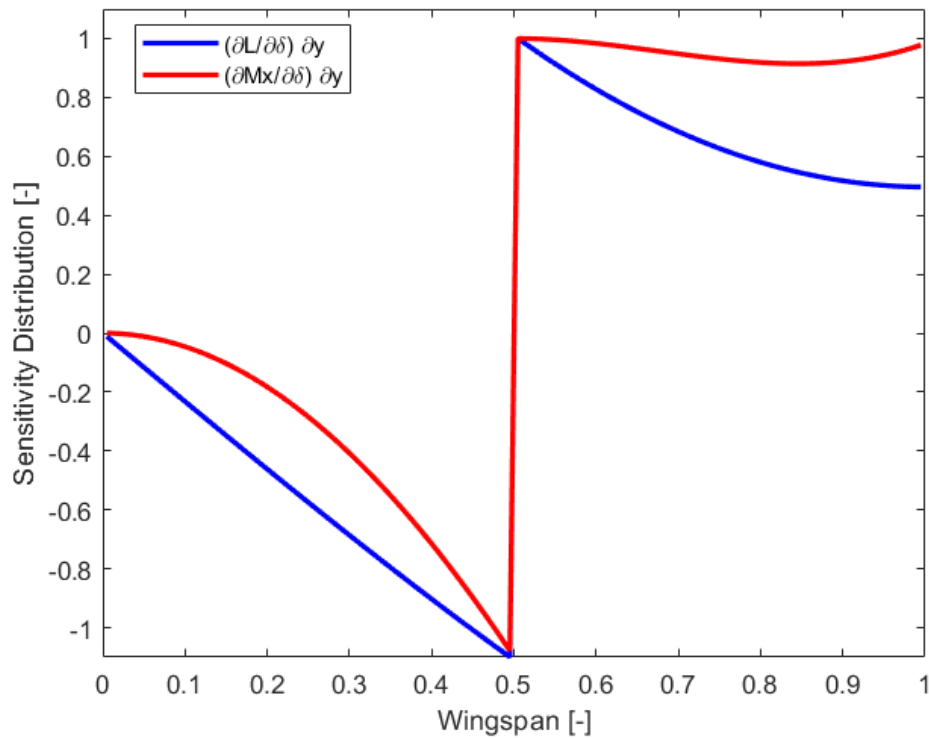


Figure 11: Contribution of each section to the global sensitivity.

d.2 $U_R/U_D > 0.5$.

Due to the geometric configuration of the shear center, the control reversal velocities are always higher than the half of the divergence speed. This is caused by using a distributed wing loading of both, extra lift generation and extra torsion moment generation. Making the 2D system more efficient than the 1D system studied at the lecture 2. As it is easier to have a total positive contribution of the control surface even if some parts of the wing are not contributing to extra lift generation Figure 11.

e) Opinion about the subject

- I think that the way this subject is structured is quite balance between theory and problems, as every lecture there is a proposed problem that might be solved using the taught information.
- The scope of the theory is quite similar to the one done at the subject of vehicle done by Oriol Casamor. But, at that subject the same information was given very fast and without understanding the basis of the coupling between structure and aerodynamics.
- I think that this subject might need a bit more projects evaluation than exam, as the problems are complex enough to be made using programming. And the written examen should be more about the physics of the problems rather than solving extremely simplified cases.



Project



Project



74

Setup of a virtual laboratory for studying aeroelastic problems

Goal: Implement a set of MATLAB functions to perform different kinds of aeroelastic analysis (e.g. assess divergence conditions, flutter study, unsteady aerodynamics, etc.).

Code requirements:

- Structures:
 - Use of 3D FEM code to obtain effective properties.
 - MATLAB implementation of a beam's FEM algorithm.
- Aerodynamics:
 - For steady aerodynamics: MATLAB implementation of lifting-line solution by horseshoe elements.
 - For unsteady aerodynamics: MATLAB implementation of Theodorsen's model.
- Coupling:
 - MATLAB implementation of transfer matrices: structures output (displacements vector) to aerodynamics input (angle of attack) and aerodynamics output (lift distribution) to structures input (force vector).
- Solvers:
 - Divergence speed + modes.
 - Flutter speed.

Results:

- For a clamped-free straight panel with a constant NACA0012 airfoil section, obtain:
 - Divergence speed for different wing aspect ratios.
 - First modes associated to divergence conditions for different aspect ratios.
 - Stability plots for flutter.

Evaluation:

75% Report + Code

- 50% - Minimum requirements
- 10% - Report quality
- 15% - Bonus (up to 30%)

25% Presentation

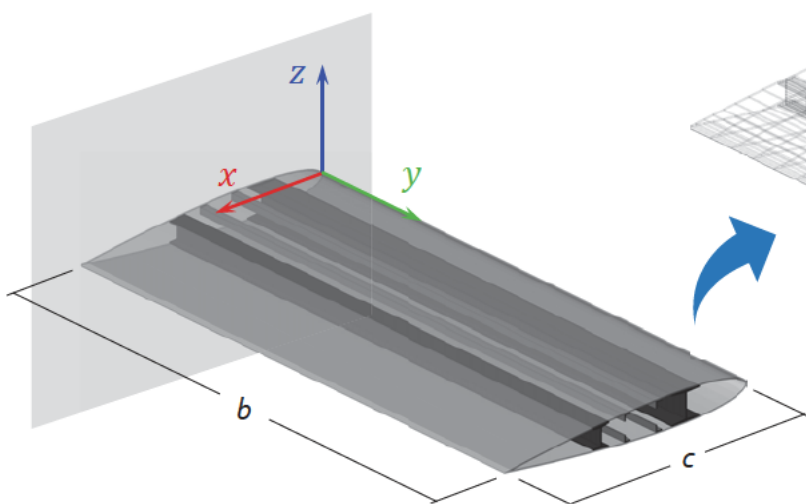
Bonus:

15% of the project qualification will come from devoting some extra effort to go beyond the minimum requirements. The nature and level of this extra effort can be awarded with an additional 15% (accounting ~10% of the global course grade!). Some ideas:

- Performing an analysis on a swept wing and/or with variable chord length.
- Implementing more complex structural/aerodynamic models.
- Implementing wake rollup for unsteady aerodynamic computation.
- ...

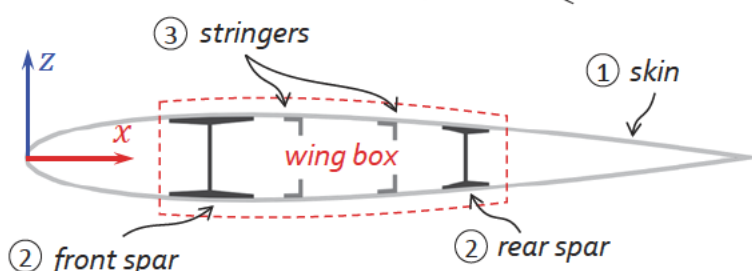


3D FEM Analysis – Experimental structural test



Material properties

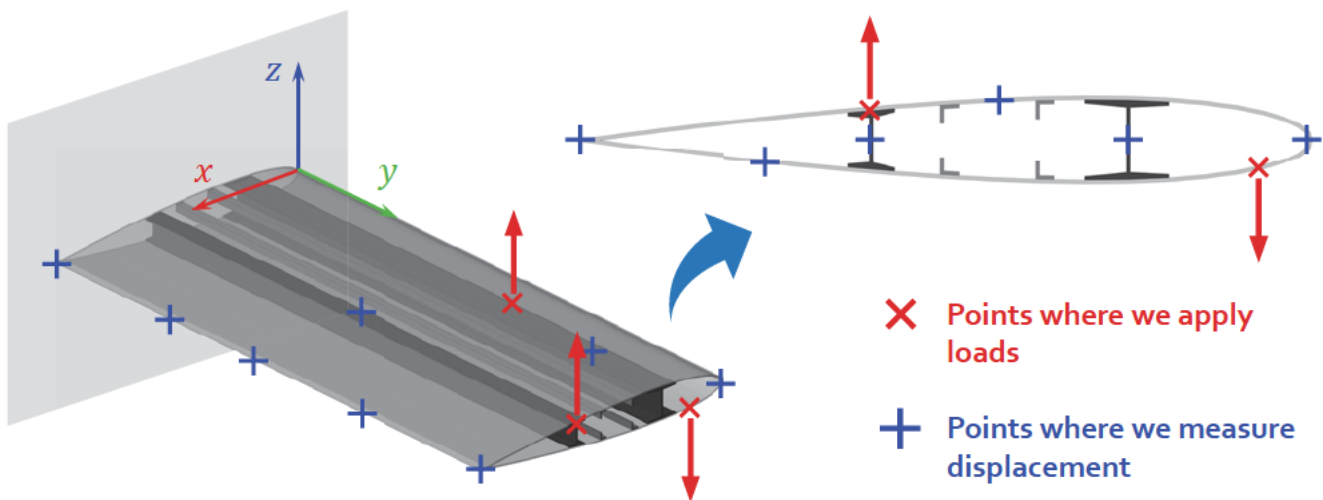
Material	Density (kg m ⁻³)	Young's Modulus (GPa)	Poisson's ratio
(1) Skin	2000	9	0.27
(2) Spars	1800	150	0.30
(3) Stringers	2300	70	0.35



NACA0012

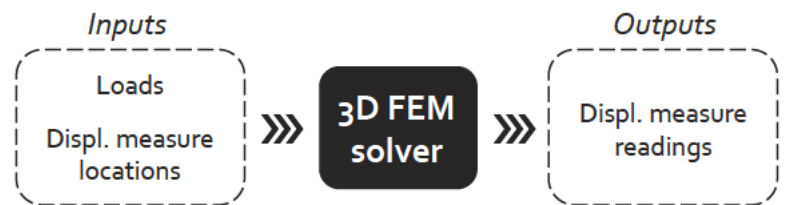


3D FEM Analysis – Experimental structural test



The goal is to obtain:

- Shear center position: $x_{sc}(y)$
- Torsional stiffness: $\overline{GJ}(y)$
- Bending stiffness: $\overline{EI}(y)$



3D FEM Analysis – Experimental structural test

Assumptions:

- Small displacements and deformations (this implies also small angles and linear elasticity).
- Effective response can be described by elemental beam theory:

$$\begin{Bmatrix} T \\ M \end{Bmatrix} = \underbrace{\begin{bmatrix} \overline{GJ} & 0 \\ 0 & \overline{EI} \end{bmatrix}}_{[E]} \begin{Bmatrix} d\theta/dy \\ d^2h/dy^2 \end{Bmatrix}$$

This is our hypothesis. We want to verify whether this hypothesis is satisfied and, if so, find $[E]$.

In the experiment, we are applying forces and measuring displacements. Since we cannot guarantee, a priori, that bending and torsion are structurally uncoupled (i.e. $k = 0$), it is better to work with the following constitutive relation instead:

$$\begin{Bmatrix} \bar{\theta}' \\ \bar{h}'' \end{Bmatrix} = \underbrace{\begin{bmatrix} S_{11} & S_{12} \\ S_{21} & S_{22} \end{bmatrix}}_{[E]^{-1}} \begin{Bmatrix} T \\ M \end{Bmatrix}$$

From applying a pure torsional load ($M = 0$):

$$S_{11} = \bar{\theta}'/T, \quad S_{21} = \bar{h}''/T$$

From applying a pure shear load ($T = 0, M' = -Q$):

$$S_{12} = \bar{\theta}'/M = -\bar{\theta}''/Q, \quad S_{22} = \bar{h}''/M = -\bar{h}'''/Q$$

To apply a pure shear load, we need to find the shear center first!

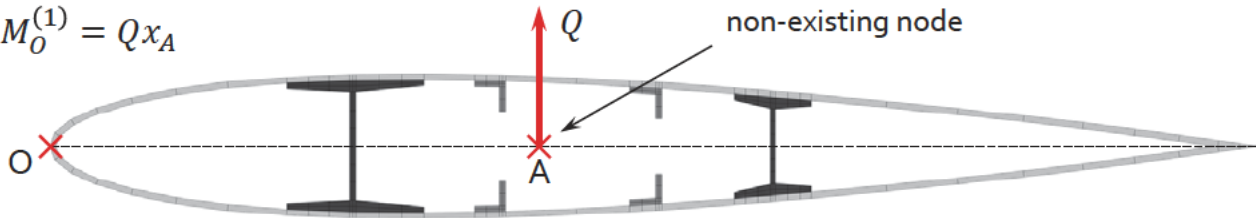


3D FEM Analysis – Experimental structural test

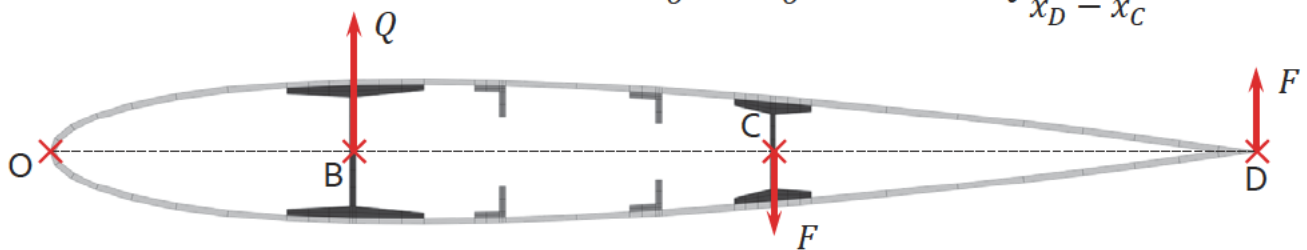
Considerations:

- The effect of applying a shear load in a particular point can be replaced by applying the same load at a different point and adding a compensating torque:

$$M_O^{(1)} = Qx_A$$



$$\text{III } M_O^{(1)} = M_O^{(2)} \rightarrow F = Q \frac{x_A - x_B}{x_D - x_C}$$



$$M_O^{(2)} = Qx_B + F(x_D - x_C)$$

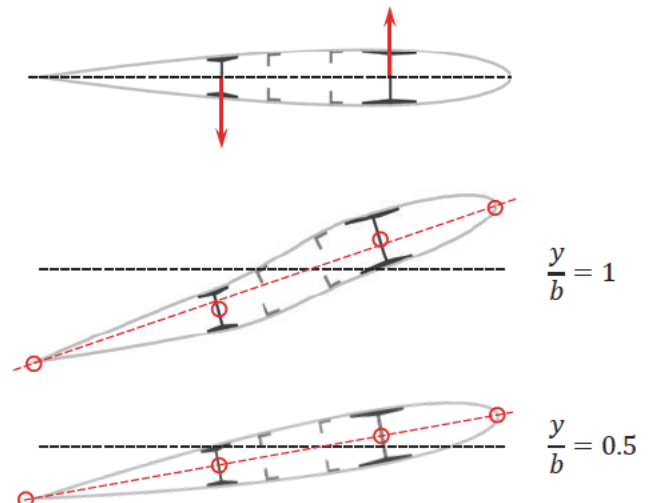
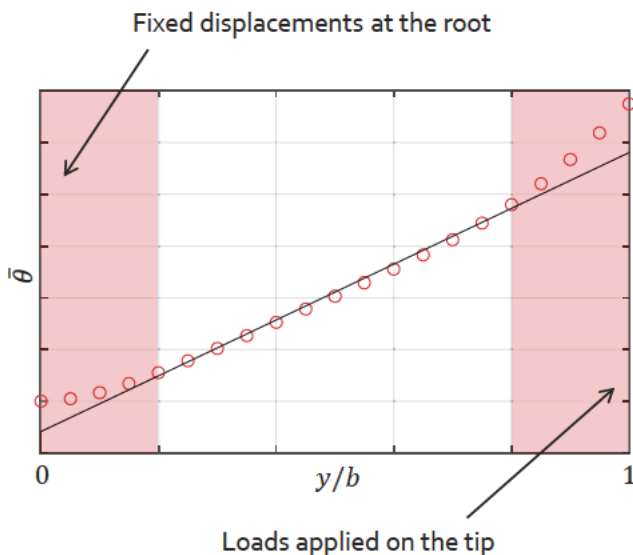


3D FEM Analysis – Experimental structural test

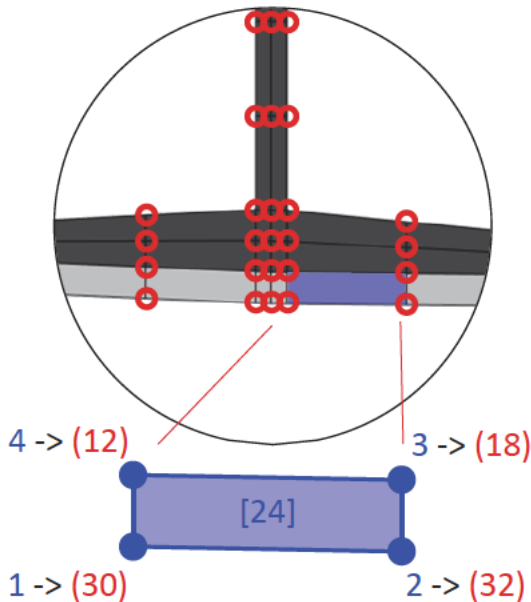
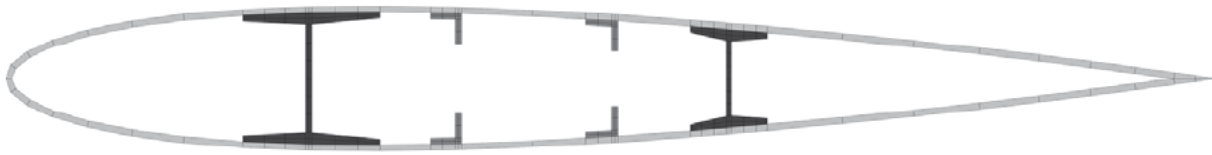
Considerations:

- We are applying point forces in a 3D FEM model. This means that deformations near the load application points may *distort* the average twist $\bar{\theta}$ and deflection \bar{h} on neighbouring sections. The same may be true for sections around the root, where the boundary conditions are applied. This must be taken into account when choosing the measuring points to obtain $\bar{\theta}$ and \bar{h} .

Results of applying a pure torque



2D FEM Analysis – Section properties



Determination of section properties:

Nodal coordinates $[\mathbf{x}] = \begin{bmatrix} \vdots \\ x^{(i)} & y^{(i)} & z^{(i)} \\ \vdots \end{bmatrix} = \begin{bmatrix} \vdots \\ \mathbf{x}^{(i)} \\ \vdots \end{bmatrix}$

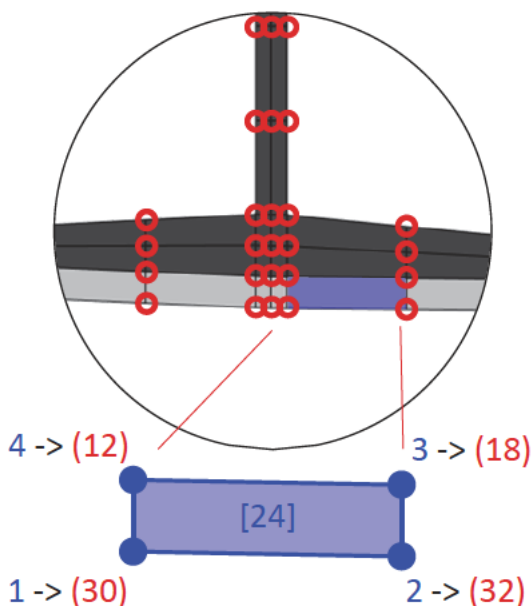
Nodal connectivities $[\mathbf{T}_n] = \begin{bmatrix} (i)_1^{[e]} & (i)_2^{[e]} & (i)_3^{[e]} & (i)_4^{[e]} \\ \vdots & \vdots & \vdots & \vdots \end{bmatrix}$

Material properties $[\mathbf{m}] = \begin{bmatrix} \vdots \\ \rho^{(m)} \\ \vdots \end{bmatrix}$

Material connectivities $[\mathbf{T}_m] = \begin{bmatrix} \vdots \\ (m)^{[e]} \\ \vdots \end{bmatrix}$



2D FEM Analysis – Section properties



Determination of section properties:

For each element $[e]$:

1. Obtain the coordinates and material:

$$\mathbf{x}_j^{[e]} = [\mathbf{x}]([\mathbf{T}_n]^{(e,j)}), \quad j = 1 \dots 4$$

$$\rho^{[e]} = [\mathbf{m}]([\mathbf{T}_m]^{(e)})$$

2. Determine the centroid coordinates:

$$\mathbf{x}^{[e]} = \frac{1}{4} \sum_{j=1}^4 \mathbf{x}_j^{[e]}$$

3. Determine the area of each element $[e]$:

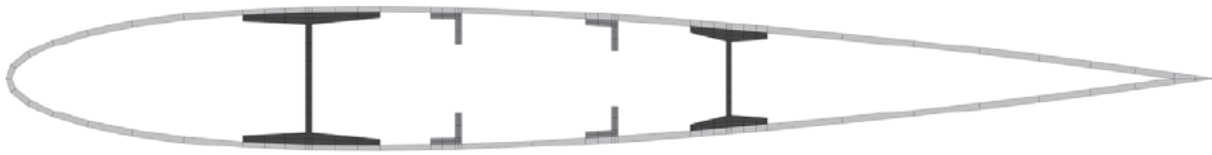
$$a = \mathbf{x}_1^{[e]} - \mathbf{x}_4^{[e]}; \quad b = \mathbf{x}_2^{[e]} - \mathbf{x}_1^{[e]}$$

$$c = \mathbf{x}_3^{[e]} - \mathbf{x}_2^{[e]}; \quad d = \mathbf{x}_4^{[e]} - \mathbf{x}_3^{[e]}$$

$$A^{[e]} = \frac{1}{2}(a \times b + c \times d)$$



2D FEM Analysis – Section properties



Determination of section properties:

Then, compute:

1. Total mass p.u. length:

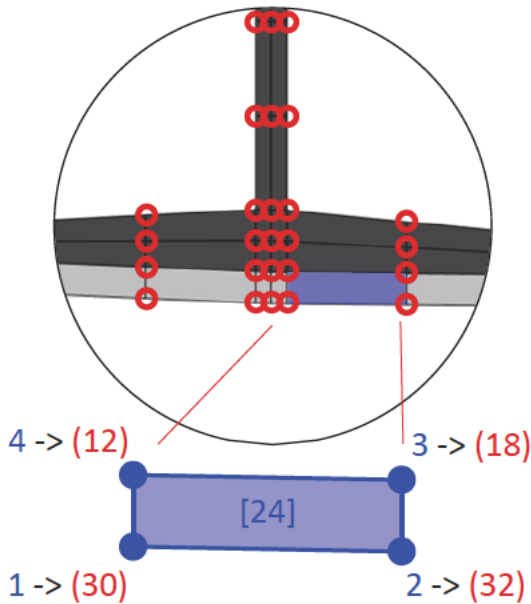
$$m = \sum_e \rho^{[e]} A^{[e]}$$

2. Center of mass:

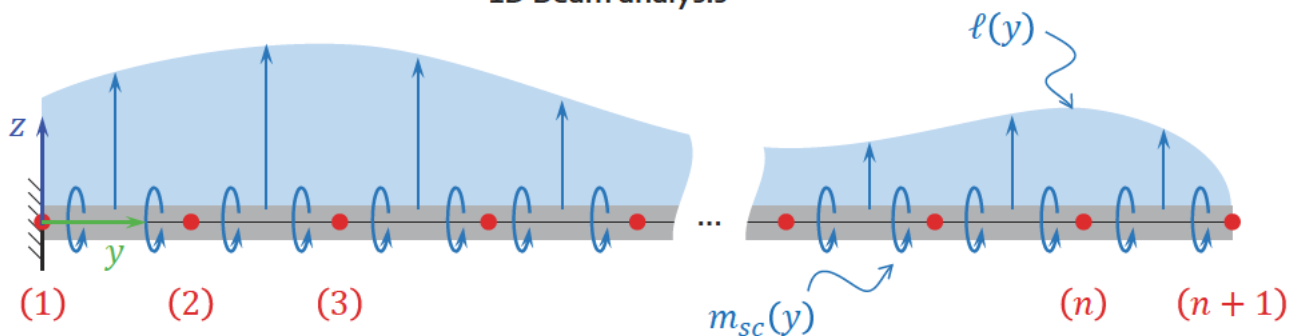
$$\mathbf{x}_{cm} = \frac{1}{m} \sum_e \mathbf{x}^{[e]} \rho^{[e]} A^{[e]}$$

3. Inertia about the shear center p.u. length:

$$I_{sc} = \sum_e (\mathbf{x}^{[e]} - \mathbf{x}_{sc})^2 \rho^{[e]} A^{[e]}$$



1D Beam analysis



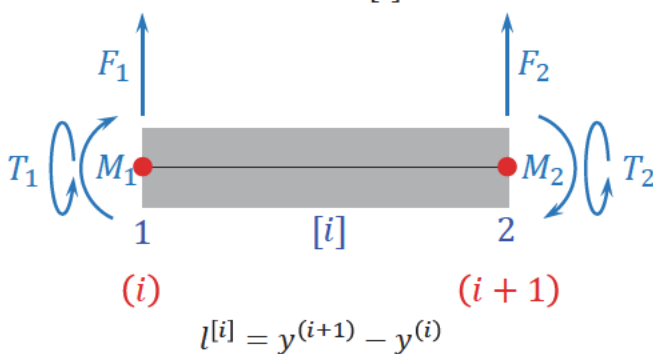
Nodal coordinates: $[\mathbf{y}]^{(i)} = y^{(i)}$

Nodal connectivities: $[\mathbf{T}_n]^{(i,1)} = i$; $[\mathbf{T}_n]^{(i,2)} = i + 1$

Element equilibrium equation

$$[\mathbf{M}^{[i]}] \{\ddot{\mathbf{u}}^{[i]}\} + [\mathbf{K}^{[i]}] \{\mathbf{u}^{[i]}\} = \{\mathbf{f}^{[i]}\}$$

Element $[i]$



$$\{\mathbf{u}^{[i]}\} = \begin{Bmatrix} \theta^{(i)} \\ h^{(i)} \\ \gamma^{(i)} \\ \theta^{(i+1)} \\ h^{(i+1)} \\ \gamma^{(i+1)} \end{Bmatrix}; \quad \{\mathbf{f}^{[i]}\} = \begin{Bmatrix} T_1^{[i]} \\ F_1^{[i]} \\ M_1^{[i]} \\ T_2^{[i]} \\ F_2^{[i]} \\ M_2^{[i]} \end{Bmatrix}$$



1D Beam analysis – Element matrices

Stiffness matrix:

$$[\mathbf{K}^{[i]}] = \frac{\overline{GJ}}{l^{[i]}} \begin{bmatrix} 1 & 0 & 0 & -1 & 0 & 0 \\ 0 & 0 & 0 & 0 & 0 & 0 \\ 0 & 0 & 0 & 0 & 0 & 0 \\ -1 & 0 & 0 & 1 & 0 & 0 \\ 0 & 0 & 0 & 0 & 0 & 0 \\ 0 & 0 & 0 & 0 & 0 & 0 \end{bmatrix} + \frac{\overline{EI}}{(l^{[i]})^3} \begin{bmatrix} 0 & 0 & 0 & 0 & 0 & 0 \\ 0 & 12 & 6l^{[i]} & 0 & -12 & 6l^{[i]} \\ 0 & 6l^{[i]} & 4(l^{[i]})^2 & 0 & -6l^{[i]} & 4(l^{[i]})^2 \\ 0 & 0 & 0 & 0 & 0 & 0 \\ 0 & -12 & -6l^{[i]} & 0 & 12 & -6l^{[i]} \\ 0 & 6l^{[i]} & 4(l^{[i]})^2 & 0 & -6l^{[i]} & 4(l^{[i]})^2 \end{bmatrix}$$

Mass matrix (lumped):

$$[\mathbf{M}^{[i]}] = \frac{l^{[i]}}{2} \begin{bmatrix} I_{sc} & md & 0 & 0 & 0 & 0 \\ md & m & 0 & 0 & 0 & 0 \\ 0 & 0 & 0 & 0 & 0 & 0 \\ 0 & 0 & 0 & I_{sc} & md & 0 \\ 0 & 0 & 0 & md & m & 0 \\ 0 & 0 & 0 & 0 & 0 & 0 \end{bmatrix}; \quad d = x_{sc} - x_{cm}$$



1D Beam analysis – Matrices assembly

Given the element stiffness and mass matrices, $[K^{[i]}]$ and $[M^{[i]}]$, respectively, one can obtain the global stiffness and mass matrix with the following assembly algorithm:

- 1) Initialize global matrices. Remember that, in this case, we have 3 degrees of freedom (DoFs) per node ($\theta, h, \gamma \equiv h'$). Therefore, the total number of DoFs, $N = 3(n + 1)$:

$$[\mathbf{K}] = [\mathbf{0}]_{N \times N}, \quad [\mathbf{M}] = [\mathbf{0}]_{N \times N}$$

- 2) For each element $i = \{1 \dots n\}$:

For each element node $a = \{1, 2\}$

For each degree of freedom $j = \{1 \dots 3\}$

$$p = 3 \times (a - 1) + j$$

$$I = 3 \times ([\mathbf{T}_n]^{(i,a)} - 1) + j$$

For each element node $b = \{1, 2\}$

For each degree of freedom $k = \{1 \dots 3\}$

$$q = 3 \times (b - 1) + k$$

$$J = 3 \times ([\mathbf{T}_n]^{(i,b)} - 1) + k$$

$$[\mathbf{K}]^{(I,J)} = [\mathbf{K}]^{(I,J)} + [\mathbf{K}^{[i]}]^{(p,q)}, \quad [\mathbf{M}]^{(I,J)} = [\mathbf{M}]^{(I,J)} + [\mathbf{M}^{[i]}]^{(p,q)}$$

Next k

Next b

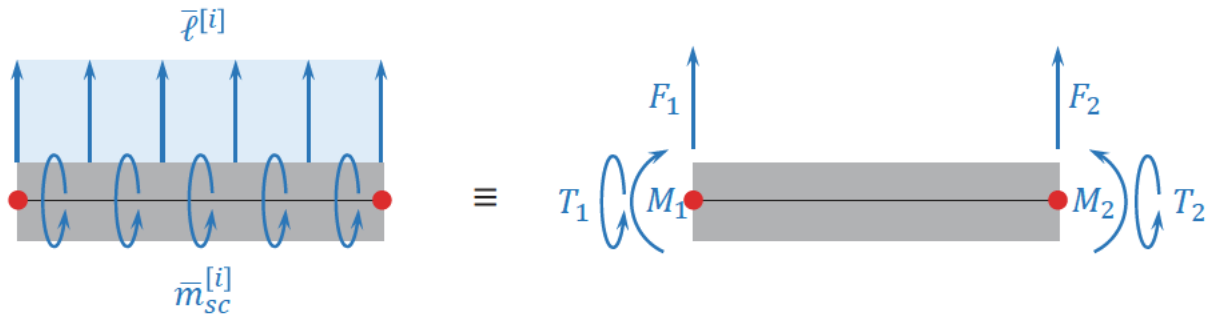
Next j

Next a

Next i



1D Beam analysis – Element force vector



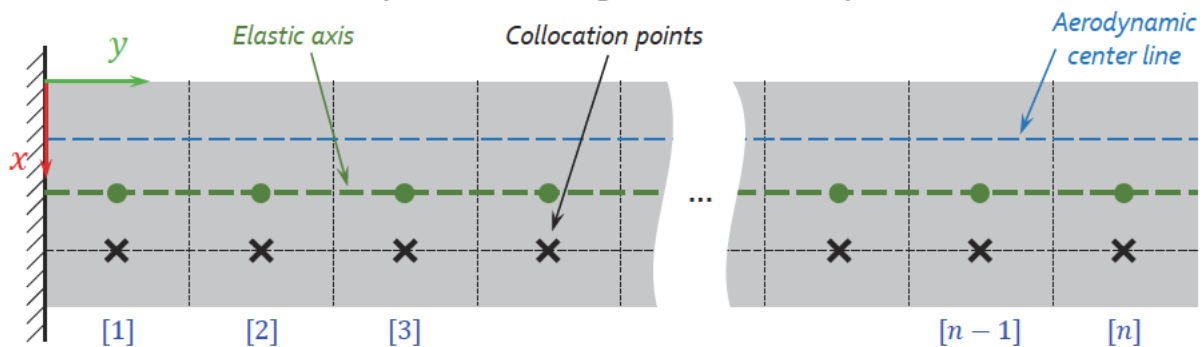
Force vector:

$$\{\mathbf{f}^{[i]}\} = \frac{l^{[i]}}{2} \begin{bmatrix} 0 & 1 \\ l^{[i]}/6 & 0 \\ 0 & 1 \\ 1 & 0 \\ -l^{[i]}/6 & 0 \end{bmatrix} \begin{Bmatrix} \bar{p}^{[i]} \\ \bar{m}_{sc}^{[i]} \end{Bmatrix}$$

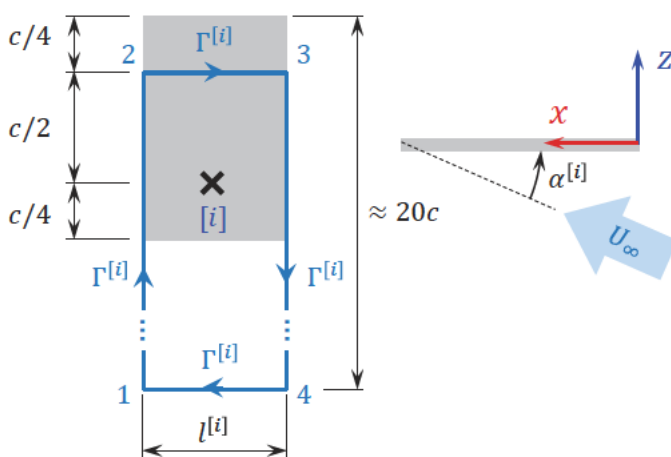
This information comes from the aerodynamic analysis!



Aerodynamics – Lifting-line surface analysis



Horseshoe element $[i]$:



Discretization:

- Surface area of the element: $S^{[i]}$
- Normal vector of the element: $\mathbf{n}^{[i]}$
- Coordinates of collocation point: $\mathbf{x}^{[i]}$

Kutta condition for each element:

$$\left(\sum_{j=1}^n (v_{12}^{[j]} + v_{23}^{[j]} + v_{34}^{[j]}) \Big|_{\mathbf{x}=\mathbf{x}^{[i]}} + \mathbf{U}_\infty \right) \cdot \mathbf{n}^{[i]} = 0$$

Aerodynamics – Lifting-line surface analysis

Induced velocity at point \mathbf{x} due to a vortex segment from \mathbf{x}_j to \mathbf{x}_k with vorticity $\Gamma^{[i]}$:

$$\mathbf{v}_{jk}^{[i]}(\mathbf{x}) = \frac{\Gamma^{[i]}}{4\pi} \frac{\mathbf{r}_j \times \mathbf{r}_k}{\|\mathbf{r}_j \times \mathbf{r}_k\|^2} \left(\frac{\mathbf{l}^{[i]} \cdot \mathbf{r}_j}{r_j} - \frac{\mathbf{l}^{[i]} \cdot \mathbf{r}_k}{r_k} \right); \quad \mathbf{r}_j = \mathbf{x} - \mathbf{x}_j; \quad \mathbf{l}^{[i]} = \mathbf{x}_k - \mathbf{x}_j$$

System of equations:

$$[\mathbf{A}]\{\Gamma\} = -U_\infty\{\alpha\}$$

$$\begin{bmatrix} A_{11} & A_{12} & \cdots & A_{1n} \\ A_{21} & A_{22} & \cdots & A_{2n} \\ \vdots & \vdots & \ddots & \vdots \\ A_{n1} & A_{n2} & \cdots & A_{nn} \end{bmatrix} \begin{Bmatrix} \Gamma^{[1]} \\ \Gamma^{[2]} \\ \vdots \\ \Gamma^{[n]} \end{Bmatrix} = -U_\infty \begin{Bmatrix} \alpha^{[1]} \\ \alpha^{[2]} \\ \vdots \\ \alpha^{[n]} \end{Bmatrix}$$

where $[\mathbf{A}]$ is the aerodynamic influence coefficients matrix:

$$A_{ij} = \left(\mathbf{v}_{12}^{[j]}(\mathbf{x}^{[i]}) + \mathbf{v}_{23}^{[j]}(\mathbf{x}^{[i]}) + \mathbf{v}_{34}^{[j]}(\mathbf{x}^{[i]}) \right) \Big|_{\Gamma^{[i]=1}} \cdot \mathbf{n}^{[i]}$$

Total lift on the element:

$$L^{[i]} = \rho_\infty U_\infty S^{[i]} \Gamma^{[i]} \quad \rightarrow \quad \{\mathbf{L}\} = -\rho_\infty U_\infty^2 [\mathbf{S}][\mathbf{A}]^{-1} \{\alpha\}; \quad [\mathbf{S}] = \begin{bmatrix} S^{[1]} & & 0 \\ & \ddots & \\ 0 & & S^{[n]} \end{bmatrix}$$



Systems coupling – Force vector assembly

- 1) Express the lift vector $\{\mathbf{L}\}$ in terms of the structural unknown vector $\{\mathbf{u}\}$. In this case, this means finding an interpolation matrix between $\{\alpha\}$ and $\{\mathbf{u}\}$. For our aerodynamic model:

$$\alpha^{[i]} = \theta^{[i]} = \frac{1}{2} \begin{bmatrix} 1 & 0 & 0 & 1 & 0 & 0 \end{bmatrix} \begin{Bmatrix} \theta^{(i)} \\ h^{(i)} \\ \gamma^{(i)} \\ \theta^{(i+1)} \\ h^{(i+1)} \\ \gamma^{(i+1)} \end{Bmatrix} = [\mathbf{I} \quad \mathbf{I}] \begin{Bmatrix} \mathbf{u}^{(i)} \\ \mathbf{u}^{(i+1)} \end{Bmatrix}$$

$$\{\alpha\} = \begin{Bmatrix} \alpha^{[1]} \\ \alpha^{[2]} \\ \vdots \\ \alpha^{[n]} \end{Bmatrix} = \begin{bmatrix} \mathbf{I} & \mathbf{I} & \mathbf{0} & \cdots & \mathbf{0} & \mathbf{0} \\ \mathbf{0} & \mathbf{I} & \mathbf{I} & \cdots & \mathbf{0} & \mathbf{0} \\ \vdots & \vdots & \vdots & \ddots & \vdots & \vdots \\ \mathbf{0} & \mathbf{0} & \mathbf{0} & \cdots & \mathbf{I} & \mathbf{I} \end{bmatrix} \begin{Bmatrix} \mathbf{u}^{(1)} \\ \mathbf{u}^{(2)} \\ \mathbf{u}^{(3)} \\ \vdots \\ \mathbf{u}^{(n)} \\ \mathbf{u}^{(n+1)} \end{Bmatrix} = [\mathbf{I}]\{\mathbf{u}\}$$

$$\{\mathbf{L}\} = -\rho_\infty U_\infty^2 [\mathbf{S}][\mathbf{A}]^{-1} [\mathbf{I}]\{\mathbf{u}\}$$



Systems coupling – Force vector assembly

- 2) Express each element's $\bar{\rho}^{[i]}$ and $\bar{m}_{sc}^{[i]}$ in terms of $L^{[i]}$. Since $L^{[i]}$ is the total lift on each element, we can express:

$$\begin{bmatrix} \bar{\rho}^{[i]} \\ \bar{m}_{sc}^{[i]} \end{bmatrix} = \frac{1}{l^{[i]}} \begin{bmatrix} 1 \\ e \end{bmatrix} L^{[i]}, \quad e = x_{sc} - x_{ac}$$

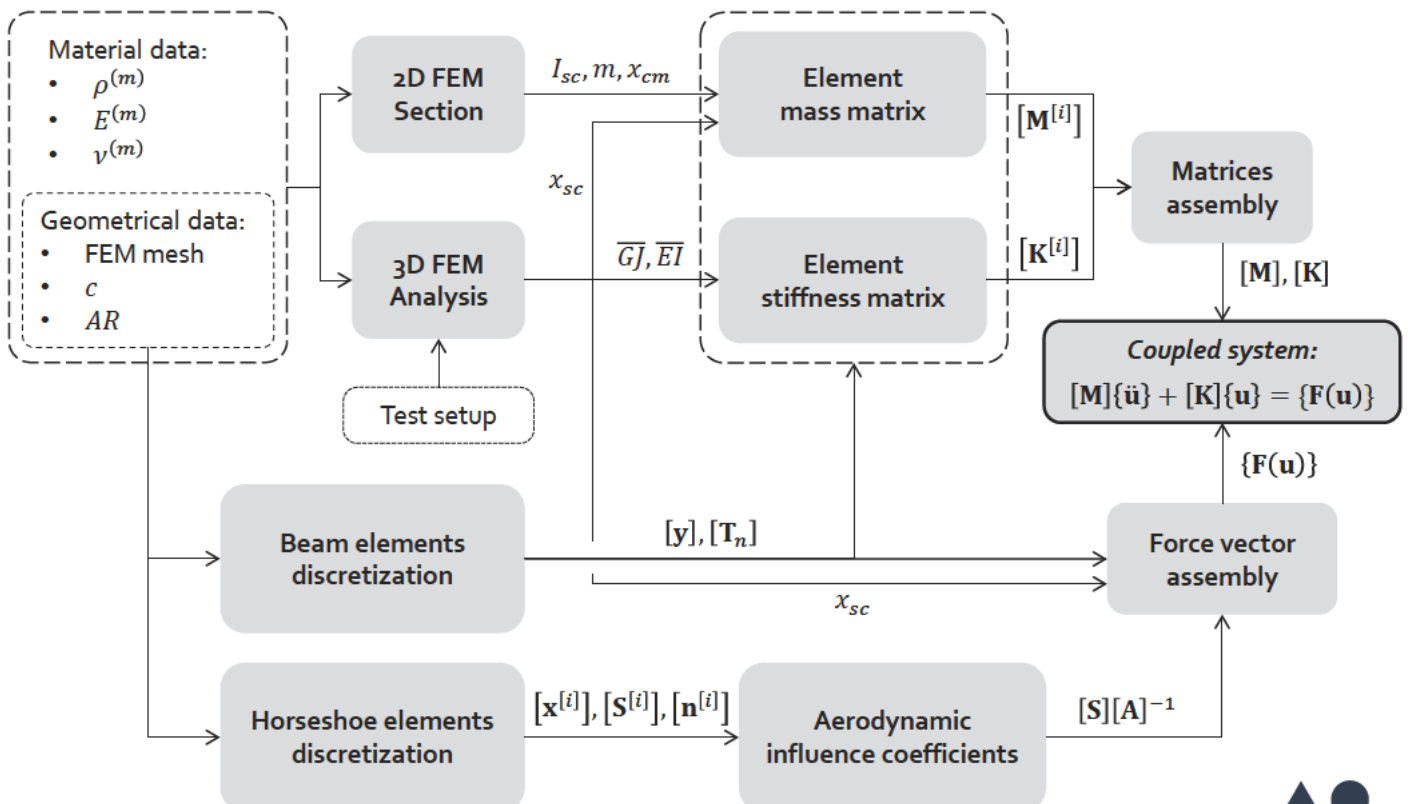
- 3) Obtain the element force assembly matrix:

$$\{f^{[i]}\} = \frac{l^{[i]}}{2} \begin{bmatrix} 0 & 1 \\ 1 & 0 \\ l^{[i]}/6 & 0 \\ 0 & 1 \\ 1 & 0 \\ -l^{[i]}/6 & 0 \end{bmatrix} \frac{1}{l^{[i]}} \begin{bmatrix} 1 \\ e \end{bmatrix} L^{[i]} = \frac{1}{2} \begin{bmatrix} e \\ 1 \\ l^{[i]}/6 \\ e \\ 1 \\ -l^{[i]}/6 \end{bmatrix} L^{[i]} \rightarrow \begin{Bmatrix} \mathbf{F}^{(i)} \\ \mathbf{F}^{(i+1)} \end{Bmatrix} = \frac{1}{2} \begin{bmatrix} \mathbf{Q}_1^{[i]} \\ \mathbf{Q}_2^{[i]} \end{bmatrix} L^{[i]}$$

$$\begin{Bmatrix} \mathbf{F}^{(1)} \\ \mathbf{F}^{(2)} \\ \mathbf{F}^{(3)} \\ \vdots \\ \mathbf{F}^{(n)} \\ \mathbf{F}^{(n+1)} \end{Bmatrix} = \frac{1}{2} \begin{bmatrix} \mathbf{Q}_1^{[1]} & \mathbf{0} & \dots & \mathbf{0} \\ \mathbf{Q}_2^{[1]} & \mathbf{Q}_1^{[2]} & \dots & \mathbf{0} \\ \mathbf{0} & \mathbf{Q}_2^{[2]} & \dots & \mathbf{0} \\ \vdots & \vdots & \ddots & \vdots \\ \mathbf{0} & \mathbf{0} & \dots & \mathbf{Q}_1^{[n]} \\ \mathbf{0} & \mathbf{0} & \dots & \mathbf{Q}_2^{[n]} \end{bmatrix} \begin{Bmatrix} L^{[1]} \\ L^{[2]} \\ \vdots \\ L^{[n]} \end{Bmatrix} \rightarrow \{\mathbf{F}(\mathbf{u})\} = \underbrace{-\frac{1}{2} \rho_\infty U_\infty^2 [\mathbf{Q}][\mathbf{S}][\mathbf{A}]^{-1}[\mathbf{I}]\{\mathbf{u}\}}_{q_\infty [\mathbf{K}_a]}$$



Coupled system flow diagram



Rúbrica Project

Item	Pes	Multiplicadors			Nota
		1	0.5	0	(pes x multiplicador)/
1) L'estudiant ha obtingut les característiques estructurals del perfil requerides per l'anàlisi.	1	Implementació correcta i resultats coherents	Esforç d'implementació amb algun error que condueix a resultats incorrectes	No s'aporten resultats ni implementació	A
2) L'estudiant ha implementat el model aerodinàmic proposat: obtenció de la matriu de coeficients d'influència.	0.5				B
3) L'estudiant ha implementat el model estructural proposat: obtenció de matrius de rigidesa i massa.	0.5				C
4) L'estudiant ha analitzat les condicions de divergència per diferents ratis d'aspecte de l'ala.	1				D
5) L'estudiant ha obtingut els modes associats a les condicions de divergència per diferents ratis d'aspecte de l'ala.	1				E
6) L'estudiant ha estudiat les condicions de flutter.	1				F
4) Aspectes de qualitat de l'informe	1	Compleix criteris de rigor, precisió i concisió en la presentació de resultats		No compleix els criteris de rigor, precisió i concisió en la presentació de resultats	G
5) Criteris d'excel·lència valorables	1.5	Plantejament teòric detallat de l'anàlisi de flutter (+0.5); Estudi de convergència numèrica/sensibilitat (+0.33); Altres configuracions d'ala (+0.33 per estudi extra). Màxim multiplicador (1).			H
Nota final (0-10)				(A+B+C+D+E+F+G)/0.75	



Setup of a virtual laboratory for studying aeroelastic problems

C. A. [REDACTED], C. N. [REDACTED]

Polytechnic University of Catalonia, Master's program in Aeronautical Engineering

Abstract—This project is designed for the study of aeroelastic problem through setup of a virtual laboratory. Basically, the goal is to implement a set of MATLAB functions to perform different kinds of aeroelastic analysis. These analysis could be the observation of divergence conditions, flutter study, unsteady aerodynamics, etc.

Key words—Aeroelasticity, wing, flutter, FEM, aerodynamics, horseshoe, Theodorsen.

1. INTRODUCTION

The setup of a virtual laboratory is carried out through this project to study the aeroelastic problems. In order to do so, it is required to use a set of MATLAB functions to conduct the analysis for different aeroelastic cases. These cases include divergence conditions, study of flutter, unsteady aerodynamics, etc.

The structural code requirement uses 3D FEM code to obtain effective properties where the MATLAB implementation is based on beam's FEM algorithm. The part of the steady aerodynamics condition and unsteady aerodynamics require the MATLAB code implementation of lifting-line solution by horseshoe element and Theodorsen's model respectively. The third part of this project is related to coupling that is carried out through transfer matrices. These matrices transfer the structural output (displacement vector) to aerodynamic input (angle of attack) and aerodynamic output (lift distribution) to structural input (force vector). Once computed the previous requirements successfully, a solver computes the divergence speed, modes and flutter speed.

2. PROBLEM DEFINITION

The definition of the problem relies on 3D FEM analysis of a wing that goes through experimental structural tests. The airfoil chosen for the computation of this wing is NACA0012. The material properties are shown on the Table 1.

Initially the chord of NACA0012 is considered 1 and the span is $b=5c$. This value of chord changes along the study of this problem in order to observe the influence of aspect ratio.

MATERIAL PROPERTIES

Material	ρ [$kg \cdot m^{-3}$]	E [GPa]	ν
Skin	2000	9	0.27
Spars	1800	1500	0.30
Stringers	2300	70	0.35

TABLE 1: Wing's Material properties

3. METHODOLOGY

A. Structural analysis

The goal of this first structural analysis is to obtain the shear centre position X_{sc} , the torsional stiffness GJ and the bending stiffness EI of a NACA0012 airfoil. The model of the airfoil is formed by hexahedral elements that gives more accuracy than using tetrahedras.

The starting point of the finite element code is to use a code already build that simulates what would be an experimental analysis of a wing, it has as input the loads where the forces will be applied and the magnitude. It also reads the displacement measure locations, the places of interest to locate the sensors in order to measure the displacement.

This FEM Analysis assumes small displacements and deformations, that implies also small angles and linear elasticity. The second hypothesis is that the effective response can be described by the elemental beam theory:

$$\begin{Bmatrix} T \\ M \end{Bmatrix} = \underbrace{\begin{bmatrix} \overline{GJ} & 0 \\ 0 & EI \end{bmatrix}}_{[E]} \begin{Bmatrix} d\theta/dy \\ d^2h/dy^2 \end{Bmatrix} \quad (1)$$

Here, torsion is related to the twist change although the span of the wing and the bending moment is related to the second derivative of the wing deflection. Both parameters, as the section profile is the same, will be assumed constant along the wing span and assumed uncoupled. This hypothesis will be verified in Section 4.

Since in this problem loads are being imposed and the resulting displacements are measured, the constitutive relation can be

written as:

$$\begin{Bmatrix} \bar{\theta}' \\ \bar{h}'' \end{Bmatrix} = \underbrace{\begin{bmatrix} S_{11} & S_{12} \\ S_{21} & S_{22} \end{bmatrix}}_{[\mathbf{E}]^{-1}} \begin{Bmatrix} T \\ M \end{Bmatrix} \quad (2)$$

This constitutive relation allows the user to apply pure torsional load ($M = 0$) and obtain the uncoupled effect on the twist angle and the wing deflection. It also allows the application of a pure bending load ($T = 0$) to obtain the rest of the coefficients.

Applying pure torsional load ($M = 0$) it is easy to compute:

$$S_{11} = \bar{\theta}'/T, \quad S_{21} = \bar{h}''/T \quad (3)$$

Instead of a bending load, a pure shear load ($M = 0$, $M' = -Q$) is be applied:

$$S_{12} = \bar{\theta}'/M = -\bar{\theta}''/Q, \quad S_{22} = \bar{h}''/M = -\bar{h}'''/Q \quad (4)$$

It is important to recall that the shear and bending are related so that the derivative of the bending is the shear.

To do so, the torsional load will be applied imposing two forces with the same magnitude in opposite directions separated by a certain distance. A pure shear load means a load in a specific point in a beam that does not cause torsion. This specific point is the shear centre calculated previously.

The program has a particularity that prevents the application of loads at any point and they need to be applied at predefined nodes. In order to apply forces at non existing nodes, the methodology will be the following: apply a force in a specific node accompanied by a torsional moment (same load in opposite directions in separate nodes). This is useful to compute the shear centre.

The points selected by the user to apply forces or measure displacements cannot be chosen randomly. The element that carries the structural resistance is spar because skin is too thin to have a resistance. Therefore, the point where the forces are applied are located at the spars. The measurement points will be enough to have a accurate value on the rotation and deflection.

Once the torsional stiffness \overline{GJ} and the bending stiffness are obtained, \overline{EI} the next step is to perform another numerical analysis in order to define the section properties. To do so, the wing section is discretized in 224 elements contained in the following matrices:

- Nodal coordinates $[\mathbf{x}]$: this matrix contains the x, y, z coordinates of each node.
- Nodal connectivity $[\mathbf{T}_n]$: This matrix tells us which element is connected to which node.
- Material properties $[\mathbf{m}]$: this matrix contain the density of each material.
- Material's connectivity $[\mathbf{T}_m]$: This matrix tells us which element is connected to which material.

The determination of the section properties is given by the following procedure:

- 1) Obtain the coordinates and the material of each element.
- 2) Determine the centroid coordinates of each element.
- 3) Determine the area of each element.

With this information, it is easy to compute:

- 1) The mass per unit length

$$m = \sum_e \rho^{[e]} A^{[e]} \quad (5)$$

- 2) The centre of mass

$$\mathbf{x}_{cm} = \frac{1}{m} \sum \mathbf{x}^{[e]} \rho^{[e]} A^{[e]} \quad (6)$$

- 3) The inertia about the shear centre per unit length.

$$I_{sc} = \sum_e \left(x^{[e]} - x_{sc} \right)^2 \rho^{[e]} A^{[e]} \quad (7)$$

The next step is to discretize the wing into beam elements as shown in Figure 1.

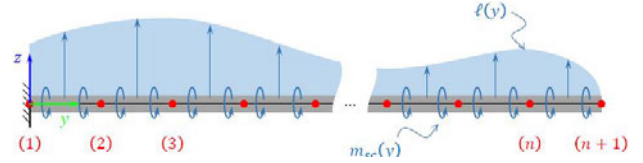


Fig. 1: 1D Beam

With this discretization, the unknowns will be located at each node. Imposing equilibrium in each element the equilibrium equation can be written as:

$$[\mathbf{M}^{[i]}] \{ \ddot{\mathbf{u}}^{[i]} \} + [\mathbf{K}^{[i]}] \{ \mathbf{u}^{[i]} \} = \{ \mathbf{f}^{[i]} \} \quad (8)$$

Where $\{ \mathbf{u} \}$ contains the 3 defined degrees of freedom of the problem (the elastic twist θ , deflection h and rotation about the x-axis γ).

$$\{ \mathbf{u}^{[i]} \} = \begin{Bmatrix} \theta^{(i)} \\ h^{(i)} \\ \gamma^{(i)} \\ \theta^{(i+1)} \\ h^{(i+1)} \\ \gamma^{(i+1)} \end{Bmatrix}; \quad \{ \mathbf{f}^{[i]} \} = \begin{Bmatrix} T_1^{[i]} \\ F_1^{[i]} \\ M_1^{[i]} \\ T_2^{[i]} \\ F_2^{[i]} \\ M_2^{[i]} \end{Bmatrix} \quad (9)$$

There will be a Torsion T , a shear load F and a Bending moment M associated to each degree of freedom. To solve the system, it is necessary to compute the stiffness matrix and the mass matrix. The expression of the stiffness matrix is formed by two sub-matrices, one containing the torsional stiffness (computed previously) and the other containing the effective bending stiffness. The mass matrix is computed using the lumped approach with the values computed in the previous analysis.

Given the element stiffness matrix and mass matrices $[\mathbf{K}^{[i]}]$ and $[\mathbf{M}^{[i]}]$, respectively, the global stiffness and mass matrices can be calculated using the developed MATLAB algorithm.

Finally, the force vector will be discussed in the aerodynamic part. As shown in Figure 2, a constant lift distribution for each beam element $\bar{l}^{[i]}$ and a constant torsion moment distribution $\bar{m}_{sc}^{[i]}$ will be assumed.

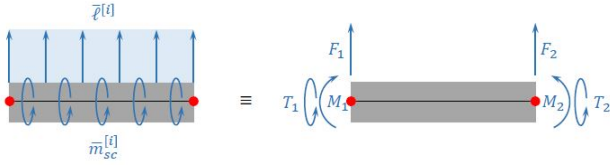


Fig. 2: Element force

Similarly to process followed in mass, the force will be separated into two load points, this relation is given in the following matrix:

$$\{\mathbf{f}^{[i]}\} = \frac{l^{[i]}}{2} \begin{bmatrix} 0 & 1 \\ 1 & 0 \\ l^{[i]}/6 & 0 \\ 0 & 1 \\ 1 & 0 \\ -l^{[i]}/6 & 0 \end{bmatrix} \begin{Bmatrix} \bar{\ell}^{[i]} \\ \bar{m}_{sc}^{[i]} \end{Bmatrix} \quad (10)$$

The half of the contribution is given to each node by multiplying the beam length and dividing by 3. This is, in fact, the interpolation of coupling between the aerodynamic and the structural part.

B. Aerodynamic analysis

The aerodynamic analysis requires a couple of pre-processes in the computation. The first step is the discretization of the panel to develop a coherent relation with beam element from the structural analysis. The association between the structural and aerodynamic degrees of freedom DoF is implemented. The unknown variables in the aerodynamic analysis are the vortex intensities $\Gamma^{[i]}$ shown of the following figure 3 as vortex lines.

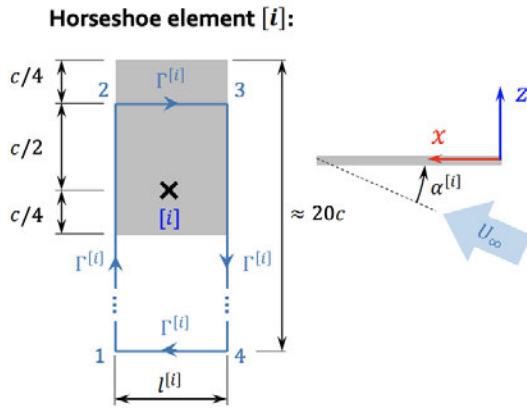


Fig. 3: Horseshoe element [i]: Vortex lines

The Horseshoe element refers to the effect of the vorticity from node 4 to 1 is considered far from the body, which leads this parameter to be null. The distance of the contribution of this vorticity, from the section's leading edge, is big enough ($\approx 20c$) to neglect its effect. Therefore, the horseshoe element considers the other three vorticities and places the vortex at $c/4$, the aerodynamic centre. The Kutta condition is applied at the collocation point 'x' shown on figure 3, at $3c/4$ of the section.

The numerical analysis is based on the discretization of the panel obtaining the effective area of each discretized section or panel $S^{[i]}$, a vertical normal vector for each panel $n^{[i]}$ and the coordinates of the collocation point $x^{[i]}$. The intensity of the vortex lines come from applying the Kutta condition (11) at each collocation point. As the U_∞ is deviated at a certain angle (elastic twist, θ_i), the projection of the corresponding axis is calculated and this links the structural part and aerodynamic part.

$$\left(\sum_{j=1}^n (v_{12}^{[j]} + v_{23}^{[j]} + v_{34}^{[j]}) \right) \Big|_{\mathbf{x}=\mathbf{x}^{[i]}} + \mathbf{U}_\infty \cdot \mathbf{n}^{[i]} = 0 \quad (11)$$

Induced velocity at point \mathbf{x} due to a vortex segment from x_j to x_k with vorticity $\Gamma^{[i]}$ is calculated as follows:

$$\mathbf{v}_{jk}^{[i]}(\mathbf{x}) = \frac{\Gamma^{[i]}}{4\pi} \frac{\mathbf{r}_j \times \mathbf{r}_k}{\|\mathbf{r}_j \times \mathbf{r}_k\|^2} \left(\frac{\mathbf{l}^{[i]} \cdot \mathbf{r}_j}{r_j} - \frac{\mathbf{l}^{[i]} \cdot \mathbf{r}_k}{r_k} \right) \quad (12)$$

$$\mathbf{r}_j = \mathbf{x} - \mathbf{x}_j; \quad \mathbf{l}^{[i]} = \mathbf{x}_k - \mathbf{x}_j \quad (13)$$

The system of equations is:

$$[A]\{\Gamma\} = -U_\infty\{\alpha\} \quad (14)$$

Where [A] is the aerodynamic influence coefficients matrix:

$$A_{ij} = \left(v_{12}^{[j]}(\mathbf{x}^{[i]}) + v_{23}^{[j]}(\mathbf{x}^{[i]}) + v_{34}^{[j]}(\mathbf{x}^{[i]}) \right) \Big|_{\Gamma^{[i]}=1} \cdot \mathbf{n}^{[i]} \quad (15)$$

Finally, the total lift as a function of $\{\alpha\}$ and U_∞ on the element is:

$$\{\mathbf{L}\} = -\rho_\infty U_\infty^2 [\mathbf{S}][\mathbf{A}]^{-1}\{\alpha\} \quad (16)$$

Where [S] is:

$$[\mathbf{S}] = \begin{bmatrix} S^{[1]} & & 0 \\ & \ddots & \\ 0 & & S^{[n]} \end{bmatrix} \quad (17)$$

The expression of lift can also be built as a function of q_∞ instead of U_∞ because it is the main variable that the problem is looking for. In that case, lift would be:

$$\{\mathbf{L}\} = -2q_\infty [\mathbf{S}][\mathbf{A}]^{-1}\{\alpha\} \quad (18)$$

C. System's coupling

The study of coupling effect in the system requires the assembly of three vectors. The first vector is based of expression the lift vector $\{\mathbf{L}\}$ in terms of the structural unknown vector $\{\mathbf{u}\}$. This is obtained finding the interpolation matrix between $\{\alpha\}$ and $\{\mathbf{u}\}$. For the expression of Lift, the positions that contain θ in the displacement vector, is related to α .

$$\begin{Bmatrix} \alpha^{[1]} \\ \alpha^{[2]} \\ \vdots \\ \alpha^{[n]} \end{Bmatrix} = \begin{bmatrix} \mathbf{I} & \mathbf{I} & \mathbf{0} & \dots & \mathbf{0} & \mathbf{0} \\ \mathbf{0} & \mathbf{I} & \mathbf{I} & \dots & \mathbf{0} & \mathbf{0} \\ & \vdots & & \ddots & \vdots & \\ \mathbf{0} & \mathbf{0} & \mathbf{0} & \dots & \mathbf{I} & \mathbf{I} \end{bmatrix} \begin{Bmatrix} \mathbf{u}^{(1)} \\ \mathbf{u}^{(2)} \\ \mathbf{u}^{(3)} \\ \vdots \\ \mathbf{u}^{(n)} \\ \mathbf{u}^{(n+1)} \end{Bmatrix}$$

Substituting the previous expression of α to the expression of Lift obtained in equation (16), the vector of lift is computed for coupling system:

$$\{\mathbf{L}\} = -\rho_{\infty} U_{\infty}^2 [\mathbf{S}][\mathbf{A}]^{-1} [\mathbf{I}]\{\mathbf{u}\} \quad (19)$$

The second vector has the average value of constant lift distribution $\bar{l}^{[i]}$ and the effective torsional moment contribution about shear centre $\bar{m}_{sc}^{[i]}$ in terms of $L^{[i]}$ (the total lift of each panel).

$$\begin{bmatrix} \bar{\ell}^{[i]} \\ \bar{m}_{sc}^{[i]} \end{bmatrix} = \frac{1}{l^{[i]}} \begin{bmatrix} 1 \\ e \end{bmatrix} L^{[i]} \quad (20)$$

where e is:

$$e = x_{sc} - x_{ac} \quad (21)$$

The element force assembly matrix is computed inserting the expression (20) into the expression (10). This way, the force of two nodes of each element is related. Now that, all the equations are sorted, the coupling effect between structural and aerodynamic part is obtained simply computing the following general equation of Force where each couple of $Q^{[i][i]}$ in column belongs to a specific element:

$$\begin{Bmatrix} \mathbf{F}^{(1)} \\ \mathbf{F}^{(2)} \\ \mathbf{F}^{(3)} \\ \vdots \\ \mathbf{F}^{(n)} \\ \mathbf{F}^{(n+1)} \end{Bmatrix} = \frac{1}{2} \begin{bmatrix} \mathbf{Q}_1^{[1]} & \mathbf{0} & \dots & \mathbf{0} \\ \mathbf{Q}_2^{[1]} & \mathbf{Q}_1^{[2]} & \dots & \mathbf{0} \\ \mathbf{0} & \mathbf{Q}_2^{[2]} & \dots & \mathbf{0} \\ \vdots & \vdots & \ddots & \vdots \\ \mathbf{0} & \mathbf{0} & \dots & \mathbf{Q}_1^{[n]} \\ \mathbf{0} & \mathbf{0} & \dots & \mathbf{Q}_2^{[n]} \end{bmatrix} \begin{Bmatrix} L^{[1]} \\ L^{[2]} \\ \vdots \\ L^{[n]} \end{Bmatrix} \quad (22)$$

Therefore, final expression of Force is:

$$\{\mathbf{F}(\mathbf{u})\} = -\underbrace{\frac{1}{2}\rho_{\infty} U_{\infty}^2 [\mathbf{Q}][\mathbf{S}][\mathbf{A}]^{-1} [\mathbf{I}]}_{q_{\infty} [\mathbf{K}_a]} \{\mathbf{u}\} \quad (23)$$

D. Flutter analysis

One of the most extensively used in aerodynamic models, capable to explain flutter induced instabilities, was developed by Theodorsen back in 1935. The goal of this section is to introduce the flutter condition in this dynamic system which means finding the appropriate set of solutions for the elastic twist and the plunch. Typically, the solutions have a harmonic shape. There are two unknowns for two equations that equalized to zero the real and the imaginary part of the determinant. The involvement of aerodynamics lead to a

non linear equation to solve a numerical approach, Newton Raphson method.

The aerodynamic expressions for the lift and moment are given by a Theodorsen function that accounts for attenuation phenomena in the lift and moment due to the wake vorticity. It is a non-dimensional parameter that is defined by a H function and a reduced frequency which is a non dimensional frequency:

$$C(\kappa) = \frac{H_1^{(2)}(\kappa)}{H_1^{(2)}(\kappa) + iH_0^{(2)}(\kappa)}, \quad \kappa = \frac{\omega b}{U_{\infty}} \quad (24)$$

Instead of working with previous expression, the following one has already been developed:

$$C(\kappa) = 1 - \frac{0.165}{1 - i\frac{0.0455}{\kappa}} - \frac{0.335}{1 - i\frac{0.3}{\kappa}} \quad (25)$$

That can be expressed as: $C(\kappa) = F(\kappa) + iG(\kappa)$

$$F(\kappa) = \frac{0.5\kappa^4 + 0.0765\kappa^2 + 1.8632 \times 10^{-4}}{\kappa^4 + 0.0921\kappa^2 + 1.8632 \times 10^{-4}} \quad (26)$$

$$G(\kappa) = \frac{-0.1080\kappa^3 - 8.8374 \times 10^{-4}\kappa}{\kappa^4 + 0.0921\kappa^2 + 1.8632 \times 10^{-4}} \quad (27)$$

Introducing this expression in our system of equations one can get:

$$\begin{Bmatrix} m_{sc}^{[i]} \\ \ell^{[i]} \end{Bmatrix} = \pi\rho_{\infty} b^2 U_{\infty}^2 \left([\hat{\mathbf{A}}_R(\kappa)] + i [\hat{\mathbf{A}}_I(\kappa)] \right) [\mathbf{I} \quad \mathbf{I}] \begin{Bmatrix} \hat{\mathbf{u}}^{(i)} \\ \hat{\mathbf{u}}^{(i+1)} \end{Bmatrix} \quad (28)$$

And the element force vector becomes:

$$\{\mathbf{f}^{[i]}\} = b \begin{bmatrix} \hat{\mathbf{Q}}_1^{[i]} \\ \hat{\mathbf{Q}}_2^{[i]} \end{bmatrix} \begin{Bmatrix} m_{sc}^{[i]} \\ \ell^{[i]} \end{Bmatrix} \quad (29)$$

It is assumed that the degree of freedom referring to the vertical displacement, h , is non-dimensionalized by the half-chord, b , when writing $\hat{\mathbf{u}}^{[i]}$. Additionally, to make the units consistent, all equations referring to forces are multiplied by b . In practice, this means that $l^{[i]} = \ell^{[i]}/b$ in the definition of $\hat{\mathbf{Q}}$ and that rows and columns of both $[\mathbf{K}]$ and $[\mathbf{M}]$ corresponding to the second degree of freedom of each node, must be multiplied by b .

Doing algebra manipulations and applying the boundary conditions the system yields:

$$\underbrace{\left([\hat{\mathbf{K}}_{LL}]^{-1} [\hat{\mathbf{M}}_{LL}] + \frac{1}{\mu\kappa^2} [\hat{\mathbf{K}}_{LL}]^{-1} [\hat{\mathbf{F}}_{LL}(\kappa)] - \lambda[\mathbf{1}] \right)}_{[\hat{\mathbf{D}}_{LL}(\kappa)]} \{\hat{\mathbf{u}}\} = \{0\}$$

And the flutter condition is given by:

$$\det \left([\hat{\mathbf{D}}(\kappa_F)] - \lambda_F[\mathbf{1}] \right) = 0 \quad (30)$$

E. Code development

The code developed to perform this structural analysis has the following structure:

1) Inputs and test set up:

- Material data: ρ^m , E^m , ν^m .
- Geometrical data: FEM mesh, c , AR;

- 2) 3D FEM Analysis.
 - a) Find the shear centre.
 - b) Apply pure torsional load.
 - c) apply pure shear load.
 - d) Compute \overline{GJ} and \overline{EI} .
- 3) 2D FEM Section.
 - a) Compute the section properties: I_{sc} , m , x_{cm} .
- 4) Element mass and element stiffness matrix computation.
- 5) Beam elements discretization.
- 6) Horseshoe elements discretization.
- 7) Aerodynamic influence coefficients.
- 8) System coupling.
- 9) Final calculations and print results.

4. RESULTS

The results of the first structural analysis are not very accurate, this is due to the coarse mesh used for our computational cost limitations. It has been checked that the memory required grows exponentially with the number of elements used.

To get the shear centre position X_{sc} , the torsional stiffness GJ and the bending stiffness EI of the airfoil some loads have been applied. The first load applied is a pure torsional load. It has been imposed two forces with the same magnitude in opposite directions separated a certain distance, the selected points are the location of the ribs, $0.25*c$ and $0.6*c$, both at the section located at the span. Figure 4 shows the undeformed wing before applying the forces.

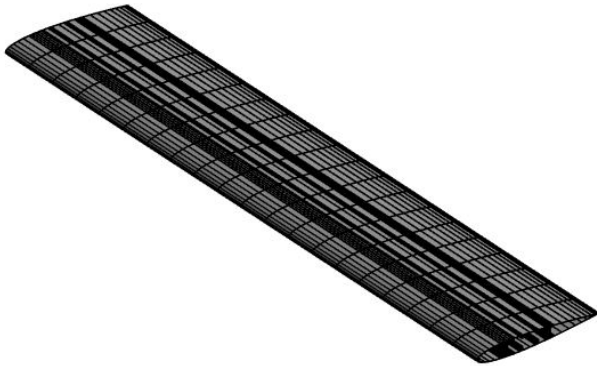


Fig. 4: Undeformed wing

Figure 5 shows the deformed shape of a section when applying torsional load of a magnitude $F = 24522$ N. It's possible to appreciate the deformation done by the forces applied in opposite directions

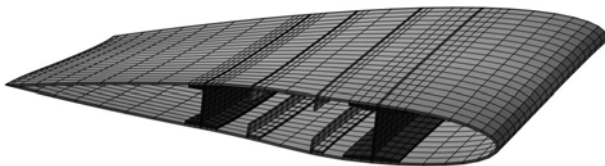


Fig. 5: Deformed wing

Additionally, Figure 6 and Figure 7 shows the elastic twist and the deflection of the wing along the span. It can be seen that, as expected, both varies linearly. In addition, the twist angle is equal to zero at the root of the wing which validates the code.

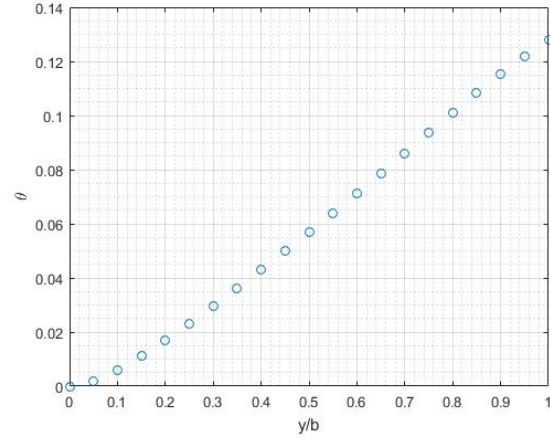


Fig. 6: Twist along the span

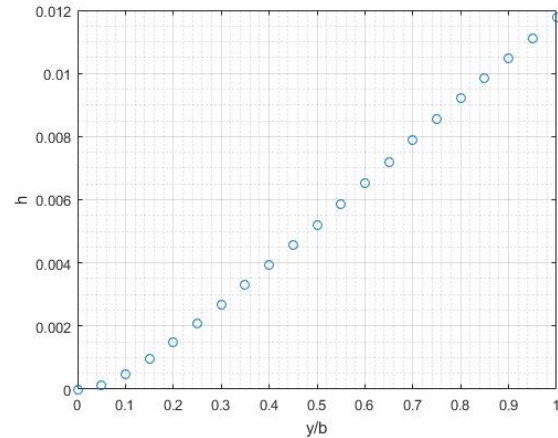


Fig. 7: Deflection along the wing

The firsts constitutive relation terms can be obtained by doing the first derivative of the twist and the deflection:

$$S_{11} = \bar{\theta}' = 3.1408e - 06; \quad (31)$$

$$S_{21} = \bar{h}'' = 2.2423e - 08; \quad (32)$$

The next step was to obtain the shear centre Applying a force in a specific node accompanied by a torsional moment. Results are shown the the Figure 8, it shows the twist angle distribution when applying different forces, from this plot the shear centre has been obtained by interpolating and finding the point where the twist is equal to zero. The point found is:

$$x_{sc} = 0.3521$$

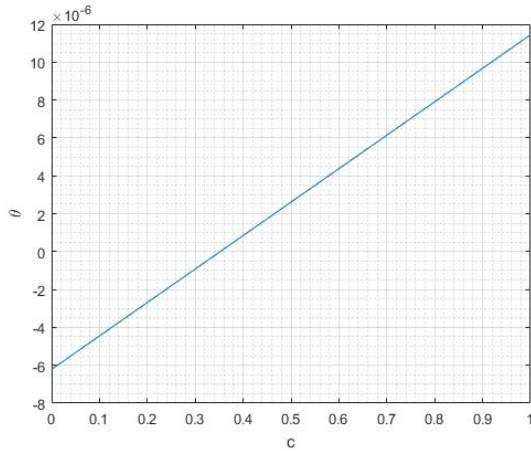


Fig. 8: Twist along the chord

The last coefficients have been obtained applying pure shear load, to do so, a force has been imposed at the shear centre, it can be checked that the twist is at the order of 10^{-8} which is practically zero. Figure 9 shows the deformed wing when applying the force.



Fig. 9: Deformed wing

The last two constitutive relation terms can be obtained by doing the first derivative of the twist and the second derivative of the deflection:

$$S_{12} = \bar{\theta}' = -5.3501e - 09; \quad (33)$$

$$S_{22} = \bar{h}'' = 1.1626e - 06; \quad (34)$$

With all the constitutive terms the E matrix is obtained by doing the inverse:

$$[\mathbf{E}] = \begin{bmatrix} 3.18e + 05 & 1.46e + 03 \\ -6.14e + 03 & 8.60e + 05 \end{bmatrix} \quad (35)$$

And, the torsional stiffness GJ and the bending stiffness EI :

$$\overline{GJ} = 318\text{KNm}^2$$

$$\overline{EI} = 860\text{KNm}^2$$

It is observed that the hypothesis done previously that there is no coupling between the torsion (T) and the bending moment (M), the order of magnitude of the coupling terms are low but not enough to be considered negligible.

Figure 10 shows the wing section discretized in 224 element that corresponds with a different colour, each element contains 5 nodes. The blue dot represents the position of the canter of mass. The properties of the section are described in the Table 2.

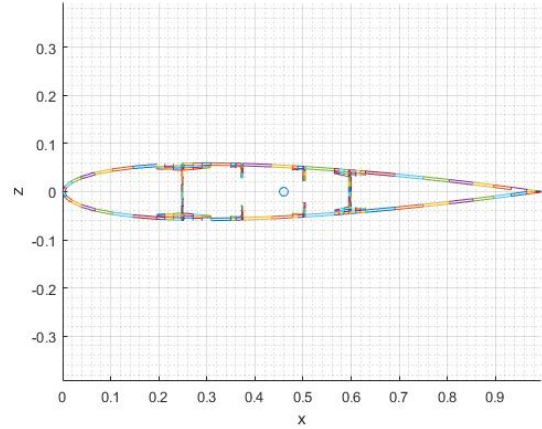


Fig. 10: Discretized wing section

Total mass	Mass center	Inertia
28.1590 Kg	x = 0.46 m	$I_x = 2.19\text{Kgm}^2$
	y = 0 m	$I_y = 0$
	z = 0 m	$I_z = 0.05\text{kgm}^2$

TABLE 2: Section properties

As explained in section 3.2, the aim of the aerodynamic part of this project is to obtain Lift force following the series of equations shown in the same section. In order to obtain this force, it is required to compute the matrices [A] and [S] and define the parameters U_∞ and ρ .

For the calculation of the coefficients of the matrix [A] it is considered that the segment 4-1 is far away and, as a consequence, its induced velocity is negligible. As there are three different segments to work with, according to the Horseshoe element, x_j and x_k take different values depending on the induced velocity of the segment in question. Applying this criteria, the following result([A] matrix (4) computed for 5 elements) is obtained. It can be observed that for each column and row of the matrix [A], the values change. The diagonal terms refer to the data of the same element. The matrix [S] (36) is also computed for 5 elements in order to make it computationally compatible with [A]. Finally, Lift force is obtained for each element applying the equation (16).

$$[\mathbf{A}] = \begin{bmatrix} -0.768 & 0.163 & 0.026 & 0.010 & 0.005 \\ 0.163 & -0.768 & 0.163 & 0.026 & 0.010 \\ 0.026 & 0.163 & -0.768 & 0.163 & 0.026 \\ 0.010 & 0.026 & 0.163 & -0.768 & 0.163 \\ 0.005 & 0.010 & 0.026 & 0.163 & -0.768 \end{bmatrix}$$

$$[\mathbf{S}] = \begin{bmatrix} 1 & 0 & 0 & 0 & 0 \\ 0 & 1 & 0 & 0 & 0 \\ 0 & 0 & 1 & 0 & 0 \\ 0 & 0 & 0 & 1 & 0 \\ 0 & 0 & 0 & 0 & 1 \end{bmatrix} \quad (36)$$

Once the relevant parameters and matrices are computed, the study of the problem takes another step forward and leads to the data that defines the eigenvalues and eigenvectors. The

matrices computed during the computational process, lead to the determination of divergence condition which is one of the aims targeted in this project. Since the matrices [K], [Q], [S], [A] and [I] are known, the matrix [Ka] can be determined without further complication. The expression of $\{F(u)\}$, equation (23) is easily calculated as a function of q_∞ and $\{u\}$ is the displacement vector(unknown). As the problem is being resolved in homogeneous approach, the right side of the equation (23) is zero. The first approach to solve this part is to remove the fixed degrees of freedom (in this case the first three) which belong to the first three rows and the first three columns of [K] and [Ka]. The results auto-values correspond to $-1/q_\infty$.

Using the modes of the auto-values that are not nulls, the divergence velocity is calculated through the dynamic pressure: $qD = -1/L(2(n+1))$ where n is the number of elements or panels. The values of the divergence speed are stored in L and the order goes from the smallest value to biggest value in negative. The smallest value is the one that marks the minor divergence velocity in the vector of L. The dynamic pressure is:

$$qD = 9.962 \cdot 10^5 \text{ Pa}$$

Using the following expression, the divergence velocity is calculated:

$$q_\infty = \frac{1}{2} \rho_\infty U_\infty^2$$

$$\text{DivergenceVelocity} = 1.2625 \cdot 10^3 \text{ m/s}$$

The results of the eigenvectors and eigenvalues are ordered in a specific way as seen in the case of divergence speed. Usually, these values go from the highest to lowest. The exception happens when there are zeros and they are relocated to the first positions, because they are singular modes of the matrix, gathering the real numbers together. In this problem, due to the type of aerodynamic loads (influenced by just torsional load) and structurally, the torsion and flexion are uncoupled which means that the degrees of freedom related to flexion are singular. This explains the resulting matrix with 2/3 of columns of zeros.

The autovector stores different modes in column where the twist θ , deflexion h and rotation γ are grouped in this order (the first one is torsion and the last two are flexion).

However, the first five modes are represented on the Figure 11. The eigenvector of twist, first degree of freedom, is plotted as a function of normalized span b. As observed, the mode 1 is uniformly distributed while the rest of the modes follow a sinus or cosine function. As the Figure shows the different modes of deformed wing are coherent with the type of aerodynamic loads applied. There are sinusoidal modes because it is like the decomposition in Fourier series of the degrees of freedom or rotation. The higher order modes oscillate more than lower order modes. In order to fulfil the boundary condition $y=0$, a zero has been inserted in the first position.

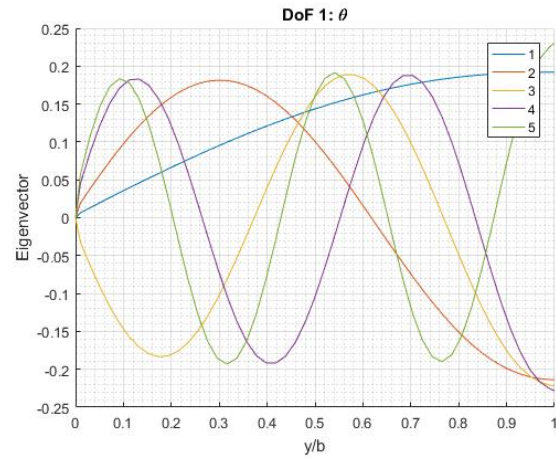


Fig. 11: Modes of the DoF 1

The Figure 12 shows the second degree of freedom that indicates deflexion and follows the same criteria than the first degree of freedom.

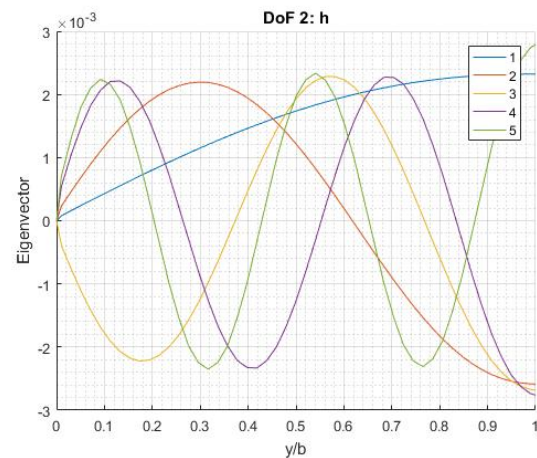


Fig. 12: Modes of the DoF 2

Finally the figure 13 shows the third degree of freedom that is linked to the rotation about x-axis.

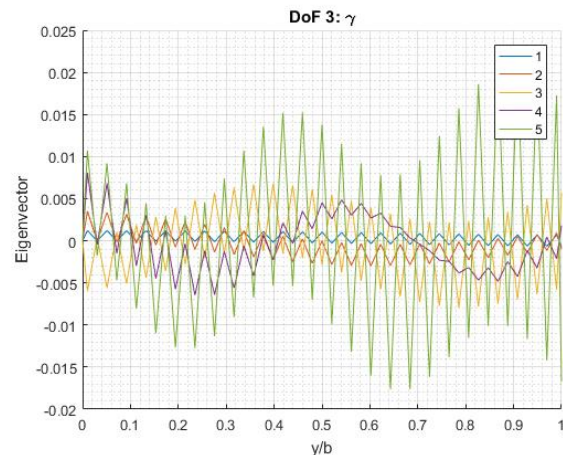


Fig. 13: Modes of the DoF 3

The following Figure 14 is the result of a test ran for different aspect ratio of the wing. By means of observation, it can be stated that the divergence speed decreases as the aspect ratio increases.

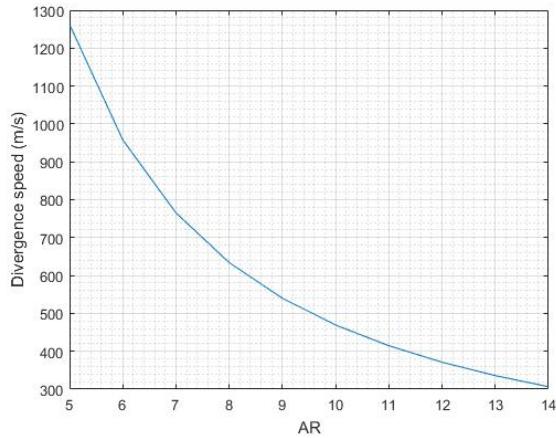


Fig. 14: Divergence speed vs Aspect Ratio

The computation of torsional force T , shear load F and bending moment M have been also carried out. Their behaviour along the wing span is shown on the Figure 15, Figure 16 and Figure 17. The torsional force and shear load share the progress along the non-dimensionalized span, the only difference is their order of magnitude. The last figure of bending moment grows towards negative values as it approaches the tip of the wing.

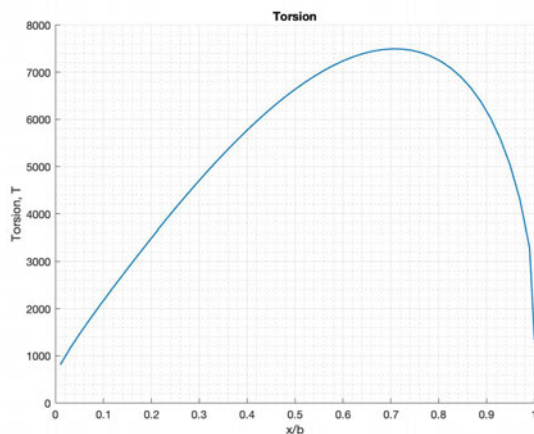


Fig. 15: Torsional Force

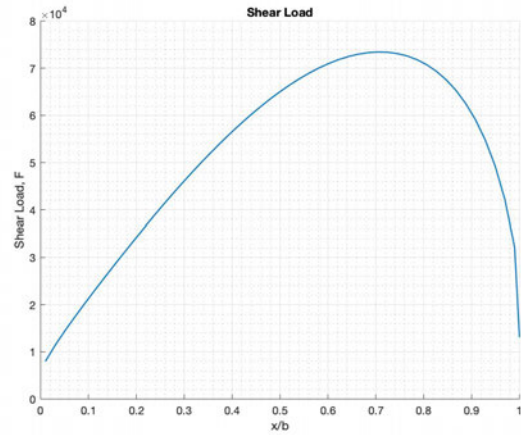


Fig. 16: Shear Load

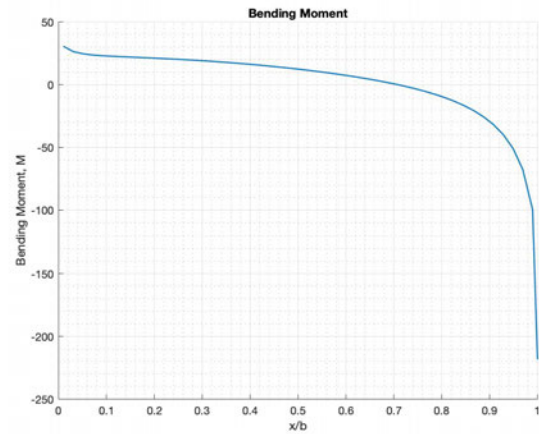


Fig. 17: Bending Moment

5. CONCLUSIONS

This report has studied the aeroelastic problem by means of a set of functions in MATLAB. The cases include divergence conditions, theoretical study of flutter, unsteady aerodynamics, etc.

To perform the analysis a 3D FEM code has been used to obtain some of the needed parameters for the future study or the divergence condition. During the process, it is seen that there is a clear coupling between the torsional load and the bending load. The last part of this project has been related to the coupling that is carried out through transfer matrices. These matrices transfer the structural output (displacement vector) to aerodynamic input (angle of attack) and aerodynamic output (lift distribution) to structural input (force vector). Once computed the previous requirements successfully, a solver computes the divergence speed, modes and flutter speed.

Finally, it is studied that the Finite Element Code is more accurate for large Aspect Ratio than smaller ones because of the use of Euler-Bernoulli approach. Also, it has been observed that, for future analysis or real wings it's convenient to have low aspect ratios if the divergence condition wants to be avoided.

Project Aeroelasticity:

3D FEM Analysis – Experimental structural test

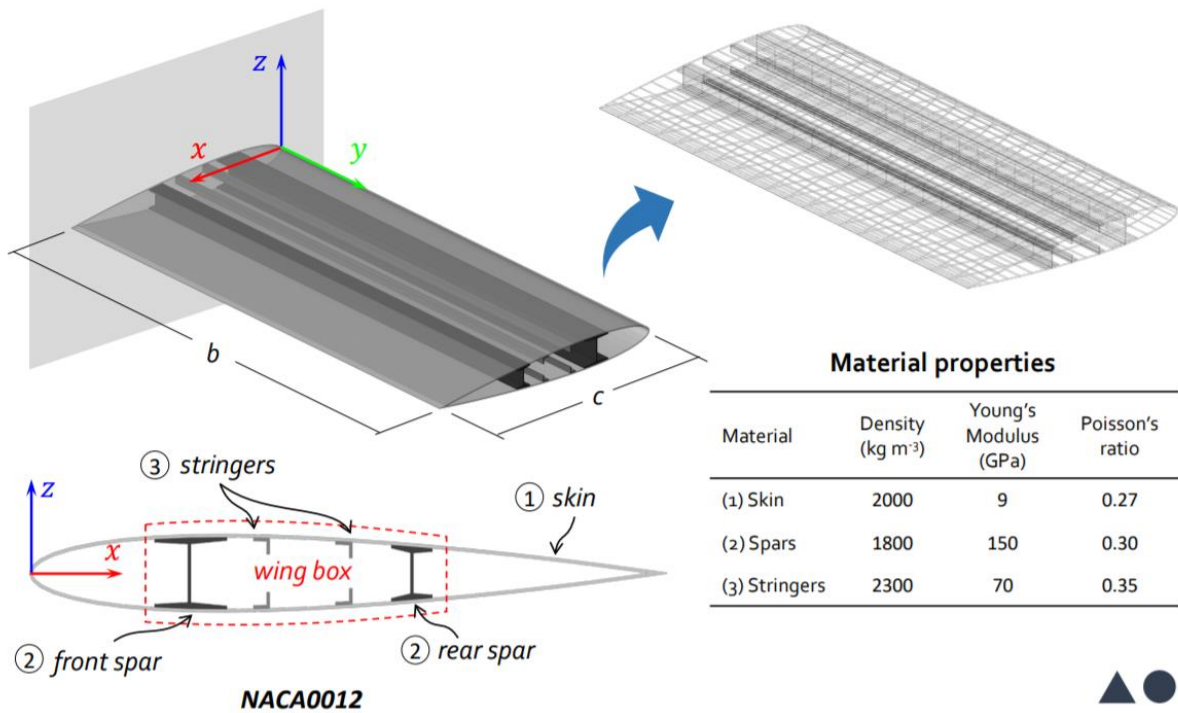


Figure 1: NACA0012 air foil experiment that will be analysed in this project.

M [REDACTED], D [REDACTED]
G [REDACTED], R [REDACTED]

This is an aero elastic study for a clamped-free straight panel with a constant NACA0012 airfoil section done with a setup of a virtual laboratory. The main goal is to implement a set of Mat lab functions to perform different kinds of aero elastic analysis, as the flutter study, the divergence condition and effective stiffness.

To realise this study, a Finite Element code (FEM) is implemented to analyse the effective structural properties of the wing.

The idea is to use it has a black box in order to simulate an experimental analysis. Commonly, loads are putted at different points of the wing and with known inputs the displacement at given points are measured and recorded.

So to simulate this experiment the finite element code is used. The inputs are the loads and the displacement measure location. Then introducing it in the finite element solver the outputs that are the displacement measure at the reading points defined are obtained.

To this end, the study is separated in 3parts: Regarding the structure, a 3D FEM code is used to obtain the effective properties. Considering the wing as a flat plate and implementing the beam's FEM algorithm the shear centre, the effective torsional stiffness and the effective bending stiffness is found. Then for steady aerodynamics the lifting-line solution by horseshoe elements is implemented, and for unsteady aerodynamics the Theodorsen's model is implemented and a flutter study is made.

After a coupling between both is done, by implementing the transfer matrices: from the structures output (displacements vector) to the aerodynamics input (angle of attack), and then from the aerodynamics output (lift distribution) to structures input (force vector).

Finally the analysis results of this clamped-free straight panel with a constant NACA0012 airfoil section are discussed. That principally are:

- Divergence speed for different wing aspect ratios.
- First modes associated to divergence conditions for different aspect ratios.
- Stability plots for flutter speed.

Table of contents:

3D FEM Analysis, experimental structural test:.....	4
2D FEM Analysis, Section properties:	6
1D Beam analysis:	8
a) Element matrices:	8
b) Matrices assembly:.....	9
c) Element force vector:	10
Aerodynamic, Lifting line surface analysis:.....	10
System coupling: force vector assemble:	12
Solver part: Flutter analysis:.....	13
Results.....	16
Steady aerodynamics	17
Unsteady aerodynamics	19
Conclusion and discussion:.....	20
References:	21

3D FEM Analysis, experimental structural test:

To simulate a real experiment, a code where a set of coordinate are defined in which the measurement are made and a set of coordinates where we apply the loads is implemented.

The inputs are the loads and the displacement measure location. Then introducing it in the finite element solver, the outputs that are the displacement measure at the reading points defined are obtained.

With that information, the shear centre of the airfoil section, the torsional stiffness and the bending stiffness is obtained.

Assumptions:

- Small displacements and deformations that implies small angles and linear elasticity.
- Effective response of the flat surface described by elemental beam theory.

$$\begin{Bmatrix} T \\ M \end{Bmatrix} = \begin{bmatrix} \overline{GJ} & 0 \\ 0 & \overline{EI} \end{bmatrix} = \begin{Bmatrix} d\theta/dy \\ d^2h/dy^2 \end{Bmatrix}$$

$$[E] = \begin{bmatrix} \overline{GJ} & 0 \\ 0 & \overline{EI} \end{bmatrix}$$

(Eq.1)

The torsion is related to twist derivative through this torsional stiffness. The bending moment M is related to the second derivative of the deflection of the wing through this bending stiffness and is assumed constant thought out to the whole wing.

- This both phenomenon have to be uncoupled.

It should be verified if this uncoupled hypothesis can be reasonable made. There is a composed structure where the section have different elements with different materials properties. So the torsion and bending moment should be strictly uncoupled. To guarantee it, the following constitutive matrix is used:

$$\begin{Bmatrix} \overline{\theta}' \\ \overline{h}'' \end{Bmatrix} = \begin{bmatrix} S_{11} & S_{12} \\ S_{21} & S_{22} \end{bmatrix} \begin{Bmatrix} T \\ M \end{Bmatrix} = [E]^{-1} = \begin{Bmatrix} T \\ M \end{Bmatrix}$$

(Eq.2)

A function that calculus the deflection in different points of the wing is created. Also a set of coordinates along the wing in a vector, which are the points where the loads are applied.

First, a pure torsional load forces (M=0) is applied, by applying 2 loads with the same magnitude in opposite directions, to get S_{11} and S_{21} .

$$S_{11} = \overline{\theta}'/T$$

$$S_{21} = \overline{h}''/T$$

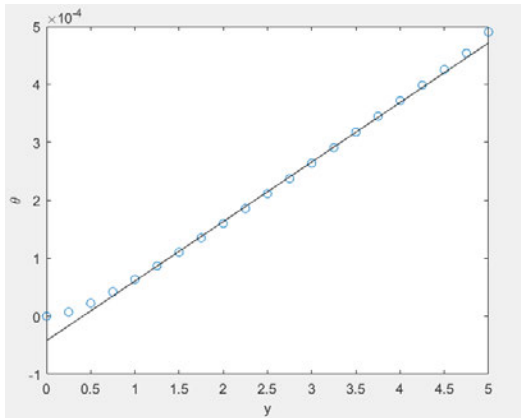


Image 2: Twist angle for a pure torsion.

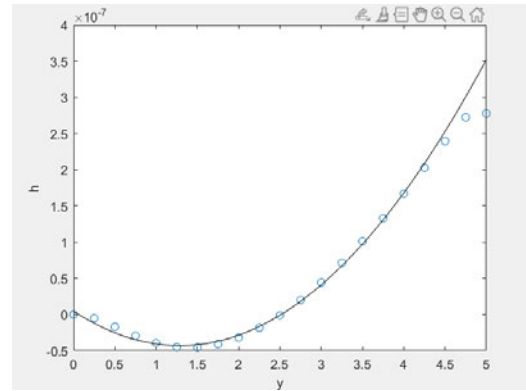


Image 3: Deflection of the wing for a pure torsion.

Secondly a shear load is applied in the shear centre x_{sc} to not cause any torsion (is related with bending $T=0, M'=-Q$) in order to find S_{12} and S_{22} that are defined as follows:

$$S_{12} = \overline{\theta} / Q$$

$$S_{22} = \frac{\overline{h}''}{M} = -\frac{\overline{h}'''}{Q}$$

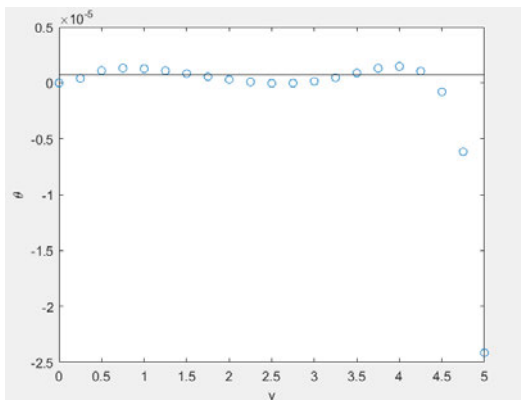


Image 4: Twist angle for a pure bending moment.

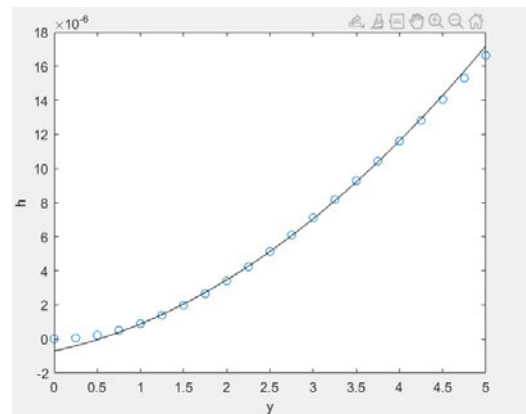


Image 5: Deflection for a pure bending moment.

Then the shear centre needs to be found. To determine it, a force is applied and it is moved between the two spars in order to find the point where no matter what force causes the wing, there is only to bending but not twist. So to determine the shear centre the following equation have to be solve:

$$x_{sc} \rightarrow \frac{\partial \theta}{\partial y} = 0 \tag{Eq1.3}$$

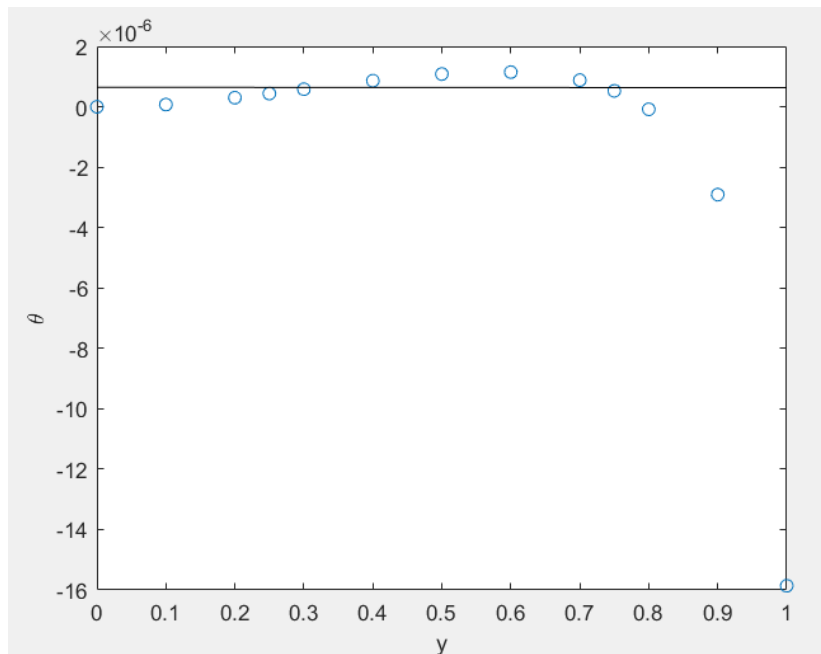


Image 5: Plot of the twist angle ϑ for each defined point measure.

Thanks to FEM solver we found the shear centre position in function of the chord:

$$x_{sc} = 0,33064 * C$$

Finally, we found for this matrix E^{-1} expressed previously in equation 2:

S11	1.0327e-04
S12	-1.1559e-08
S21	-2.6619e-07
S22	5.3585e-07

2D FEM Analysis, Section properties:

In this finite element analysis integrals over the section was done in order to obtain the section properties. There is a NACA0012 profile file (Mat Lab script file) in which there are the nodal coordinates, the nodal connectivity's, and the material connectivity's of the section of this case.

So a 2D FEM script is computed that allows to obtain this section properties thanks to this following formulas:

$$\text{Nodal coordinates } [x] = \begin{bmatrix} \ddot{x}^{(i)} & \ddot{y}^{(i)} & \ddot{z}^{(i)} \\ \dots & \dots & \dots \end{bmatrix} = \begin{bmatrix} \ddot{x}^{(i)} \\ \dots \end{bmatrix}$$

$$\text{Nodal connectivities } [T_n] = \begin{bmatrix} \ddot{(i)}_1^e & \ddot{(i)}_2^e & \ddot{(i)}_3^e & \ddot{(i)}_4^e \\ \dots & \dots & \dots & \dots \end{bmatrix}$$

$$\text{Material connectivities } [T_m] = \begin{bmatrix} \ddot{(m)}^{(e)} \\ \dots \end{bmatrix}$$

(Eq1.4)

A function is implemented to select the vectors data of each coordinate x, y and z, and the connections between the nodes.

The properties material matrix is used and the data are separated in order to calculate the position and the number of elements and nodes for each element (that is 4 for each one). With this 4 nodes the centre of each element is calculated.

Then the material properties matrix is defined as a vector:

$$\text{Material properties } [m] = \begin{bmatrix} \dots \\ \rho^{(m)} \\ \dots \end{bmatrix} \quad (\text{Eq1.5})$$

With this matrix the properties of each section are determined. The nodal coordinates give the coordinates of each node, (is a finite element discretization of the section). This mesh is defined by assigning the coordinates of each points. Then the number of the nodes are assigned and in order to connect it to each element the vertices of each element are implemented (corresponding to each row by identifying the numbers of the corresponding nodes).

The same procedure is done for material properties: a matrix with the different material properties is defined, here there are 3 different materials so the obtained matrix have 3 rows. And then a vector is defined, assigning at each element corresponding to each row of this vector, the index of the material corresponding to this element.

To obtain the properties for each element [e] those following algorithms are used:

$$\text{Coordinates: } x_j^{[e]} = [x]^{([T_m]^{(e,j)})}, \quad j = 1, \dots, 4$$

$$\text{Material: } \rho^{[e]} = [m]^{([T_m]^{(e)})}$$

$$\text{Centroid coordinates: } x^{[e]} = \frac{1}{4} \sum_{j=1}^4 x_j^{[e]}$$

$$\text{Area: } A^{[e]} = \frac{1}{2} (a \cdot b + c \cdot d)$$

$$a = x_1^{[e]} - x_4^{[e]}; \quad b = x_1^{[e]} - x_2^{[e]}$$

$$c = x_3^{[e]} - x_2^{[e]}; \quad d = x_4^{[e]} - x_3^{[e]}$$

(Eq1.6)

Once determined for each element the coordinates and the material, a function to determine the centre of each element is defined. Thanks to the vectors a, b, c and d, a Mat lab function is used to calculus the area of each element.

By ordering this data a matrix "elem" is created where:

- the first column is the x position of the element centre
- the second column is the z position of the element centre
- the thirds column is the area of each element
- the four column is the total mass per unit length of each element

A similar matrix is obtained for properties of each element that gives the kind of material (1, 2, or 3 depending on which material), the density, the young module and the Poisson module for each element.

Finally by summing the columns of the element vectors, the total mass, the centre of mass of the full profile in x and z coordinates, and the inertia using the shear centre founded previously are determined.

The mass per unit length is computed, also the centre of mass and the inertia along the shear centre per unit length making an algorithm with this following equations:

$$\begin{aligned}
 \text{Total mass per unit length: } m &= \sum_e \rho^{[e]} A^{[e]} \\
 \text{Center of mass: } x_{cm} &= \frac{1}{m} \sum_e x^{[e]} \rho^{[e]} A^{[e]} \\
 \text{Inertia of shear center per unit length: } I_{sc} &= \sum_e (x^{[e]} - x_{sc})^2 \rho^{[e]} A^{[e]}
 \end{aligned}
 \tag{Eq1.7}$$

The following plot shows the different properties of the 3 materials that compose this wing profile. It is clearly differentiate by colours the stringers in brown, the spars in green and the skin in blue.

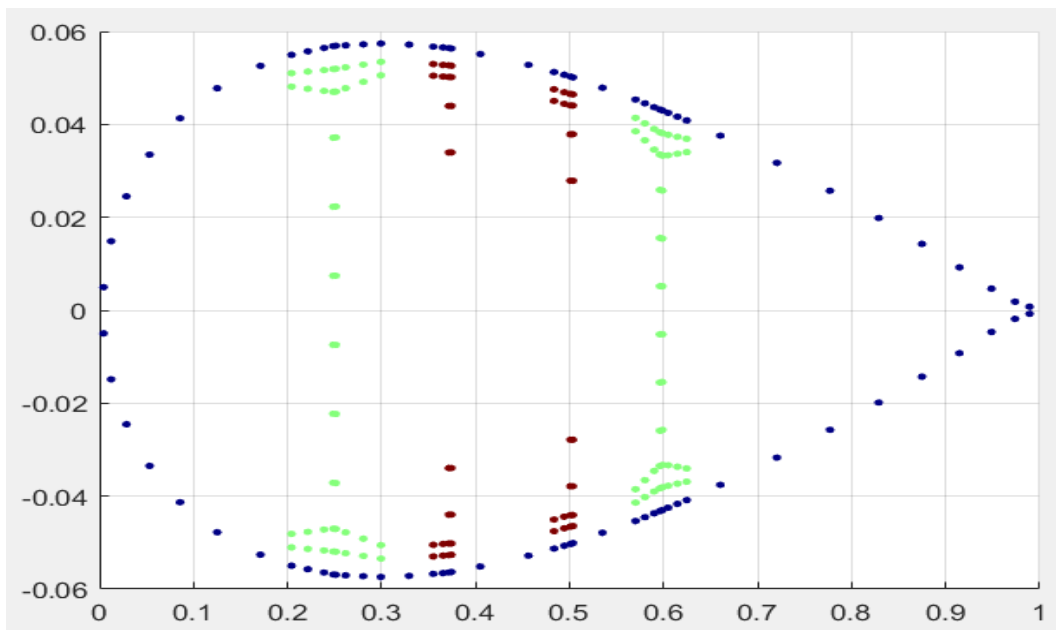


Image 6: Plot showing the different section properties of the wing.

1D Beam analysis:

The goal of this part is to obtain the stiffness and the mass matrices, assuming that the wing is discretised by beam elements.

a) Element matrices:

Imposing an element equilibrium, a system as follows is obtained:

$$[M^{(i)}]\{u^{(i)}\} + [k^{(i)}]\{u^{(i)}\} = \{f^{(i)}\}$$

$$\{u^{(i)}\} = \begin{pmatrix} \theta^{(i)} \\ h^{(i)} \\ \gamma^{(i)} \\ \theta^{(i+1)} \\ h^{(i+1)} \\ \gamma^{(i+1)} \end{pmatrix} ; \{f^{(i)}\} = \begin{pmatrix} T_1^{(i)} \\ F_1^{(i)} \\ M_1^{(i)} \\ T_2^{(i)} \\ F_2^{(i)} \\ M_2^{(i)} \end{pmatrix} \quad (\text{Eq1.8})$$

There are here 3 degrees of freedom for each node associated to the elastic twist $\theta^{(i)}$, the deflection $h^{(i)}$ and the first derivative of the deflection (according to beams theory) $\gamma^{(i)}$ that corresponds to the section rotation about the x axis. When a certain deflection is applied, the section of the wing will also rotate a certain angle. So in this case the elastic axis is always perpendicular to the section of the beam (that works more accurate for large aspect ratio beams).

Associated to this displacement of degrees of freedom, the torsion, the shear load and the bending moment is obtained.

This following expression is used to determine the stiffness matrix $K^{(i)}$ and the mass matrix (lumped) $M^{(i)}$ per unit length:

$$[K^{(i)}] = \frac{\overline{GJ}}{l^{(i)}} \begin{bmatrix} 1 & 0 & 0 & -1 & 0 & 0 \\ 0 & 0 & 0 & 0 & 0 & 0 \\ 0 & 0 & 0 & 0 & 0 & 0 \\ -1 & 0 & 0 & 1 & 0 & 0 \\ 0 & 0 & 0 & 0 & 0 & 0 \\ 0 & 0 & 0 & 0 & 0 & 0 \end{bmatrix} + \frac{\overline{EI}}{(l^{(i)})^3} \begin{bmatrix} 0 & 0 & 0 & 0 & 0 & 0 \\ 0 & 12 & 6l^{(i)} & 0 & \overline{EI} & 6l^{(i)} \\ 0 & 6l^{(i)} & 4(l^{(i)})^2 & 0 & 6l^{(i)} & 4(l^{(i)})^2 \\ 0 & 0 & 0 & 0 & 0 & 0 \\ 0 & \overline{EI} & -6l^{(i)} & 0 & \overline{EI} & -6l^{(i)} \\ 0 & 6l^{(i)} & 4(l^{(i)})^2 & 0 & -6l^{(i)} & 4(l^{(i)})^2 \end{bmatrix}$$

$$l^{(i)} = y^{(i+1)} - y^{(i)}$$

$$[M^{(i)}] = \frac{l^{(i)}}{2} \begin{bmatrix} I_{sc} & md & 0 & 0 & 0 & 0 \\ md & m & 0 & 0 & 0 & 0 \\ 0 & 0 & 0 & 0 & 0 & 0 \\ 0 & 0 & 0 & I_{sc} & md & 0 \\ 0 & 0 & 0 & md & m & 0 \\ 0 & 0 & 0 & 0 & 0 & 0 \end{bmatrix} ; d = x_{sc} - x_{cm}$$

(Eq1.8)

b) Matrices assembly:

Then the global mass and stiffness matrices have to be obtained following this matrix assembly approach. In this case there are 3 degrees of freedom (DoF) per node, so the total number of DoFs is: $N=3(n+1)$.

$$\text{Initialise global matrices: } [K] = [0]_{N \times N} \text{ and } [M] = [0]_{N \times N}$$

(Eq1.9)

The algorithm determine for each element $i=\{1\dots n\}$, for each node $a=\{1,2\}$ and for each degree of freedom $j=\{1\dots 3\}$:

$$p = 3(a - 1) + j \quad ; \quad I = 3([T_n]^{(i,a)} - 1) + j$$

(Eq1.10)

Then for each element node $b=\{1,2\}$ and for each degree of freedom $k=\{1...3\}$:

$$q = 3(b - 1) + k \quad ; \quad J = 3([T_n]^{(i,b)} - 1) + k$$

(Eq1.11)

Finally the matrices assembly is computed:

$$[K]^{(I,J)} = [K]^{(I,J)} + [K^{(i)}]^{(p,q)}$$

$$[M]^{(I,J)} = [M]^{(I,J)} + [M^{(i)}]^{(p,q)}$$

(Eq1.12)

c) Element force vector:

The force vector is related to the aerodynamic part because the load system for aero elastic problems come from this aerodynamic part. From the structural part a constant lift distribution for each beam element and a constant torsion moment distribution is assumed. And then the contribution of the mass in the both point's loads at each node configuring the element are accounted. This relation is given through this matrix:

$$\{f^{(i)}\} = \frac{l^{(i)}}{2} \begin{bmatrix} 0 & 1 \\ 1 & 0 \\ l^{(i)}/6 & 0 \\ 0 & 1 \\ 1 & 0 \\ -l^{(i)}/6 & 0 \end{bmatrix} \begin{Bmatrix} \overline{l^{(i)}} \\ m_{sc}^{(i)} \end{Bmatrix}$$

(Eq1.13)

Basically for the lift and torsion moment, half of the contribution to each node by multiplying by "l" the beam length and dividing it by 2 are given.

This is the interpolation or coupling matrix between the aerodynamic and the structural part.

Aerodynamic, Lifting line surface analysis:

In this part the discretization panels that correspond to the beam elements from the structural analysis are defined. For this numerical analysis it's important to obtain:

-Surface area of the element: $S^{[i]}$

-Normal vector of the element (vertical): $n^{[i]}$

-Coordinates of collocation points (3/4 length of the element, in the middle): $x^{[i]}$

The system that can be used to obtain the unknown, in this case the intensity of the vortex line $\Gamma^{[i]}$, comes from applying the Kutta condition at each collocation point:

$$\left(\sum_{j=1}^n (v_{12}^{[j]} + v_{23}^{[j]} + v_{34}^{[j]})_{X=X^{[i]}} + U_{\infty} \right) \cdot n^{[i]} = 0$$

$$\text{Induced velocity: } (v_{12}^{[j]} + v_{23}^{[j]} + v_{34}^{[j]})_{X=X^{[i]}}$$

$$\text{Total velocity: } U_{\infty}$$

(Eq1.14)

A small angles approximation is assumed so the freestream velocity is the normal times the angle of attack of each section. In our case the angle of attack correspond to the elastic twist because is how it is defines in the aero elastic analysis.

So this is the link between the structural and the aerodynamic part. There is the angle of attack in one hand and through the definition of the lift obtained by solving the system described in Eq1.15, it is related to the force vector in the structural analysis. An algorithm is implemented to found out the induced velocity at point x due to a vortex segment from x_j to x_k with vorticity $\Gamma^{[i]}$ is:

$$v_{jk}^{[i]} = \frac{\Gamma^{[i]}}{4\pi} \frac{r_j x r_k}{\|r_j x r_k\|^2} \cdot \left(\frac{l^{[i]} \cdot r_j}{r_j} - \frac{l^{[i]} \cdot r_k}{r_k} \right)$$

$$r_j = x - x_j ; \quad l^{[i]} = x_k - x_j$$

(Eq1.15)

Then the following system of equations where [A] is the aerodynamic influence coefficients matrix is found.

$$[A]\{\Gamma\} = -U_\infty\{\alpha\}$$

$$\begin{bmatrix} A_{11} & A_{12} & \dots & A_{1n} \\ A_{21} & A_{22} & \dots & \dots \\ \dots & \dots & \dots & \dots \\ A_{n1} & A_{n2} & \dots & A_{nn} \end{bmatrix} \begin{Bmatrix} \Gamma^{[1]} \\ \Gamma^{[2]} \\ \dots \\ \Gamma^{[n]} \end{Bmatrix} = -U_\infty \begin{Bmatrix} \alpha^{[1]} \\ \alpha^{[2]} \\ \dots \\ \alpha^{[n]} \end{Bmatrix}$$

(Eq1.16)

The coefficients of [A] are obtained by applying this formula, that involve the induce velocity at each point:

$$A_{ij} = (v_{12}^{[j]}(x^{[i]}) + v_{23}^{[j]}(x^{[i]}) + v_{34}^{[j]}(x^{[i]}))_{\Gamma^{[i]=1} \cdot n^{[i]}}$$

(Eq1.17)

Then using the lift definition of Eq1.18 the total lift {L} at each panel in terms of the angle of attack is found.

$$\text{Total lift on the element: } L^{[i]} = \rho_\infty U_\infty S^{[i]} \Gamma^{[i]}$$

$$\{L\} = -\rho_\infty U_\infty^2 [S][A]^{-1}\{\alpha\}$$

(Eq1.18)

Where [S] is a diagonal matrix involving the plane form surface area of each panel:

$$[S] = \begin{bmatrix} S^{[1]} & \dots & 0 \\ \dots & S^{[i]} & \dots \\ 0 & \dots & S^{[n]} \end{bmatrix}$$

System coupling: force vector assemble:

Finally, what rest to do is the system coupling. In one hand the lift [L] have to be expressed in terms of the unknown vector from the structural part {u}. That means finding an interpolation matrix between {α} that only the twist angle and {u} that have 3 DoFs are important. The relationship comes from the matrix [I]. So for this aerodynamic model the following equation have to be solved:

$$\alpha^{[i]} = \theta^{[i]} = \frac{1}{2} \begin{bmatrix} 1 & 0 & 0 & 1 & 0 & 0 \end{bmatrix} \begin{pmatrix} \theta^{(i)} \\ h^{(i)} \\ \gamma^{(i)} \\ \theta^{(i+1)} \\ h^{(i+1)} \\ \gamma^{(i+1)} \end{pmatrix} = [I \quad I] \begin{Bmatrix} u^{(i)} \\ u^{(i+1)} \end{Bmatrix}$$

$$\{\alpha\} = \begin{Bmatrix} \alpha^{[1]} \\ \alpha^{[2]} \\ \dots \\ \alpha^{[n]} \end{Bmatrix} = \begin{bmatrix} I & I & 0 & \dots & 0 & 0 \\ 0 & I & I & \dots & 0 & 0 \\ \dots & \dots & \dots & \dots & \dots & \dots \\ 0 & 0 & 0 & \dots & I & I \end{bmatrix} \begin{Bmatrix} u^{(1)} \\ u^{(2)} \\ u^{(3)} \\ \dots \\ u^{(n)} \\ u^{(n+1)} \end{Bmatrix} = [I] \{u\}$$

$$\{L\} = -\rho_{\infty} U_{\infty}^2 [S] [A]^{-1} [I] \{u\}$$

(Eq1.20)

Then the force vector is assembled. To do it, the expression defined previously for the element force vector, with the effective/average value of the constant distribution in each section $l^{[i]}$ and the effective torsion moment contribution about the shear centre $m_{sc}^{[i]}$ is recalled. And this is related to the total lift $L^{[i]}$ of each panel through this simple expression.

$$\begin{bmatrix} \overline{l^{[i]}} \\ \overline{m_{sc}^{[i]}} \end{bmatrix} = \frac{1}{l^{[i]}} \begin{bmatrix} 1 \\ e \end{bmatrix} L^{[i]}, \quad e = x_{sc} - x_{ac}$$

(Eq1.21)

After it is introduced into (Eq1.13) defined previously and the element force assembly matrix becomes:

$$\{f^{(i)}\} = \frac{l^{(i)}}{2} \begin{bmatrix} 0 & 1 \\ 1 & 0 \\ 0 & 1 \\ 1 & 0 \\ -l^{(i)}/6 & 0 \end{bmatrix} \frac{1}{l^{(i)}} \begin{bmatrix} 1 \\ e \end{bmatrix} L^{[i]} = \frac{1}{2} \begin{bmatrix} l^{(i)}/6 & 1 \\ 0 & l^{(i)}/6 \\ 1 & 1 \\ 0 & l^{(i)}/6 \\ -l^{(i)}/6 & 0 \end{bmatrix} L^{[i]}$$

(Eq1.22)

Then the force value at each pair of nodes corresponding to the same element by this following expression that depend on the lift of each section can be determined:

$$\begin{Bmatrix} F^{(i)} \\ F^{(i+1)} \end{Bmatrix} = \frac{1}{2} \begin{bmatrix} Q_1^{[i]} \\ Q_2^{[i]} \end{bmatrix} L^{[i]}$$

$$\begin{pmatrix} F^{(1)} \\ F^{(2)} \\ F^{(3)} \\ \dots \\ F^{(n)} \\ F^{(n+1)} \end{pmatrix} = \frac{1}{2} \begin{bmatrix} Q_1^{[1]} & 0 & \dots & 0 \\ Q_2^{[2]} & Q_1^{[2]} & \dots & 0 \\ 0 & Q_2^{[2]} & \dots & 0 \\ \dots & \dots & \dots & \dots \\ 0 & 0 & \dots & Q_1^{[n]} \\ 0 & 0 & \dots & Q_2^{[n]} \end{bmatrix} \begin{pmatrix} L^{[1]} \\ L^{[2]} \\ \dots \\ L^{[n]} \end{pmatrix}$$

(Eq1.23)

With this final matrix that relate the total force vector to the total lift vector, the final expression that gives the coupling between the 2 pars is found.

$$\{F(u)\} = -\frac{1}{2}\rho_{\infty}U_{\infty}^2[Q][S][A]^{-1}[I]\{u\} = q_{\infty}[K_a]$$

(Eq1.24)

In this last expression the aerodynamic pressure q_{∞} (that is constant) can be identified.

Solver part: Flutter analysis:

A constant NACA0012 section with different aspect ratios is studied. The divergence speed and the different modes associated are obtained solving the model problem to this divergent condition.

Also flutter speed is carried out in order to study the stability in terms of the freestream velocity, and to get stability plots for the flutter analysis.

In order to solve (Eq1.24) the Theodorsen's aerodynamic model is used. The idea is to non-dimensionalize the system following a procedure explained in this section. The system have several degrees of freedom (depending on the number of elements in the discretization), which is not a major issue in terms of the procedure.

Theodorsen's aerodynamic model:

$$l(y) = \pi\rho_{\infty}b^2(u_{\infty}\dot{\theta} - ba\ddot{\theta} - \dot{h}) + 2\pi\rho_{\infty}u_{\infty}bc(k)(u_{\infty}\theta + b\left(\frac{1}{2} - a\right)\dot{\theta} - \dot{h})$$

$$\begin{aligned}
 m_{sc}(y) = & -\pi\rho_{\infty}b^3\left(u_{\infty}\left(\frac{1}{2} - a\right)\dot{\theta} + b\left(\frac{1}{8} + a^2\right)\ddot{\theta} + a\dot{h}\right) \\
 & + 2\pi\rho_{\infty}u_{\infty}b^2c(k)\left(a + \frac{1}{2}\right)\left(u_{\infty}\theta + b\left(\frac{1}{2} - a\right)\dot{\theta} - \dot{h}\right)
 \end{aligned}$$

(Eq1.25)

Where: $b = \frac{c}{2}$, $a = \frac{x_{sc}}{b-1}$, $c(k) = \frac{H_1^{(2)}(K)}{H_1^{(2)}(K) + iH_0^{(2)}(K)}$, $K = \frac{wb}{u_{\infty}}$: reduced frequency

For this case the Theodorsen's function can be approximated as follows:

$$C(K) = 1 - \frac{0,165}{1 - i\frac{0,0455}{k}} - \frac{0,335}{1 - i\frac{0,3}{k}}$$

(Eq1.26)

Then expressing $C(K)=F(K)+I g(k)$, it is possible to get:

$$F(K) = \frac{0,5K^4 + 0,0765K^2 + 1,8632 \cdot 10^{-4}}{K^4 + 0,0921K^2 + 1,8632 \cdot 10^{-4}} \quad \text{and} \quad G(K) = \frac{-0,1080K^3 - 8,8374 \cdot 10^{-4}K}{K^4 + 0,0921K^2 + 1,8632 \cdot 10^{-4}} \quad (\text{Eq1.27})$$

$$\text{In this case: } \begin{Bmatrix} m_{sc}^{[i]} \\ l^{[i]} \end{Bmatrix} = \pi \rho_{\infty} b^2 u_{\infty}^2 ([\hat{A}_R(K)] + i[\hat{A}_I(K)]) [I \ I] \begin{Bmatrix} \hat{u}^i \\ \hat{u}^{(i+1)} \end{Bmatrix}$$

$$\text{With: } \hat{A}_R(K) = K^2 \begin{bmatrix} \frac{1}{8} + a^2 & a \\ a & 1 \end{bmatrix} + KG(K) \begin{bmatrix} 2a^2 - \frac{1}{2} & 2a + 1 \\ 2a - 1 & 2 \end{bmatrix} + F(K) \begin{bmatrix} 1 + 2a & 0 \\ 2 & 0 \end{bmatrix}$$

$$\hat{A}_I(K) = K \begin{bmatrix} a - 1/2 & 0 \\ 1 & 0 \end{bmatrix} - KF(K) \begin{bmatrix} 2a^2 - \frac{1}{2} & 2a + 1 \\ 2a - 1 & 2 \end{bmatrix} + G(K) \begin{bmatrix} 1 + 2a & 0 \\ 2 & 0 \end{bmatrix}$$

$$I = \begin{bmatrix} 1/2 & 0 & 0 \\ 0 & 1/2 & 0 \end{bmatrix}$$

(Eq1.28)

$$\text{So the element force vector becomes: } \{f^{[i]}\} = b \begin{bmatrix} \hat{Q}_1^{[i]} \\ \hat{Q}_2^{[i]} \end{bmatrix} \begin{Bmatrix} m_{sc}^{[i]} \\ l^{[i]} \end{Bmatrix} \quad (\text{Eq1.29})$$

$$\text{With: } \hat{Q}_1^{[i]} = \frac{\hat{l}^{[i]}}{2} \begin{bmatrix} 1 & 0 \\ 0 & 1 \end{bmatrix}, \quad \hat{Q}_2^{[i]} = \frac{\hat{l}^{[i]}}{2} \begin{bmatrix} 1 & 0 \\ 0 & -1 \end{bmatrix}, \quad \hat{l}^{[i]} = l^{[i]}/b$$

$$\text{Therefore: } \{F\} = \pi \rho_{\infty} b^3 u_{\infty}^2 [\hat{Q}][\hat{A}(K)][\hat{I}]\{\hat{u}\} \quad (\text{Eq1.30})$$

And the coupling matrices are defined in this project as follows:

$$[\hat{Q}] = \begin{bmatrix} \hat{Q}_1^{[1]} & 0 & \dots & 0 \\ \hat{Q}_2^{[1]} & \hat{Q}_1^{[2]} & \dots & 0 \\ 0 & \hat{Q}_2^{[2]} & \dots & 0 \\ \dots & \dots & \dots & \dots \\ 0 & 0 & \dots & \hat{Q}_1^{[n]} \\ 0 & 0 & \dots & \hat{Q}_2^{[n]} \end{bmatrix}, \quad [\hat{I}] = \begin{bmatrix} I & I & 0 & \dots & 0 & 0 \\ 0 & I & I & \dots & 0 & 0 \\ \dots & \dots & \dots & \dots & \dots & \dots \\ 0 & 0 & 0 & \dots & I & I \end{bmatrix}$$

(Eq1.31)

It is assumed that the degree of freedom referring to the vertical displacement, h , is nondimensionalized by the half-chord, b , when writing $\hat{u}^{[i]}$. Additionally, to make the units consistent, all equations referring to forces are multiplied by b . So $\hat{l}^{[i]} = l^{[i]}/b$ in the definition of $[\hat{Q}]$ and, rows and columns of both $[K]$ and $[M]$ corresponding to the second degree of freedom of each node, must be multiplied by b . The non-dimensionalization of these matrices is done by:

$$[\hat{M}] = \frac{1}{mb^3} [B]^T [M] [B], \quad [\hat{K}] = \frac{1}{mb^3 \omega_{\theta}^2} [B]^T [K] [B], \quad [B] = \begin{bmatrix} b & \dots & 0 \\ \dots & \dots & \dots \\ 0 & \dots & 0 \end{bmatrix}, \quad b = \begin{bmatrix} 1 & 0 & 0 \\ 0 & b & 0 \\ 0 & 0 & 1 \end{bmatrix}$$

(Eq1.32)

Where $\omega_\theta^2 = \overline{GJ}/I_{sc}b^2$ for instance. Then the system can be expressed as follows:

$$(mb^3\omega_\theta^2[\widehat{K}] - mb^3\omega^2[\widehat{M}])\{\hat{u}\} = \pi\rho_\infty b^3 U_\infty^2 [\widehat{Q}][\widehat{A(K)}][\widehat{I}]\{\hat{u}\} \quad (\text{Eq1.33})$$

Dividing everything by $\pi\rho_\infty b^3 U_\infty^2$ the following equations are obtained:

$$\left(\frac{mb^3\omega_\theta^2}{\pi\rho_\infty b^3 U_\infty^2} [\widehat{K}] - \frac{mb^3\omega^2}{\pi\rho_\infty b^3 U_\infty^2} [\widehat{M}] - [\widehat{Q}][\widehat{A(K)}][\widehat{I}] \right) \{\hat{u}\} = \{0\}$$

$$\left(\frac{m}{\pi\rho_\infty b^2} \frac{b^2\omega^2}{U_\infty^2} \frac{\omega_\theta^2}{\omega^2} [\widehat{K}] - \frac{m}{\pi\rho_\infty b^2} \frac{b^2\omega^2}{U_\infty^2} [\widehat{M}] - [\widehat{F}(K)] \right) \{\hat{u}\} = \{0\} \quad (\text{Eq1.34})$$

Then, defining: $\lambda = \frac{\omega_\theta^2}{\omega^2}$, $\mu = \frac{m}{\pi\rho_\infty b^2}$, $k = \frac{b^2\omega^2}{U_\infty^2}$ and after applying the boundary conditions (that allows to take out the first 3 rows and columns of all matrices, the resulting system yields:

$$([\widehat{K}_{LL}]^{-1}[\widehat{M}_{LL}] + \frac{1}{\mu k^2} [\widehat{K}_{LL}]^{-1}[\widehat{F}_{LL}(K)] - \lambda[1])\{\hat{u}\} = \{0\}$$

$$\text{Where: } [\widehat{D}_{LL}(K)] = [\widehat{K}_{LL}]^{-1}[\widehat{M}_{LL}] + \frac{1}{\mu k^2} [\widehat{K}_{LL}]^{-1}[\widehat{F}_{LL}(K)] \quad (\text{Eq1.35})$$

Finally the **flutter condition** is given by: $\det([\widehat{D}_{(k_F)}] - \lambda_F[1]) = 0$ (Eq1.36)

To solve the flutter analysis, first a set of k_F is specified. Then for each k_F the eigenvalues λ_F of $\widehat{D}_{(k_F)}$ are found. That allows to obtain for each eigenvalues $\omega_F = \frac{\omega_\theta}{\sqrt{\lambda_F}}$ (complex valued) and $U_F = \frac{bRe(\omega_F)}{k_F}$. Then the modes and K_F for which $\text{Im}(\omega_F) < 0$ (unstable) are found. Finally the limits of the K_F obtained are interpolated to found the U_F corresponding to flutter boundary.

Regarding the flutter analysis several modes (or eigenvalues) for each trial kappa are found. From all those modes, only in those that may cause instabilities, (have associated non-null negative imaginary components of the resulting frequency, ω_F) are interesting.

To guess at which kappa range the flutter boundary is found (the point where the imaginary component of the frequency changes sign), a sweep from 1e-3 to 1e3 in a logarithmic scale is done. This way a huge range in the same computation is cover and the chances of capturing the sign change for some modes is increased.

Results

The study has been performed for a rectangular wing with aspect ratio of 5 with a NACA 0012 airfoil, clamped in one end and free in the other. In this study 3 different wing configurations are studied varying the aspect ratio in values of 2, 5 and 10.

The study is started by measuring the displacements of the wing when applied some forces to the structure. The forces needed are a torsional load and a shear load in order to find GJ and EI as well as the shear center. When the forces are applied the wing deforms in a certain way, as it can be seen in the images 1, 2, 3 and 4 from the 3D FEM analysis explanation.

By applying a pure torsional load and a pure shear load on the wing using the test FEM Matlab program provided can be found the stiffness of the wing and the shear center.

	AR =2	AR =5	AR =10
GJ [Nm/rad]	18396	47289	96392
EI [Nm]	1302500	1004800	1303000
X_{sc}	0.3491	0.3746	0.3903

Analysing the 2D section of the airfoil using the FEM method can be obtained the mass per unit length of the wing the center of mass and the inertia at the shear center:

	AR =2	AR =5	AR =10
Mass (kg/m)	28.159	28.159	28.159
CM	0.4597	0.4597	0.4597
I_{sc}[kg m²]	2.2101	2.0697	2.0016

Steady aerodynamics

Using this data, the wing is simplified to a beam, where can be extracted the K and M matrices. Using the lifting line method is obtained the Ka matrix which is applied to the system. To find the divergence speed for this system it is needed to perform the eigenvalues and eigenvectors of the K and Ka matrices.

This way are obtained the different divergence speeds (U_D) and their correspondent modes, taking into account a standard air density of 1.225 Kg/m^3 :

U_{modes} [m/s]	Mode 1	Mode 2	Mode 3	Mode 4	Mode 5
AR=2	200.71	782.60	1599.7	2598.3	3753.3
AR=5	89.64	315.75	612.22	969.77	1382.6
AR=10	54.02	177.89	327.48	501.39	698.59

	AR=2	AR=5	AR=10
U_D [m/s]	200.71	89.64	54.02

As the AR increases, the divergence speed gets lower as the wing is less stiff and thus is more susceptible to flutter.

When the different modes are represented can be seen how the variation in the theta and h directions of the wing strongly related and react the same way to the divergence conditions:

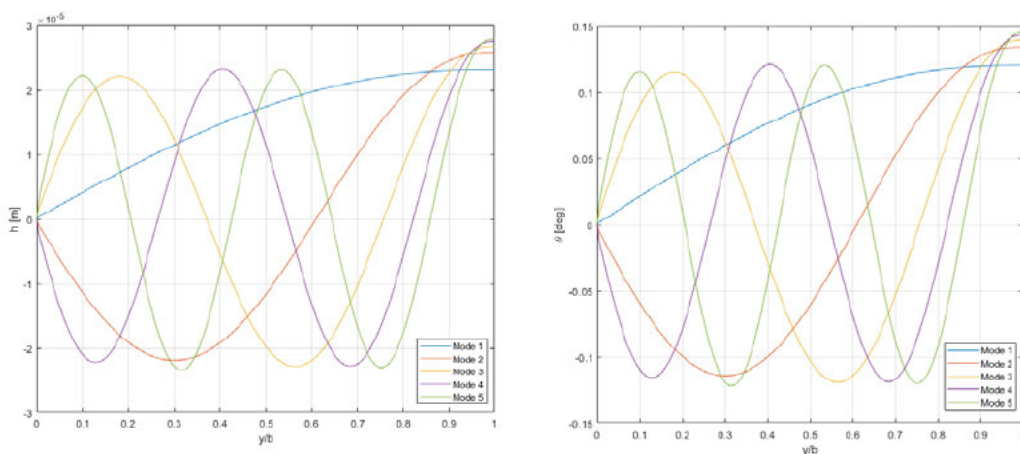


Image 7: Modal oscillation in ϑ and h for AR=5

In the gamma deflection graph is presented that the deflections in gamma angle, are really small and oscillate back and forth between two values, while slowly drifting in value altogether.

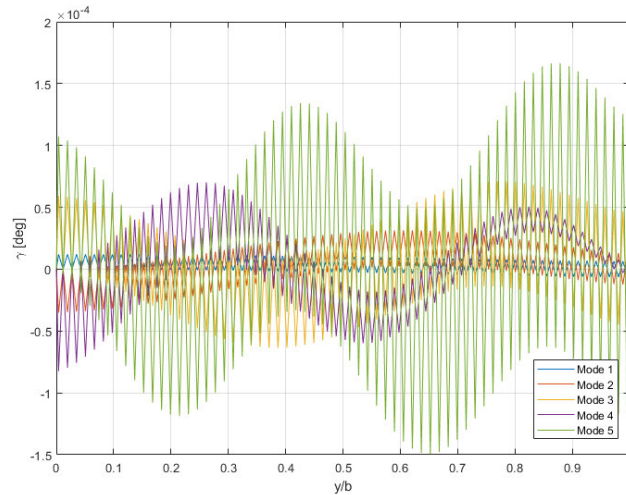


Image 8: Modal oscillation in γ for AR=5.

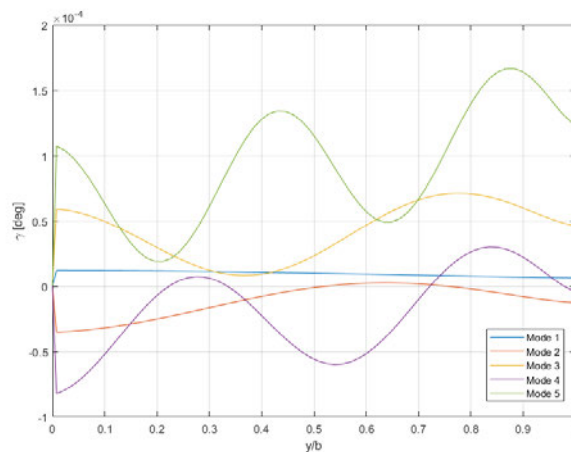


Image 9: Modal oscillation drift in γ for AR=5.

When only one side of the oscillation is plotted, can be seen clearly the different drifts of the modes and how as higher the mode higher is the amplitude of the oscillations.

For the other two degrees of freedom the modes are very similar, with slightly different frequencies, and different amplitudes, for the AR=10 case are higher movements and lower for the AR=2 case, they are not presented here because the information they add is not relevant.

Unsteady aerodynamics

Theodorsen's approximation of the aerodynamic forces give an approximation to an unsteady aerodynamic model, that can be coupled with the structural matrices calculated earlier can be used to calculate the flutter speed of the wing with more accuracy than using the lifting line method.

The Theodorsen method uses an initial approximation of the parameter κ , so by sweeping through different values the flutter speed stabilizes as the κ is higher.

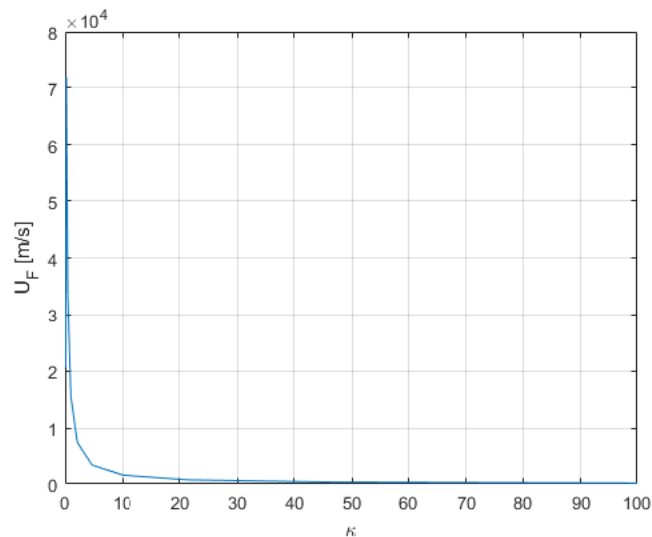


Image 9: U_F vs. κ for $AR=10$.

Using the convergence plot it can be deduced that the flutter speed converges as kappa gets higher, so to find the flutter speed is taken a value of kappa=100.

	AR=2	AR=5	AR=10
U_F	43253	154.78	112.30

The velocities obtained are higher than in the steady aerodynamics case, and also go lower as the aspect ratio of the wing increases so it is confirmed that when the wing is slim and long (high aspect ratio) is more susceptible to flutter. Must also be noticed that the value for $AR = 2$ is very high this can be due to some problems with the Theodorsen model implementation that fails when the aspect ratio is low, because this velocity does not look correct.

Conclusion and discussion:

First the "experimental test" was done and the location of the "shear centre", "inertial bending", and the "inertial torsion" was found.

Then the response the aerodynamic model with the "lifting line" and the "Theodorsen model" was analysed in order to found the divergence

Some checks were made to see how is the distribution of the lift in the lifting-line to verify that it is elliptical, and to see what happens when the "aspect ratio" is varied, and finally to see how the divergence varies with the "aspect ratio".

Results shows that the model diverges with lower speeds when the aspect ratio or the wing size is increased, this happens because the structure is the same but the wing is longer, has more inertia and so is less stiff.

Finally, to solve the flutter studied with the Theodorsen model, all the equations were none dimensioned in order to have the reduced frequency " k " with which we have found the solution later.

The final results obtained in the steady aerodynamic method look reasonable, how the divergence speed is lower for higher aspect ratios, and the absolute values look correct.

The modes for the θ and h seem also correct, and the plot for the γ modes seems to do strange things, but looking at the calculations don't seem to be bad, and so maybe the results are ok and it is the real movement of the wing, as it is really small.

The Theodorsen method has caused more trouble, as it is more complex and difficult. The equations have been applied the way the guides and classes explained, and the results seem ok, giving flutter speeds a bit lower than in the steady case, which is reasonable, and the speed also decreases with the aspect ratio. For the case with $AR=2$ the result is clearly not okay. Also, to obtain the results the part of the solving of the equation with D the path taken to do so, the method is not the one explained by the teacher in the explanations, but is the one that has given us better results so has been done all the possible to get accurate results and is the better we have been able to perform in the time we had.

Overall, the behaviour of the wing has been studied and can be obtained some approximations of the speeds and situations where flutter can appear, from here the analysis can be further expanded by making sure the unsteady aerodynamics approach is correctly calculated, and then the shape of the wing and the airfoil may be changed, the shape can be more easily changed in the program, because if the airfoil is changed the 3d FEM program may be changed and the meshes redone, and this is not easy.

References:

[1] Project pdf, ATENEA,

https://atenea.upc.edu/pluginfile.php/3674362/mod_resource/content/1/Project.pdf



UNIVERSITAT POLITÈCNICA DE CATALUNYA
BARCELONATECH

Escola Superior d'Enginyeries Industrial,
Aeroespacial i Audiovisual de Terrassa

POLYTECHNIC UNIVERSITY OF CATALONIA

ADVANCED AEROELASTICITY

MASTER'S DEGREE IN AEROSPACE ENGINEERING

**Project: Setup of a virtual laboratory to
study aeroelastic problems**

Students:

I [REDACTED] B [REDACTED]
P [REDACTED] S [REDACTED]

Professor:

David Roca Cazorla

January 21th 2021

Contents

1	Introduction	3
2	3D FEM analysis - Experimental structural test	5
3	2D FEM Analysis - Section properties	8
4	1D Beam analysis	9
4.1	Element matrices	9
4.2	Matrices assembly	9
4.3	Element force vector	10
5	Aerodynamics	11
5.1	Lifting line surface analysis	11
5.2	Theodorsen's aerodynamic model	11
6	Systems coupling - Force vector assembly	13
6.1	Divergence analysis	13
6.2	Flutter analysis	14
7	Code structure	16
8	Results	17
8.1	Divergence speed for different wing aspect ratios	17
8.2	First modes associated to divergence conditions for different aspect ratios	18
8.3	Flutter stability plots	19
9	Conclusions	23
10	Code	24
10.1	Main	24
10.2	Functions	30

List of Figures

1	Setup of the experiment and characteristics of the wing studied. . . .	3
2	Pure torsion load.	5
3	Pure shear load.	5
4	Displacement in different sections obtained when using function poly- fit with the y values of the sensors.	6
5	Displacement in different sections obtained with the solver.	6
6	How to obtain an equivalent force to one applied at a non-existing node.	7
7	Displacement in the different sections when applying a pure shear load.	7
8	Quadrilateral element of the mesh.	8
9	Stiffness and mass matrix of the wing.	9
10	Element discretization at the beam.	10
11	Element forces discretization.	10
12	Element forces vector.	10
13	System of equations to find Γ	11
14	Lift and moment in Theodorsen's model.	11
15	Aerodynamic forces in Theodorsen's model.	12
16	$\hat{\mathbf{A}}_R(k)$, $\hat{\mathbf{A}}_I(k)$ and \mathbf{I} matrices definition.	12
17	Coefficients $F(k)$ and $G(k)$ of Theodorsen's function.	12
18	Expression of α in terms of the structural unknown vector.	13
19	RHS of the equation.	14
20	RHS of the equation.	14
21	Shape of the element force vector.	14
22	Equilibrium equation for the non-steady case.	15
23	Values of λ , μ and κ	15
24	Resulting system for the non-steady case.	15
25	Divergence speeds of the wing for different aspect ratios.	17
26	AR = 1.	18
27	AR = 4.	18
28	AR = 5.	18
29	AR = 6.	18
30	AR = 8.	18
31	AR = 10.	18
32	First five modes for different AR.	18
33	W_f for $k = 10^{-2}$ to 10^3	19
34	W_f for $k = 10$ to 100	20
35	W_f for $k = 1$ to 2	21
36	Minimum flutter speeds for $k = 10^{-2}$ to 10^3	22

1. Introduction

The objective of this assignment is to simulate in *MATLAB* the setup of a virtual laboratory to study aeroelastic problems. The setup will simulate a semi-wing of airfoil NACA0012 inside a wind tunnel. The section and properties are constant, as seen in Figure 1, and $\alpha = 0$.

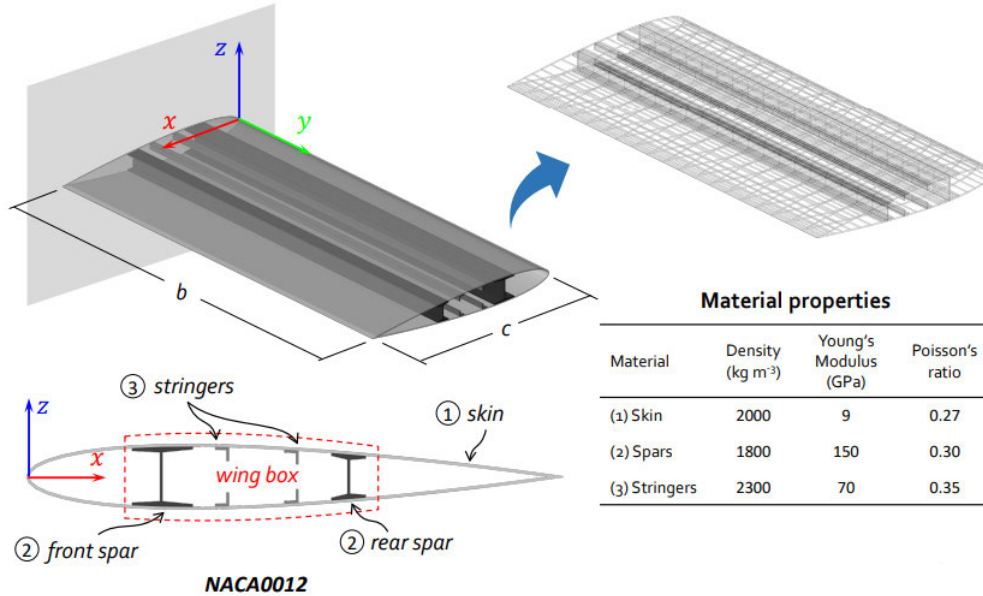


Figure 1: Setup of the experiment and characteristics of the wing studied.

The analysis is done by solving the equilibrium equation (Equation 1) for a set of panels along the span, treating the wing as a beam.

$$[\mathbf{M}]\{\ddot{\mathbf{u}}\} + [\mathbf{K}]\{\mathbf{u}\} = \{\mathbf{f}\} \quad (1)$$

To take into account that the whole wing is a 3D structure, effective properties of the beam structure are obtained with FEM, and matrices \mathbf{M} and \mathbf{K} of the beam structure are obtained with the properties of the wing. To account for the lift of a whole 3D wing, Prandtl lifting-line surface theory is used to obtain the divergence speed and the modes, as it can also be applied to a panel division of a beam. For the unsteady problem, Theodorsen's unsteady aerodynamic model is used.

The virtual laboratory code has the following requirements.

Structures: Use of 3D FEM code to obtain effective properties and MATLAB implementation of a beam's FEM algorithm.

Aerodynamics: For steady aerodynamics: MATLAB implementation of lifting-line solution by horseshoe elements. And for unsteady aerodynamics: MATLAB implementation of Theodorsen's model.

Coupling: MATLAB implementation of transfer matrices: structures output (displacements vector) to aerodynamics input (angle of attack) and aerodynamics output (lift distribution) to structures input (force vector).

Solvers: Divergence speed + modes and flutter speed.

Results: Obtain the stability plots for flutter, first modes associated to divergence conditions for different aspect ratios and divergence speed for different wing aspect ratios for a clamped-free straight panel with a constant NACA0012 airfoil section.

2. 3D FEM analysis - Experimental structural test

The aim is to obtain the shear center position $x_{sc}(y)$, the torsional stiffness $\overline{GJ}(y)$ and the bending stiffness $\overline{EI}(y)$. For the loading tests, sensors are placed along the mesh (wing span and chord) with the help of function *getNode*, that gets the closest structure node to a determined point. Equidistant 6 sensor (from 0.1c to 1c) placements along the span from 1.5m to 4m distance from the root have been chosen in order to avoid distorted values of the extremes. A 3D FEM solver provided will be used to get to know the displacements.

Assumptions:

- Small displacements and deformations (small angles and linear elasticity too).
- Effective response can be described by elemental beam theory (Equation 2).

$$\begin{Bmatrix} T \\ M \end{Bmatrix} = \begin{bmatrix} \overline{GJ} & 0 \\ 0 & \overline{EI} \end{bmatrix} \begin{Bmatrix} d\theta/dy \\ d^2h/dy^2 \end{Bmatrix} = [\mathbf{E}] \begin{Bmatrix} d\theta/dy \\ d^2h/dy^2 \end{Bmatrix} \quad (2)$$

Since it is not assumed that bending and torsion are uncoupled Equation 3 will be used for the experiment.

$$\begin{Bmatrix} \bar{\theta}' \\ \bar{h}'' \end{Bmatrix} = \begin{bmatrix} S_{11} & S_{12} \\ S_{21} & S_{22} \end{bmatrix} \begin{Bmatrix} T \\ M \end{Bmatrix} = [\mathbf{E}^{-1}] \begin{Bmatrix} T \\ M \end{Bmatrix} \quad (3)$$

Loading tests with pure torsional load and pure shear load are performed. The first one to be performed is the pure torsional load, in order to find the $x_{sc}(y)$, because it is where the load is applied in the second test.

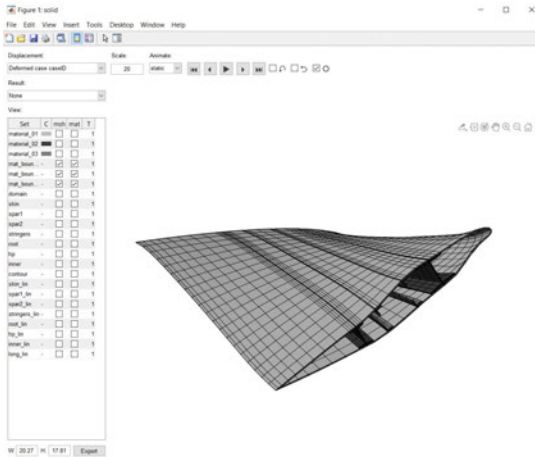


Figure 2: Pure torsion load.

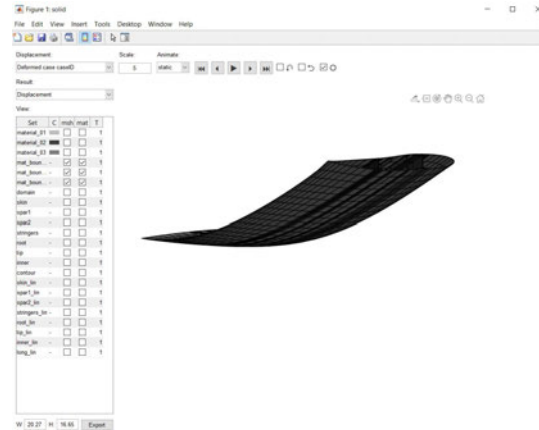


Figure 3: Pure shear load.

To apply a pure torsional load, two forces of equal value but opposite direction are applied at the wingtip at 0.1c and 0.6c. The elastic axis ($x_{sc}(y)$) can be obtained because it will be the point along the chord that will remain at $y = 0$. S_{11} and S_{21} can be obtained too, because when applying a pure torsional load $M = 0$, so:

$$S_{11} = \bar{\theta}'/T, \quad S_{21} = \bar{h}''/T \quad (4)$$

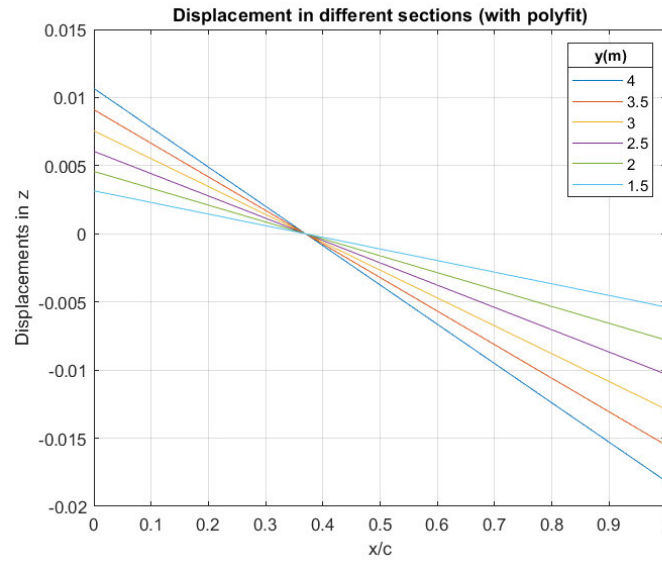


Figure 4: Displacement in different sections obtained when using function polyfit with the y values of the sensors.

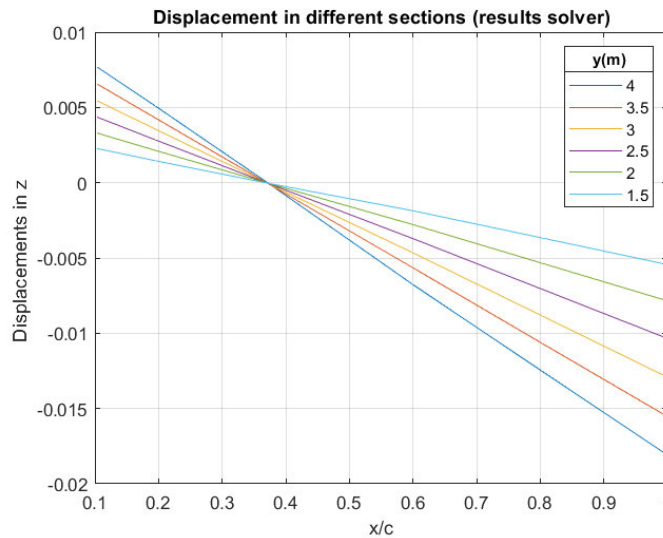


Figure 5: Displacement in different sections obtained with the solver.

Figures 4 and 5 show very similar results. They are the prove that the polynomial expressions to describe the displacements are well adjusted and it is possible to use them to obtain the derivatives. This check would be very necessary in the generic case that the deformations do not adjust to a linear regression and form a curve that needs to be described with a higher degree polynomial.

Once the shear center position is known, a pure shear load is applied in the wingtip. It is not possible to apply the force in the shear center because the structure does not exist along all $y = 0$ and the mesh is not infinite, but an equivalent force with 0 resultant moment can be calculated as the sum of different forces in 3 coordinates, as it can be seen in Figure 6.

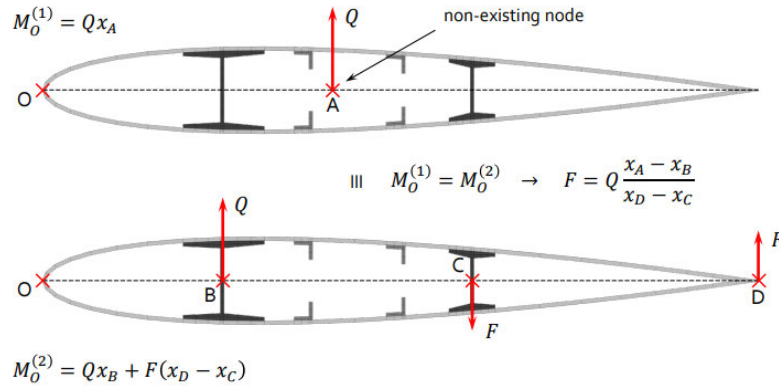


Figure 6: How to obtain an equivalent force to one applied at a non-existing node.

When applying a pure torsional load, $T = 0$ and $M' = -Q$ so S_{12} and S_{22} can be obtained as seen in Equation 5.

$$S_{12} = \bar{\theta}' / M = -\bar{\theta}'' / Q, \quad S_{22} = \bar{h}'' / M = -\bar{h}''' / Q \tag{5}$$

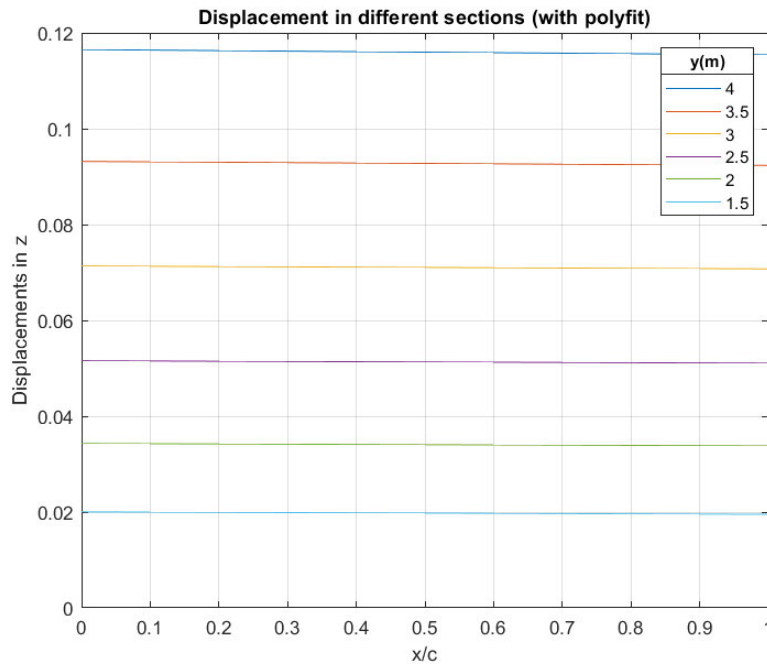


Figure 7: Displacement in the different sections when applying a pure shear load.

In both cases all displacements from the sections where the sensors are are evaluated to obtain the derivative values that will be used to obtain \mathbf{E}^{-1} matrix, that will be inverted to find \mathbf{E} , \overline{EI} and \overline{GJ} . These values are calculated for a wing of $c = 1$ and $AR = 5$, but are considered constant for the rest of the problem regardless of the aspect ratio.

3. 2D FEM Analysis - Section properties

As a first step, all the properties of the section are calculated. In this problem, as properties are constant, properties of the first section are calculated and they are applied to the whole span taking into account that they are calculated per unit of length.

To calculate the section properties it is necessary to use the connectivity matrices (T_n and T_m). The four points of the square section are obtained along with its density (specified in Figure 1). With these data the centroid coordinates, the area of each element and the density of each element can be obtained to calculate the total mass per unit of length, the center of mass in x and the inertia about the shear center per unit of length.

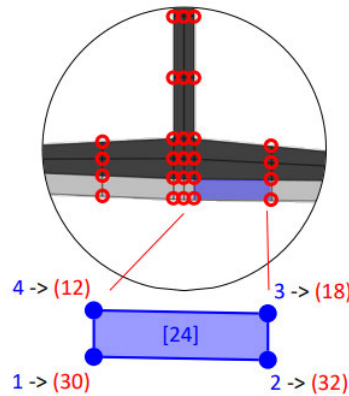


Figure 8: Quadrilateral element of the mesh.

To calculate the area of the mesh, it is assumed that the quadrilateral elements have an almost rectangular shape to apply the following assumption (Equation 6). Where a , b , c and d are the sides of the quadrilateral calculated as the distance between the (x, z) coordinates of adjacent nodes because they are in the same section y .

$$A^{[e]} = \frac{1}{2}(ab + cd) \quad (6)$$

For the centroid, as the airfoil is symmetric in z and only coordinate x is needed, only x coordinates of each node are accounted for.

4. 1D Beam analysis

Once the properties per unit of length are calculated, it is possible to proceed to 1D analysis. The span of the wing is divided into elements (*n_ely*) for this purpose, the more elements, the more numerical accuracy the results will have. In this assignment the results presented for the divergence speed and the first modes will be corresponding to a 40 elements division.

4.1. Element matrices

The matrices K^e and M^e can be calculated for all the elements. In this case, as properties per unit of length are constant only one K^e and one M^e are needed, and they will be applied to all the elements. At this point, the aspect ratio of the wing becomes relevant because the length of each element is calculated. The variation of the aspect ratio is made by changing the span of the wing, to avoid variations in the calculated shape and matrices that are made with $c = 1$.

Stiffness matrix:

$$[\mathbf{K}^{[i]}] = \frac{\overline{GJ}}{l^{[i]}} \begin{bmatrix} 1 & 0 & 0 & -1 & 0 & 0 \\ 0 & 0 & 0 & 0 & 0 & 0 \\ 0 & 0 & 0 & 0 & 0 & 0 \\ -1 & 0 & 0 & 1 & 0 & 0 \\ 0 & 0 & 0 & 0 & 0 & 0 \\ 0 & 0 & 0 & 0 & 0 & 0 \end{bmatrix} + \frac{\overline{EI}}{(l^{[i]})^3} \begin{bmatrix} 0 & 0 & 0 & 0 & 0 & 0 \\ 0 & 12 & 6l^{[i]} & 0 & -12 & 6l^{[i]} \\ 0 & 6l^{[i]} & 4(l^{[i]})^2 & 0 & -6l^{[i]} & 4(l^{[i]})^2 \\ 0 & 0 & 0 & 0 & 0 & 0 \\ 0 & -12 & -6l^{[i]} & 0 & 12 & -6l^{[i]} \\ 0 & 6l^{[i]} & 4(l^{[i]})^2 & 0 & -6l^{[i]} & 4(l^{[i]})^2 \end{bmatrix}$$

Mass matrix (lumped):

$$[\mathbf{M}^{[i]}] = \frac{l^{[i]}}{2} \begin{bmatrix} I_{sc} & md & 0 & 0 & 0 & 0 \\ md & m & 0 & 0 & 0 & 0 \\ 0 & 0 & 0 & 0 & 0 & 0 \\ 0 & 0 & 0 & I_{sc} & md & 0 \\ 0 & 0 & 0 & md & m & 0 \\ 0 & 0 & 0 & 0 & 0 & 0 \end{bmatrix}; \quad d = x_{sc} - x_{cm}$$

Figure 9: Stiffness and mass matrix of the wing.

4.2. Matrices assembly

After obtaining the element matrices they are assembled to find global structural M and K. There are $3(n_{ely} + 1)$ DOFs because \mathbf{u} will be evaluated at each side of each element, as seen in Figure 10.

$$[\mathbf{K}]^{(I,J)} = [\mathbf{K}]^{(I,J)} + [\mathbf{K}^{[i]}]^{(p,q)} \quad (7)$$

$$[\mathbf{M}]^{(I,J)} = [\mathbf{M}]^{(I,J)} + [\mathbf{M}^{[i]}]^{(p,q)} \quad (8)$$

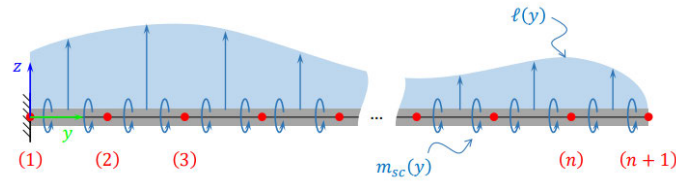


Figure 10: Element discretization at the beam.

4.3. Element force vector

The forces at each element can be discretized assigning the forces of the panel to its nodes as seen in Figure 11. The distributed lift force is converted into two forces and two moments applied (one of each) at each node of the element, while the moment is converted into two moments applied one at each node.

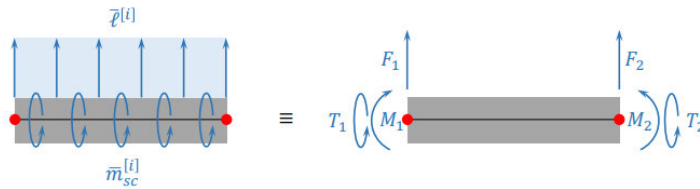


Figure 11: Element forces discretization.

$$\{\mathbf{f}^{[i]}\} = \frac{l^{[i]}}{2} \begin{bmatrix} 0 & 1 \\ 1 & 0 \\ l^{[i]}/6 & 0 \\ 0 & 1 \\ 1 & 0 \\ -l^{[i]}/6 & 0 \end{bmatrix} \begin{Bmatrix} \bar{q}^{[i]} \\ \bar{m}_{sc}^{[i]} \end{Bmatrix}$$

Figure 12: Element forces vector.

5. Aerodynamics

Once structural calculations have been done, it is time to evaluate the aerodynamic side of the problem. Two different methods will be used to account for steady and unsteady aerodynamics.

5.1. Lifting line surface analysis

The objective of the aerodynamic analysis is to find the aerodynamic forces seen in Figure 12, that, as seen in Section 6, can be obtained from the total lift on the elements matrix (\mathbf{L}). The lift on an element can be expressed as seen in Equation 9.

$$L^{[i]} = \rho_{\infty} U_{\infty} S^{[i]} \Gamma^{[i]} \quad (9)$$

Where the surface of each element can be directly calculated and Γ can be obtained through the system in Figure 13.

$$\begin{aligned} & \mathbf{[A]}\{\Gamma\} = -U_{\infty}\{\alpha\} \\ & \begin{bmatrix} A_{11} & A_{12} & \cdots & A_{1n} \\ A_{21} & A_{22} & \cdots & A_{2n} \\ \vdots & \vdots & \ddots & \vdots \\ A_{n1} & A_{n2} & \cdots & A_{nn} \end{bmatrix} \begin{Bmatrix} \Gamma^{[1]} \\ \Gamma^{[2]} \\ \vdots \\ \Gamma^{[n]} \end{Bmatrix} = -U_{\infty} \begin{Bmatrix} \alpha^{[1]} \\ \alpha^{[2]} \\ \vdots \\ \alpha^{[n]} \end{Bmatrix} \end{aligned}$$

where $\mathbf{[A]}$ is the aerodynamic influence coefficients matrix:

$$A_{ij} = \left(\mathbf{v}_{12}^{[j]}(\mathbf{x}^{[i]}) + \mathbf{v}_{23}^{[j]}(\mathbf{x}^{[i]}) + \mathbf{v}_{34}^{[j]}(\mathbf{x}^{[i]}) \right) \Big|_{\Gamma^{[i]}=1} \cdot \mathbf{n}^{[i]}$$

Figure 13: System of equations to find Γ .

So the total lift can be expressed as:

$$\{\mathbf{L}\} = -\rho_{\infty} U_{\infty}^2 [\mathbf{S}][\mathbf{A}]^{-1} \{\alpha\} \quad (10)$$

And, as seen in Figure 13, the aerodynamic influence coefficients matrix can be calculated using the lifting line surface analysis. Induced velocities are calculated at collocation points of each panel at $3/4c$ as the sum of the contributions of the horseshoe vortex segments. As a summary, the aerodynamic analysis' outputs are matrices $[\mathbf{S}]$ (surface of each element) and $[\mathbf{A}]$ (aerodynamic influence coefficients).

5.2. Theodorsen's aerodynamic model

According to Theodorsen's model the aerodynamic expressions for the lift and the moment are:

$$\begin{aligned} \ell(y) &= \pi \rho_{\infty} b^2 (U_{\infty} \dot{\theta} - ba\ddot{\theta} - \ddot{h}) + 2\pi \rho_{\infty} U_{\infty} b C(\kappa) \left(U_{\infty} \theta + b \left(\frac{1}{2} - a \right) \dot{\theta} - \dot{h} \right) \\ m_{sc}(y) &= -\pi \rho_{\infty} b^3 \left(U_{\infty} \left(\frac{1}{2} - a \right) \dot{\theta} + b \left(\frac{1}{8} + a^2 \right) \ddot{\theta} + a\ddot{h} \right) + 2\pi \rho_{\infty} U_{\infty} b^2 C(\kappa) \left(a + \frac{1}{2} \right) \left(U_{\infty} \theta + b \left(\frac{1}{2} - a \right) \dot{\theta} - \dot{h} \right) \end{aligned}$$

Figure 14: Lift and moment in Theodorsen's model.

The objective of the aerodynamic analysis is to find the aerodynamic forces seen in Figure 12. In this case, the aerodynamic forces seen in Figure 12 can be expressed as:

$$\begin{Bmatrix} m_{sc}^{[i]} \\ \ell^{[i]} \end{Bmatrix} = \pi \rho_{\infty} b^2 U_{\infty}^2 ([\hat{\mathbf{A}}_R(\kappa)] + i[\hat{\mathbf{A}}_I(\kappa)]) [\mathbf{I} \quad \mathbf{I}] \begin{Bmatrix} \hat{\mathbf{u}}^{(i)} \\ \hat{\mathbf{u}}^{(i+1)} \end{Bmatrix}$$

Figure 15: Aerodynamic forces in Theodorsen's model.

Where:

$$\begin{aligned} \hat{\mathbf{A}}_R(\kappa) &= \kappa^2 \begin{bmatrix} 1/8 + a^2 & a \\ a & 1 \end{bmatrix} + \kappa G(\kappa) \begin{bmatrix} 2a^2 - 1/2 & 2a + 1 \\ 2a - 1 & 2 \end{bmatrix} + F(\kappa) \begin{bmatrix} 1 + 2a & 0 \\ 2 & 0 \end{bmatrix} \\ \hat{\mathbf{A}}_I(\kappa) &= \kappa \begin{bmatrix} a - 1/2 & 0 \\ 1 & 0 \end{bmatrix} - \kappa F(\kappa) \begin{bmatrix} 2a^2 - 1/2 & 2a + 1 \\ 2a - 1 & 2 \end{bmatrix} + G(\kappa) \begin{bmatrix} 1 + 2a & 0 \\ 2 & 0 \end{bmatrix} \\ \mathbf{I} &= \begin{bmatrix} 1/2 & 0 & 0 \\ 0 & 1/2 & 0 \end{bmatrix} \end{aligned}$$

Figure 16: $\hat{\mathbf{A}}_R(k)$, $\hat{\mathbf{A}}_I(k)$ and \mathbf{I} matrices definition.

Where a and b are:

$$a = x_{sc}/b - 1, \quad b = c/2 \quad (11)$$

and the Theodorsen's function $C(k) = F(k) + iG(k)$ (to account for attenuation by wake vorticity) is given by the equation in Figure 17 in this case.

$$F(\kappa) = \frac{0.5\kappa^4 + 0.0765\kappa^2 + 1.8632 \times 10^{-4}}{\kappa^4 + 0.0921\kappa^2 + 1.8632 \times 10^{-4}}, \quad G(\kappa) = \frac{-0.1080\kappa^3 - 8.8374 \times 10^{-4}\kappa}{\kappa^4 + 0.0921\kappa^2 + 1.8632 \times 10^{-4}}$$

Figure 17: Coefficients $F(k)$ and $G(k)$ of Theodorsen's function.

6. Systems coupling - Force vector assembly

6.1. Divergence analysis

The \mathbf{L} matrix of the steady aerodynamic analysis is expressed in terms of α , and needs to be expressed in terms of the structural unknown vector to be coupled into the system. $\alpha^{[i]}$ ($= \theta^{[i]}$) is also calculated for every element, and needs to be applied to the nodes. Figure 18 illustrates how this conversion is made to obtain Equation 12.

$$\{\mathbf{L}\} = -\rho_{\infty} U_{\infty}^2 [\mathbf{S}][\mathbf{A}]^{-1} [\mathbf{I}]\{\mathbf{u}\} \quad (12)$$

$$\alpha^{[i]} = \theta^{[i]} = \frac{1}{2} [1 \quad 0 \quad 0 \quad 1 \quad 0 \quad 0] \begin{Bmatrix} \theta^{(i)} \\ h^{(i)} \\ \gamma^{(i)} \\ \theta^{(i+1)} \\ h^{(i+1)} \\ \gamma^{(i+1)} \end{Bmatrix} = [\mathbf{I} \quad \mathbf{I}] \begin{Bmatrix} \mathbf{u}^{(i)} \\ \mathbf{u}^{(i+1)} \end{Bmatrix}$$

$$\{\boldsymbol{\alpha}\} = \begin{Bmatrix} \alpha^{[1]} \\ \alpha^{[2]} \\ \vdots \\ \alpha^{[n]} \end{Bmatrix} = \begin{bmatrix} \mathbf{I} & \mathbf{I} & \mathbf{0} & \cdots & \mathbf{0} & \mathbf{0} \\ \mathbf{0} & \mathbf{I} & \mathbf{I} & \cdots & \mathbf{0} & \mathbf{0} \\ & \vdots & \vdots & \ddots & \vdots & \vdots \\ \mathbf{0} & \mathbf{0} & \mathbf{0} & \cdots & \mathbf{I} & \mathbf{I} \end{bmatrix} \begin{Bmatrix} \mathbf{u}^{(1)} \\ \mathbf{u}^{(2)} \\ \mathbf{u}^{(3)} \\ \vdots \\ \mathbf{u}^{(n)} \\ \mathbf{u}^{(n+1)} \end{Bmatrix} = [\mathbf{I}]\{\mathbf{u}\}$$

Figure 18: Expression of α in terms of the structural unknown vector.

Now, the aerodynamic forces are ready to be coupled into the element equilibrium equation:

$$[\mathbf{M}^{[i]}\{\ddot{\mathbf{u}}^{[i]}\} + [\mathbf{K}^{[i]}\{\mathbf{u}^{[i]}\} = \{\mathbf{f}^{[i]}\} \quad (13)$$

where $\{\ddot{\mathbf{u}}\}$ is 0 because it is a steady problem and where (only θ is considered):

$$\{\mathbf{u}^{[i]}\} = \begin{Bmatrix} \theta^{(i)} \\ h^{(i)} \\ \gamma^{(i)} \\ \theta^{(i+1)} \\ h^{(i+1)} \\ \gamma^{(i+1)} \end{Bmatrix} = \begin{Bmatrix} \theta^{(i)} \\ 0 \\ 0 \\ \theta^{(i+1)} \\ 0 \\ 0 \end{Bmatrix}; \quad \{\mathbf{f}^{[i]}\} = \begin{Bmatrix} T_1^{[i]} \\ F_1^{[i]} \\ M_1^{[i]} \\ T_2^{[i]} \\ F_2^{[i]} \\ M_2^{[i]} \end{Bmatrix} \quad (14)$$

Each element's lift and moment is expressed in terms of \mathbf{L} , and the force assembly matrix \mathbf{Q} is obtained to get:

$$\{\mathbf{F}(\mathbf{u})\} = -\underbrace{\frac{1}{2}\rho_{\infty}U_{\infty}^2[\mathbf{Q}][\mathbf{S}][\mathbf{A}]^{-1}[\mathbf{I}]\{\mathbf{u}\}}_{q_{\infty}[\mathbf{K}_a]}$$

Figure 19: RHS of the equation.

So:

$$[\mathbf{K}]\{\mathbf{u}\} = \{\mathbf{F}(\mathbf{u})\} = -q_{\infty}[\mathbf{K}_a]\{\mathbf{u}\} \quad (15)$$

$$([\mathbf{K}_s] + q_{\infty}[\mathbf{K}_a])\{\mathbf{u}\} = 0 \quad (16)$$

To get the divergence speed and nodes, the first 3 DOFs of each matrix are prescribed and the structural stiffness matrix is adimensionalized with the analytical solution for the divergence condition ($Q_{Da} = \pi^2/4b^2 \quad GJ/ceCl_{,\alpha}$) for a wing with constant properties. The aerodynamic stiffness matrix (\mathbf{K}_a) needs to be inverted to solve the system and find the eigenvalues but as there are 0s in the diagonal it is not possible to invert it. the solution to this numerical problem has been adding an almost negligible value (1×10^{-10}) to the diagonal of the matrix to be able to invert it. The eigenvalues and eigenvectors of the system have been found.

The adimensional divergence condition Q_D is given by the minimum eigenvalue. To find U_D the value is dimensionalized multiplying it by Q_{Da} and later obtaining the U_D (ρ is known). The first five modes are found at the end of the eigenvector matrix. So the minimum divergence speed and the first five modes of the wing are obtained.

6.2. Flutter analysis

In this case, having obtained the aerodynamic element forces as a function of k , when adding the element force vector, the \mathbf{F} matrix is:

$$\{\mathbf{F}\} = \pi\rho_{\infty}b^3U_{\infty}^2[\widehat{\mathbf{Q}}][\widehat{\mathbf{A}}(\kappa)][\widehat{\mathbf{I}}]\{\widehat{\mathbf{u}}\}$$

Figure 20: RHS of the equation.

The element force vector and the force assembly matrix in this case are:

$$\{\mathbf{f}^{[i]}\} = b \begin{bmatrix} \widehat{\mathbf{Q}}_1^{[i]} \\ \widehat{\mathbf{Q}}_2^{[i]} \end{bmatrix} \begin{Bmatrix} m_{sc}^{[i]} \\ \ell^{[i]} \end{Bmatrix}$$

$$\widehat{\mathbf{Q}}_1^{[i]} = \frac{\hat{l}^{[i]}}{2} \begin{bmatrix} 1 & 0 \\ 0 & 1 \\ 0 & \hat{l}^{[i]}/6 \end{bmatrix}, \quad \widehat{\mathbf{Q}}_2^{[i]} = \frac{\hat{l}^{[i]}}{2} \begin{bmatrix} 1 & 0 \\ 0 & 1 \\ 0 & -\hat{l}^{[i]}/6 \end{bmatrix}, \quad \text{and } \hat{l}^{[i]} = l^{[i]}/b$$

Figure 21: Shape of the element force vector.

To solve the system, matrices \mathbf{M} and \mathbf{K} are adimensionalized and the system is expressed:

$$\left(\frac{mb^3\omega_\theta^2}{\pi\rho_\infty b^3 U_\infty^2} [\hat{\mathbf{K}}] - \frac{mb^3\omega^2}{\pi\rho_\infty b^3 U_\infty^2} [\hat{\mathbf{M}}] - [\hat{\mathbf{Q}}][\hat{\mathbf{A}}(\kappa)][\hat{\mathbf{I}}] \right) \{\hat{\mathbf{u}}\} = \{\mathbf{0}\}$$

Figure 22: Equilibrium equation for the non-steady case.

Applying the definitions in Figure 23 and the boundary conditions (prescribing the first 3 DOFs) the system to be solved becomes as in Figure 24.

$$\lambda = \frac{\omega_\theta^2}{\omega^2}, \quad \mu = \frac{m}{\pi\rho_\infty b^2}, \quad \kappa = \frac{\omega b}{U_\infty}$$

Figure 23: Values of λ , μ and κ .

$$\left(\underbrace{[\hat{\mathbf{R}}_{LL}]^{-1}[\hat{\mathbf{M}}_{LL}] + \frac{1}{\mu\kappa^2}[\hat{\mathbf{R}}_{LL}]^{-1}[\hat{\mathbf{F}}_{LL}(\kappa)]}_{[\hat{\mathbf{D}}_{LL}(\kappa)]} - \lambda[\mathbf{1}] \right) \{\hat{\mathbf{u}}\} = \{\mathbf{0}\}$$

Figure 24: Resulting system for the non-steady case.

The flutter condition is given by $\det([\hat{\mathbf{D}}(\kappa_F)] - \lambda_F[\mathbf{1}]) = 0$. To solve the system a set of values for κ are defined to be tried in different iterations and all the values that depend on it are recalculated each time. The eigenvalues of $\hat{\mathbf{D}}_{LL}$ are obtained. For every iteration, values ω_F and U_F are calculated and stored with their corresponding κ . The values of ω_F that have a non-null negative imaginary part are identified, because it means that those modes may cause instabilities. To evaluate this, the positions of all the modes that create instability are stored in a matrix, so that they can later be identified and associated to their κ . The minimum U_F for each κ with instability is evaluated as well.

7. Code structure

1. **Input data and geometric parameters calculation:** Input data given is read from the mesh file *naca0012*. The geometry of the entire wing problem is defined, total number of beams and plates, total number of nodes, number of nodes for each element, etc. Physical and material properties (Young's modulus, densities, etc). Also all the sensors needed to store the displacements through the span and sections.
2. **Find shear center:** First loading test with the given functions, with a pure torsional load. Evaluate displacements and find the elastic axis.
3. **Compute the pure shear load:** Second loading test with a force placed in the elastic axis.
4. **Obtain E matrix:** Calculation of the derivatives of the displacements and θ angles. Computation of E with S11, S12, S21 and S22.
5. **Compute section properties:** Obtainment of I_{sc} , total mass per unit length and the center of mass.
6. **Obtainment of K[e] and M[e] and the corresponding assembly.**
7. **Lifting-line surface analysis:** Computation of all the induced velocities due to the vortex in all the discretized panels along the wing. Create the aerodynamic influence coefficients matrix. And the matrix assembly of K_{aero} needed to solve the total lift of the elements. Introduce the element force vector assembly.
8. **Divergence analysis:** Solve the determinant of the system and find the eigenvalues and first five modes (eigenvectors). And plot the comparison between aspect ratios.
9. **Iteration for different aspect ratios** (Return to step 6)
10. **Flutter analysis:** Solve the instabilities for a $AR = 5$ and 5 elements in the span. Analysis of the behaviour near the boundary flutter speeds. Plot the refinement iterations between closer values of k_f .

8. Results

8.1. Divergence speed for different wing aspect ratios

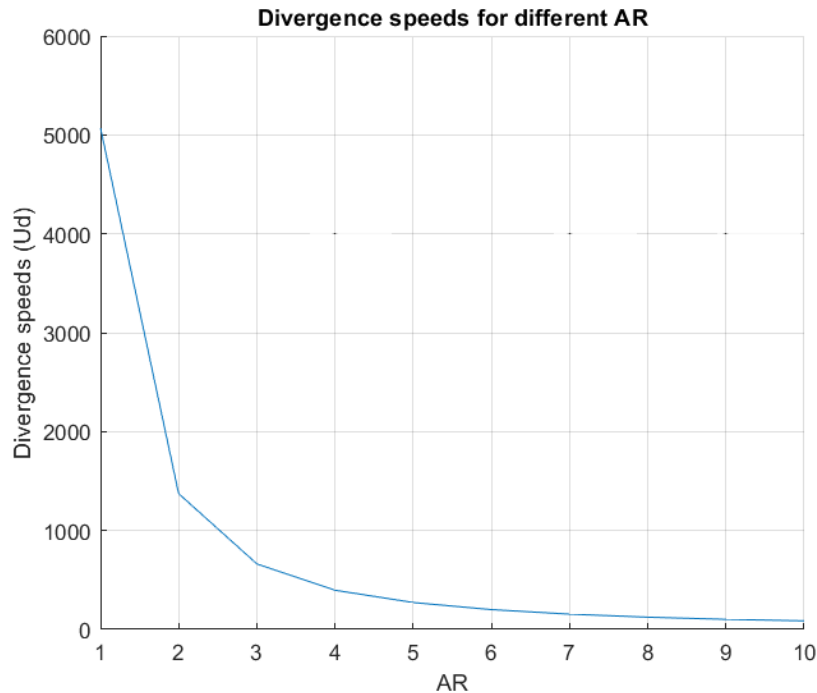


Figure 25: Divergence speeds of the wing for different aspect ratios.

Divergence occurs when the increase in the aerodynamic moment is bigger than the increase in restoring moment from the wing's torsional stiffness. Figure 25 shows how divergence speed decreases with the aspect ratio. This happens because the higher the aspect ratio is, the more span (c is constant) the torsion has to make an influence on θ . A very high speed for a square wing (as seen in Figure 25) makes sense because the necessary lift to twist the wing enough to reach divergence is very high.

AR	1	2	3	4	5
U_D [m/s]	5070.3	1372.4	662.8	396.2	272.0
AR	6	7	8	9	10
U_D [m/s]	200.4	154.5	123.7	101.9	86.8

Table 1: Divergence speeds for aspect ratios 1 to 10.

8.2. First modes associated to divergence conditions for different aspect ratios

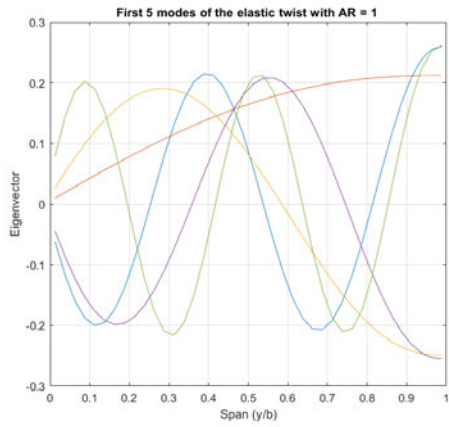


Figure 26: AR = 1.

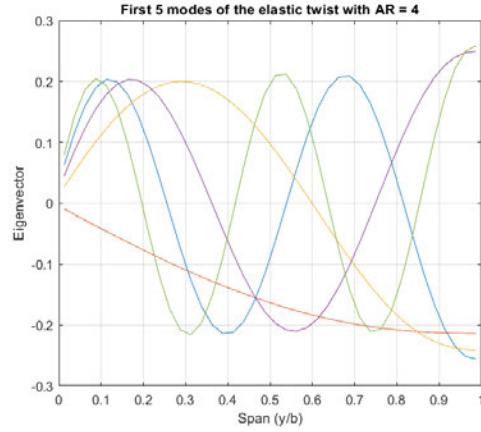


Figure 27: AR = 4.

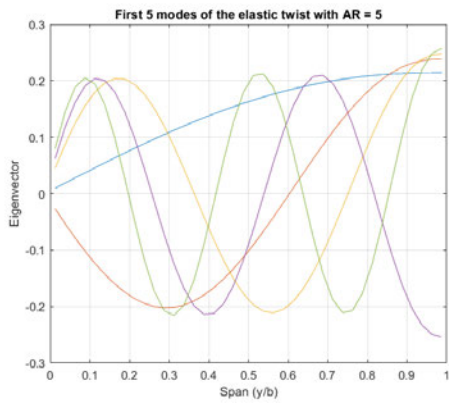


Figure 28: AR = 5.

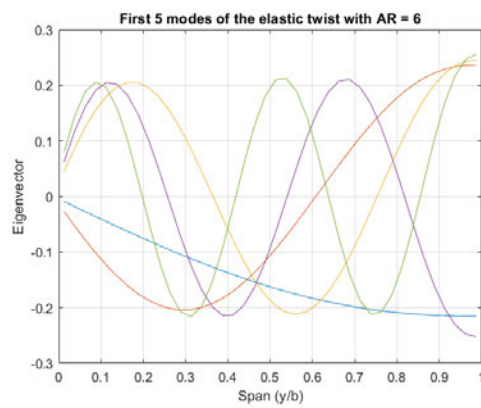


Figure 29: AR = 6.

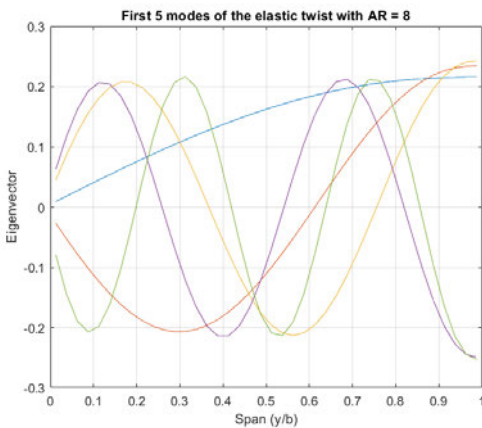


Figure 30: AR = 8.

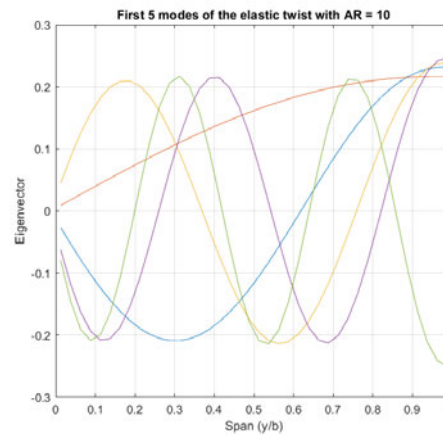


Figure 31: AR = 10.

Figure 32: First five modes for different AR.

8.3. Flutter stability plots

For the flutter analysis, κ has been evaluated using a logarithmic distribution from $\kappa = 10^{-3}$ to $\kappa = 10^3$, since the aim is to guess at which κ range the flutter boundary appears (point where the imaginary component of ω_F changes sign). In this way, a wide range is covered in the same computation. Figures 33 and 36 show plots of the ω_F and minimum U_F for these κ s. These results have been evaluated for the simple case of 5 elements.

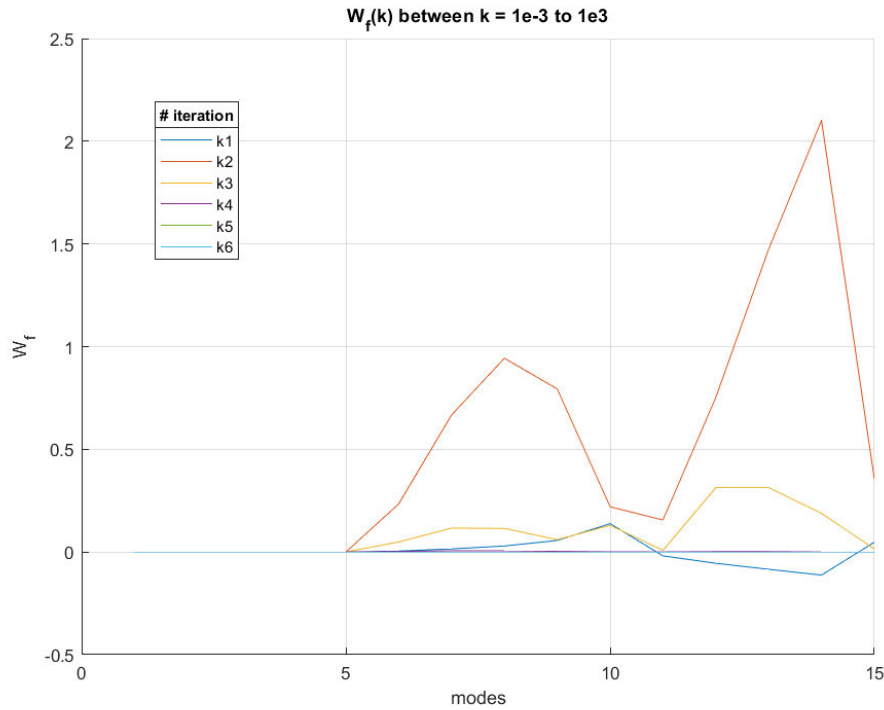


Figure 33: W_f for $k = 10^{-2}$ to 10^3 .

Figure 33 and Table 2 show that the ω_F has non-null negative imaginary component for $\kappa = 0.001$ and for $\kappa > 10$. The very small value of κ has an associated speed that is not reachable in the problem's conditions, so the search for the flutter boundary is made around $\kappa = 10$.

k_f	Minimum unstable speed [m/s]	Unstable modes
0.001	69044.40	11, 12, 13, 14
0.01	-	-
0.1	-	-
1	-	-
10	24.88	12, 13, 14
100	2.488	12, 13, 14
1000	0.25	12, 13, 14

Table 2: Minimum unstable speed and unstable modes for κ 0.001 to 1000.

In the first refinement between $\kappa = 1$ and $\kappa = 10$, the change can be seen between $\kappa = 1$ and $\kappa = 2$ (see Figure 34 and Table 3). This leads to a second refinement.

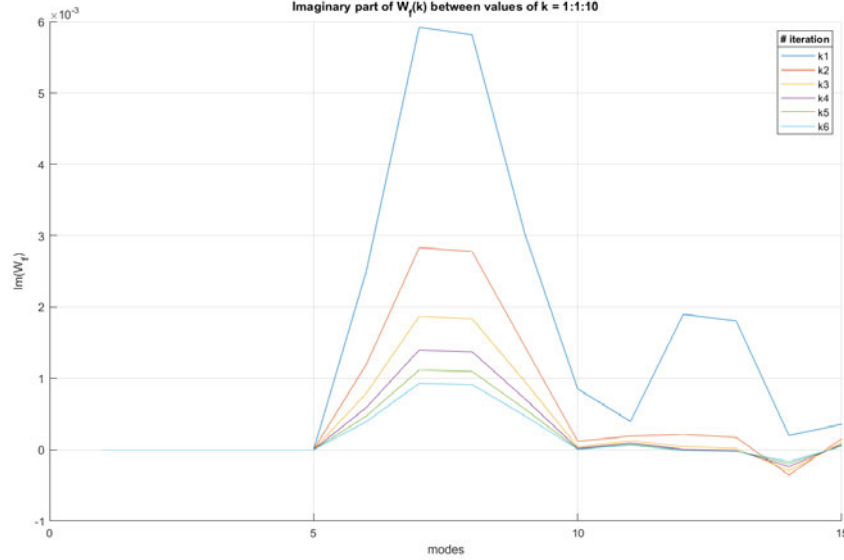
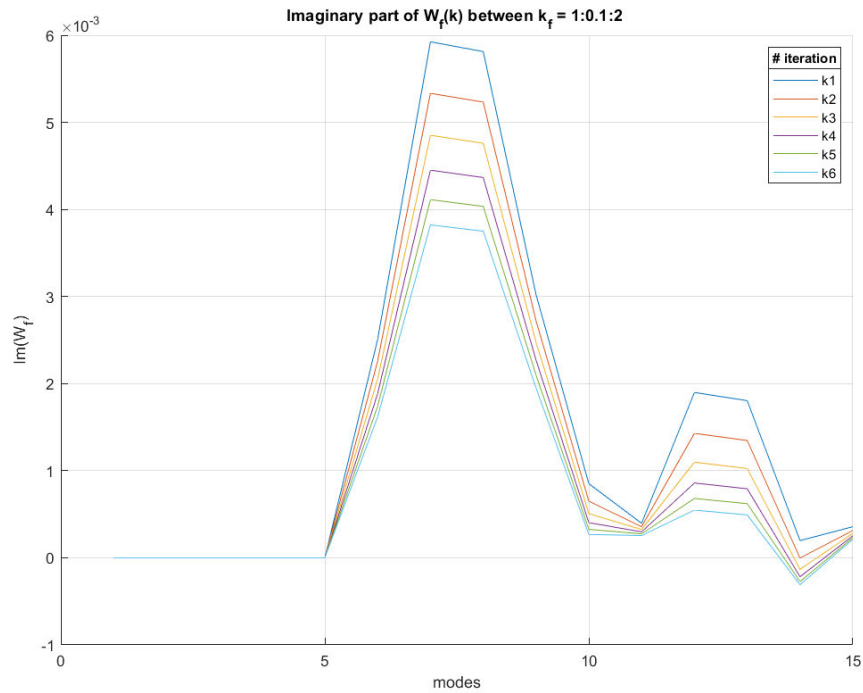


Figure 34: W_f for $k = 10$ to 100.

k_f	Minimum unstable speed [m/s]	Unstable modes
1	-	-
2	244.21	14
3	162.81	14
4	96.90	13, 14
5	49.77	12, 13, 14
6	41.47	12, 13, 14
7	35.55	12, 13, 14
8	31.10	12, 13, 14
9	27.65	12, 13, 14
10	24.88	12, 13, 14

Table 3: Minimum unstable speed and unstable modes for κ 1 to 10.

The second refinement is made between $\kappa = 1$ and $\kappa = 2$ (see Table 4). This process should be iterative and automatized, but it has not been implemented in the code. In Figure 35, a more clear tendency of the imaginary part getting smaller until it gets positive can be seen, especially between iteration 1 and 2, corresponding to $\kappa = 1$ and $\kappa = 1.1$. The value of the minimum flutter speed is around $444m/s$ as it can be seen in the table and appears in mode 14.

Figure 35: W_f for $k = 1$ to 2.

k_f	Minimum unstable speed [m/s]	Unstable modes
1	-	-
1.1	444.03	14
1.2	407.02	14
1.3	375.71	14
1.4	348.88	14
1.5	325.62	14
1.6	305.27	14
1.7	287.31	14
1.8	271.35	14
1.9	257.07	14
2	244.21	14

Table 4: Minimum unstable speed and unstable modes for κ 1 to 2.

Including Figure 33 has been considered interesting, not because it provides interesting flutter data but because it gives information about the tendency of the eigenvalues and it is a useful way to test that the code works properly even in the nodes that may not cause instabilities.

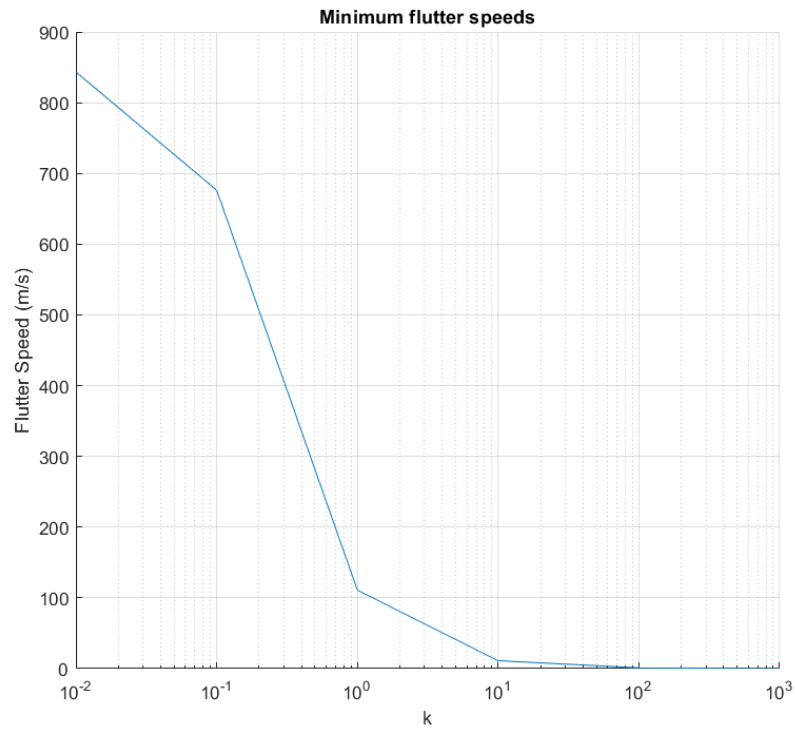


Figure 36: Minimum flutter speeds for $k = 10^{-2}$ to 10^3 .

9. Conclusions

In this assignment, it can be seen that simulating 3D conditions when doing an aeroelastic beam analysis is possible. When solving a problem of this kind, it is important to know how to couple the different systems, so that the DOFs and the equations of every system match with each other.

An analysis for a stable case and an unstable case have been performed. A method to perform further iterations in the refinement of the unstable case could be performed as an improvement. Further improvements could include variations on different parameters of the structure, such as the AR, to see how it affects flutter. Other assessments could include the variation of material properties.

Since the unsteady case study is complex, 5 elements have been used to perform calculations. Increasing the number of elements would be interesting too. For the steady case, mirroring in the horseshoe vortex for the study of the behavior of a whole wing can be included.

To approximate the study to a more real wing, other features could be added to the wing, such as sweep, dihedral or taper ratio. But to include these kind of features the 3D structure model should be changed, just like changing the wing that is going to be studied in a wind tunnel.

10. Code

10.1. Main

```

1
2 % Initialize
3 clear
4 close all
5 clc
6
7 %% Data
8
9 % Geometry data
10 meshfile = 'naca0012';
11 c = 1;      % Chord
12 b = 5*c;   % Span
13 AR = b/c;  % Aspect Ratio
14
15 Xsc = 0;    % shear center (later will be computed)
16
17 n_ely = 5; % #elements in the span
18
19 % Material data
20 mat = [
21     % Density      Young      Poisson
22     2000,         9e9,      0.27; % Skin
23     1800,        150e9,    0.30; % Spars
24     2300,         70e9,    0.35; % Stringers
25 ];
26
27
28 %% Setup lab
29
30 [probData,vLab] = SetupTest(meshfile,c,b,mat);
31
32 %% Setup displacement sensors
33
34 % - Each row correspond to the coordinates of a 'sensor' on the
35   % setup:
36 X_app = [0.1, 4, 0      % sensor 1 s1
37          0.2, 4, 0      % sensor 2 s1
38          0.4, 4, 0      % sensor 3 s1
39          0.6, 4, 0      % sensor 4 s1
40          0.8, 4, 0      % sensor 5 s1
41          1,   4, 0      % sensor 6 s1
42
43          0.1, 3.5, 0     % sensor 1 s2
44          0.2, 3.5, 0     % sensor 2 s2
45          0.4, 3.5, 0     % sensor 3 s2
46          0.6, 3.5, 0     % sensor 4 s2
47          0.8, 3.5, 0     % sensor 5 s2
48          1,   3.5, 0     % sensor 6 s2
49
50          0.1, 3, 0       % sensor 1 s3
51          0.2, 3, 0       % sensor 2 s3
52          0.4, 3, 0       % sensor 3 s3

```

```

52     0.6, 3, 0 % sensor 4 s3
53     0.8, 3, 0 % sensor 5 s3
54     1, 3, 0 % sensor 6 s3
55
56     0.1, 2.5, 0 % sensor 1 s4
57     0.2, 2.5, 0 % sensor 2 s4
58     0.4, 2.5, 0 % sensor 3 s4
59     0.6, 2.5, 0 % sensor 4 s4
60     0.8, 2.5, 0 % sensor 5 s4
61     1, 2.5, 0 % sensor 6 s4
62
63     0.1, 2, 0 % sensor 1 s5
64     0.2, 2, 0 % sensor 2 s5
65     0.4, 2, 0 % sensor 3 s5
66     0.6, 2, 0 % sensor 4 s5
67     0.8, 2, 0 % sensor 5 s5
68     1, 2, 0 % sensor 6 s5
69
70     0.1, 1.5, 0 % sensor 1 s6
71     0.2, 1.5, 0 % sensor 2 s6
72     0.4, 1.5, 0 % sensor 3 s6
73     0.6, 1.5, 0 % sensor 4 s6
74     0.8, 1.5, 0 % sensor 5 s6
75     1, 1.5, 0]; % sensor 6 s6
76
77 [~,X_nod] = probData.MeshData{1}.getNodes(X_app);
78
79
80 %% Pure torsion load force set CASE ID = 1
81
82 % forces to pure torsion load
83 cas = 1;
84 [fext_T, T] = set_forces(cas,Xsc);
85
86 % PURE TORSION CASE (case ID = 1)
87 [rep_F_T,rep_D_T,rep_R_T,vLab,T_T,M_T] = LoadingTest(probData,
88     fext_T,X_nod,vLab,'caseID',1);
89
90 %% Postprocessing results
91
92 % study of the sections displacements (in this case solution of the
93     shear center)
94 [Xsc, d_theta_T, dd_h_T, dd_theta_T, ddd_h_T] = findshearcenter(
95     X_nod, rep_D_T, cas, Xsc);
96
97 %% Compute the pure shear load (bending) case (case ID = 2)
98
99 % forces to pure bending load
100 cas = 2;
101 [fext_M, M_test] = set_forces(cas, Xsc);
102
103 % solutions of the loading test
104 [rep_F_M, rep_D_M, rep_R_M, vLab, T_M, M_M] = LoadingTest(probData,
105     fext_M, X_nod, vLab, 'caseID', 2);
106
107 % study of the sections displacements

```

```

105 [Xsc, d_theta_M, dd_h_M, dd_theta_M, ddd_h_M] = findshearcenter(
      X_nod, rep_D_M, cas, Xsc);
106
107 % obtain the matrix of the assumed uncoupled structure
108 [E] = obtain_E(T,M_test,d_theta_T,dd_h_T,dd_theta_M,ddd_h_M);
109
110 %% compute all the section section properties
111 ii = 0;
112
113 % import the data from profile
114 [Tn,Tm,Xnod] = import_mesh();
115
116 [Isc, d, mass_tot] = section_properties(Xnod, Tn, Tm, mat, Xsc);
117
118 for b = 1:1:5
119
120     [K, M, GJ, EI] = obtain_K_M(b, n_ely, E, Isc, mass_tot, d);
121
122     [M_ass, K_ass, Tn_y, Y_coord] = assembly(K, M, n_ely, b);
123
124     %% Horsheshoe elements discretization
125     [K_aero, e, RHO] = lift_line(b, Y_coord, Xsc, n_ely);
126
127     % SOLVERS %
128
129     %% Divergence speed + modes
130     % midterm problem
131     [V_theta_5, lambda_prima, Ud] = divergence(K_aero, K_ass, GJ, b
          , e, c, RHO, Y_coord, n_ely);
132
133     ii = ii+1;
134     Ud_min(ii) = min(Ud);
135
136 end
137
138 % plot different divergence speeds
139
140 figure(20)
141 hold on
142 plot(1:1:5, Ud_min);
143 title('Divergence speeds for different AR');
144 xlabel('AR');
145 ylabel('Divergence speeds (Ud)');
146 grid on;
147
148 %% Flutter analysis %%%%%%%%%%%%%%%
149
150 % theodorsen
151
152 % wing geometry
153
154 AR = 5;
155 c = 1;
156 b = AR * c;
157 l_elem = b/n_ely;
158
159 % nodal connectivities en 1D

```

```

160 for e = 1:n_ely
161     Tnod(e,1) = e;
162     Tnod(e,2) = e+1;
163 end
164
165 % utilizamos las matrices y valores para el AR = 5 del analisis
166 anterior
167 % creamos la nueva matriz Q
168 Q_mat = zeros(3*n_ely, 3*n_ely);
169
170 Q = (l_elem/(2*b))*[ 1 0;
171                    0 1;
172                    0 l_elem/(6*b);
173                    1 0;
174                    0 1;
175                    0 -l_elem/(6*b)];
176
177 for e = 1:n_ely
178     Q_mat((3*(e-1)+1:3*(e-1)+6), (3*e-2):(3*e-1) ) = Q;
179 end
180
181 % iniciamos con parametros
182 B = c/2;
183 a = (Xsc/B)-1;
184
185 W_theta = sqrt(GJ/(Isc*B^2));
186
187 %% Matrices A de theodorsen
188 AR_a = [1/8+a^2  a;
189         a        1];
190 AR_b = [2*a^2-0.5  2*a+1;
191         2*a-1      2];
192 AR_c = [1+2*a  0;
193         2       0];
194
195 AI_a = [a-0.5  0;
196         1       0];
197 AI_b = [2*a^2-0.5  2*a+1;
198         2*a-1      2];
199 AI_c = [1+2*a  0;
200         2       0];
201
202 I = [0.5  0  0;
203      0  0.5  0];
204
205 I_mat = zeros(3*n_ely,n_ely*3);
206
207 for e = 1:n_ely
208     I_mat((3*e-2):(3*e-1), 1+3*(e-1):6+3*(e-1)) = [I I];
209 end
210
211 %% Modificar las matrices estructurales
212 b_mat = [1 0 0;
213          0 B 0;
214          0 0 1];
215

```

```

216 B_mat = zeros(n_ely*3,n_ely*3);
217 B_mat = diag(b);
218
219 M_theo = zeros(n_ely*3,n_ely*3);
220 M_theo = (1/(mass_tot*B^3))*B_mat'*M_ass*B_mat;
221
222 K_theo = zeros(n_ely*3,n_ely*3);
223 K_theo = (1/(mass_tot*W_theta^2*B^3))*B_mat'*K_ass*B_mat;
224
225 % prescribed DOF
226 K_theo = K_theo(4:(n_ely*3+3),4:(n_ely*3+3));
227 M_theo = M_theo(4:(n_ely*3+3),4:(n_ely*3+3));
228
229 %% Solver system
230 % from pdf flutter analysis
231 U_inf = 1;
232 rho = 1;
233
234 mu = mass_tot/(pi*rho*B^2);
235
236 % initial value for k
237 k = 10^-3;
238
239 % para n_ely=5 vemos aparicion de flutter de k = 10 a 100
240 % refinamos esa area para estudiar mejor
241 % k_min = 10;
242 % k_max = 100;
243 % ite = 0;
244
245 w_f = zeros(10,n_ely);
246 U_f = zeros(10,n_ely);
247 mode = zeros(n_ely, 10);
248
249 % comienza las iteraciones para valores de k
250 % Specify a set of a trial values for k_F
251
252 for ite = 1:6
253 % for k = k_min:10:k_max
254
255     %ite = ite + 1;
256
257     F = (0.5*k^4 + 0.0765*k^2 + 1.8632*10^-4)/(k^4 + 0.0921*k^2 +
258         1.8632*10^-4);
259     G = (-0.1080*k^3 - 8.8374*k*10^-4)/(k^4 + 0.0921*k^2 +
260         1.8632*10^-4);
261
262     A_R = k^2*AR_a + k*G*AR_b + F*AR_c;
263     A_I = k*AI_a - k*F*AI_b + G*AI_c;
264
265     A_mat = zeros(n_ely*3, n_ely*3);
266
267     for i = 1:n_ely
268         A_mat(1+3*(i-1):2+3*(i-1),1+3*(i-1):2+3*(i-1)) = A_R + 1i*
269             A_I;
270     end
271
272 % system to solve

```

```

270     F_LL = Q_mat*A_mat*I_mat;
271     F_LL = F_LL(4:(n_ely*3+3),4:(n_ely*3+3));
272
273     D_LL = inv(K_theo)*M_theo + ((mu*k^2)^(-1))*inv(K_theo)*F_LL;
274
275     % For each k_F, find the eigenvalue of D(k), which correspond
276     % to lambda_F.
277     [vectors_flutt, lambda_flutt] = eig(D_LL);
278     lambda_flutt = diag(lambda_flutt);
279
280     % For each eigenvalue lambda_F, and the corresponding k, obtain
281     % :
282     mod = 1;
283
284     for e = 1:size(lambda_flutt,1)
285         w_f(ite,e) = W_theta/sqrt(lambda_flutt(e));
286         % Find modes and K_f ranges for which Im(w_F)<0 (unstable).
287
288         U_f(ite,e) = B * real(w_f(ite,e))/k;
289
290         % find modes and k ranges for which Im(wf)<0
291         % unstable
292         if imag(w_f(ite,e))<0 && real(U_f(ite,e))>0
293             % # modes where unstable
294             mode_range(ite,mod) = e;
295             U_f_danger(ite,mod) = U_f(ite,e);
296             mod = mod + 1;
297
298         end
299
300         % number of modes in unstable conditions
301         mod_ite(ite) = mod;
302
303     end
304
305     % find the minimum real values for flutter speed for each k
306     [U_f_min(1,ite), index(1,ite)] = min(real(U_f(ite,:)));
307     % the eigenvalue lambda to the minimum uf of the iteration
308     lambda_min(1,ite) = lambda_flutt(index(1,ite));
309
310     %Repeat for the next k
311     %sweep from 1e-3 to 1e3 in a logarithmic scale.
312     k = k * 10;
313     k_mat(1,ite) = k;
314
315 end
316
317 % plot the minimum real flutter speeds
318 figure(30)
319 hold on
320 plot(k_mat(1,:),U_f_min(1,:));
321 title('Minimum flutter speeds')
322 xlabel('k')
323 ylabel('Flutter Speed (m/s)')
324 set(gca, 'XScale', 'log')
325 grid on

```

```

325 % plot the imaginary part of w_f to see when is <0
326 figure(40)
327 hold on
328 for ite = 1:6
329     plot(1:1:n_ely*3, imag(w_f(ite,:)));
330 end
331 title('W_f(k)')
332 xlabel('modes')
333 ylabel('W_f')
334 leg = legend('k1','k2','k3','k4','k5','k6','k7','k8','k9','k10');
335 title(leg, '# iteration')
336 grid on
337
338 % Interpolate the limits of the k_F ranges obtained to obtained to
339 % obtain the U_F corresponding to flutter boundary.
340
341
342 %% RESULTS REQUIRED %%
343
344 % For a clamped-free straight panel with constant NACA0012 airfoil
345 % section, obtain:
346
347 % 1 - Divergence speed for different wing aspect ratios.
348 % 2 - First modes associated to divergence conditions for different
349 %    aspect
350 %    ratios.
351 % 3 - Stability plots for flutter.

```

10.2. Functions

```

1 function [M_ass, K_ass, Tn_y, Y_coord] = assembly(K, M, n_ely, span
2 )
3 % 1D beam analysis
4
5 l_elem = span/n_ely; % define criteria to set the length of each
6 element
7
8 for i = 1:n_ely
9     % nodal connectivities en y
10    Tn_y(i,1) = i ;
11    Tn_y(i,2) = i + 1 ;
12
13    % nodal coordinate
14    Y_coord(i) = (l_elem/2) + l_elem*(i-1);
15
16 end
17
18 K_ass = zeros(3*(n_ely + 1), 3*(n_ely + 1));
19 M_ass = zeros(3*(n_ely + 1), 3*(n_ely + 1));
20
21 for e = 1:n_ely
22     for nod = 1:2
23         for dof = 1:3

```

```

24
25         p = 3* (nod - 1) + dof;
26         I = 3* ((Tn_y(e,nod)) - 1) + dof;
27
28         for nod_b = 1:2
29             for dof_2 = 1:3
30
31                 q = 3*(nod_b-1) + dof_2;
32                 J = 3*((Tn_y(e,nod_b))-1) + dof_2;
33
34                 K_ass(I,J) = K_ass(I,J) + K(p,q);
35                 M_ass(I,J) = M_ass(I,J) + M(p,q);
36
37             end
38         end
39
40     end
41 end
42 end
43
44 end

```

```

1 function [V_theta_5, lambda_prima, Ud] = divergence(Ka, Ks, GJ, b,
2           e, C, rho, y, n_ely)
3 %% boundary conditions --> prescribe the first 3 dof in each matrix
4 Ka = Ka(4:end, 4:end);
5 Ks = Ks(4:end, 4:end);
6
7 % analitical solution for constant properties;
8 Cl_alpha = 2*pi;
9 QD = (pi^2 * GJ) / (4 * b^2 * Cl_alpha * e * C);
10
11 %% solve the eigenvalues
12 Ks = Ks/QD;
13
14 Ka = Ka + eye(length(Ka(1,:)))*10^-10;
15
16 % eigenvalues of the matrix
17 [V,lambda_prima] = eig(-Ka\Ks);
18 lambda_prima = diag(lambda_prima);
19
20 % positives
21 lambda_prima = lambda_prima(lambda_prima>0);
22 min_lambda = min(lambda_prima);
23
24 j=0;
25
26 for i=1:n_ely
27     if lambda_prima(i)>0
28         j=1+j;
29
30         % divergence condition given by the minimum value of the
31         lambda prima
32         qD(1,j) = lambda_prima(i);

```

```

33     % divergence speed at each panel
34     Ud(1,j) = sqrt(QD*qD(1,j)*2/rho);
35     end
36 end
37
38 % to evaluate divergence its interesting the minimum value of the
39 % qD
40 min_qd = min(qD);
41 % only interest the ones corresponding to theta values
42 V_theta = V(1:3:end,:);
43
44 % the y/N in the x-axis of the plot
45 modes_y_adim = zeros(1,n_ely);
46 for i=1:n_ely
47     modes_y_adim(1,i)=y(i)/b;
48 end
49
50 %% the first 5 ones
51
52 nummodes = 5;
53
54 j=n_ely*3;
55 for i = 1:nummodes
56     V_theta_5(:,i) = V_theta(:,j);
57     j = j - 1;
58 end
59
60 % plot the 5 modes
61
62 figure(10)
63 hold on
64 for mode=1:nummodes
65     modes_x = V_theta_5(:,mode);
66     plot(modes_y_adim, modes_x);
67 end
68 grid on
69 box on
70 title('First 5 modes of the elastic twist with AR = 1 ');
71 xlabel('Span (y/b)');
72 ylabel('Eigenvector');
73 xlim([0 1]);
74
75 end

```

```

1 function [Xsc_new, d_theta, dd_h, dd_theta, ddd_h]=findshearcenter(
2     X_nod, rep_D, cas, Xsc)
3
4 % CASE ID = 1 PURE TORSION LOAD
5
6 % regresion linial de los displacement
7
8 disp_X_s1=rep_D(1:6,4); % X displacement s1
9 disp_Y_s1=rep_D(1:6,5); % Y displacement s1
10 disp_Z_s1=rep_D(1:6,6); % Z displacement s1

```

```

11
12 disp_X_s2=rep_D(7:12,4); % X displacement s2
13 disp_Y_s2=rep_D(7:12,5); % Y displacement s2
14 disp_Z_s2=rep_D(7:12,6); % Z displacement s2
15
16 disp_X_s3=rep_D(13:18,4); % X displacement s3
17 disp_Y_s3=rep_D(13:18,5); % Y displacement s3
18 disp_Z_s3=rep_D(13:18,6); % Z displacement s3
19
20 disp_X_s4=rep_D(19:24,4); % X displacement s3
21 disp_Y_s4=rep_D(19:24,5); % Y displacement s3
22 disp_Z_s4=rep_D(19:24,6); % Z displacement s3
23
24 disp_X_s5=rep_D(25:30,4); % X displacement s3
25 disp_Y_s5=rep_D(25:30,5); % Y displacement s3
26 disp_Z_s5=rep_D(25:30,6); % Z displacement s3
27
28 disp_X_s6=rep_D(31:36,4); % X displacement s3
29 disp_Y_s6=rep_D(31:36,5); % Y displacement s3
30 disp_Z_s6=rep_D(31:36,6); % Z displacement s3
31
32 X=X_nod(1:6,1); % X coordinate (chord)
33 Y=X_nod(1:6:31,2);
34
35 figure()
36 plot(X, disp_Z_s1, X, disp_Z_s2, X, disp_Z_s3, X, disp_Z_s4, X,
37 disp_Z_s5, X, disp_Z_s6);
38 ylabel('Displacements in z ');
39 xlabel('x/c');
40 title('Displacement in different sections (results solver)');
41 grid on;
42 leg = legend('4', '3.5', '3', '2.5', '2', '1.5');
43 title(leg, 'y(m)')
44
45 x=[0:0.1:1]; % point to evaluate the
46 polynomial
47
48 p1=polyfit(X,disp_Z_s1,1); % linial curve
49 y1_fit = polyval(p1,x);
50
51 p2=polyfit(X,disp_Z_s2,1); % linial curve
52 y2_fit = polyval(p2,x);
53
54 p3=polyfit(X,disp_Z_s3,1); % linial curve
55 y3_fit = polyval(p3,x);
56
57 p4=polyfit(X,disp_Z_s4,1); % linial curve
58 y4_fit = polyval(p4,x);
59
60
61 p5=polyfit(X,disp_Z_s5,1); % linial curve
62 y5_fit = polyval(p5,x);
63
64
65

```

```

66 p6=polyfit(X,disp_Z_s6,1); % linial curve
67 y6_fit = polyval(p6,x);
68
69
70 figure()
71 plot(x, y1_fit , x, y2_fit , x, y3_fit, x, y4_fit, x, y5_fit, x,
    y6_fit);
72 ylabel('Displacements in z');
73 xlabel('x/c');
74 title('Displacement in different sections (with polyfit)');
75 grid on;
76 leg = legend('4','3.5','3','2.5','2','1.5');
77 title(leg,'y(m)')
78
79 % Theta values for each section
80 theta = [atand(p1(1)); atand(p2(1)); atand(p3(1)); atand(p4(1));
    atand(p5(1)); atand(p6(1))];
81
82 % intersection of the torsion lines
83 % A1x+B1=A2x+B2
84 if cas==1
85     f1 = @(x1) p6(1)*x1+p6(2)-p1(1)*x1-p1(2);
86     Xsc1 = fsolve(f1,1);
87
88     f2 = @(x2) p5(1)*x2+p5(2)-p2(1)*x2-p2(2);
89     Xsc2 = fsolve(f2,1);
90
91     f3 = @(x3) p3(1)*x3+p3(2)-p1(1)*x3-p1(2);
92     Xsc3 = fsolve(f3,1);
93
94     f4 = @(x4) p4(1)*x4+p4(2)-p2(1)*x4-p2(2);
95     Xsc4 = fsolve(f4,1);
96
97     f5 = @(x5) p5(1)*x5+p5(2)-p3(1)*x5-p3(2);
98     Xsc5 = fsolve(f5,1);
99
100    f6 = @(x6) p6(1)*x6+p6(2)-p4(1)*x6-p4(2);
101    Xsc6 = fsolve(f6,1);
102
103    % Determinar shear center
104    Xsc_new=(Xsc1+Xsc2+Xsc3+Xsc4+Xsc5+Xsc6)/6;
105 end
106
107 p = 0; % counter
108 X = X_nod(1:6,1); % position of the sensors on the chord
109
110 % find matrix for shear center displaments
111
112 for i = 1:6:31
113
114     p = p+1;
115
116     % Z displacement section i
117     disp_Z = rep_D(i:(i+5),6);
118
119     % h values at each section (using the shear center position)
120     disp_Z_pol = polyfit(X, disp_Z, 3);

```

```

121     h(p,1)         = polyval(disp_Z_pol, Xsc);
122
123 end
124
125 switch cas
126
127     case 1 % when applying pure torsion load
128
129         fun_theta = polyfit(Y,theta,1); %se puede sacar mas si se
130             necesita mayor derivada
131         d_theta   = fun_theta(1);
132         dd_theta  = 0; % null
133
134         fun_h     = polyfit(Y,h,2); % second grade
135         dd_h      = 2*fun_h(1);
136         ddd_h     = 0;
137
138     case 2 % when pure bending load
139
140         fun_theta = polyfit(Y,theta,2); %se puede sacar mas si se
141             necesita mayor derivada
142         d_theta   = fun_theta(2);
143         dd_theta  = 2*fun_theta(1);
144
145         fun_h     = polyfit(Y,h,3); %se puede sacar mas si se
146             necesita mayor derivada
147         dd_h      = 2*fun_h(2);
148         ddd_h     = 3*2*fun_h(1);
149
150         Xsc_new=Xsc;
151
152 end
153
154 end

```

```

1 function [F] = force_vector(L)
2
3 F = 0.5*L*[0 1;
4           1 0;
5           L/6 0;
6           0 1;
7           1 0;
8           -L/6 0];
9
10 end

```

```

1 function [Tn,Tm,Xnod] = import_mesh()
2
3 addpath(genpath('./Mesh')); % open the main folder
4
5 naca0012();
6
7 naca0012_profile();
8
9 Tm = Tmat;

```

```

10 Tn = Tnod;
11 Xnod = xnod;
12
13 end

```

```

1 function [Ka_mat, e, RHO] = lift_line(b, Y_coord, x_sc, n_ely)
2
3 %% discretization (constant properties)
4
5 % AoA
6
7 alpha = 0; %geometric angle of attack in degrees
8 beta = 0; %geometric lateral angle (positive angle turns towards
9         positive y)
10
11 U_inf = 1;
12 U_inf_vect = [U_inf*cosd(alpha)*cosd(beta), U_inf*sind(beta)*cosd(
13               alpha), U_inf*sind(alpha)]; %free stream velocity components
14 RHO = 1;
15
16 %%%%%%%%%%%%%%%%%%%%%%%%%%%%%%%%%%%%%%%%%
17 %geometry discretization
18 %%%%%%%%%%%%%%%%%%%%%%%%%%%%%%%%%%%%%%%%%
19
20 TR = 1; % Tapper ratio
21 sweep = 0; % Sweep angle in degrees (
22         positive angles sweep backwards)
23 dihedral = 0; % dihedral angle in degrees (
24         positive angles tilt upwards)
25 twist = 0; % geometric twist in degrees
26
27 l_elem = b/n_ely; % span
28
29 rootC = (2*b^2/b)/(b*(1+TR)); % root chord calculation
30
31 tipC = TR*rootC; % tip chord calculation
32
33 angle_TR = atand((rootC-tipC)/(2*b)); % angulo de TR
34
35 meanAeroChord=2/3*rootC*(1+TR+TR^2)/(1+TR); % mean aerodynamic
36         chord calculation
37
38 S_tot = (rootC+tipC)/2*b; % wing surface calculation
39
40 chord = zeros(n_ely,1);
41
42 for e = 1:n_ely
43     % chord of the airfoil/panel
44     chord(e) = rootC - (rootC-tipC)/(b/2)*abs(Y_coord(e));
45
46     % Surface of the element
47     S(e) = l_elem * chord(e);
48 end
49
50 % Normal vector of the element
51 n_vect = [sind(-alpha); 0; cosd(-alpha)];

```

```

47
48 %% Kutta condition for each element
49 % induced velocity at point x_coll due to a vortex segment between
      corners
50 % of the HS
51
52 % induced velocities computation
53
54 A = zeros(n_ely,n_ely);
55
56 for i = 1:n_ely      % FOR EACH CONTROL POINT
57     for j = 1:n_ely % EVERY VORTEX INFLUENCE
58
59         % Coordinatres of collocation point
60         x_coll = [3/4*chord(j) Y_coord(i) 0];
61
62         % coordinates of 4-points HS (square)
63         x_inf = chord(i)*20 + chord(i)*0.25;
64         x_ac = 0.25*chord(i);
65
66         x_HS_1 = [x_inf, Y_coord(j)-0.5*l_elem, 0];
67         x_HS_2 = [x_ac, Y_coord(j)-0.5*l_elem, 0];
68         x_HS_3 = [x_ac, Y_coord(j)+0.5*l_elem, 0];
69         x_HS_4 = [x_inf, Y_coord(j)+0.5*l_elem, 0];
70
71         v_12 = vel_ind(x_HS_2, x_HS_1, x_coll);
72
73         v_23 = vel_ind(x_HS_3, x_HS_2, x_coll);
74
75         v_34 = vel_ind(x_HS_4, x_HS_3, x_coll);
76
77         V = v_34 + v_23 + v_12;
78
79         % A is the aerodynamic influence coefficients matrix
80         A(i,j) = dot(V,n_vect);
81
82     end
83 end
84
85 %% Aerodynamic influence coefficient
86 S_mat = diag(S);
87
88 %% Element Force vector assembly
89
90 %%% porque se anulan los demas componentes
91 %%% es para simplificar y solo nos importa torsion
92
93 e = x_sc - x_ac;
94
95 [f_vect] = force_vector(l_elem);
96 Q = f_vect*[1; e];
97
98 dof = 3;
99 I_mat = zeros(n_ely,(n_ely+1)*dof);
100 n = 0;
101
102 for i = 1:3:((n_ely)*3)

```

```

103     n = n+1;
104     I_mat(n,i:1:(i+5)) = [0.5 0 0 0.5 0 0];
105     Q_mat(i:1:(i+5), n) = Q;
106 end
107
108 % quitamos los ceros de la matriz y nos quedamos solo con torsion
109 U_mat = repmat([1;0;0;], n_ely+1, 1);
110
111 % F(u) = q_inf*[Ka]*{u}
112 Ka_mat = Q_mat * S_mat* inv(A) * I_mat;
113 F_mat = Ka_mat * U_mat;
114
115 % for steady problem ----> (K_fem - q_inf*K_aero) (theta) = Q
116
117
118 end

```

```

1 function [E2]=obtain_E(T, Q, d_theta_T, dd_h_T, dd_theta_M, ddd_h_M
2 )
3 %from applyinmg a pure torsional load (M=0)
4 S_11= d_theta_T/T;
5 S_21= dd_h_T/T; % es para pure torsional
6
7 %from applying a pure shear load
8 S_12= - dd_theta_M/Q; % segunda der
9 S_22= - ddd_h_M/Q; % tercera der
10
11 % uncoupled E
12 E = [ S_11 S_12
13       S_21 S_22];
14
15 E2 = inv(E);
16
17 end

```

```

1 function [K, M]=obtain_K_M(L, E, I_sc, m, d)
2
3 E=inv(E);
4
5 GJ=E(1,1);
6 EI=E(2,2);
7
8 A(e)= [1 0 0 -1 0 0;
9        0 0 0 0 0 0;
10       0 0 0 0 0 0;
11       -1 0 0 1 0 0;
12       0 0 0 0 0 0;
13       0 0 0 0 0 0];
14
15 % podemos variar el criterio de L entre materiales
16
17 B(e)= [0 0 0 0 0 0;
18       0 12 6*L(e) 0 -12 6*L(e);
19       0 6*L(e) 4*(L(e))^2 0 -6*L(e) 4*(L(e))^2];

```

```

20     0 0      0      0      0      0;
21     0 -12    -6*L(e)  0      12    -6*L(e);
22     0 6*L(e)  4*(L(e))^2  0    -6*L(e)  4*(L(e))^2];
23
24 K(e)= (GJ/L(e)).*A(e)+(EI/(L(e)^3)).*B(e);
25
26 % Isc=;
27 % md=;
28 % m=;
29
30 C(e)= [Isc md 0 0 0 0;
31        md m 0 0 0 0;
32        0 0 0 0 0 0;
33        0 0 0 Isc md 0;
34        0 0 0 md m 0;
35        0 0 0 0 0 0];
36
37 M(e)=(L(e)/2).*C(e);
38
39
40 end

```

```

1 function [K, M, GJ, EI]=obtain_K_M(span, n_ely, E, Isc, m_tot, d)
2
3 l_elem = (span/n_ely); % define criteria to set the length of each
4 element
5 %%% make sure that are positive values %%%
6 GJ = abs(E(1,1));
7 EI = abs(E(2,2));
8
9
10 A = [1 0 0 -1 0 0;
11      0 0 0 0 0 0;
12      0 0 0 0 0 0;
13      -1 0 0 1 0 0;
14      0 0 0 0 0 0;
15      0 0 0 0 0 0];
16
17 % podemos variar el criterio de L entre materiales
18
19 B = [0 0      0      0      0      0;
20      0 12    6*l_elem  0    -12    6*l_elem;
21      0 6*l_elem 4*(l_elem)^2  0    -6*l_elem  4*(l_elem)^2;
22      0 0      0      0      0      0;
23      0 -12   -6*l_elem  0      12    -6*l_elem;
24      0 6*l_elem 4*(l_elem)^2  0    -6*l_elem  4*(l_elem)^2];
25
26 K = (GJ/l_elem)*A+(EI/(l_elem^3))*B;
27
28 l = (l_elem/2);
29
30 M =      [l*Isc      l*m_tot*d 0 0      0      0;
31           l*m_tot*d  l*m_tot  0 0      0      0;
32           0          0      0 0      0      0;
33           0          0      0 l*Isc  l*m_tot*d 0;

```

```

34         0         0         0  l*m_tot*d  l*m_tot  0;
35         0         0         0  0         0         0];
36
37 end

```

```

1 function [I_sc, D, mass_tot] = section_properties(x, Tn, Tm, mat,
2         Xsc)
3 n_element = size(Tm,1);
4
5 I_sc = 0;
6
7 for e = 1:n_element
8
9     % obtain the coordinates and material
10    % no estamos leyendo todas las coordenadas
11    % las
12
13    x_j(:,e) = x(Tn(e,:),1)'; % four point of the square section
14    z_j(:,e) = x(Tn(e,:),3)';
15
16    rho(e) = mat(Tm(e,1)); % density for each element
17
18    % determine the centroid coordinates
19
20    x_cent(e) = 0.25 * sum(x_j(:,e)) ;
21    z_cent(e) = 0.25 * sum(z_j(:,e)) ;
22
23    % determine the area of each element
24
25    a = sqrt((x_j(1,e)-x_j(4,e))^2+(z_j(1,e)-z_j(4,e))^2);
26    b = sqrt((x_j(2,e)-x_j(1,e))^2+(z_j(2,e)-z_j(1,e))^2);
27    c = sqrt((x_j(3,e)-x_j(2,e))^2+(z_j(3,e)-z_j(2,e))^2);
28    d = sqrt((x_j(4,e)-x_j(3,e))^2+(z_j(4,e)-z_j(3,e))^2);
29
30    A(e) = 0.5 * (a*b+c*d);
31
32 end
33
34 mass_tot = 0;
35 cent_mass = 0;
36
37 for e = 1:n_element
38     % total mass p.u.
39     mass_tot = rho(e)*A(e) + mass_tot;
40
41     % center of mass in x coordinates
42     cent_mass = x_cent(e)*rho(e)*A(e) + cent_mass;
43
44 end
45
46 cent_mass = (1/mass_tot)*cent_mass;
47
48 D = Xsc - cent_mass;
49
50 % inertia about the shear center p.u. lenght

```

```

51 for e = 1:n_element
52     I_sc = (x_cent(e)-Xsc)^2*rho(e)*A(e)+I_sc;
53 end
54
55 end

```

```

1 function [fext, f_ref]=set_forces(cas, Xsc)
2
3 switch cas
4
5     case 1 % ITERATION TO DETERMINE SHEAR CENTER
6         % set 2 forces that create a pure moment
7
8
9         Xa1 = 0.100; % Q1 distance to LE
10        Xa2 = 0.600; % Q2 distance to LE
11
12        Q1 = 5000;
13        Q2 = -5000;
14
15        fext = [Xa1,    5, 0, 0, 0,  Q1
16                Xa2,    5, 0, 0, 0,  Q2;
17                ];
18
19        f_ref = Q1;
20
21     case 2
22
23         % ITERATION TO DETERMINE PURE SHEAR LOAD
24         % set the bending force placed in the shear center
25
26        Xa = Xsc; % M distance to LE
27
28        Xb = 0.2475; % distance to Q eq
29        Xc = 0.5948; % distance to F eq
30        Xd = 1.0000; % distance to -F
31
32        M = 10000;
33        F = M*(Xa-Xb)/(Xd-Xc);
34
35        fext = [0.2475,    5, 0, 0, 0,  M
36                0.5948,    5, 0, 0, 0, -F
37                1,          5, 0, 0, 0,  F;
38                ];
39
40        f_ref = M;
41
42 end
43
44 end

```

```

1
2 function V_jk = vel_ind(x_k, x_j, x_coll)
3
4

```

```
5 r_j = x_coll - x_j;  
6 r_k = x_coll - x_k;  
7  
8 l = x_k - x_j;  
9  
10 %circulacion unitaria  
11 circ = 1;  
12  
13 V_jk = circ/(4*pi)*cross(r_j,r_k)/(norm(cross(r_j,r_k))^2)*(dot(l,  
    r_j)/norm(r_j)-dot(l,r_k)/norm(r_k));  
14  
15 end
```



**UNIVERSITAT POLITÈCNICA DE CATALUNYA
BARCELONATECH**

**Escola Superior d'Enginyeries Industrial,
Aeroespacial i Audiovisual de Terrassa**

**Project:
Setup of a virtual laboratory for studying
aeroelastic problems**

Màster Universitari en Enginyeria Aeronàutica

Advanced Aeroelasticity (220351)

Students:

M [REDACTED], Á [REDACTED]
S [REDACTED], A [REDACTED]

Prof. in charge:

Roca Cazorla, David

11th of January of 2021

Universitat Politècnica de Catalunya

Escola Superior d'Enginyeries Industrial, Aeroespacial i Audiovisual de
Terrassa

Contents

1	Aim and scope	2
2	Requirements	2
2.1	Code requirements	2
2.2	Results demanded	3
3	Theoretical background	3
3.1	FEM analysis	3
3.1.1	3D FEM analysis	3
3.1.2	2D FEM analysis	6
3.1.3	1D Beam analysis	7
3.2	Aerodynamics	8
3.2.1	Steady Aerodynamics: Lifting-line surface analysis	9
3.2.2	Unsteady aerodynamics: Theodorsen's model	10
3.3	Systems coupling	12
3.3.1	Force vector assembly	12
3.4	Resolution of the system	12
3.4.1	Divergence condition	13
3.4.2	Flutter condition	13
4	Results	14
4.1	Processing results	14
4.2	Final results	19
4.2.1	First modes associated to divergence conditions for different AR	19
4.2.2	Divergence speed for different Aspect Ratios	25
4.2.3	Stability plots for flutter	26
5	Conclusions	27
6	Bibliography	28

1 Aim and scope

The aim of this project is to implement a set of MATLAB functions to perform different kinds of aeroelastic analysis (e.g. assess divergence conditions, flutter study, unsteady aerodynamics, etc.).

2 Requirements

A series of requirements are demanded for the implementation of the project [1]. They can be classified in code or results depending on the demanded requirement.

2.1 Code requirements

4 main sections for the code have been demanded in order to solve the problem of joining aerodynamics and structures.

- Structures
 1. Use of 3D FEM code to obtain effective properties
 2. MATLAB implementation of a beam's FEM algorithm
- Aerodynamics
 1. For steady aerodynamics: MATLAB implementation of lifting-line solution by horseshoe elements
 2. For unsteady aerodynamics: MATLAB implementation of Theodorsen's model
- Coupling
 1. MATLAB implementation of transfer matrices: structures output (displacements vector) to aerodynamics input (angle of attack) and aerodynamics output (lift distribution) to structures input (force vector)
- Solvers
 1. Divergence speed + modes
 2. Flutter speed

2.2 Results demanded

The outputs demanded for a clamped free-straight panel with a constant NACA0012 airfoil section are listed below:

- Divergence speed for different wing aspect ratios
- First modes associated to divergence conditions for different aspect ratios
- Stability plots for flutter

3 Theoretical background

In this section, the different theoretical methodologies [1] used for the code implementation will be commented. They will be based on the requirements given in Section 2.

3.1 FEM analysis

3.1.1 3D FEM analysis

The wing proposed, with a NACA0012 airfoil constant section is depicted in the Figure 1. As it can be noticed, different elements will be the constituents of this wing: skin, rear spar, front spar and stringers.

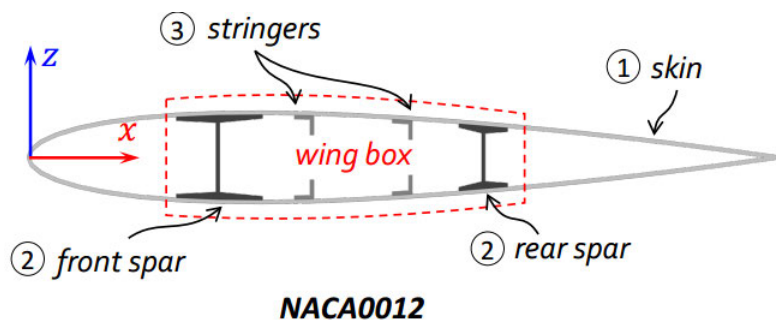


Figure 1: Elements used for the structural modelisation of the wing [1]

Different properties (density, Young's modulus and Poisson's ratio) have been associated to the structural elements, which have been taken into account for the resolution of the problem. They are presented in the Figure 2. These material relations are already given in the mesh functions.

Material properties

Material	Density (kg m ⁻³)	Young's Modulus (GPa)	Poisson's ratio
(1) Skin	2000	9	0.27
(2) Spars	1800	150	0.30
(3) Stringers	2300	70	0.35

Figure 2: Material properties structural modelisation of the wing [1]

The process used in this section is based on obtaining displacement measure readings by introducing loads and displacement measure locations in the 3D FEM solver. The main goal following this procedure is to get: Shear center position ($x_{SC}(y)$), Torsional stiffness ($\overline{GJ}(y)$) and Bending stiffness ($\overline{EI}(y)$).

Shear center position calculation: For the calculation of the shear center 4 points are taken: 2 at the center of the front spar and rear spar, 1 at the leading edge and 1 at the trailing edge. To find the shear center position, a moment is created by applying 2 forces of the same magnitude in opposite directions, which causes a pure torsional moment at the wing.

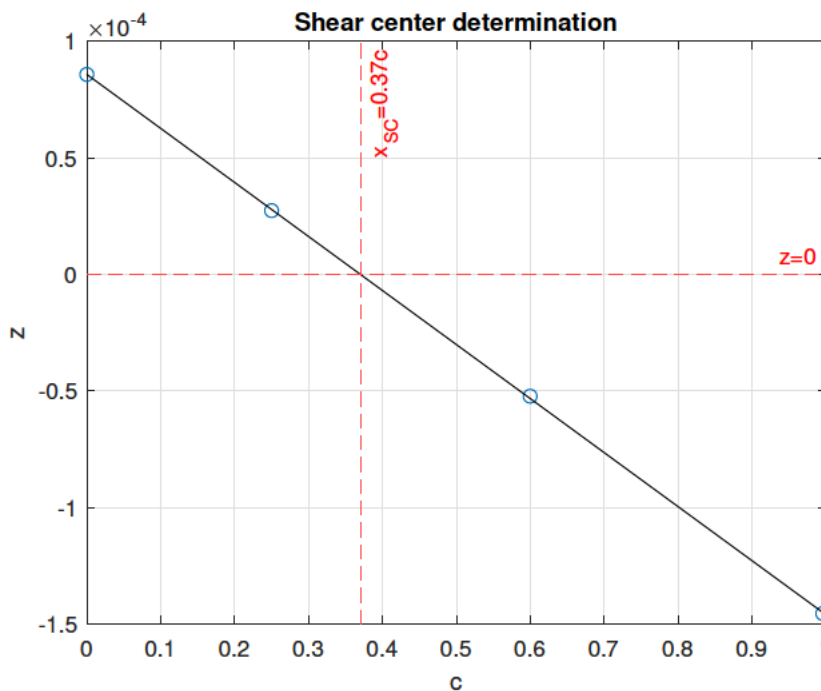


Figure 3: Shear center determination

The main objective is to look for a point where the z is 0, as the structure consists in a symmetrical airfoil section. With 4 different points an interpolation can be done and a point where the z is zero can be obtained, so the x position of this point is the shear center position x_{SC} . The result obtained is $x_{SC} \simeq 0.37$, as shown in Figure 3.

Torsional and bending stiffness: For the calculation of these 2 parameters an initial hypothesis is taken to find the matrix E (2x2) of the next system:

$$\begin{Bmatrix} T \\ M \end{Bmatrix} = \begin{Bmatrix} \overline{GJ} & 0 \\ 0 & EI \end{Bmatrix} \begin{Bmatrix} d\theta/dy \\ d^2h/dy^2 \end{Bmatrix} \quad (1)$$

The assumptions taken are small displacements and deformations, which basically implies small angles and linear elasticity. It also is considered that the effective response can be described by elemental beam theory presented on the Equation 1. Since it is not guaranteed that bending and torsion are structurally uncoupled, the following constitutive relation is used to solve the problem instead, where the 2x2 matrix correspond to E^{-1} .

$$\begin{Bmatrix} \bar{\theta}' \\ \bar{h}'' \end{Bmatrix} = \begin{Bmatrix} S_{11} & S_{12} \\ S_{21} & S_{22} \end{Bmatrix} \begin{Bmatrix} T \\ M \end{Bmatrix} \quad (2)$$

where $S_{11} = \bar{\theta}'/T$, $S_{21} = \bar{h}''/T$, $S_{12} = \bar{\theta}'/M = -\bar{\theta}''/Q$, $S_{22} = \bar{h}''/M = -\bar{h}'''/Q^2$

Firstly, is determined the $\bar{\theta}'$ for points between $0.2b$ and $0.8b$, where b is the span of the wing, in order to avoid distortions on the averaged twist, and also considering different stations of the chord of the airfoil. Those points are: 0 , $c/4$, $0.6c$ and c . This derivative has been obtained with the polyfit function for each section and applying also the next expression:

$$\bar{\theta} = \arctan(\bar{\theta}') \quad (3)$$

By doing this polyfit of first order (it would be equivalent to a linear regression of the points), it is possible to find the slope of the interval, which is the mean variation of $\bar{\theta}$. The second order derivative, is calculated through a second order polyfit. For the \bar{h} , a similar procedure is used, although for this case, a third order polyfit is necessary due to the calculation of the S_{22} term. The procedure is also repeated for each section, just as the $\bar{\theta}$ case. Nevertheless, the forces need a special treatment commented below.

The forces applied for the torsional case are applied at the center of the front spar and rear spar ($0.25c$ and $0.6c$) with a value of 100N in opposite senses.

In order to apply a shear load in the shear center, it is needed the treatment of replacing this load by applying it at a different point and adding a compensating torque, since the

¹ S_{11} and S_{21} from applying a torsional load ($M=0$)

² S_{12} and S_{22} from applying a pure shear load ($T=0$, $M'=-Q$)

shear center point is a non-existing node in the mesh used. The input value of Q has been again of 100N.

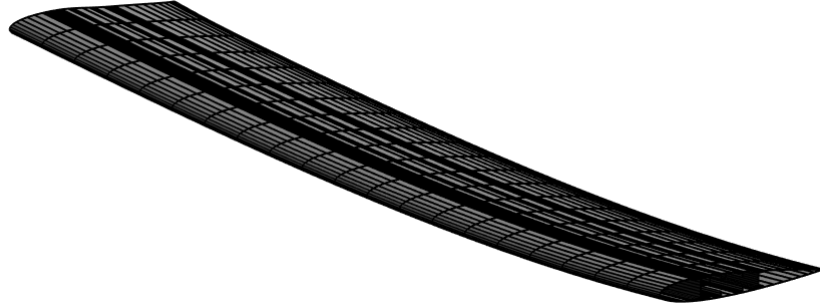


Figure 4: Replacing of a shear load at a different point adding a compensating torque

Finally, once the values of S_{11} , S_{12} , S_{21} and S_{22} are obtained, it is able to determine the elasticity matrix by just doing the inverse. The resultant matrix E has been:

$$E = \begin{bmatrix} \overline{GJ} & 0 \\ 0 & \overline{EI} \end{bmatrix} = \begin{bmatrix} 874579.503 & 462.546 \\ 12881.944 & 25089.088 \end{bmatrix} \quad (4)$$

As it can be noticed, the values on the diagonal are significantly higher than the non-diagonal terms, and although not being 0, the assumption of developing a correct process up to this point is taken.

3.1.2 2D FEM analysis

For the 2D FEM analysis, the nodal coordinates, nodal connectivities, material properties and material connectivities matrixes are needed for the treatment of the problem in elements. These matrixes have been supplied by the professor. For the section properties calculation, the process followed has basically been the one presented in the slides.

1. The coordinates and materials for each element composed of 4 nodes are obtained.

$$x_j^{[e]} = [x]^{([T_n]^{(e,j)})} \quad (5)$$

2. Determination of the centroid coordinates is done as an average of the position of the 4 nodes:

$$x^{[e]} = \frac{1}{4} \sum_{j=1}^4 x_j^{[e]} \quad (6)$$

3. The area of each element is determined, again as an average of the rectangular area

formed by each pair of nodes (1-4,1-2) and (3-2,3-4):

$$a = x_1^{[e]} - x_4^{[e]}, \quad b = x_2^{[e]} - x_1^{[e]}, \quad c = x_3^{[e]} - x_2^{[e]} \quad d = x_4^{[e]} - x_3^{[e]} \quad (7)$$

$$A^{[e]} = \frac{1}{2}(a \times b + c \times d) \quad (8)$$

4. The mass per unit length is calculated by using the element area, as well as the density as:

$$m = \sum_e \rho^{[e]} A^{[e]} \quad (9)$$

5. The center of mass is obtained by using:

$$x_{cm} = \frac{1}{m} \sum_e x^{[e]} \rho^{[e]} A^{[e]} \quad (10)$$

6. Finally, the inertia about the shear center per unit length is calculated as:

$$I_{sc} = \sum_e (x^{[e]} - x_{sc})^2 \rho^{[e]} A^{[e]} \quad (11)$$

3.1.3 1D Beam analysis

For the 1D Beam analysis, taking an element i formed by 2 nodes, the nodal coordinates, nodal connectivities and length per element can be determined by using the following procedure:

- **Nodal coordinates:**

$$[y]^i = y^{(i)} \quad (12)$$

- **Nodal connectivities:**

$$[T_x]^{(i,1)} = i, \quad [T_x]^{(i,2)} = i + 1 \quad (13)$$

- **Length:**

$$l^{[i]} = y^{(i+1)} - y^{(i)} \quad (14)$$

Computation of element matrices:

Once these lengths are calculated, computation of the stiffness and mass matrix are possible as they are basically dependant on Torsional and bending stiffness obtained in the 3D analysis, and the Inertia about the shear center and masses obtained in the 2D analysis.

Stiffness matrix:

$$[\mathbf{K}^{[i]}] = \frac{\overline{GJ}}{l^{[i]}} \begin{bmatrix} 1 & 0 & 0 & -1 & 0 & 0 \\ 0 & 0 & 0 & 0 & 0 & 0 \\ 0 & 0 & 0 & 0 & 0 & 0 \\ -1 & 0 & 0 & 1 & 0 & 0 \\ 0 & 0 & 0 & 0 & 0 & 0 \\ 0 & 0 & 0 & 0 & 0 & 0 \end{bmatrix} + \frac{\overline{EI}}{(l^{[i]})^3} \begin{bmatrix} 0 & 0 & 0 & 0 & 0 & 0 \\ 0 & 12 & 6l^{[i]} & 0 & \overline{EI} & 6l^{[i]} \\ 0 & 6l^{[i]} & 4(l^{[i]})^2 & 0 & -6l^{[i]} & 4(l^{[i]})^2 \\ 0 & 0 & 0 & 0 & 0 & 0 \\ 0 & \overline{EI} & -6l^{[i]} & 0 & \overline{EI} & -6l^{[i]} \\ 0 & 6l^{[i]} & 4(l^{[i]})^2 & 0 & -6l^{[i]} & 4(l^{[i]})^2 \end{bmatrix}$$

Mass matrix (lumped):

$$[\mathbf{M}^{[i]}] = \frac{l^{[i]}}{2} \begin{bmatrix} I_{sc} & md & 0 & 0 & 0 & 0 \\ md & m & 0 & 0 & 0 & 0 \\ 0 & 0 & 0 & 0 & 0 & 0 \\ 0 & 0 & 0 & I_{sc} & md & 0 \\ 0 & 0 & 0 & md & m & 0 \\ 0 & 0 & 0 & 0 & 0 & 0 \end{bmatrix}; \quad d = x_{sc} - x_{cm}$$

Figure 5: Element matrices computation [1]

Please, notice that the diagonal terms of the stiffness second matrix should be 12 instead of \overline{EI} and -12 for the non-diagonal terms which contain \overline{EI} .

Assembly of matrices: Global matrices calculation:

Once the element matrices $[K^{[i]}]$ and $[M^{[i]}]$ are computed, their assembly is done initializing global matrices with 3 degrees of freedom (DoFS) per node, being the total number of DoFs, $N = 3(n+1)$ with $\theta, h, \gamma == h'$ as DoFs. Then, using several for loops (element, element node twice, degree of freedom twice), global matrices are computed.

3.2 Aerodynamics

For the aerodynamics section, the Lifting-line surface analysis is considered in order to analyse the problem. This analysis consists on dividing the wing in elements, each one as a horseshoe element that makes influence on the other ones for the static part of the code.

On the other hand, for the dynamic part of the code, the implementation of Theodorsen's model is done.

3.2.1 Steady Aerodynamics: Lifting-line surface analysis

The discretization is done by assigning a surface area for each element obtained as:

$$S^{[i]} = l^{[i]} \cdot c \quad (15)$$

A normal vector is associated to each element in a constant direction in z of $n = [0, 0, 1]$. Finally, the collocation point is computed at $3c/4$ of each element.

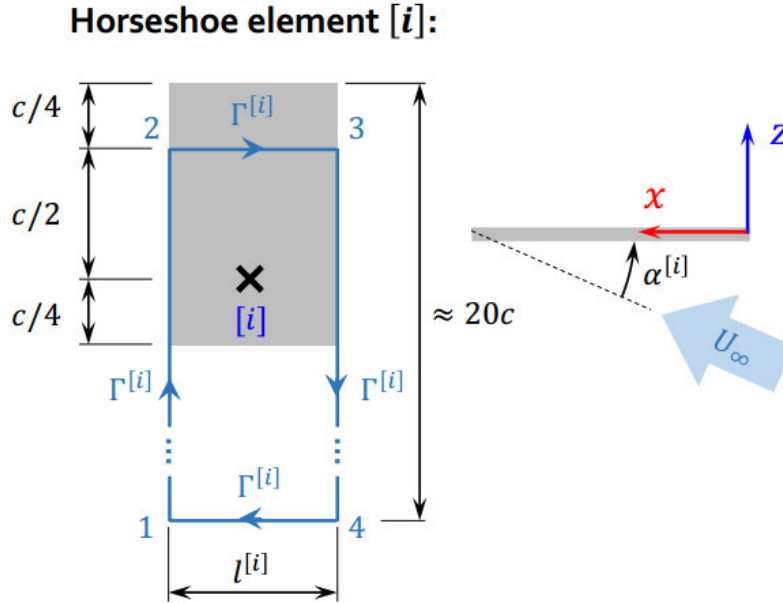


Figure 6: Horseshoe element discretization [1]

Taking these indications into consideration, it is possible to calculate the following system of equations:

$$[A][\Gamma] = -U_\infty[\alpha]$$

$$\begin{bmatrix} A_{11} & A_{12} & \dots & A_{1n} \\ A_{21} & A_{22} & \dots & A_{2n} \\ \dots & \dots & \dots & \dots \\ A_{n1} & A_{n2} & \dots & A_{nn} \end{bmatrix} \begin{Bmatrix} \Gamma^{[1]} \\ \Gamma^{[2]} \\ \dots \\ \Gamma^{[n]} \end{Bmatrix} = -U_\infty \begin{Bmatrix} \alpha^{[1]} \\ \alpha^{[2]} \\ \dots \\ \alpha^{[n]} \end{Bmatrix} \quad (16)$$

where $[A]$ is the aerodynamic influence coefficients matrix, Γ is the circulation supposed as 1 initially for the system resolution, U_∞ is an unknown and the α is the angle of attack that will be later commented. The steps taken to calculate each item are done as follows:

1. Induced velocity at point x with vorticity $\Gamma^{[i]} = 1$ calculation:

$$v_{jk}^{[i]} = \frac{\Gamma^{[i]}}{4\pi} \frac{r_j \times r_k}{\|r_j \times r_k\|^2} \left(\frac{l^{[i]} \cdot r_j}{r_j} - \frac{l^{[i]} \cdot r_k}{r_k} \right); \quad r_j = x - x_j; \quad l^{[i]} = x_k - x_j \quad (17)$$

2. **Aerodynamic influence coefficients matrix [A] calculation:**

$$A_{ij} = (v_{12}^{[j]}(x^{[i]}) + v_{23}^{[j]}(x^{[i]}) + v_{34}^{[j]}(x^{[i]})) \cdot n^{[i]} \quad (18)$$

3. **Surface:** With the surface calculation for each element presented in the Equation 15, it is possible to create a diagonal matrix with the surfaces located in the diagonal of a matrix S:

$$[S] = \begin{bmatrix} S^{[1]} & & 0 \\ & \dots & \\ 0 & & S^{[n]} \end{bmatrix} \quad (19)$$

4. **Angle of attack $[\alpha]$ calculation:** In order to determine an expression for the angle of attack, the aerodynamic model considers an interpolation matrix between α and u . Then, for this specific problem:

$$\alpha^{[i]} = \theta^{[i]} = \frac{1}{2} \begin{bmatrix} 1 & 0 & 0 & 1 & 0 & 0 \end{bmatrix} \begin{Bmatrix} \theta^{(i)} \\ h^{(i)} \\ \gamma^{(i)} \\ \theta^{(i+1)} \\ h^{(i+1)} \\ \gamma^{(i+1)} \end{Bmatrix} = \begin{bmatrix} I & I \end{bmatrix} \begin{Bmatrix} u^{(i)} \\ u^{(i+1)} \end{Bmatrix} \quad (20)$$

then, applying the relation for n angles of attack:

$$\{\alpha\} = \begin{Bmatrix} \alpha^{[1]} \\ \alpha^{[2]} \\ \dots \\ \alpha^{[n]} \end{Bmatrix} = \begin{bmatrix} I & I & 0 & \dots & 0 & 0 \\ 0 & I & I & \dots & 0 & 0 \\ \dots & \dots & \dots & \dots & \dots & \dots \\ 0 & 0 & 0 & \dots & I & I \end{bmatrix} \begin{Bmatrix} u^{(1)} \\ u^{(2)} \\ u^{(3)} \\ \dots \\ u^{(n)} \\ u^{(n+1)} \end{Bmatrix} = [I] \{u\} \quad (21)$$

3.2.2 Unsteady aerodynamics: Theodorsen's model

The methodology used to analyse the flutter is the Theodorsen model [2] [3], developed in 1935. Before starting the resolution of the problem, a series of parameters definitions are needed:

$$b = c/2 \quad a = \frac{X_{sc}}{b-1} \quad k_T = \frac{GJ}{l} \quad \omega_\theta = \sqrt{\frac{k_T}{I_{sc}}} \quad \mu = \frac{m}{\pi \rho_\infty b^2} \quad (22)$$

Where the ρ_∞ is taken as $1.225kg/m^3$.

It is also needed the Theodorsen's function, which is a transfer function that accounts for attenuation by the wake vorticity. The approximation used is in the form of: $C(k) = F(k) + iG(k)$.

$$C(k) = \frac{0.5k^4 + 0.0765k^2 + 1.8632 \cdot 10^{-4}}{k^4 + 0.0921k^2 + 1.8632 \cdot 10^{-4}} + i \frac{-0.1080k^3 - 8.8374 \cdot 10^{-4}k}{k^4 + 0.0921k^2 + 1.8632 \cdot 10^{-4}} \quad (23)$$

Where k is defined as the reduced frequency $k = \frac{\omega b}{U_\infty}$, which contains two unknowns of the problem.

As in the case of steady aerodynamics, a system coupling is needed through the defined matrices given in Section 3.3. However, in this case it is also required an extra column of zeros to adjust the dimensions of the problem.

For the definition of the system of equations to solve, it is also needed the A matrices definitions given by:

$$\begin{aligned} [\hat{A}_R(k)] &= k^2 \begin{bmatrix} 1/8 + a^2 & a \\ a & 1 \end{bmatrix} + kG(k) \begin{bmatrix} 2a^2 - 1/2 & 2a + 1 \\ 2a - 1 & 2 \end{bmatrix} + F(k) \begin{bmatrix} 1 + 2a & 0 \\ 2 & 0 \end{bmatrix} \\ [\hat{A}_R(k)] &= k^2 [\hat{M}'] + kG(k) [\hat{C}'] + F(k) [\hat{K}'] \end{aligned} \quad (24)$$

$$\begin{aligned} [\hat{A}_I(k)] &= k \begin{bmatrix} a - 1/2 & 0 \\ 1 & 0 \end{bmatrix} - kF(k) \begin{bmatrix} 2a^2 - 1/2 & 2a + 1 \\ 2a - 1 & 2 \end{bmatrix} + G(k) \begin{bmatrix} 1 + 2a & 0 \\ 2 & 0 \end{bmatrix} \\ [\hat{A}_I(k)] &= k [\hat{C}'] - kF(k) [\hat{C}'] + G(k) [\hat{K}'] \end{aligned} \quad (25)$$

Once this procedure is done, an adjustment on the parameters of the mass and stiffness matrices is also required, so the dimensions of the different elements are consistent. The steady matrices K and M are adjusted³ as a consequence as:

$$[\hat{M}] = \frac{[M]}{mb^2} \quad (26)$$

$$[\hat{K}] = \frac{[K]}{m\omega_\theta b^2} \quad (27)$$

Where m stands for the total mass per unit length. Finally, having the non-dimensionalised matrices, the system obtained in function of the defined parameters is the following:

³It has also been necessary to add a diagonal term close to 0 to allow the computation of the K matrix

$$([\hat{K}]^{-1} [\hat{M}] + \mu^{-1} [\hat{K}]^{-1} ([\hat{M}'] + ik^{-1}([\hat{C}'''] - (F(k) + iG(k)) [\hat{C}''']) + k^{-2}(F(k) + iG(k)) [\hat{K}'''] - \lambda[1]) \{\bar{x}\} = \{0\} \quad (28)$$

or, re-expressing the left-hand side term with the matrix D:

$$([\hat{D}(k_F)] - \lambda[1]) \{\bar{x}\} = \{0\} \quad (29)$$

At this point, it is possible to impose the flutter condition, so the unknowns of the problem can be determined following the procedure which is going to be explained in the Section 3.4.2.

3.3 Systems coupling

3.3.1 Force vector assembly

Once the aerodynamic part is determined, it is possible to assembly the element force vector through the definition of a $[Q]$ matrix formed by $Q_1^{[i]}$ and $Q_2^{[i]}$ as:

$$Q_1^{[i]} = \frac{1}{2} \begin{bmatrix} e \\ 1 \\ l^{[i]}/6 \end{bmatrix} \quad Q_2^{[i]} = \frac{1}{2} \begin{bmatrix} e \\ 1 \\ -l^{[i]}/6 \end{bmatrix} \quad (30)$$

$$[Q] = \frac{1}{2} \begin{bmatrix} Q_1^{[1]} & 0 & \dots & 0 \\ Q_2^{[1]} & Q_1^{[2]} & \dots & 0 \\ 0 & Q_2^{[2]} & \dots & 0 \\ \dots & \dots & \dots & \dots \\ 0 & 0 & \dots & Q_1^{[n]} \\ 0 & 0 & \dots & Q_2^{[n]} \end{bmatrix} \quad (31)$$

Then, the element force assembly matrix is calculated as:

$$[F(u)] = -\frac{1}{2} \rho_\infty U_\infty^2 [Q][S][A]^{-1}[I][u] = q_\infty [K_a] \quad (32)$$

as $q_\infty = \frac{1}{2} \rho_\infty U_\infty^2$ and $[K_a] = [Q][S][A]^{-1}[I][u]$.

3.4 Resolution of the system

Once the aerodynamic matrix is obtained, the boundary conditions to the total stiffness matrix are applied, basically meaning that the torsion angle at the fixed extreme

(corresponding to the first term of the matrix) is 0. The aerodynamic matrix, is also adjusted by adding to it a diagonal matrix with non-zero values but very close to it, in order to avoid obtaining discontinuities when solving the system. The matrices are also non-dimensionalised with the dynamic pressure to avoid additional terms multiplying the system.

3.4.1 Divergence condition

To obtain the divergence condition [4] [5], what is wanted is to equalize to zero the eigenvalues of the system. For the problem it is obtained that:

$$\left[\hat{K}_s \right] \left\{ u \right\} + \hat{q} \left[\hat{K}_a \right] \left\{ u \right\} = 0 \quad (33)$$

By multiplying both sides of the equation with the $[\hat{K}_a^{-1}]$ term, the system can be re-structured as:

$$\left(\left[\hat{K}_a^{-1} \right] \left[\hat{K}_s \right] + \hat{q} \left[1 \right] \right) \left\{ u \right\} = 0 \quad (34)$$

Then, the divergence condition is determined by setting:

$$\det \left(\left[\hat{K}_a^{-1} \right] \left[\hat{K}_s \right] + \hat{q} \left[1 \right] \right) \left\{ u \right\} = 0 \quad (35)$$

taking the divergence dynamic pressure as the minimum eigenvalue obtained applying the previous condition. Finally, once the dynamic pressure is obtained, the speed can be directly calculated as follows:

$$u_D = \sqrt{\frac{2 \cdot \hat{q}_D \cdot q_{Danalyt}}{\rho_\infty}} \quad (36)$$

where $q_{Danalyt} = \frac{\pi^2}{4b^2} \frac{GJ}{ceC_{l,\alpha}}$ corresponds to the analytical solution used to non-dimensionalise the divergence dynamic pressure.

3.4.2 Flutter condition

Starting from the Equation 29, the flutter condition [2] [3] can be obtained in terms of λ_F and k_F , which are defined as follows:

$$\lambda_F = \frac{\omega_F^2}{\omega_\theta^2} = \frac{\omega_R^2 - \omega_I^2}{\omega_\theta^2} + i \frac{2\omega_R\omega_I}{\omega_\theta^2} \quad (37)$$

$$k_F = \frac{\omega_F b}{U_F} = \frac{\omega_R b}{U_F} + i \frac{\omega_I b}{U_F} \quad (38)$$

The objective is to find the instability condition, which is produced when ω_I goes from positive to negative values. In the limit, $\omega_I = 0$, which means $\lambda_R > 0$ and $\lambda_I = 0$. Then, to obtain the flutter condition it is necessary to find the $k_F \in \Re$ for which $\lambda_F > 0 \in \Re$ taking into account the Equation 29:

$$\det([\hat{D}(k_F)] - \lambda_F[1]) = 0 \quad (39)$$

Finally, for each λ_F obtained, it can be calculated the velocity and the frequency.

4 Results

This section shows the results obtained with the code in order to verify the procedure, and the final results demanded as outputs of the program.

4.1 Processing results

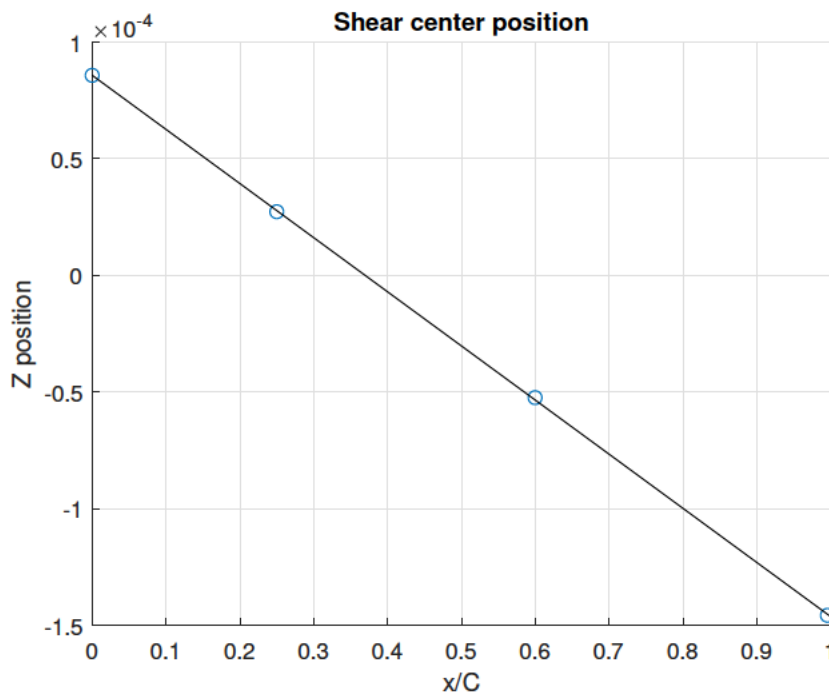


Figure 7: Shear center position

By applying a pure torsional load on the wing, the deviation in height of the points along the chord can be obtained. With this, the point with 0 deviation is the shear center. (See Section 3.1.1 for further details.

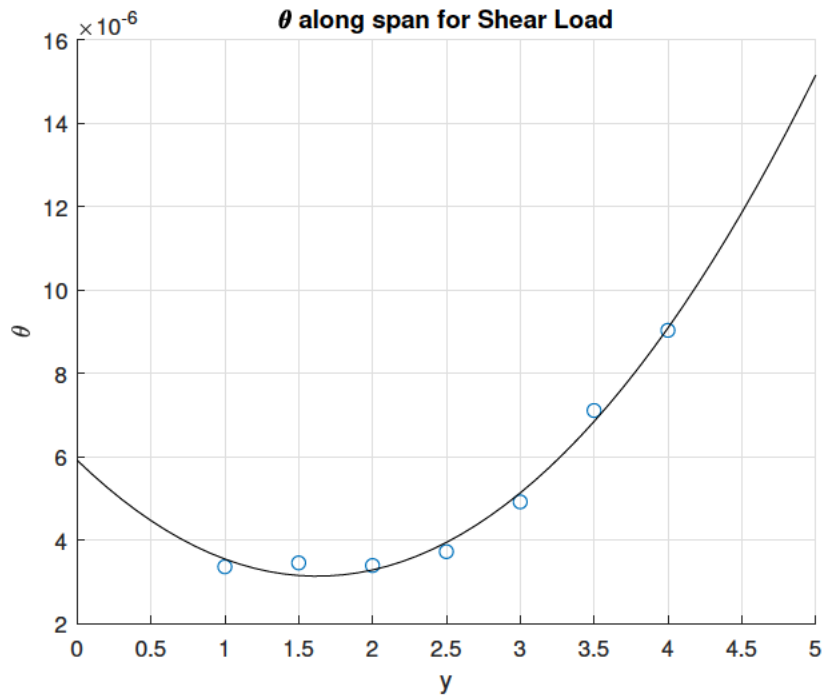


Figure 8: θ along the span

In the Figure 8, it can be seen the tendency of the θ angle along the span when the system is under a pure shear load.

It is believed that the tendency of the system should remain constant, but due to the structure nature, when approaching the tip of the wing, the θ angle increases, creating a bigger effect as a consequence. However, notice that the values are of orders that could be consider close to 0, so the variations between the points are very close between them. For further details about the forces applied to achieve this tendency, see further details in Section 3.1.1.

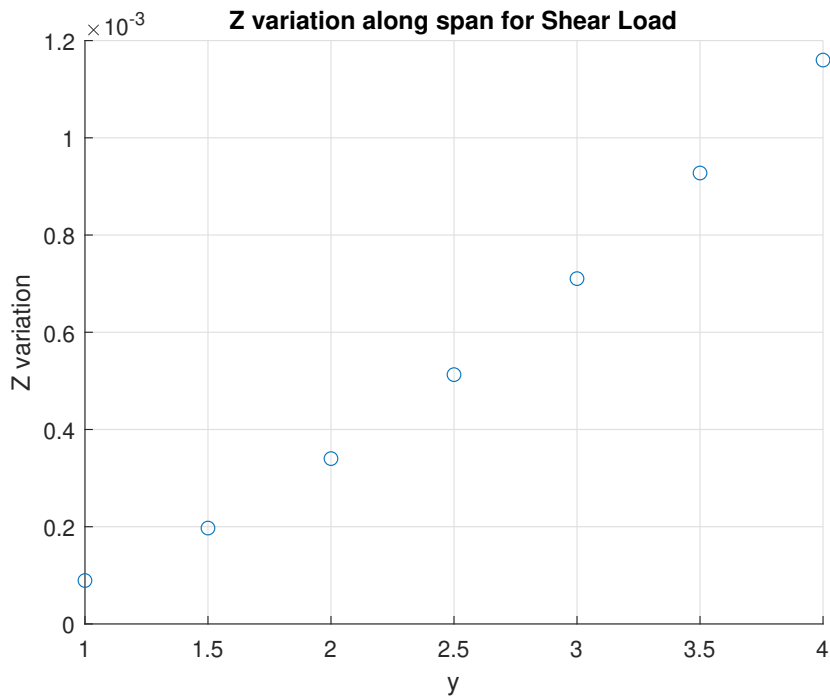


Figure 9: Z position along the span

As it can be seen, the Z position of the section increases with the span. As the main objective is to see the overall tendency, the tip (where the forces are being applied) and the joint (where the wing is fixed), are not shown, since at these points the variation doesn't follow the same tendency.

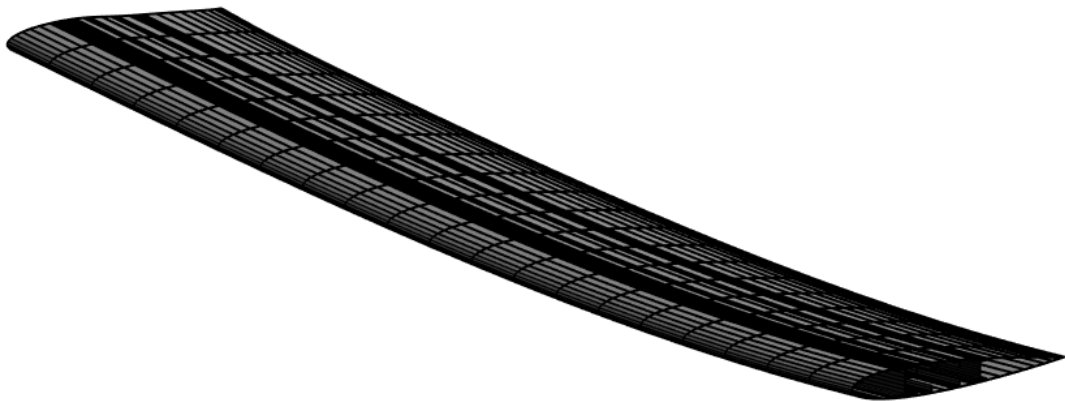


Figure 10: Shear load case

This Figure 10 shows a representation of the system under shear load conditions in order to observe the tendency of it.

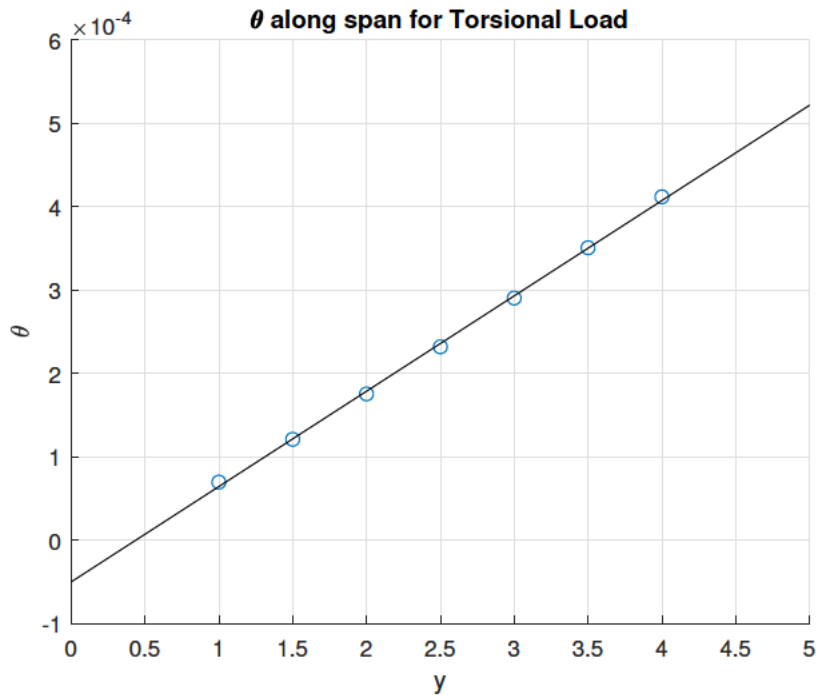


Figure 11: θ along the span

In the Figure 11, it can be seen the tendency of the θ angle along the span when the system is under a pure torsional load.

The angle θ should have a tendency to increase along the span, which it does, basically meaning that we will observe bigger angles at the tip, whereas for the sections near to the clamped part, the angle will have values closer to 0.

As it can be seen in the Figure 12, the Z position of the section decreases with the span. As the main objective is to see the overall tendency, the tip (where the forces are being applied) and the joint (where the wing is fixed), are not shown, since at these points the variation doesn't follow the same tendency. This Z variation is not supposed to happen, since the overall load has value 0 in the Z direction.

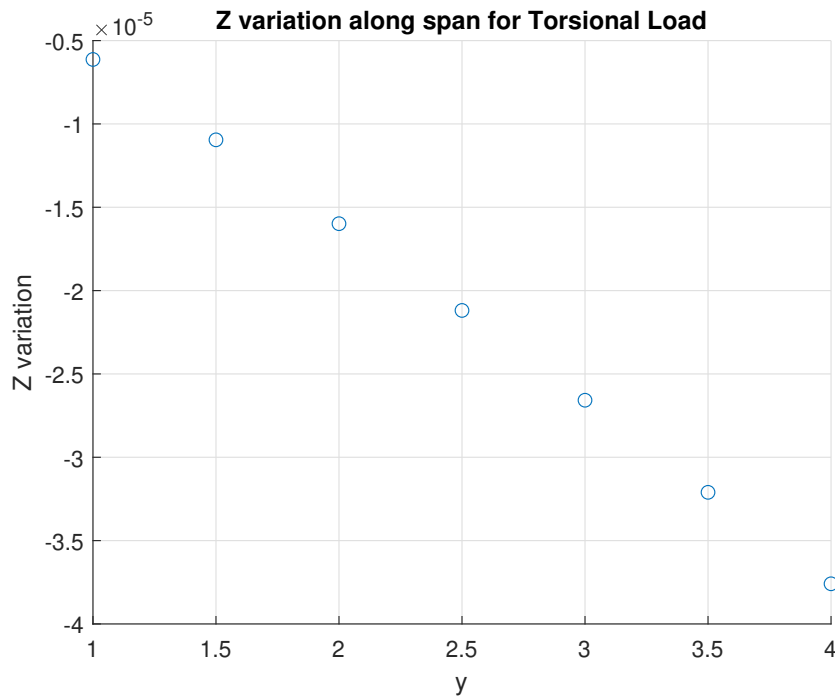


Figure 12: Z position along the span

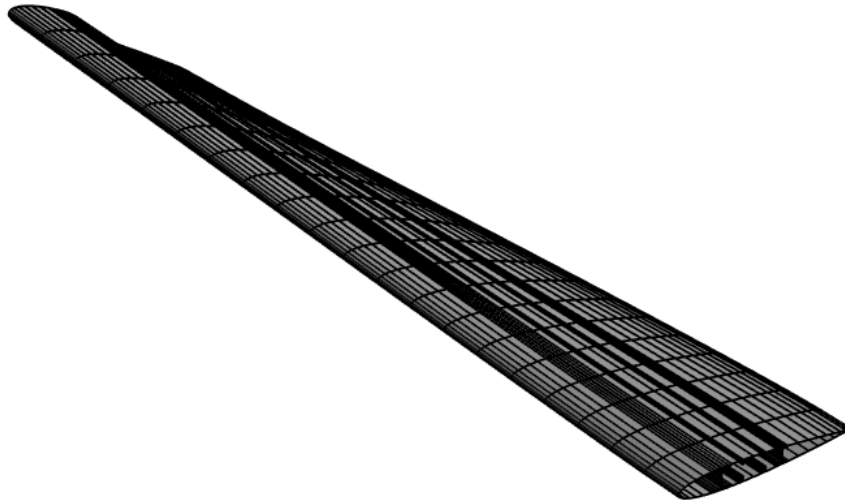


Figure 13: Torsional load case

The Figure 13 shows a representation of the system under torsional load conditions in order to observe the tendency of it. Notice that the effect in the free-tip is higher than the clamped one.

4.2 Final results

The results obtained developing the methodologies exposed in the Section 3 are shown below.

4.2.1 First modes associated to divergence conditions for different AR

The first modes associated to divergence conditions for different Aspect Ratios are shown in the Figures below. The values chosen for the aspect ratio will vary between 1 and 10 being the first 5 modes shown for each configuration.

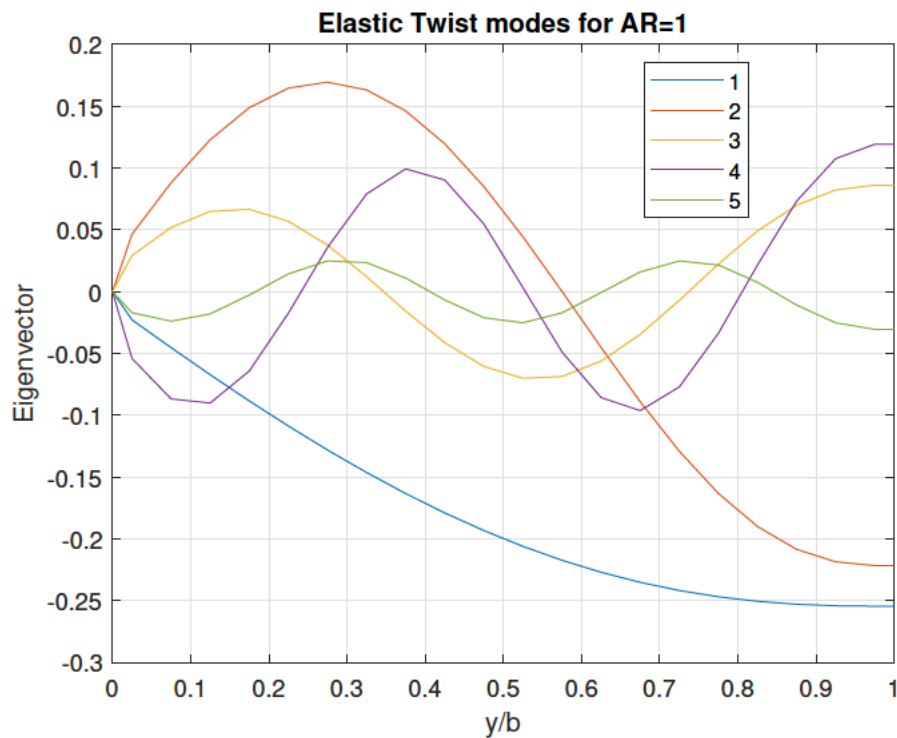


Figure 14: First modes for Aspect Ratio 1

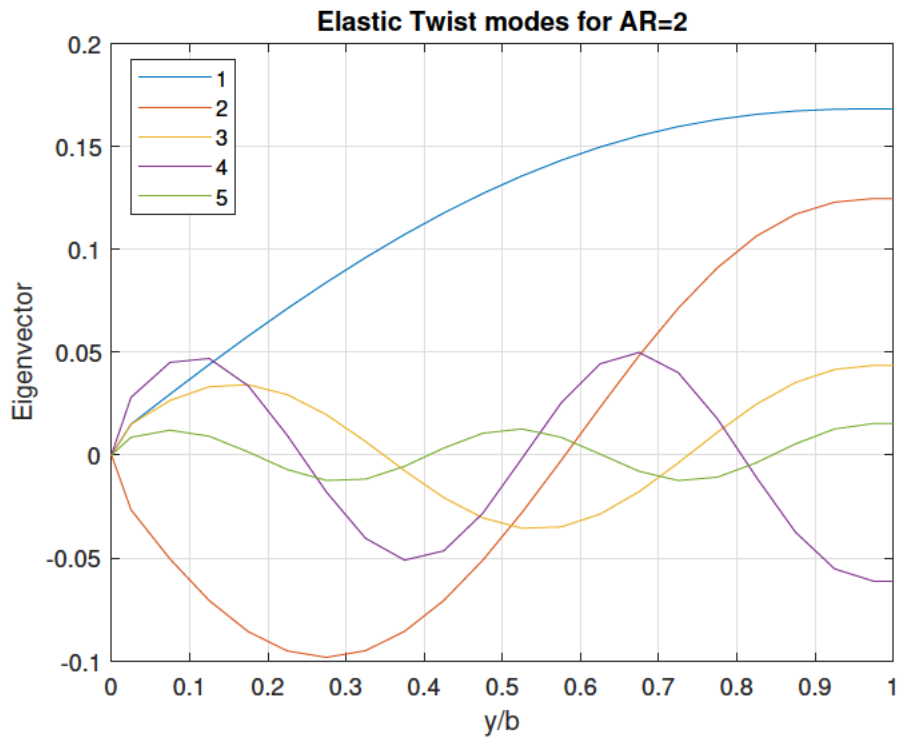


Figure 15: First modes for Aspect Ratio 2

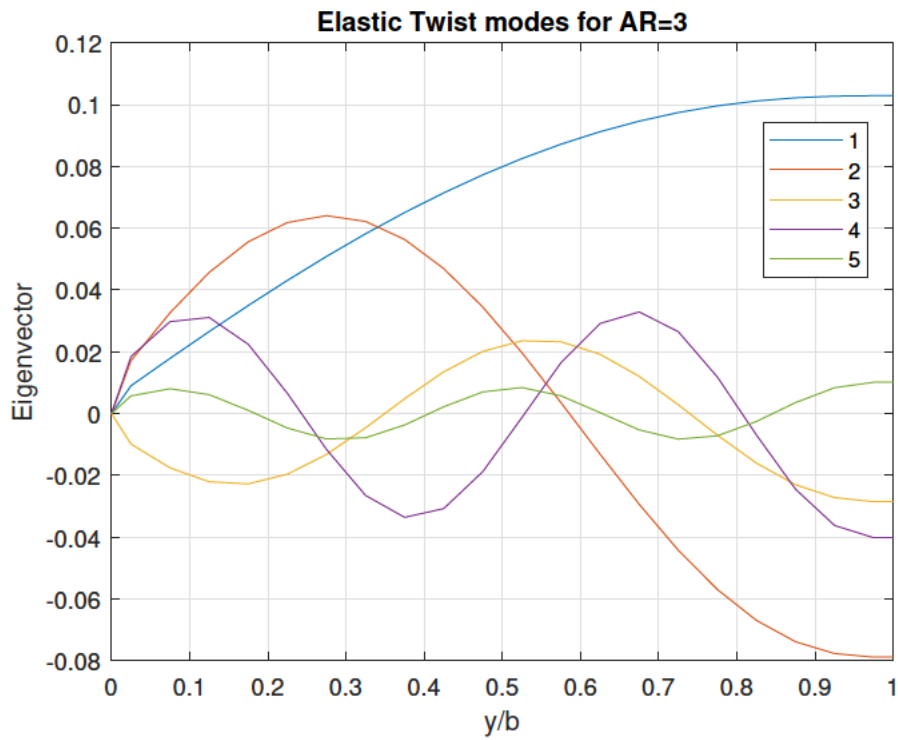


Figure 16: First modes for Aspect Ratio 3

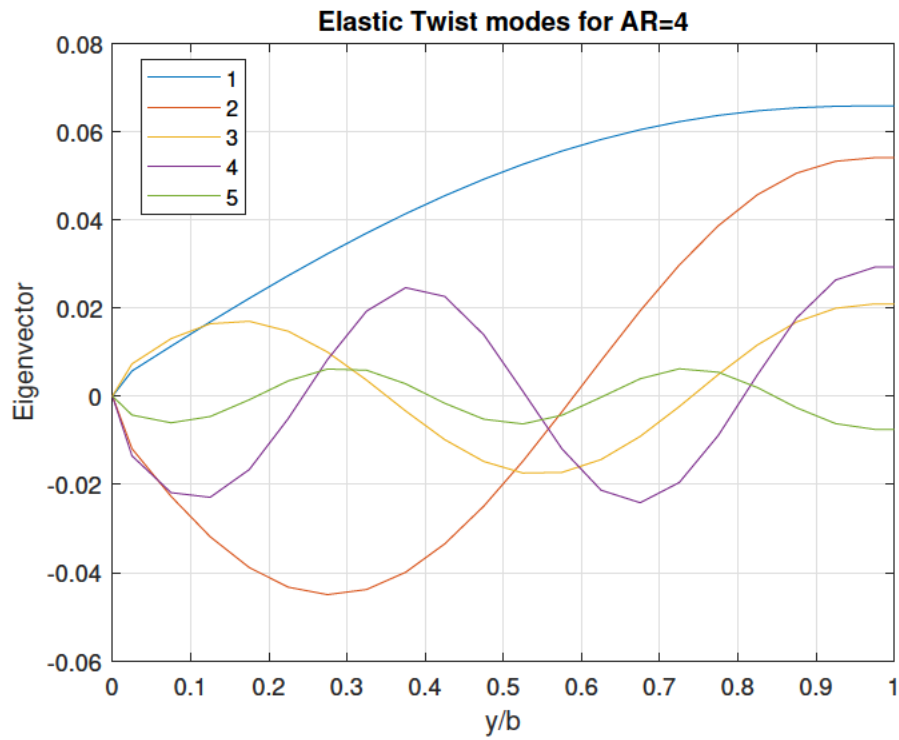


Figure 17: First modes for Aspect Ratio 4

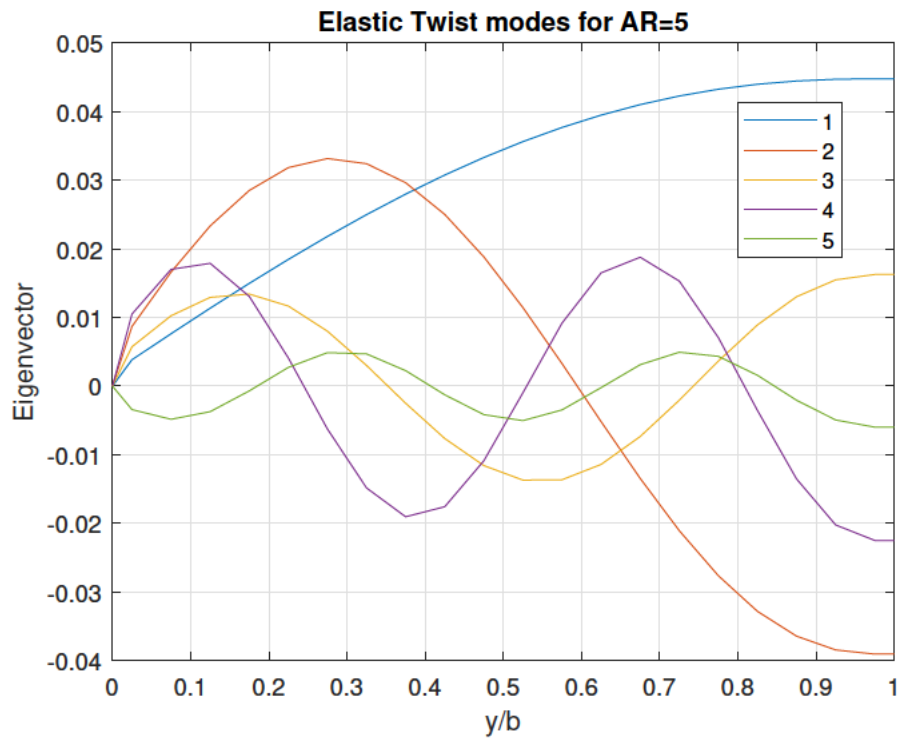


Figure 18: First modes for Aspect Ratio 5

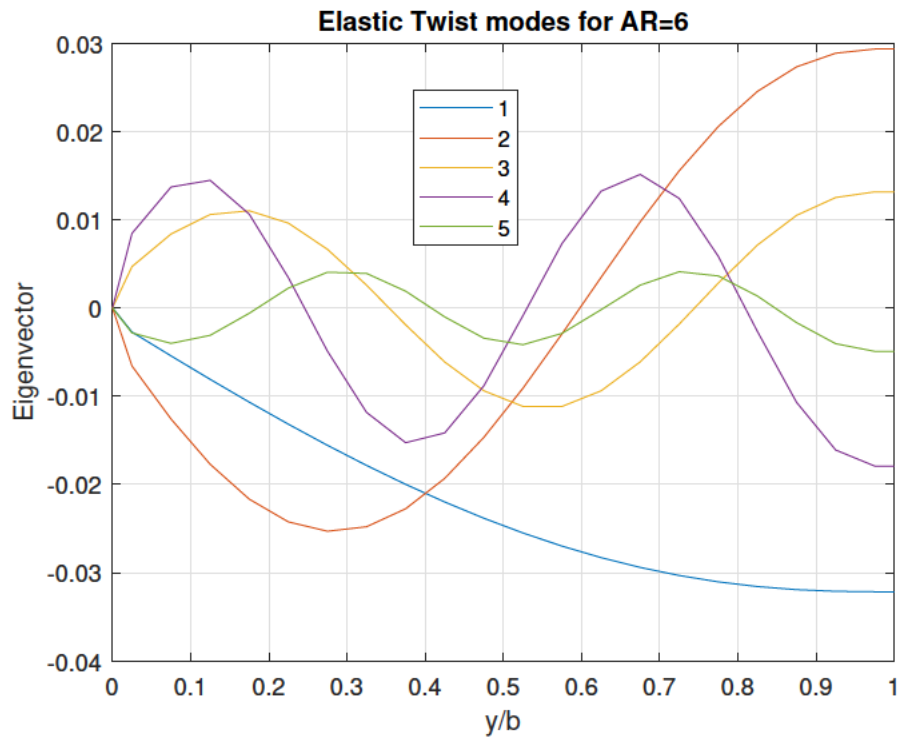


Figure 19: First modes for Aspect Ratio 6

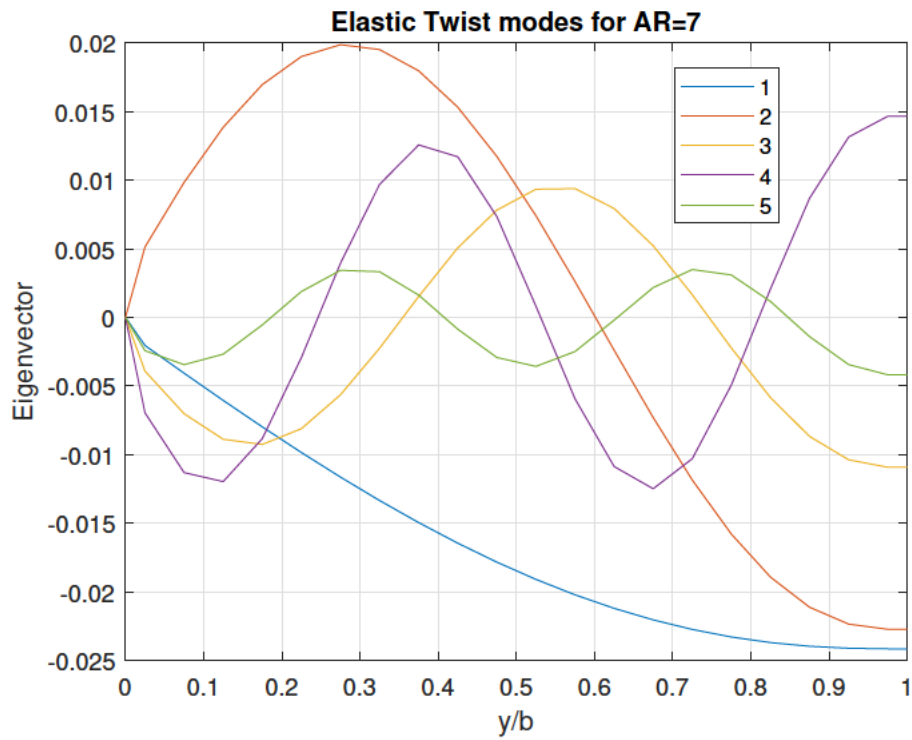


Figure 20: First modes for Aspect Ratio 7

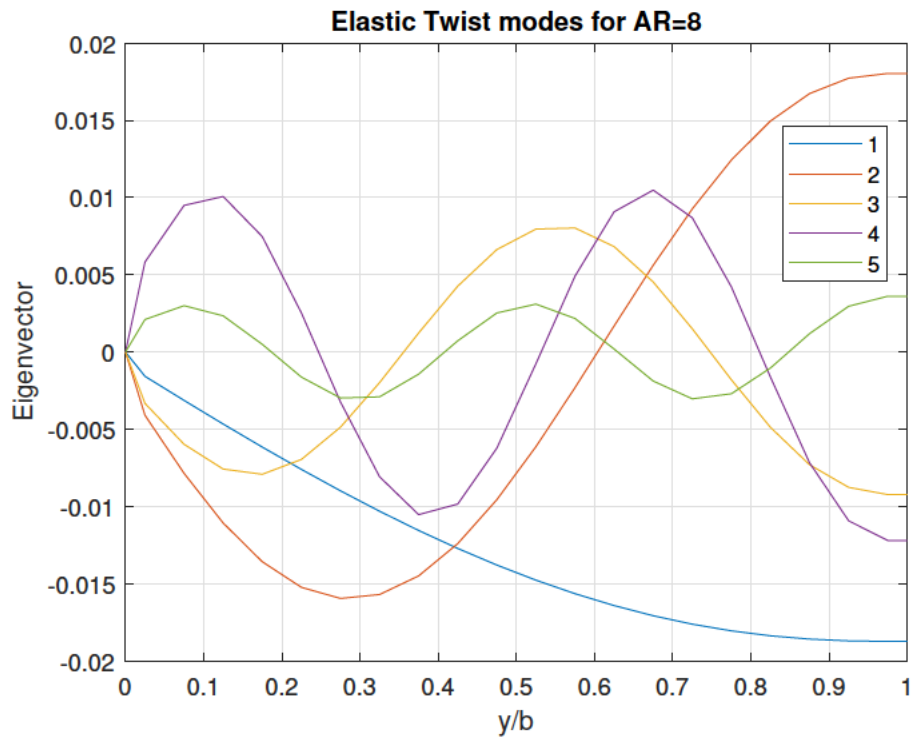


Figure 21: First modes for Aspect Ratio 8

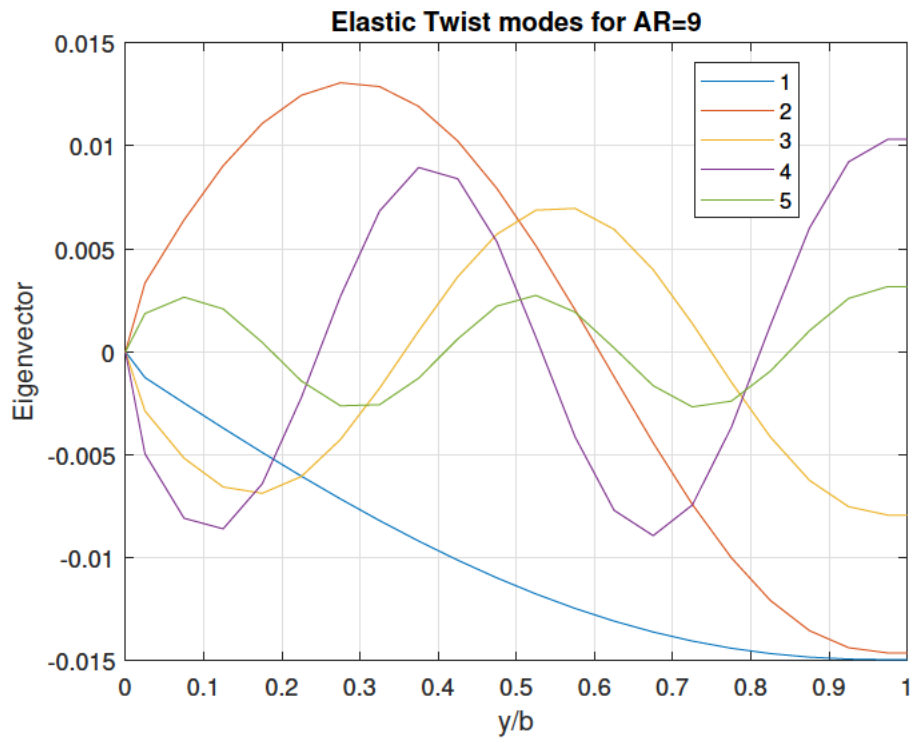


Figure 22: First modes for Aspect Ratio 9

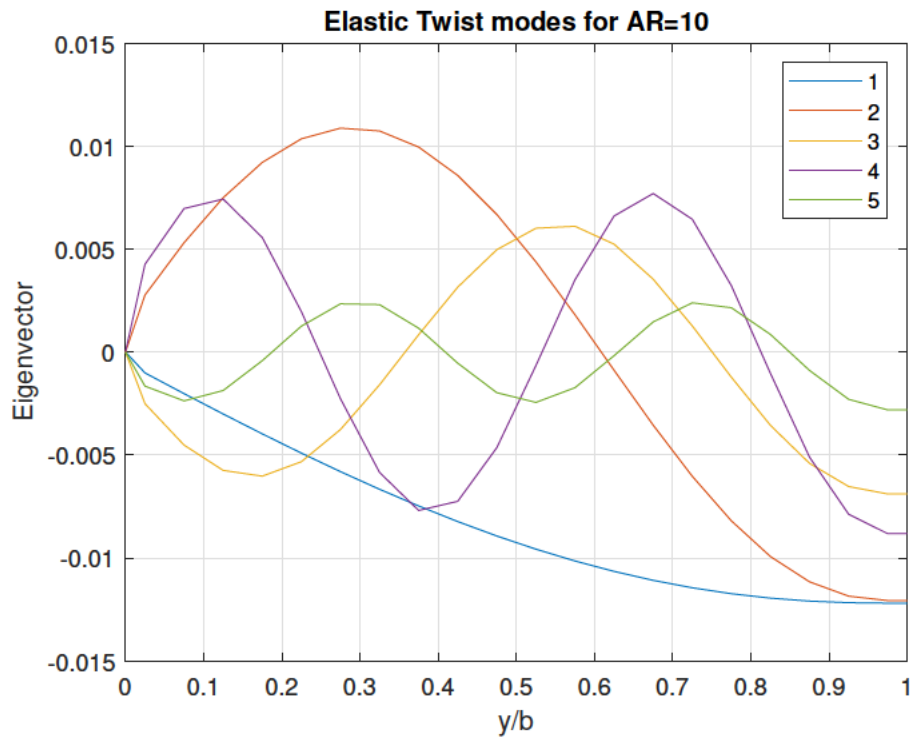


Figure 23: First modes for Aspect Ratio 10

As it can have been observed in the previous Figures, the modes associated to each Aspect Ratio vary significantly.

Taking into account the definition of Aspect Ratio, $AR = \frac{b^2}{S} = \frac{b^2}{b \cdot c} = \frac{b}{c}$ for this case. So, for lower values of AR, we are basically considering a square-wing with the highest values observed for the eigenvector than any other case. On the contrary, while making the wing more slender (increasing AR), a reduction of these eigenvectors values is observed, which it is believed it could be associated to the speed reduction necessary to achieve the divergence condition. It would also be relevant to comment the fact that a filter has been done for each case, since the order of the modes varies depending on the case analysed.

4.2.2 Divergence speed for different Aspect Ratios

The Figure 24 shows the tendency of the divergence speed when changing the Aspect Ratio.

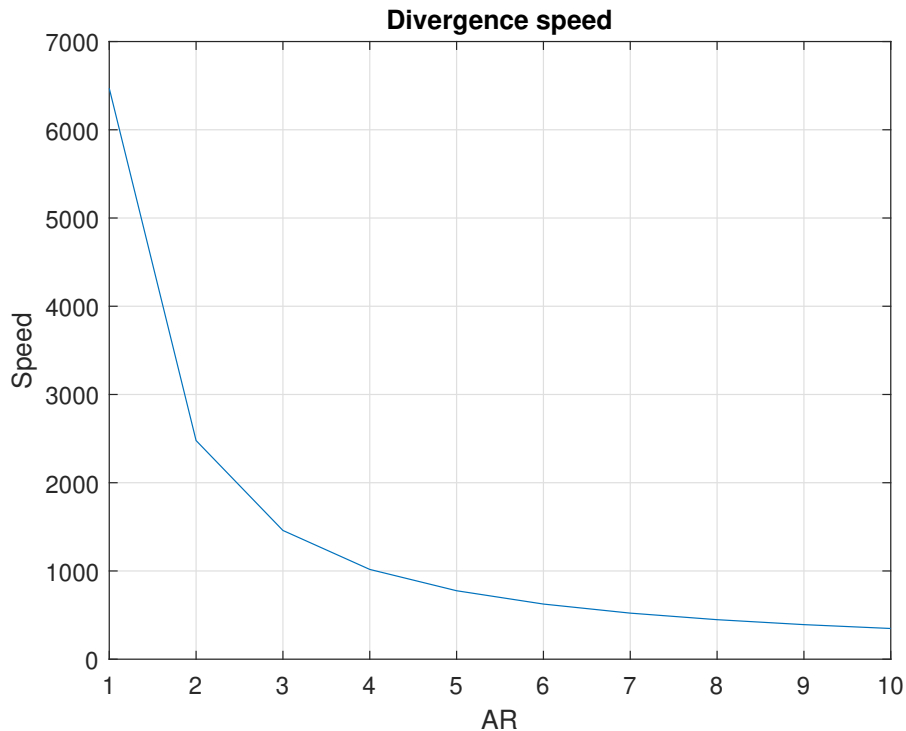


Figure 24: Divergence speed (m/s) for different wing Aspect Ratios

As it can be seen, when increasing the Aspect Ratio of the wing, the divergence speed decreases, approaching the 0 value as the Aspect Ratio increases. This result shows that, when the span is large enough, any variation in the wing instantly creates the divergence condition, and thus, the wing would be certainly uncontrollable.

For the most critical situation it would be inside the ranges of a typical commercial aircraft. For instance, in the case of an Airbus A320, which has an AR of approximately 10.3, the cruise speed is of the 830km/h order, being below the 1000km/h where the divergence phenomena would appear. However, this does not always happen. Then, it would be interesting to find tools to avoid this kind of condition as, generally, divergence is a non-desired effect. Making stiffer structural elements would be a solution, although this stiffness increase it is usually achieved in expenses of having more weight on the aircraft. So, it's always a trade-off depending on the application and ranges of operation of the aircraft.

4.2.3 Stability plots for flutter

The calculation of the Flutter speed is developed by using the Theodorsen's model 3.2.2 and applying the resolution explained in 3.4.2. Taking this into account, the multiple solutions that give the lowest velocity are shown in the Figure 25.

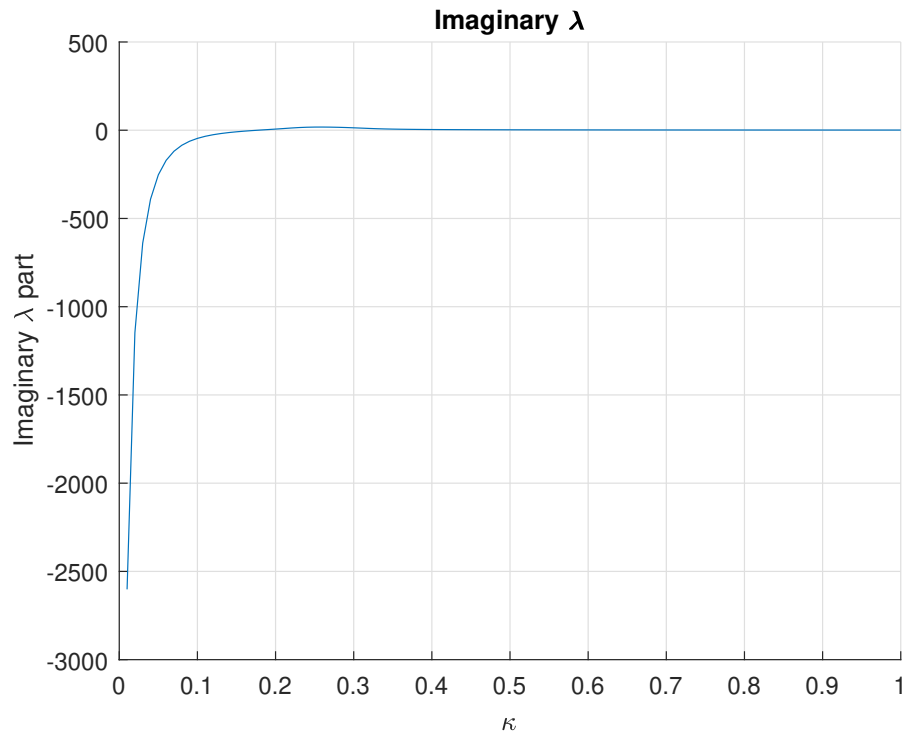


Figure 25: Imaginary parts of λ vs κ

By forcing the imaginary part of λ to be 0, the flutter speed is obtained: 218.7 m/s. At this velocity, the system will make a transition from stability to instability achieving the aforementioned flutter. As it can be seen, the order calculated is similar to the one obtained for the divergence for relatively slender wings.

In the Figure 26, the velocity vs κ evolution is represented. Following the Equation 38, it can be seen how the tendency of increasing κ while decreasing the speed is accomplished.

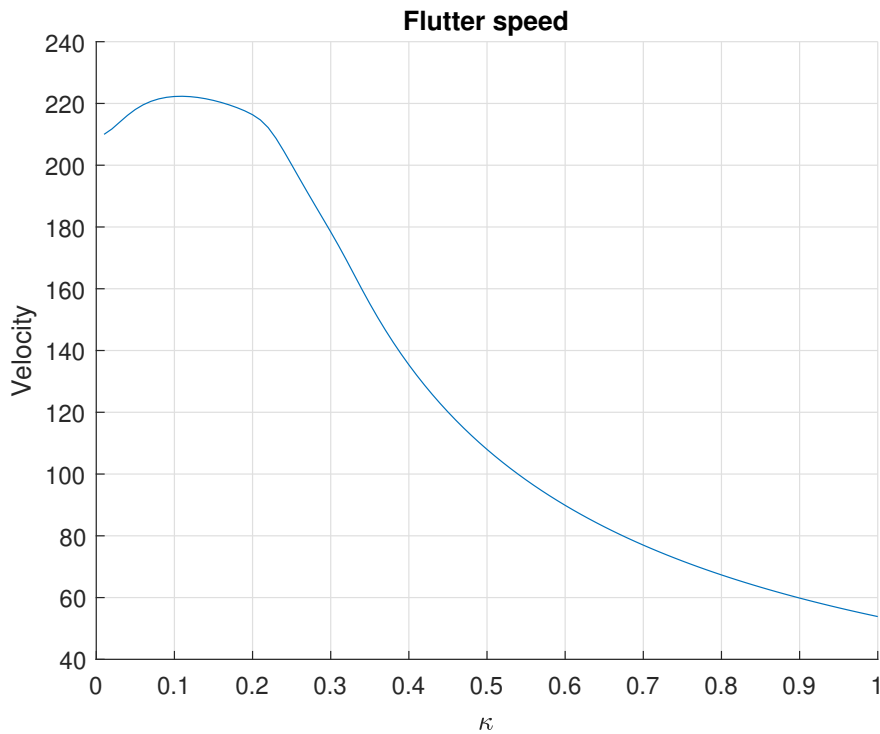


Figure 26: Velocity (m/s) vs κ

5 Conclusions

Once the results are obtained, some conclusions can be extracted about the project. The results obtained are generally outputs expected from what the theory and problems given in class have presented. The orders for the velocities and the tendencies achieved seem to have logical values. All the demanded results presented in the requirements are obtained and justified accomplishing with the aim and scope of the project. The code obtained is an interesting tool that could be used to verify and test future developments, based on the concepts presented here: basically divergence and flutter speed for both steady and unsteady aerodynamics. Some improvements for the development could pass from working with more sophisticated aerodynamic methods such as Vortex Lattice, where instead of using only one horseshoe vortex per wing, as in LLT, it uses a lattice of horseshoe vortices. For the dynamic part it could also be interesting to consider other methodologies, apart from the Theodorsen's one presented taking care of the computational cost they would require. Additional considerations on the structural part could also be considered, for instance improving the mesh input of the program with a more detailed structure, adding more complex or detailed elements to the mesh, among others.

6 Bibliography

References

- [1] D. Roca, “Project,” *Universitat Politècnica de Catalunya. Escola Superior d'Enginyeries Industrial, Aeroespacial i Audiovisual de Terrassa*, pp. 1–20, 2020.
- [2] D. Roca, “Dynamics of an airfoil,” *Universitat Politècnica de Catalunya. Escola Superior d'Enginyeries Industrial, Aeroespacial i Audiovisual de Terrassa*, pp. 1–9, 2020.
- [3] D. Roca, “Problem 5,” *Universitat Politècnica de Catalunya. Escola Superior d'Enginyeries Industrial, Aeroespacial i Audiovisual de Terrassa*, pp. 1–12, 2020.
- [4] D. Roca, “Wing model,” *Universitat Politècnica de Catalunya. Escola Superior d'Enginyeries Industrial, Aeroespacial i Audiovisual de Terrassa*, pp. 1–15, 2020.
- [5] D. Roca, “Problem 3,” *Universitat Politècnica de Catalunya. Escola Superior d'Enginyeries Industrial, Aeroespacial i Audiovisual de Terrassa*, pp. 1–9, 2020.

Advanced Aeroelasticity: Project

Finite wing divergence and flutter phenomena

A  

Table of contents

1. Introduction	3
2. Wing model	4
2.1. Structural model.....	4
2.2. Aerodynamic model	6
2.2.1. Horseshoe method.....	6
2.2.2. Theodorsen method.....	7
2.3. Discretization.....	8
2.3.1. Aerodynamic symmetry condition	8
2.4. Divergence.....	9
2.5. Flutter	9
3. Implementation.....	10
3.1. Divergence condition	10
3.1.1. Torsion eigenmodes	10
3.1.2. Aspect ratio sensitivity	11
3.1.3. Swept wing	12
3.1.4. Trapezoidal wing	13
3.2. Flutter condition.....	14
4. Conclusions	15

1. Introduction

The aeroelasticity phenomenon is a critical design point in different industries. Nowadays, it is not just a phenomenon of interest for increasing the safety in the aerospace industry, but it is also critical for designing more efficient wind turbines, or even it is applied in the motorsport industry for achieving better aerodynamic performance of the race cars.

This phenomenon is based on a coupling between the structural deformation of certain aerodynamic surfaces and its effects in the aerodynamic forces. Achieving a feedback loop that may blow the stability of the system depending on the design and the boundary conditions.

It can be studied using different approach, on one hand, it is possible to build a model with certain mechanical and aerodynamics configuration a test it on a wind tunnel. This may result in highly accurate results of certain geometry, but it will not be very cost-effective, as many models might be manufactured to study different configurations and their effects.

On the other hand, it is possible to model this event using different degrees of complexity. The most accurate solution may be using a complete CFD of the element with a Finite Element structure that is deformed dynamically under certain conditions. As in the previous case, this will result in accurate solution of the problem, but it will be high computational and engineering expensive. There exist simplified models that are suitable for understanding the causes and the effects of different parameters, concretely they can be divided into two parts, the quasi-static model, the structure is modelled using static beam elements and the aerodynamic is modelled using a horseshoe potential model. The dynamic model is based on dynamic beam elements structural modelling and the aerodynamics are modelled using the Theodorsen's aerodynamics model.

This study proposes a virtual testing environment based on a simplified beam modelling for the structural part, whose properties will be extracted from a detailed finite element analysis of the whole wing structure. And the aerodynamics will be modelled using the horseshoe method for analysing the divergence condition and the Theodorsen's aerodynamic model for analysing the flutter stability condition.

2. Wing model

In this section, the model is described in detail. Concretely it will be divided in two sections the structural modelling and the aerodynamic modelling.

2.1. Structural model

The structure will be modelled using the Finite Element Method with hexahedral elements. Each part of the wing will be modelled using different properties.

Once the structure is completely defined, it will be tested under different load cases. The first load case objective is determining the shear centre of the structure. To find this point the definition of the shear centre will be used: the shear centre is the point where a shear force does not cause twisting deformation. It is necessary to determine a feasible way to place a force at different chord locations, to do so an equivalent force and moment method will be used, as described in figure 1.

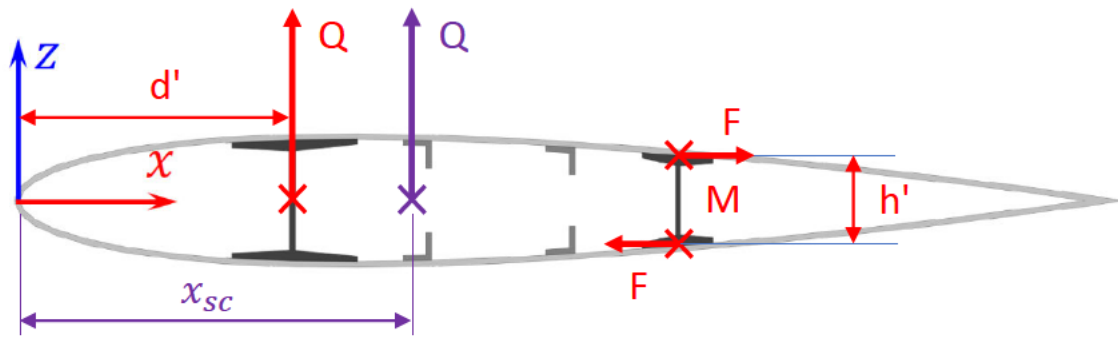


Figure 1: Equivalent shear force and position.

The equation that determines the position of the equivalent shear force is:

$$x_{sc} = \frac{Qd' + M}{Q} = \frac{Qd' + Fh'}{Q}$$

The solver that will be used is based on a Bolzano algorithm, supposing that the shear centre is between the chord of the wing.

After finding the shear centre, two load cases will be used to determine the bending and torsion stiffness of the beam. To do so a polynomial fitting of the central nodes' deformation will be used as shown in figure 2.

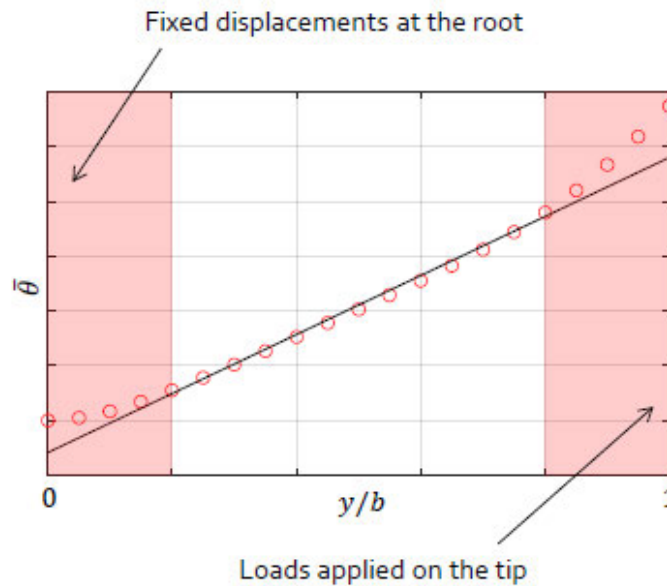


Figure 2: Deformation fitting using 1D beam elements. Torsion case.

The equations that determine the equivalent beam properties, supposing that there is not twisting bending coupling, are:

$$\widehat{EI} = -\frac{\partial^3 h}{\partial y^3}; \quad \widehat{GJ} = \frac{\partial \theta}{\partial y}$$

Once the equivalent beam structural properties are obtained, the inertial properties must be determined, to do so the polar inertia of the section, the mass per unit length and the centre of gravity position must be obtained. They will be obtained by integrating the mass of each element using the following expressions:

$$\widehat{m} = \sum \rho^{[e]} A^{[e]}; \quad x_{cm} = \frac{\sum x^{[e]} \rho^{[e]} A^{[e]}}{\widehat{m}}; \quad \widehat{I}_{cm} = \sum (x_{cm} - x^{[e]})^2 \rho^{[e]} A^{[e]}$$

Finally, those magnitudes can be scaled by using the chord size at each section using the following expressions:

$$EI^{[e]} = \widehat{EI} \cdot \left(\frac{c^{[e]}}{\hat{c}}\right)^4; \quad GJ^{[e]} = \widehat{GJ} \cdot \left(\frac{c^{[e]}}{\hat{c}}\right)^4; \quad m^{[e]} = \widehat{m} \cdot \left(\frac{c^{[e]}}{\hat{c}}\right)^2; \quad I_{cm}^{[e]} = \widehat{I}_{cm} \cdot \left(\frac{c^{[e]}}{\hat{c}}\right)^4$$

And then it is possible to obtain the elemental matrices as:

$$[K]^{[e]} = \frac{GJ^{[e]}}{l^{[e]}} \begin{bmatrix} +1 & 0 & 0 & -1 & 0 & 0 \\ 0 & 0 & 0 & 0 & 0 & 0 \\ 0 & 0 & 0 & 0 & 0 & 0 \\ -1 & 0 & 0 & +1 & 0 & 0 \\ 0 & 0 & 0 & 0 & 0 & 0 \\ 0 & 0 & 0 & 0 & 0 & 0 \end{bmatrix} + \frac{EI^{[e]}}{(l^{[e]})^3} \begin{bmatrix} 0 & 0 & 0 & 0 & 0 & 0 \\ 0 & 12 & 6l^{[e]} & 0 & -12 & 6l^{[e]} \\ 0 & 6l^{[e]} & 4(l^{[e]})^2 & 0 & -6l^{[e]} & 4(l^{[e]})^2 \\ 0 & 0 & 0 & 0 & 0 & 0 \\ 0 & -12 & -6l^{[e]} & 0 & 12 & -6l^{[e]} \\ 0 & 6l^{[e]} & 4(l^{[e]})^2 & 0 & -6l^{[e]} & 4(l^{[e]})^2 \end{bmatrix}$$

$$[M]^{[e]} = \frac{l^{[e]}}{2} \begin{bmatrix} I_{cm} + md^2 & md & 0 & 0 & 0 & 0 \\ md & m & 0 & 0 & 0 & 0 \\ 0 & 0 & 0 & 0 & 0 & 0 \\ 0 & 0 & 0 & I_{cm} + md^2 & md & 0 \\ 0 & 0 & 0 & md & m & 0 \\ 0 & 0 & 0 & 0 & 0 & 0 \end{bmatrix}; \quad d = x_{sc} - x_{cm}$$

2.2. Aerodynamic model

Two different aerodynamic models will be used depending on the type of analysis that will be performed, if the analysis objective is determining the divergence modes the horseshoe method will be used. Whereas, if the analysis objective is determining the flutter condition, the Theodorsen's aerodynamic model will be used.

2.2.1. Horseshoe method

The horseshoe method is based on the extension of the discrete vortex for a 2D airfoil analysis, it is based on constant vortex lines that have an attach part at the aerodynamic centre of each section and two unattached vortex that are parallel to the free stream velocity. As in the 2D airfoil analysis each section has a collocation point where the flow through the surface must be zero obtaining the following system of equations:

$$\left(\sum_{j=1}^n (v_{12}^{[j]} + v_{23}^{[j]} + v_{34}^{[j]}) |_{x=x^{[i]} + U_{\infty}} \right) \cdot n^{[i]} = 0$$

Which can be written in matrix form:

$$[A]\{\Gamma\} = -U_{\infty}\{\alpha\}$$

Then the lift contribution of each element is:

$$L^{[i]} = \rho_{\infty} U_{\infty} S^{[i]} \Gamma^{[i]} \rightarrow [L] = -2 \cdot q_{\infty} [S][A]^{-1} \{\alpha\}$$

Where S is a diagonal matrix with the aerodynamic surface of each element.

And the torsional moment of each element is:

$$[M_{sc}] = [L]d$$

2.2.2. Theodorsen method

The Theodorsen method is based on a linear approximation of the 2D airfoil wake dynamics based on the coupling of the different degrees of freedom of the model and the Theodorsen's transfer function that accounts the attenuation by the wake vorticity.

$$\begin{aligned}
 l^{[i]} &= \pi\rho_{\infty}b^2(U_{\infty}\theta - ba\theta - h) + 2\pi\rho_{\infty}U_{\infty}bC(\kappa)\left(U_{\infty}\theta + b\left(\frac{1}{2} - a\right)\theta - h\right) \\
 m_{sc} &= -\pi\rho_{\infty}b^3\left(U_{\infty}\left(\frac{1}{2} - a\right)\theta + b\left(\frac{1}{8} + a^2\right)\theta + ah\right) + \\
 &\quad + 2\pi\rho_{\infty}U_{\infty}b^2C(\kappa)\left(a + \frac{1}{2}\right)\left(U_{\infty}\theta + b\left(\frac{1}{2} - a\right)\theta - h\right)
 \end{aligned}$$

Where $C(\kappa)$ is the Theodorsen transfer function and κ is the reduced frequency:

$$C(\kappa) = 1 - \frac{0.165}{1 - \frac{i0.0455}{\kappa}} - \frac{0.335}{1 - \frac{i0.3}{\kappa}}; \quad \kappa = \frac{\omega b}{U_{\infty}}$$

The Theodorsen function can be written in complex form as:

$$F(\kappa) = \frac{0.5\kappa^4 + 0.0765\kappa^2 + 1.8632 \cdot 10^{-4}}{\kappa^4 + 0.0921\kappa^2 + 1.8632 \cdot 10^{-4}}; \quad G(\kappa) = \frac{-0.1080\kappa^3 - 8.8374 \cdot 10^{-4}\kappa}{\kappa^4 + 0.0921\kappa^2 + 1.8632 \cdot 10^{-4}}i$$

Finally, it is possible to write the Theodorsen aerodynamic model in matrix form for each element as:

$$\begin{aligned}
 [\widehat{A}_R(\kappa)]^{[e]} &= \kappa^2 \begin{bmatrix} \frac{1}{8} + a^2 & a & 0 \\ a & 1 & 0 \\ 0 & 0 & 0 \end{bmatrix} + \kappa G(\kappa) \begin{bmatrix} 2a^2 - \frac{1}{2} & 2a + 1 & 0 \\ 2a - 1 & 2 & 0 \\ 0 & 0 & 0 \end{bmatrix} + F(\kappa) \begin{bmatrix} 1 + 2a & 0 & 0 \\ 2 & 0 & 0 \\ 0 & 0 & 0 \end{bmatrix} \\
 [\widehat{A}_I(\kappa)]^{[e]} &= \kappa \begin{bmatrix} a - \frac{1}{2} & 0 & 0 \\ 1 & 0 & 0 \\ 0 & 0 & 0 \end{bmatrix} - \kappa F(\kappa) \begin{bmatrix} 2a^2 - \frac{1}{2} & 2a + 1 & 0 \\ 2a - 1 & 2 & 0 \\ 0 & 0 & 0 \end{bmatrix} + G(\kappa) \begin{bmatrix} 1 + 2a & 0 & 0 \\ 2 & 0 & 0 \\ 0 & 0 & 0 \end{bmatrix}
 \end{aligned}$$

2.3. Discretization

Once the elemental matrices have been defined, it is time to discretize the problem using the following method. A staggered mesh will be used using the structural nodes as center of the aerodynamic element as shown in the following figure, two extra nodes will be added at the fuselage and at the wing tip.

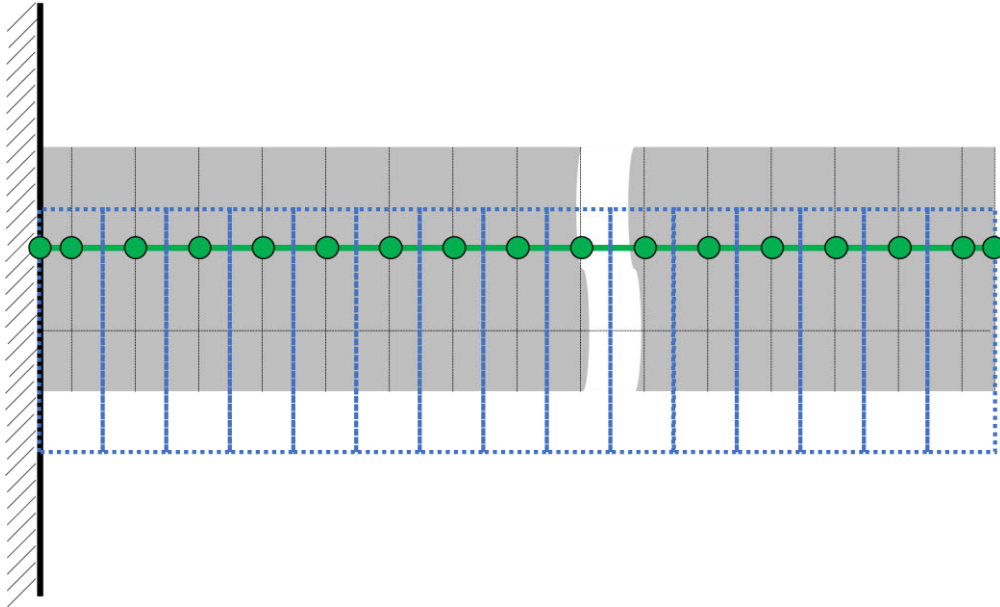


Figure 3: Wing discretization using staggered mesh. In green: Elastic axis and structural nodes position. In blue: horseshoes of each aerodynamic element. In grey: rectangular wing representation. In black: Fuselage boundary condition (it can be considered as a symmetry plane).

As it can be seen, at wing tip and at the symmetry plane, an extra aerodynamic element with null effective surface must be added to have the same number of nodes.

2.3.1. Aerodynamic symmetry condition

It is possible to account for the aerodynamic symmetry condition by creating a fictitious symmetric aerodynamic mesh that will be reduced using the symmetry conditions as:

$$\Gamma(y) = \Gamma(-y) \rightarrow K_{aero_{sym}} [i,j] = K_{aero} \left[\frac{N_{elem}}{2} + i, \frac{N_{elem}}{2} + j \right] + K_{aero} \left[\frac{N_{elem}}{2} + i, \frac{N_{elem}}{2} - j + 1 \right]; \quad i, j = 1: N_{elem}$$

If K_{aero} is a 4x4 matrix, then $K_{aero_{sym}}$ will be 2x2 matrix with the following values:

$$K_{aero} = \begin{bmatrix} K_{11} & K_{12} & K_{13} & K_{14} \\ K_{21} & K_{22} & K_{23} & K_{24} \\ K_{31} & K_{32} & K_{33} & K_{34} \\ K_{41} & K_{42} & K_{43} & K_{44} \end{bmatrix} \rightarrow K_{aero_{sym}} = \begin{bmatrix} K_{33} + K_{32} & K_{34} + K_{31} \\ K_{43} + K_{42} & K_{44} + K_{41} \end{bmatrix}$$

2.4. Divergence

The divergence condition is a quasi-static aero-elastic phenomenon that occurs when the following conditions is satisfied:

$$([K_{aero}]^{-1}[K] - \lambda)\{x\} = 0$$

In our problem the inverse of the aerodynamic matrix does not exist as there are rows and columns with null values, then the inverse problem must be solved:

$$\left([K]^{-1}[K_{aero}] - \frac{1}{\lambda}\right)\{x\} = 0$$

The main disadvantage of solving the inverse problem is that there will appear other eigenvalues associated to the diagonalization of the stiffness matrix that are not related with the divergence problem, that is caused by a torsion in the wing.

2.5. Flutter

The flutter condition is a dynamic aero-elastic phenomenon that occurs when the following conditions is satisfied:

$$\left(-\frac{\omega^2}{\pi\rho_\infty b^2 U_\infty^2} [M] + \frac{1}{\pi\rho_\infty b^2 U_\infty^2} [K] - ([\widehat{A}_R(\kappa)] + i[\widehat{A}_I(\kappa)])\right)\{x\} = \{0\}$$

Which can be converted to an eigenvalue problem using the adimensionalization as:

$$\left([\widehat{K}]^{-1}([\widehat{M}] + (\kappa^{-2} \cdot \mu^{-1})([\widehat{A}_R(\kappa)] + i[\widehat{A}_I(\kappa)])) - \lambda\right)\{x\} = 0$$

Where the solutions of this eigenvalue problem are:

$$\omega = \frac{\omega_\theta}{\sqrt{\lambda}}; \quad U_\infty = \frac{b\omega}{\kappa}$$

In fact, the flutter condition occurs when:

$$\min(U_\infty > 0 \ \& \ Im(\omega = 0))$$

3. Implementation

In this section an analysis of different parameters will be assess. Starting with the divergence condition and finally the flutter phenomena.

3.1. Divergence condition

In this section a detailed analysis of the divergence phenomena will be done, the first step will be analysing the divergence eigenmodes that appear in a simple rectangular wing. Then, a detailed analysis on the wing aspect ratio will be done. To continue, the swept wing angle effect will be analysed. Finally, a trapezoidal wing will be simulated.

3.1.1. Torsion eigenmodes

As the aerodynamic matrices are only dependent on the torsion angle, the only eigenmodes that will be analysed are the ones that have a non-null distribution of torsion angles. However, when solving the eigenvalues problem other bending eigenmodes will appear they are not related with the divergence effect. Concretely the case that will be analysed is a constant chord wing with an aspect ratio of five.

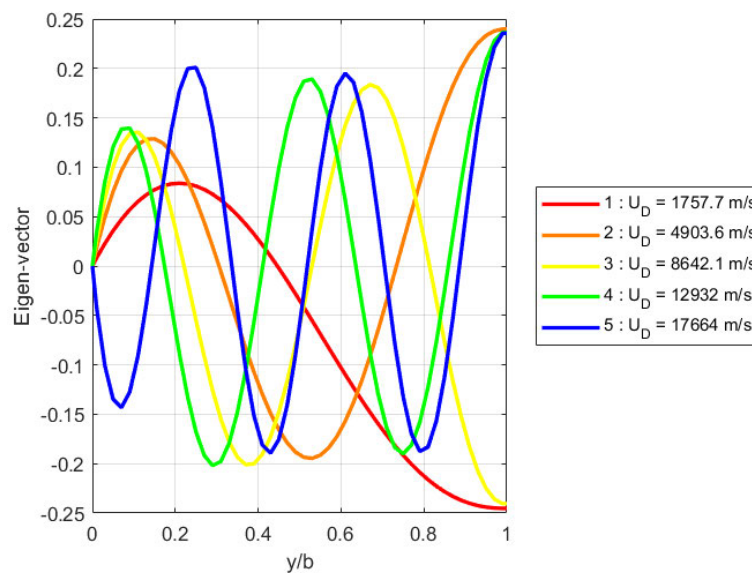


Figure 4: Divergent conditions first 5th torsion eigenmodes, AR=5.

With this wing configuration, it can be seen that the first possible eigenmode correspond to the second wing mode, as it has one relative maximum and minimum.

3.1.2. Aspect ratio sensitivity

After a detailed overview of the shape of the eigenmodes, the wing aspect ratio will be analysed making a sweep through a range between one and twenty.

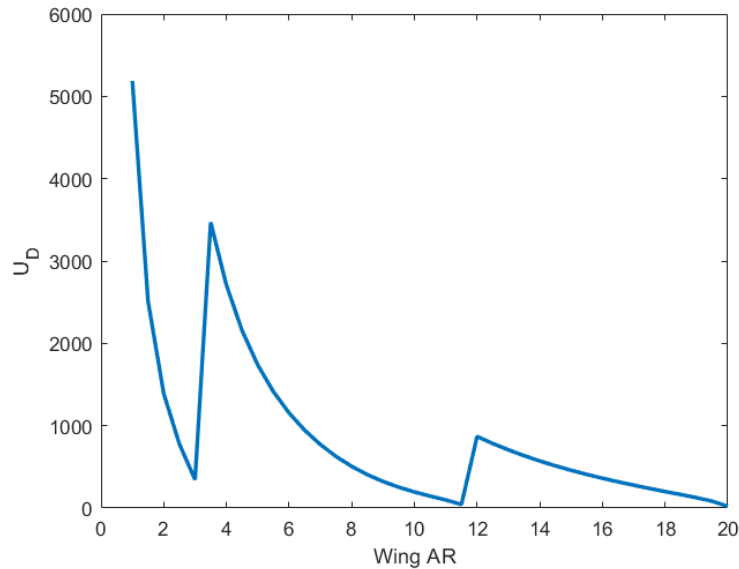


Figure 5: Divergence speed of the first divergence mode aspect ratio sensitivity.

It can be seen a tooth shaped curve; this is caused by making infeasible the first modes when increasing the aspect ratio as shown in the figure x. The first feasible eigen mode of the first curve is a single relative maximum, while in the second tooth it is a relative minimum and a relative maximum, finally the last tooth is a 3-relative maximum-minimum shape.

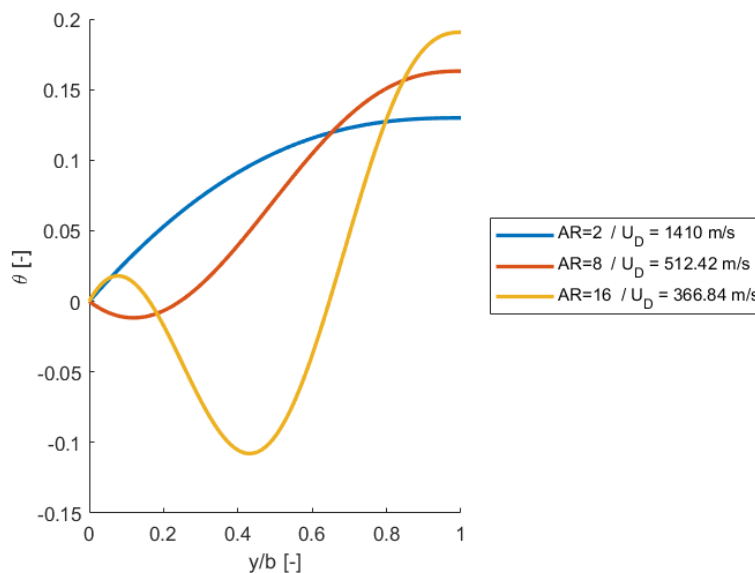


Figure 6: First divergence eigen modes at different aspect ratios.

3.1.3. Swept wing

A similar study has been performed with a swept wing. A similar effect is seen when increasing the swept angle, this may be caused by an increment of the structural elements length a thus reducing the structural stiffness.

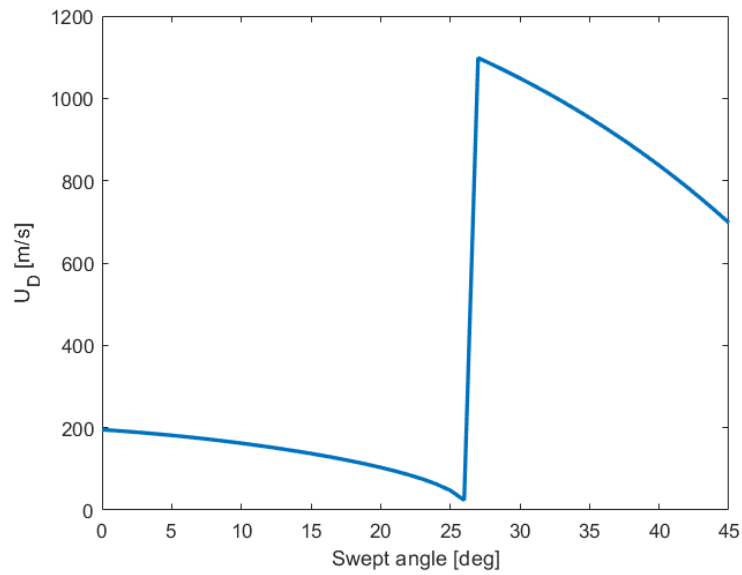


Figure 7: Swept wing first mode divergence speed. Wing AR of 10.

3.1.4. Trapezoidal wing

The last wing shape analysis that has been performed is a modification of the wing tip and root chords while maintaining the aspect ratio constant ($AR=10$) and the mean aerodynamic chord constant ($C_{mac} = 1$). The obtained results are shown in the following figures.

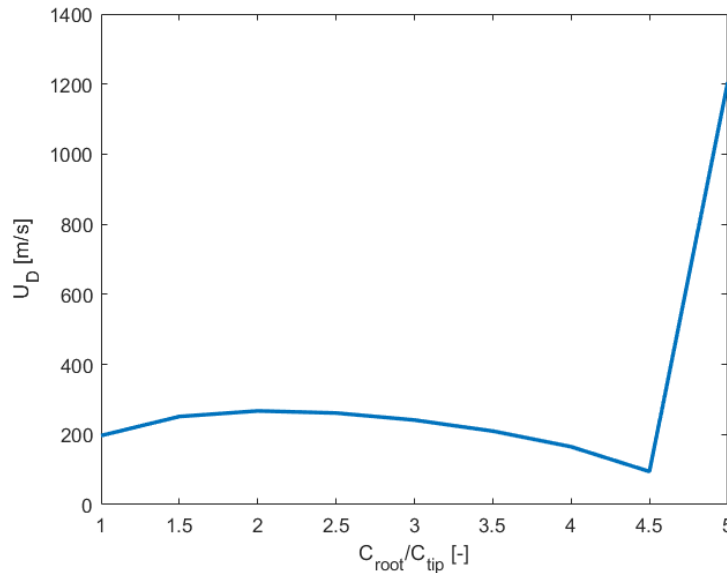


Figure 8: Divergence speed for different wing tip chord ratios. AR=10.

It can be seen that there exists an optimal wing tip ratio when the divergence speed is maximum in the range between one and 4.5. After that point, a change in the first feasible divergence mode is achieved increasing the divergence speed.

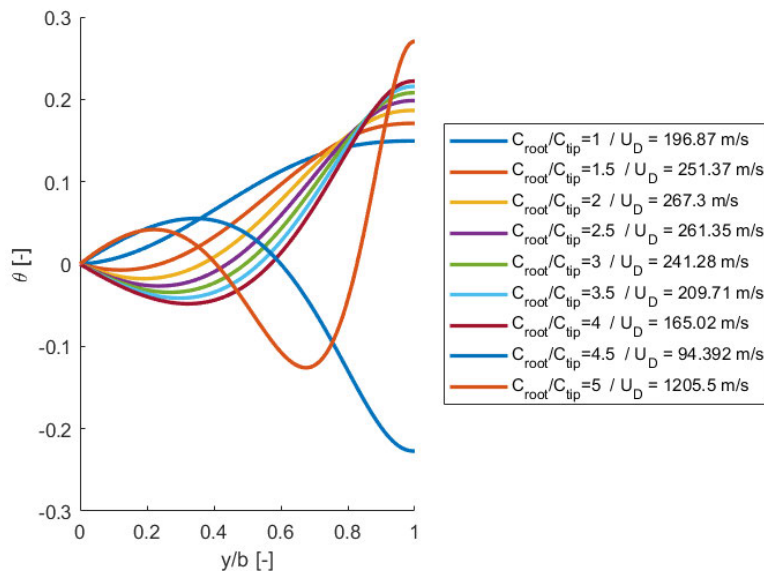


Figure 9: Divergence torsion modes for different wing tip chord ratios. AR=10.

3.2. Flutter condition

The flutter problem will be solved iteratively using a range of κ between 10^{-3} and 10^1 obtaining the following figure.

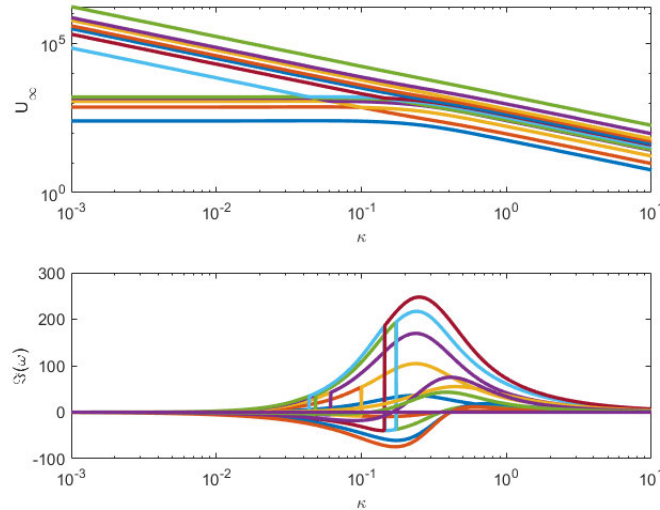


Figure 10: Flutter map for a 7 elements mesh and wing AR of 10.

As it can be seen the modes are not perfectly ordered due to the ordering factor used, the freestream velocity. In this graph, it can be seen that there are a few modes that are always stable, the imaginary component of the ω is always positive, and some others that for big κ and low speed they are stable and at certain point this stability is lost reaching negative values. Concretely, the flutter condition will occur when the first mode crosses the x axis line.

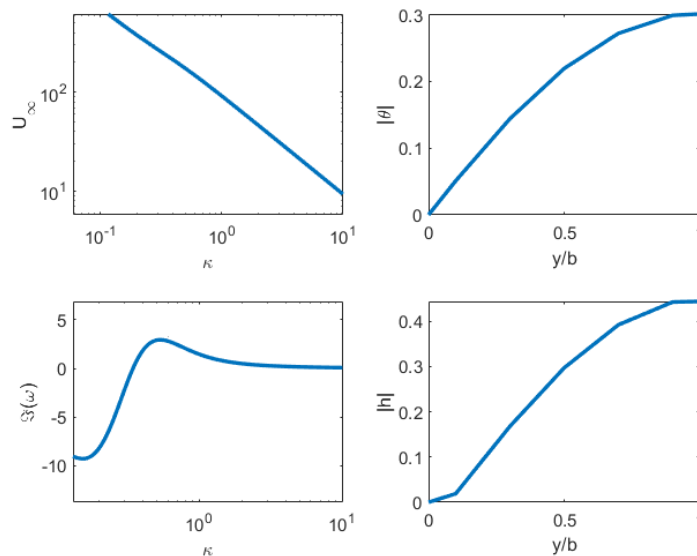


Figure 11: Flutter condition for a 7-element mesh and a wing aspect ratio of 10.
Flutter speed of: $U_{\infty_f} = 241.07$ m/s, and $\kappa = 0.3424$.

4. Conclusions

During this study, it has been proven the feasibility of studying the divergence and flutter phenomena using simple structural and aerodynamic models while capturing the principal causes and effects of those phenomena and the key design parameters.

The self-implemented MATLAB software has shown a good performance on modelling aeroelastic cases.

It has been seen that the divergence is very dependent on the geometric parameters of the wing, modifying the apparition of the first's divergence modes. Also, the flutter phenomenon has been more difficult to assess due to the randomness of the apparition of the modes, making difficult the tracking of the imaginary part of the flutter frequency.